We are committed to providing [accessible customer service](#).
If you need accessible formats or communications supports, please [contact us](#).

Nous tenons à améliorer [l'accessibilité des services à la clientèle](#).
Si vous avez besoin de formats accessibles ou d'aide à la communication, veuillez [nous contacter](#).

Geophysical
Assessment Report
on the
Martin Kenty Property

Heronry, Dogpaw and Brooks Lake Area
Kenora Mining District
Ontario, Canada

Project Location

Latitude: 49.232° North; Longitude 93.767°
NAD 83 UTM co-ordinates, Zone 15U, 710500mE and 534100mN

Prepared for:

Big Gold Inc.
Suite 2702 - 401 Bay Street
Toronto, Ontario Canada, M5H 2Y4

Prepared by:
Robert G. Komarechka, P.Geo.

Bedrock Research Corp.
545 Granite Street
Sudbury, Ontario, Canada, P3C 2P4
February 25, 2022

SIGNATURE PAGE

This report titled

"**Geophysical Assessment Report on the Martin Kenty Property**
Heronry, Dogpaw, and Brooks Lake Area
Kenora Mining District
Ontario, Canada"

Project Location

Latitude: 49.232° North; Longitude 93.767°

NAD 83 UTM co-ordinates, Zone 15U, 710500mE and 534100mN

and dated

February 25, 2022

was prepared for

Big Gold Inc.
Client Number 10005912

Suite 2702 - 401 Bay Street
Toronto, Ontario Canada, M5H 2Y4

and signed by the author,

Robert Komarechka, P.Geo.

Dated at

February 25, 2022
Sudbury Ontario Canada

February 25, 2022
"Robert G. Komarechka"
Revised: June, 2022

TABLE OF CONTENTS

LIST OF TABLES

TABLE OF FIGURES

PHOTOS

APPENDICES

Item 1: Summary

Bedrock Research Corp. of Sudbury, Ontario was contracted by Big Gold Inc. (BG) to review historic data for the Martin Kenty Property (the "Property"), identify its merits, propose an appropriate exploration program and budget for exploration on the Property, and prepare a Technical Report (the "Report") compliant with NI 43-101 standards suitable for listing on an exchange from which this geophysical assessment report has been prepared.

The Property is located in Dogpaw Lake, Heronry Lake and Brooks Lake Areas within the Kenora Mining Division of Ontario, Canada, approximately 76 km SE of Kenora. The center of the Property is located at approximately 49.2316° North Latitude and 93.7674° West Longitude or in NAD 83 UTM co-ordinates, Zone 15U, 710500mE and 534100mN. The Property is located in the Kenora Ministry of Natural Resources District within the MNR Northwest Region.

The Property is comprised of 265 unpatented single unit mineral claims (the Claims) with a total approximate area of 5,579 hectares and further described in Table 1. The Property was acquired by way of an Asset Purchase Agreement dated July 19, 2021, from the Vendor, 2060014 Ontario Inc. a corporation incorporated under the laws of the province of Ontario. The owner of the Claims, currently shown on the Ontario government's Mineral Land Acquisition System (MLAS) records is Steven Anderson, acting as agent both for the Vendor, 2060014 Ontario Inc. and the purchaser Big Gold Inc. These Claims were sold to BG in return for 4,000,000 common shares of BG with the Vendor retaining a 2% net smelter return royalty (NSR) on the Property. The geophysical work was done on 132 of these claims as shown in Table 2 and Figures 3 and 3a.

The Property is located in the Archean Kakagi-Rowan Lake Greenstone Belt within the western Wabigoon Subprovince. The Wabigoon Subprovince, located in the southwestern part of the Superior Province, is composed mainly of volcanic rocks of tholeiitic to calc-alkaline affinity and sedimentary rocks, which are crosscut or intruded by large batholiths. It is over 900 km long and has been divided in three regions, namely the eastern, central, and western Wabigoon (Blackburn et al., 1991). On a local scale, each segment of greenstone belts has been given a unique name, along with each distinct batholith.

The Kakagi-Rowan Lake Greenstone Belt is composed of a complete mafic-felsic volcanic cycle which was initiated by a vast effusion of massive, pillowed and plagioclase-phyric mafic volcanic flows intruded by synvolcanic gabbro sills. Together these early mafic sequences are referred to as the Snake Bay formation. The Snake Bay formation, to the east off the property, is unconformably overlain by an equally thick succession of intermediate to felsic pyroclastic rocks estimated to be in the order of over 3 kilometers. Intrusive into the pyroclastics are cosanginous, differentiated ultramafic to gabbroic sills referred to as the Kakagi Lake sills. Together, these two distinct rock units form the Kakagi Lake group.

The latter part of the volcanic cycle is represented by thin units of Volcanogenic sediments (siltstone) and by felsic and partially bedded ash flows. As is typical for other Archean terranes, the supracrustal volcanics and sediments are intruded by quartz porphyry dykes and plugs and by late diabase dykes. The majority of the felsic dykes are found associated with the lower mafic meta- volcanics while the diabase dykes cut across the entire stratigraphic package. The entire Complex is bounded to the west by the Aulnean Batholith, to the south by the Sabaskong Batholith and to the northeast by the regional Pipestone-Cameron Lake Fault"
Souce: *(Jagodits, Francis L. 1998, AFRI # 52F05SE2002., p7-8).*

Five mineral occurrences, 4 of gold and 1 base metal have been documented on the Ontario Mineral Inventory (OMI) database for this Property. Maps showing these sites on the Property can be found in Figures 14 and 21.

Three known gold mineralization sites occur along the east-west Kakagi Lake Shear as shown in Figure 14, these being from west to east:
1. Martin F. M. on the east side of Hay Island,
2. Kakagi Lake on the west side of East Island, and
3. Roy Martin East Occurrence on the east side of East Island.

A discretionary gold occurrence, known as Mongus Lake West Occurrence, is reported in the vicinity of Peninsula Bay near the west end of the Property and an anomalous nickel occurrence associated with mafic and ultramafic sills of the Kakagi Lake group known as the Mongus Lake Occurrence. See Figure 21.

Geophysics, prospecting, trenching and drilling have been undertaken on the 3 gold occurrences and along the Kakagi Lake Shear by earlier parties. As a result of this work the following historic estimate was reported along this shear:
1. Reserves in a zone (No. 2 Zone) 300 ft (91.4 m) by 24 ft (7.3 m) by 100 ft (30.5 m) = 120,000 tons at 0.25 opt Au (108,862 tonnes at 8.57 g/t Au).
2. At surface: No. 1 Zone is 900 ft (274.3 m) by 17 ft (5.2 m) at 0.2 opt (6.86 g/t) Au.
Source: OMI Number: MDI52F04NW00023 Martin F.M. Au Occurrence.

Note: The above grade and tonnage of <u>The Kakagi Lake Shear</u> are considered historic and the qualified person of this report has been unable to verify the information and that the information is not necessarily indicative of the mineralization on the property that is the subject of the technical report; furthermore a qualified person has not done sufficient work to classify the historical estimate as current mineral resources or mineral reserves; and the issuer is not treating the historical estimate as current mineral resources or mineral reserves.

Big Gold Inc. commissioned an initial prospecting visit to the Property in May 2021 and a field-site visit of the Property in July 2021 by the author. Select grab samples were collected and assayed from both of these prospecting visits. A later assessment report will be submitted on this work.

The helicopter airborne VTEM and magnetometer survey was conducted between October 7th and October 27th, 2021 by Geotech Ltd.

The geophysical 3D inversion of the Geotech data was done by Technoimaging and completed on January 21, 2022.

The author does not recognize any significant risks or uncertainties that would prevent the continued exploration of the Property for gold, base metals, or PGM mineralization.

The author concludes that the work completed to date indicates the Property has potential to host economic concentrations of Archean lode structural gold mineralization, VMS base metals, magmatic Nickel and PGM mineralization.

A 2 phase $350,000 2-year exploration program is proposed consisting of:

Phase 1: Year 1 - $150,000 for localized compilation, prospecting/geological mapping, line-cutting/IP and initial diamond drilling

Phase 2: Year 2 – $200,000 primarily for more diamond drilling with some further prospecting.

There is an extensive volume of data from previous operators of the present claims. The available data needs to be correlated into a clean interactive database providing targets locations to be reviewed in the field and provide direction for the exploration program. Subsequent geological mapping and prospecting can locate and verify known mineral occurrences and evaluate new targets defined by BG.

Ground geophysics such as IP and magnetometer surveys will be undertaken in specific areas to determine the extent and attitude of known and potential new targets to help refine trenching and diamond drilling locations.

Assaying and petrological work will also be undertaken to define the grade, extent and characterization of any mineralization encountered.

Item 2: Introduction

Bedrock Research Corp. of Sudbury, Ontario was contracted by Big Gold Inc. (BG) to review historic data for the Martin Kenty Property (the "Property"), identify its merits, propose an appropriate exploration program and budget for gold exploration on the property, and prepare a Technical Report (the "Report") compliant with NI 43-101 standards for listing on an exchange.

The principal sources of information for this Technical Report are:

- Assessment Files available at the Ontario Ministry of Northern Development, Mines, Natural Resources and Forestry (MNDMNRF) Assessment File Research Image Database (AFRI) retrieved from http://www.geologyontario.mndm.gov.on.ca.

- Mineral deposits information available at the Ontario Mineral Inventory (OMI) Database retrieved from http://www.geologyontario.mndm.gov.on.ca.

- Government maps and reports available at the MNDMNRF Ontario Geological Survey Publications (OGS PUB) Database retrieved from http://www.geologyontario.mndm.gov.on.ca.

- Mining claims information available at the MNDMNRF Mining Lands Administration System (MLAS) databases retrieved from

- http://www.mndm.gov.on.ca/en/mines-and-minerals/applications/mining-lands-administration-system-mlas-map-viewer

- Various corporate information, news releases and Technical Reports from SEDAR.

- A reconnaissance prospecting program of 2 days conducted by C. Johnson and D. McKinnon on May 2021 in which 20 samples were collected. A forthcoming assessment report will discuss this program and results.

- A Site Visit data conducted by the author, Robert G. Komarechka and his assistant C. Johnson on July 11 to July 20, 2021 during a prospecting program. Sites of stripping and sampling were located, photographed, and examined, with 31 samples collected. A forthcoming assessment report will discuss this program and results.

- Airborne Geophysical Preliminary VTEM Data Report completed by Geotech on December 2021 on behalf of BG.

- Airborne Geophysical interpretation of the VTEM Data completed by Technoimaging namely: Final Report Three-dimensional Inversion VTEM Electromagnetic and TMI data Martin Kenty Project Area, Nestor Falls Northwestern Ontario completed on January 24, 2022 on behalf of Big Gold. This assessment report discusses these last 2 items.

2.1 Units & Currency

Units of measure used in this report are in the metric system, unless stated otherwise. Currencies outlined in the report are in Canadian dollars unless otherwise stated.

For locations East longitude and North latitude are given in decimal degree form, as noted. Directions of strike for structural features are given in degrees of the compass and departure from north. Co-ordinates used, unless otherwise stated, are in NAD 83 UTM Zone 15U. Zone 15N is also used, it being a designation for all of Zone 15 north of the equator.

Table 1: List of Acronyms

Acronyms	Term
1VD	First Vertical Derivative
AFRI	Assessment File Report Index, Ontario
Ma	Million years
MDI	Mineral Deposit Inventory of Ontario, now replaced by OMI
MLAS	Mining Lands Acquisition System, Ontario
MNDM	Ministry of Northern Development and Mines, Ontario
MRE	Mineral resource estimate
n/a	Not applicable
N/A	Not available
NAD 83	North American Datum of 1983
nd	Not determined
NI 43-101	National Instrument 43-101
NSR	Net smelter return
NTS	National Topographic System
OGS	Ontario Geological Survey
OMI	Ontario Mineral Inventory (formerly MDI)
QA/QC	Quality assurance/quality control
QP	Qualified person (as defined in National Instrument 43-101)
SD	Standard deviation
SG	Specific gravity
TMI	Total Magnetic Intensity
Twp.	Township
UTM	Universal Transverse Mercator coordinate system
VTEM	Versatile Time Domain Electromagnetic
VMS	Volcanogenic Massive Sulphide
P.Geo.	Professional Geologist (Ontario)
P.Eng.	Professional Engineer (Ontario)
Prof.	Professional
Geol.	Geological

Table 1a: Conversion Factors for Measurements

Imperial Unit	Multiplied by	Metric Unit
1 inch	25.4	mm
1 foot	0.3048	m
1 acre	0.405	ha
1 ounce (troy)	31.1035	g
1 pound (avdp)	0.4535	kg
1 ton (short)	0.9072	t
1 ounce (troy) / ton (short)	34.2857	g/t or 1ppm

Table 1b: List of Units

Symbol	Unit
%	Percent
C$	Canadian dollar
$/t	Dollars per metric ton
°	Angular degree
°C	Degree Celsius
μm	Micron (micrometre)
cm	Centimetre
cm3	Cubic centimetre
ft	Foot (12 inches)
g	Gram
Ga	Billion years
g/cm3	Gram per cubic centimetre
g/t	Gram per metric ton (tonne)
h	Hour (60 minutes)
ha	Hectare
k	Thousand (000)
kg	Kilogram
km	Kilometre
L	Litre
lb	Pound
M	Million
m	Metre
m3	Cubic metre
Mtpa	Million ton per year
Ma	Million years
my	Million years
masl	Metres above mean sea level
mm	Millimetre
Moz	Million (troy) ounces
Mt	Million metric tons
oz	Troy ounce
oz/t	Ounce (troy) per short ton (2,000 lbs)
opt	Ounce (troy) per short ton (2,000 lbs)
ppb	Parts per billion
ppm	Parts per million (1 gm/tonne)
t	Metric tonne (1,000 kg)
ton	Short ton (2,000 lbs)
tr	trace

Table 1b: List of Units (cont'd)

US$	American dollar
wt%	Weight percent
y	Year (365 days)
yd3	Cubic yard
Au	Gold
Ag	Silver
Cu	Copper
Pb	Lead
Zn	Zinc
PGM	Platinum Group Metals

Item 3: Reliance on Other Experts

For the purposes of this report the author has relied on land ownership information provided by BG as well as claim information, geological, geophysical, structural and assessment data taken from the web site of the Ontario Ministry of Northern Development, Mines, Natural Resources and Forestry (MNDMNRF).
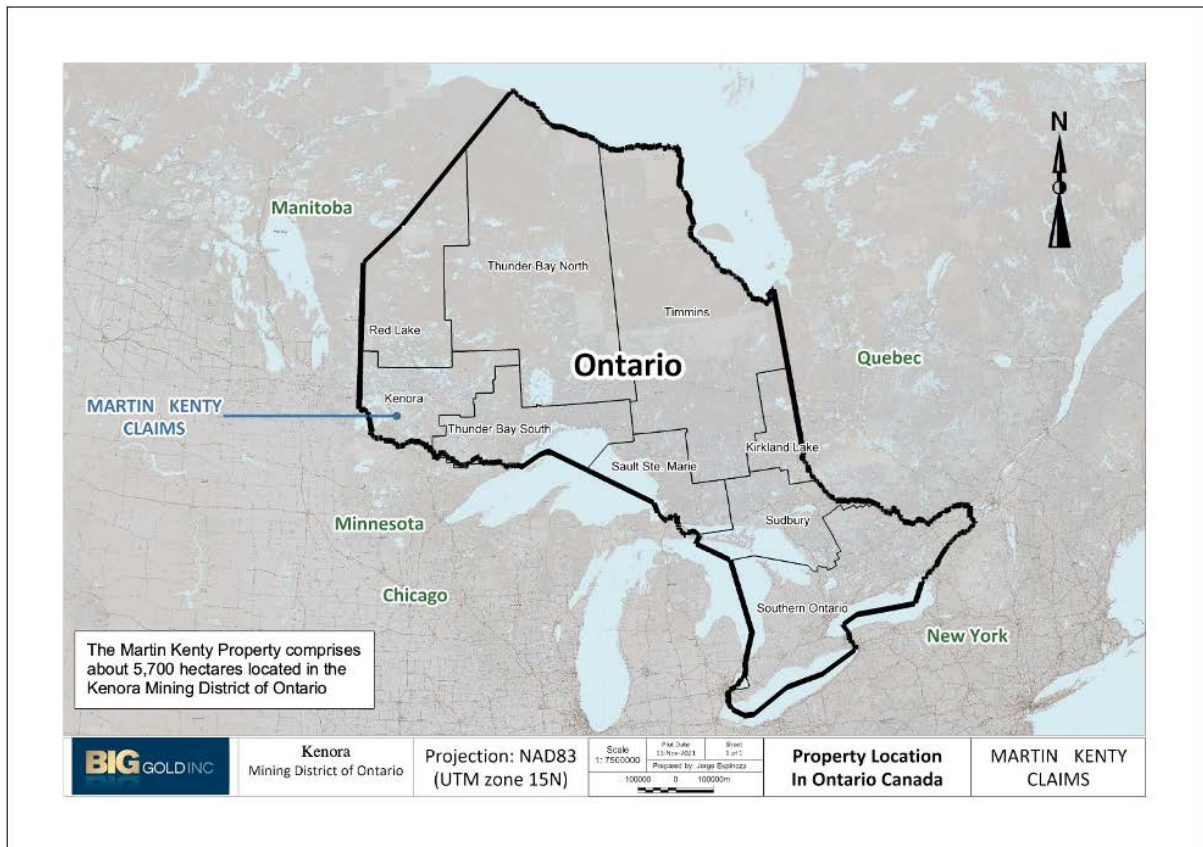

Figure 1: Martin Kenty Property Location - Source: Jorge Espinoza, Big Gold Inc. corporate files.
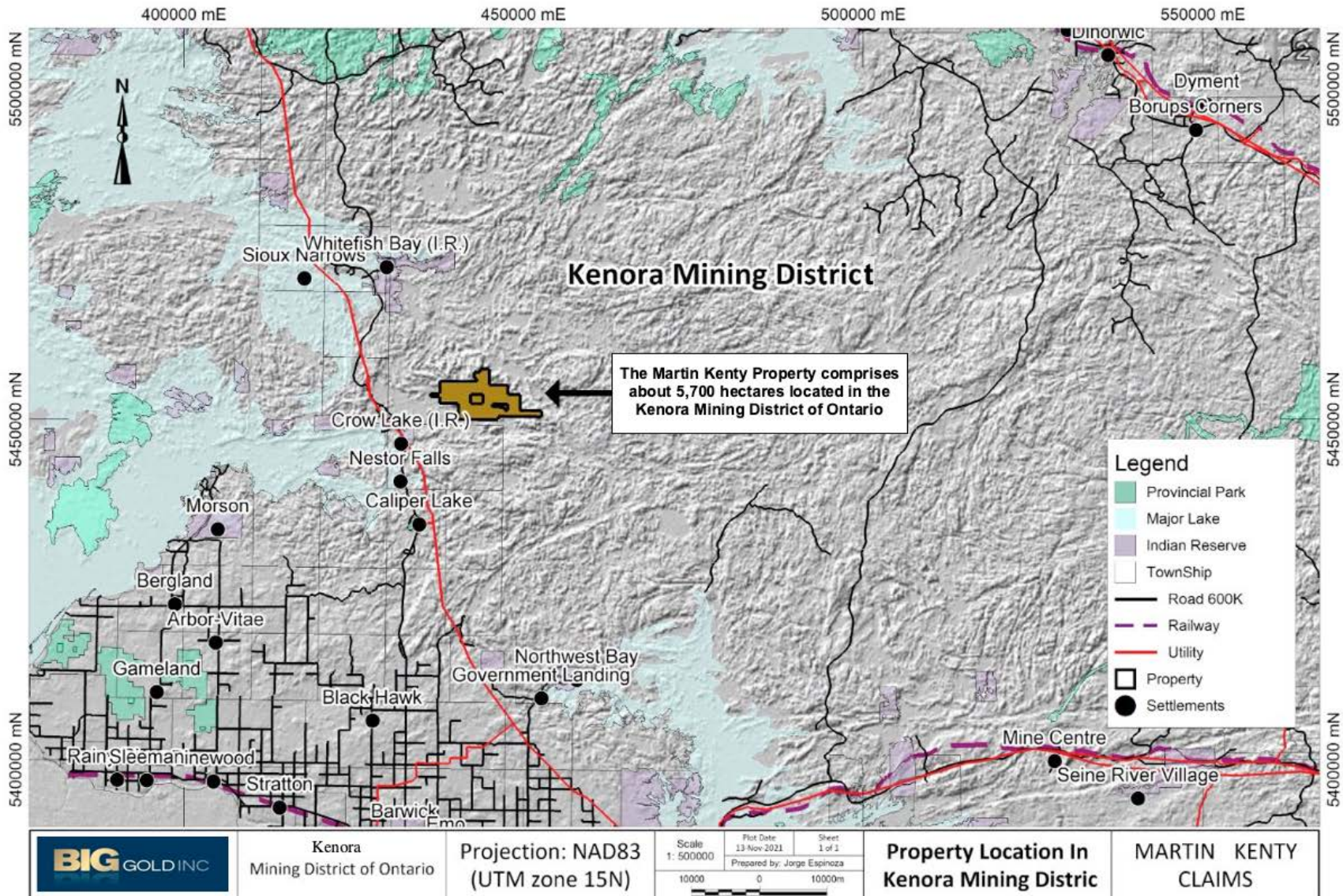
Figure 2: Property Location with nearby infrastructure - *Source: Jorge Espinoza, Big Gold Inc. corporate files.*

Item 4: Property Description and Location

The Martin Kenty Property is located in Heronry Lake, Dogpaw Lake, and Brooks Lake Areas within the Kenora Mining Division of Ontario located approximately a 104 km drive SE of the Town of Kenora (see Figure 1 and Figure 2) or a 105 km drive southeast on Hwy 7 to Fort Francis. The center of the Property is located at approximately 49.2316° North Latitude and 93.7674° West Longitude or in NAD 83 UTM co-ordinates, Zone 15U, 710500mE and 534100mN The Property is comprised of 264 unpatented single unit mineral claims (the Claims) with a total approximate area of 5,742 hectares and further described in Table 1. The Property was acquired by way of an Asset Purchase Agreement dated July 19, 2021, from the Vendor, 2060014 Ontario Inc. a corporation incorporated under the laws of the province of Ontario. The owner of the Claims, currently shown on the Ontario government's Mineral Land Acquisition System (MLAS) records is Steven Anderson, acting as agent both for the Vendor, 2060014 Ontario Inc. and the purchaser Big Gold Inc. These Claims were sold to BG in return for 4,000,000 common shares of BG with the Vendor retaining a 2% net smelter return royalty (NSR) on the Property. See Appendix 1 for the Agreement on this.

There were no carry-forward of any royalties or encumbrances on the Martin Kenty Property. The Martin Kenty Claims are shown in Table 2 and Figure 3. A copy of the Exchange Agreement with the claim list attached can be found in Appendix 1.

The 5 known mineralized zones as recorded in the OMI files as occurring on the Martin Kenty Property include: the Martin F.M. Occurrence (Au), the Kakagi Lake Occurrence (Au, Ag), the Roy Martin East Occurrence (Au), the Mongus Lake Occurrence (Au) and the Mongus Lake North Occurrence (Ni).

Figure 21 shows these occurrences relative to the Martin Kenty Property. Figure 14 shows the location of the 3 gold occurrences along the Kakagi Lake Shear, while Item 7.2 gives a description of each. To the extent known, there are no environmental liabilities to which the Property is subject.

The Ontario Mining Act requires an Exploration Permit or Plans for exploration on Crown Lands. The permit and plans are obtained from the MNDM. The processing periods are 50 days for a permit and 30 days for a plan while the documents are reviewed by MNDMNRF and presented to the Aboriginal communities whose traditional lands will be impacted by the work. The author has been informed by BG that the permits required to carry out the proposed work on the Property have been applied for. The issuance of these permits will allow the proposed work to be undertaken.

The government of Ontario requires expenditures of $400 per year per unit for mining claims, prior to expiry, to keep the claims in good standing for the following year. The report must be submitted by the expiry date of the claims to retain them.

Table 2: Martin Kenty Property Claims

No.	Claim No.	Cell No.	Township/Area	Issue Date	Due Date	Work Required	Unit Size
1	643649		Brooks Lake Area	2021-03-17	2023-03-17	$400	1
2	643648		Brooks Lake Area	2021-03-17	2023-03-17	$400	1
3	643647		Brooks Lake Area	2021-03-17	2023-03-17	$400	1
4	643646		Brooks Lake Area	2021-03-17	2023-03-17	$400	1
5	643645		Brooks Lake Area	2021-03-17	2023-03-17	$400	1
6	643644		Brooks Lake Area	2021-03-17	2023-03-17	$400	1
7	643643		Brooks Lake Area	2021-03-17	2023-03-17	$400	1
8	643642		Brooks Lake Area	2021-03-17	2023-03-17	$400	1
9	643641		Brooks Lake Area	2021-03-17	2023-03-17	$400	1
10	643640		Brooks Lake Area	2021-03-17	2023-03-17	$400	1
11	643639		Brooks Lake Area	2021-03-17	2023-03-17	$400	1
12	643638		Brooks Lake Area	2021-03-17	2023-03-17	$400	1
13	643637		Brooks Lake Area	2021-03-17	2023-03-17	$400	1
14	643636		Brooks Lake Area	2021-03-17	2023-03-17	$400	1
15	643635		Heronry Lake Area	2021-03-17	2023-03-17	$400	1
16	643634		Heronry Lake Area	2021-03-17	2023-03-17	$400	1
17	643633		Heronry Lake Area	2021-03-17	2023-03-17	$400	1
18	643632		Heronry Lake Area	2021-03-17	2023-03-17	$400	1
19	643631		Heronry Lake Area	2021-03-17	2023-03-17	$400	1
20	643630		Heronry Lake Area	2021-03-17	2023-03-17	$400	1
21	643629		Heronry Lake Area	2021-03-17	2023-03-17	$400	1
22	643628		Heronry Lake Area	2021-03-17	2023-03-17	$400	1
23	643627		Heronry Lake Area	2021-03-17	2023-03-17	$400	1
24	643626		Heronry Lake Area	2021-03-17	2023-03-17	$400	1
25	643625		Heronry Lake Area	2021-03-17	2023-03-17	$400	1
26	643624		Heronry Lake Area	2021-03-17	2023-03-17	$400	1
27	643623		Heronry Lake Area	2021-03-17	2023-03-17	$400	1
28	643622		Heronry Lake Area	2021-03-17	2023-03-17	$400	1
29	643621		Heronry Lake Area	2021-03-17	2023-03-17	$400	1
30	630973	52F04K240	Heronry Lake Area	2021-01-15	2023-01-15	$400	1
31	630972	52F04K238	Heronry Lake Area	2021-01-15	2023-01-15	$400	1
32	630971	52F04J209	Brooks Lake Area	2021-01-15	2023-01-15	$400	1
33	630970	52F04K192	Heronry Lake Area	2021-01-15	2023-01-15	$400	1
34	630969	52F04K212	Heronry Lake Area	2021-01-15	2023-01-15	$400	1
35	630968	52F04K231	Heronry Lake Area	2021-01-15	2023-01-15	$400	1
36	630967	52F04J208	Brooks Lake Area	2021-01-15	2023-01-15	$400	1
37	630966	52F04J222	Brooks Lake Area	2021-01-15	2023-01-15	$400	1
38	630965	52F04K220	Heronry Lake Area	2021-01-15	2023-01-15	$400	1
39	630964	52F04K239	Heronry Lake Area	2021-01-15	2023-01-15	$400	1

Table 2: Martin Kenty Property Claims (continued)

No.	Claim No.	Cell No.	Township/Area	Issue Date	Due Date	Work Required	Unit Size
40	630963	52F04K235	Heronry Lake Area	2021-01-15	2023-01-15	$400	1
41	630962	52F04J201	Brooks Lake Area	2021-01-15	2023-01-15	$400	1
42	630961	52F04J207	Brooks Lake Area	2021-01-15	2023-01-15	$400	1
43	630960	52F04J206	Brooks Lake Area	2021-01-15	2023-01-15	$400	1
44	630959	52F04J205	Brooks Lake Area	2021-01-15	2023-01-15	$400	1
45	630958	52F04K232	Heronry Lake Area	2021-01-15	2023-01-15	$400	1
46	630957	52F04K210	Heronry Lake Area	2021-01-15	2023-01-15	$400	1
47	630956	52F04K230	Heronry Lake Area	2021-01-15	2023-01-15	$400	1
48	630955	52F04J202	Brooks Lake Area	2021-01-15	2023-01-15	$400	1
49	630954	52F04J221	Brooks Lake Area	2021-01-15	2023-01-15	$400	1
50	630953	52F04K237	Heronry Lake Area	2021-01-15	2023-01-15	$400	1
51	630952	52F04K234	Heronry Lake Area	2021-01-15	2023-01-15	$400	1
52	630951	52F04K233	Heronry Lake Area	2021-01-15	2023-01-15	$400	1
53	630950	52F04K211	Heronry Lake Area	2021-01-15	2023-01-15	$400	1
54	630949	52F04K190	Heronry Lake Area	2021-01-15	2023-01-15	$400	1
55	630948	52F04J204	Brooks Lake Area	2021-01-15	2023-01-15	$400	1
56	630947	52F04J203	Brooks Lake Area	2021-01-15	2023-01-15	$400	1
57	630946	52F04K236	Heronry Lake Area	2021-01-15	2023-01-15	$400	1
58	630945	52F04K191	Heronry Lake Area	2021-01-15	2023-01-15	$400	1
59	630119		Heronry Lake Area	2021-01-11	2023-01-11	$400	1
60	630118		Heronry Lake Area	2021-01-11	2023-01-11	$400	1
61	630117		Heronry Lake Area	2021-01-11	2023-01-11	$400	1
62	630116		Heronry Lake Area	2021-01-11	2023-01-11	$400	1
63	630115		Heronry Lake Area	2021-01-11	2023-01-11	$400	1
64	630114		Heronry Lake Area	2021-01-11	2023-01-11	$400	1
65	630113		Heronry Lake Area	2021-01-11	2023-01-11	$400	1
66	630112		Heronry Lake Area	2021-01-11	2023-01-11	$400	1
67	630111		Heronry Lake Area	2021-01-11	2023-01-11	$400	1
68	630110		Heronry Lake Area	2021-01-11	2023-01-11	$400	1
69	630109		Heronry Lake Area	2021-01-11	2023-01-11	$400	1
70	630108		Heronry Lake Area	2021-01-11	2023-01-11	$400	1
71	630107		Heronry Lake Area	2021-01-11	2023-01-11	$400	1
72	630106		Heronry Lake Area	2021-01-11	2023-01-11	$400	1
73	630105		Heronry Lake Area	2021-01-11	2023-01-11	$400	1
74	630104		Heronry Lake Area	2021-01-11	2023-01-11	$400	1
75	630103		Brooks Lake Area	2021-01-11	2023-01-11	$400	1
76	630102		Brooks Lake Area	2021-01-11	2023-01-11	$400	1
77	630101		Brooks Lake Area	2021-01-11	2023-01-11	$400	1
78	630100		Brooks Lake Area	2021-01-11	2023-01-11	$400	1

Table 2: Martin Kenty Property Claims (continued)

No.	Claim No.	Cell No.	Township/Area	Issue Date	Due Date	Work Required	Unit Size
79	630099	52F04J082	Brooks Lake Area	2021-01-11	2023-01-11	$400	1
80	630098		Brooks Lake Area	2021-01-11	2023-01-11	$400	1
81	630097	52F04J101	Brooks Lake Area	2021-01-11	2023-01-11	$400	1
82	630096	52F04J102	Brooks Lake Area	2021-01-11	2023-01-11	$400	1
83	630095	52F04J081	Brooks Lake Area	2021-01-11	2023-01-11	$400	1
84	630094		Brooks Lake Area	2021-01-11	2023-01-11	$400	1
85	630093		Brooks Lake Area	2021-01-11	2023-01-11	$400	1
86	630092	52F04K119	Heronry Lake Area	2021-01-11	2023-01-11	$400	1
87	630091		Brooks Lake Area	2021-01-11	2023-01-11	$400	1
88	630090		Brooks Lake Area	2021-01-11	2023-01-11	$400	1
89	630089	52F04K120	Heronry Lake Area	2021-01-11	2023-01-11	$400	1
90	630088		Brooks Lake Area	2021-01-11	2023-01-11	$400	1
91	630087		Brooks Lake Area	2021-01-11	2023-01-11	$400	1
92	630086	52F04K118	Heronry Lake Area	2021-01-11	2023-01-11	$400	1
93	630085		Heronry Lake Area	2021-01-11	2023-01-11	$400	1
94	630084		Heronry Lake Area	2021-01-11	2023-01-11	$400	1
95	630083		Heronry Lake Area	2021-01-11	2023-01-11	$400	1
96	630082	52F04K100	Heronry Lake Area	2021-01-11	2023-01-11	$400	1
97	630081	52F04K099	Heronry Lake Area	2021-01-11	2023-01-11	$400	1
98	630080		Heronry Lake Area	2021-01-11	2023-01-11	$400	1
99	630079		Heronry Lake Area	2021-01-11	2023-01-11	$400	1
100	630078	52F04K093	Heronry Lake Area	2021-01-11	2023-01-11	$400	1
101	630077		Brooks Lake Area	2021-01-11	2023-01-11	$400	1
102	630076		Heronry Lake Area	2021-01-11	2023-01-11	$400	1
103	630075		Heronry Lake Area	2021-01-11	2023-01-11	$400	1
104	630074		Heronry Lake Area	2021-01-11	2023-01-11	$400	1
105	630073		Heronry Lake Area	2021-01-11	2023-01-11	$400	1
106	630072		Heronry Lake Area	2021-01-11	2023-01-11	$400	1
107	630071		Heronry Lake Area	2021-01-11	2023-01-11	$400	1
108	630070		Heronry Lake Area	2021-01-11	2023-01-11	$400	1
109	630069		Heronry Lake Area	2021-01-11	2023-01-11	$400	1
110	630068		Heronry Lake Area	2021-01-11	2023-01-11	$400	1
111	630067		Heronry Lake Area	2021-01-11	2023-01-11	$400	1
112	630066		Heronry Lake Area	2021-01-11	2023-01-11	$400	1
113	630065		Heronry Lake Area	2021-01-11	2023-01-11	$400	1
114	630064		Heronry Lake Area	2021-01-11	2023-01-11	$400	1
115	630063		Heronry Lake Area	2021-01-11	2023-01-11	$400	1
116	630062	52F04J192	Heronry Lake Area	2021-01-11	2023-01-11	$400	1
117	630061		Heronry Lake Area	2021-01-11	2023-01-11	$400	1
118	630060		Heronry Lake Area	2021-01-11	2023-01-11	$400	1

Table 2: Martin Kenty Property Claims (continued)

No.	Claim No.	Cell No.	Township/Area	Issue Date	Due Date	Work Required	Unit Size
119	630059		Heronry Lake Area	2021-01-11	2023-01-11	$400	1
120	630058		Heronry Lake Area	2021-01-11	2023-01-11	$400	1
121	630057		Heronry Lake Area	2021-01-11	2023-01-11	$400	1
122	630056	52F04K098	Heronry Lake Area	2021-01-11	2023-01-11	$400	1
123	630055		Heronry Lake Area	2021-01-11	2023-01-11	$400	1
124	630054		Heronry Lake Area	2021-01-11	2023-01-11	$400	1
125	630053		Heronry Lake Area	2021-01-11	2023-01-11	$400	1
126	630052		Heronry Lake Area	2021-01-11	2023-01-11	$400	1
127	630051		Heronry Lake Area	2021-01-11	2023-01-11	$400	1
128	630050		Heronry Lake Area	2021-01-11	2023-01-11	$400	1
129	630049		Brooks Lake Area	2021-01-11	2023-01-11	$400	1
130	630048		Heronry Lake Area	2021-01-11	2023-01-11	$400	1
131	630047		Heronry Lake Area	2021-01-11	2023-01-11	$400	1
132	630046		Heronry Lake Area	2021-01-11	2023-01-11	$400	1
133	630045		Heronry Lake Area	2021-01-11	2023-01-11	$400	1
134	630044		Heronry Lake Area	2021-01-11	2023-01-11	$400	1
135	630043		Heronry Lake Area	2021-01-11	2023-01-11	$400	1
136	630042		Heronry Lake Area	2021-01-11	2023-01-11	$400	1
137	630041		Heronry Lake Area	2021-01-11	2023-01-11	$400	1
138	630040		Heronry Lake Area	2021-01-11	2023-01-11	$400	1
139	630039		Dogpaw Lake	2021-01-11	2023-01-11	$400	1
140	630038		Dogpaw Lake	2021-01-11	2023-01-11	$400	1
141	630037		Dogpaw Lake	2021-01-11	2023-01-11	$400	1
142	630036		Dogpaw Lake	2021-01-11	2023-01-11	$400	1
143	630035		Dogpaw Lake	2021-01-11	2023-01-11	$400	1
144	630034		Dogpaw Lake	2021-01-11	2023-01-11	$400	1
145	630033		Dogpaw Lake	2021-01-11	2023-01-11	$400	1
146	630032		Dogpaw Lake	2021-01-11	2023-01-11	$400	1
147	630031		Dogpaw Lake	2021-01-11	2023-01-11	$400	1
148	630030		Dogpaw Lake	2021-01-11	2023-01-11	$400	1
149	630029		Dogpaw Lake	2021-01-11	2023-01-11	$400	1
150	630028		Dogpaw Lake	2021-01-11	2023-01-11	$400	1
151	630027		Dogpaw Lake	2021-01-11	2023-01-11	$400	1
152	630026		Dogpaw Lake	2021-01-11	2023-01-11	$400	1
153	630025		Dogpaw Lake	2021-01-11	2023-01-11	$400	1
154	630024		Dogpaw Lake	2021-01-11	2023-01-11	$400	1
155	620676	52F04K038	Brooks Lake Area	2020-11-26	2022-11-26	$400	1
156	620675	52F04K017	Brooks Lake Area	2020-11-26	2022-11-26	$400	1
157	620674	52F04K036	Brooks Lake Area	2020-11-26	2022-11-26	$400	1

Table 2: Martin Kenty Property Claims (continued)

No.	Claim No.	Cell No.	Township/Area	Issue Date	Due Date	Work Required	Unit Size
158	620673	52F04K075	Brooks Lake Area	2020-11-26	2022-11-26	$400	1
159	620672	52F04J129	Brooks Lake Area	2020-11-26	2022-11-26	$400	1
160	620671	52F04J108	Brooks Lake Area	2020-11-26	2022-11-26	$400	1
161	620670	52F04J106	Brooks Lake Area	2020-11-26	2022-11-26	$400	1
162	620669	52F04J126	Brooks Lake Area	2020-11-26	2022-11-26	$400	1
163	620668	52F04J109	Brooks Lake Area	2020-11-26	2022-11-26	$400	1
164	620667	52F04J086	Brooks Lake Area	2020-11-26	2022-11-26	$400	1
165	620666	52F04J064	Brooks Lake Area	2020-11-26	2022-11-26	$400	1
166	620665	52F04J123	Brooks Lake Area	2020-11-26	2022-11-26	$400	1
167	620664	52F04J128	Brooks Lake Area	2020-11-26	2022-11-26	$400	1
168	620663	52F04J085	Brooks Lake Area	2020-11-26	2022-11-26	$400	1
169	620662	52F04J104	Brooks Lake Area	2020-11-26	2022-11-26	$400	1
170	620661	52F04J088	Brooks Lake Area	2020-11-26	2022-11-26	$400	1
171	620660	52F04J084	Brooks Lake Area	2020-11-26	2022-11-26	$400	1
172	620659	52F04J124	Brooks Lake Area	2020-11-26	2022-11-26	$400	1
173	620658	52F04J083	Brooks Lake Area	2020-11-26	2022-11-26	$400	1
174	620657	52F04J105	Brooks Lake Area	2020-11-26	2022-11-26	$400	1
175	620656	52F04J103	Brooks Lake Area	2020-11-26	2022-11-26	$400	1
176	620655	52F04J087	Brooks Lake Area	2020-11-26	2022-11-26	$400	1
177	620654		Brooks Lake Area	2020-11-26	2022-11-26	$400	1
178	620349	52F04K112	Heronry Lake Area	2020-11-23	2022-11-23	$400	1
179	620348	52F04K111	Heronry Lake Area	2020-11-23	2022-11-23	$400	1
180	620347	52F04K151	Heronry Lake Area	2020-11-23	2022-11-23	$400	1
181	620346	52F04K110	Heronry Lake Area	2020-11-23	2022-11-23	$400	1
182	620345	52F04K156	Heronry Lake Area	2020-11-23	2022-11-23	$400	1
183	620344	52F04K155	Heronry Lake Area	2020-11-23	2022-11-23	$400	1
184	620343	52F04K152	Heronry Lake Area	2020-11-23	2022-11-23	$400	1
185	620342	52F04K132	Heronry Lake Area	2020-11-23	2022-11-23	$400	1
186	620341		Heronry Lake Area	2020-11-23	2022-11-23	$400	1
187	620340	52F04K113	Heronry Lake Area	2020-11-23	2022-11-23	$400	1
188	620339	52F04K133	Heronry Lake Area	2020-11-23	2022-11-23	$400	1
189	620338	52F04K173	Heronry Lake Area	2020-11-23	2022-11-23	$400	1
190	620337	52F04K171	Heronry Lake Area	2020-11-23	2022-11-23	$400	1
191	620336	52F04K130	Heronry Lake Area	2020-11-23	2022-11-23	$400	1
192	620335		Heronry Lake Area	2020-11-23	2022-11-23	$400	1
193	620334		Heronry Lake Area	2020-11-23	2022-11-23	$400	1
194	620333		Heronry Lake Area	2020-11-23	2022-11-23	$400	1
195	620332		Heronry Lake Area	2020-11-23	2022-11-23	$400	1
196	620331	52F04K154	Heronry Lake Area	2020-11-23	2022-11-23	$400	1

Table 2: Martin Kenty Property Claims (continued)

No.	Claim No.	Cell No.	Township/Area	Issue Date	Due Date	Work Required	Unit Size
197	620330	52F04K174	Heronry Lake Area	2020-11-23	2022-11-23	$400	1
198	620329	52F04K091	Heronry Lake Area	2020-11-23	2022-11-23	$400	1
199	620328	52F04K131	Heronry Lake Area	2020-11-23	2022-11-23	$400	1
200	620327	52F04K150	Heronry Lake Area	2020-11-23	2022-11-23	$400	1
201	620326	52F04K170	Heronry Lake Area	2020-11-23	2022-11-23	$400	1
202	620325	52F04K153	Heronry Lake Area	2020-11-23	2022-11-23	$400	1
203	620324	52F04K172	Heronry Lake Area	2020-11-23	2022-11-23	$400	1
204	620323	52F04K090	Heronry Lake Area	2020-11-23	2022-11-23	$400	1
205	620322	52F04K128	Heronry Lake Area	2020-11-23	2022-11-23	$400	1
206	620321	52F04K140	Heronry Lake Area	2020-11-23	2022-11-23	$400	1
207	620320	52F04K160	Heronry Lake Area	2020-11-23	2022-11-23	$400	1
208	620319	52F04K215	Heronry Lake Area	2020-11-23	2022-11-23	$400	1
209	620318	52F04K157	Heronry Lake Area	2020-11-23	2022-11-23	$400	1
210	620317	52F04K176	Heronry Lake Area	2020-11-23	2022-11-23	$400	1
211	620316	52F04K216	Heronry Lake Area	2020-11-23	2022-11-23	$400	1
212	620315	52F04K159	Heronry Lake Area	2020-11-23	2022-11-23	$400	1
213	620314	52F04K214	Heronry Lake Area	2020-11-23	2022-11-23	$400	1
214	620313	52F04J122	Brooks Lake Area	2020-11-23	2022-11-23	$400	1
215	620312	52F04K175	Heronry Lake Area	2020-11-23	2022-11-23	$400	1
216	620311	52F04K194	Heronry Lake Area	2020-11-23	2022-11-23	$400	1
217	620310	52F04K193	Heronry Lake Area	2020-11-23	2022-11-23	$400	1
218	620309	52F04K138	Heronry Lake Area	2020-11-23	2022-11-23	$400	1
219	620308	52F04K217	Heronry Lake Area	2020-11-23	2022-11-23	$400	1
220	620307	52F04K196	Heronry Lake Area	2020-11-23	2022-11-23	$400	1
221	620306	52F04J121	Heronry and Brooks Lake Area	2020-11-23	2022-11-23	$400	1
222	620305	52F04K139	Heronry Lake Area	2020-11-23	2022-11-23	$400	1
223	620304	52F04K177	Heronry Lake Area	2020-11-23	2022-11-23	$400	1
224	620303	52F04K158	Heronry Lake Area	2020-11-23	2022-11-23	$400	1
225	620302	52F04K195	Heronry Lake Area	2020-11-23	2022-11-23	$400	1
226	620301	52F04K213	Heronry Lake Area	2020-11-23	2022-11-23	$400	1
227	620300	52F04J149	Brooks Lake Area	2020-11-23	2022-11-23	$400	1
228	620299	52F04J148	Brooks Lake Area	2020-11-23	2022-11-23	$400	1
229	620298	52F04J188	Brooks Lake Area	2020-11-23	2022-11-23	$400	1
230	620297	52F04J147	Brooks Lake Area	2020-11-23	2022-11-23	$400	1
231	620296	52F04J189	Brooks Lake Area	2020-11-23	2022-11-23	$400	1
232	620295	52F04J186	Brooks Lake Area	2020-11-23	2022-11-23	$400	1
233	620294	52F04J169	Brooks Lake Area	2020-11-23	2022-11-23	$400	1
234	620293	52F04J168	Brooks Lake Area	2020-11-23	2022-11-23	$400	1
235	620292	52F04J166	Brooks Lake Area	2020-11-23	2022-11-23	$400	1

Table 2: Martin Kenty Property Claims (continued)

No.	Claim No.	Cell No.	Township/Area	Issue Date	Due Date	Work Required	Unit Size
236	620291	52F04J187	Brooks Lake Area	2020-11-23	2022-11-23	$400	1
237	620290	52F04J167	Brooks Lake Area	2020-11-23	2022-11-23	$400	1
238	620289	52F04J146	Brooks Lake Area	2020-11-23	2022-11-23	$400	1
239	620288	52F04J185	Brooks Lake Area	2020-11-23	2022-11-23	$400	1
240	620287		Heronry Lake Area	2020-11-23	2022-11-23	$400	1
241	620286		Heronry Lake Area	2020-11-23	2022-11-23	$400	1
242	620285		Dogpaw and Heronry Lake Area	2020-11-23	2022-11-23	$400	1
243	620284		Heronry Lake Area	2020-11-23	2022-11-23	$400	1
244	620283		Heronry Lake Area	2020-11-23	2022-11-23	$400	1
245	620282		Heronry Lake Area	2020-11-23	2022-11-23	$400	1
246	620281		Dogpaw and Heronry Lake Area	2020-11-23	2022-11-23	$400	1
247	620280		Heronry Lake Area	2020-11-23	2022-11-23	$400	1
248	620279		Dogpaw and Heronry Lake Area	2020-11-23	2022-11-23	$400	1
249	620278		Heronry Lake Area	2020-11-23	2022-11-23	$400	1
250	620277		Heronry Lake Area	2020-11-23	2022-11-23	$400	1
251	565474	52F04J184	Brooks Lake Area	2019-12-02	2022-04-02	$800	1
252	565473	52F04J183	Brooks Lake Area	2019-12-02	2022-04-02	$800	1
253	565472	52F04J182	Brooks Lake Area	2019-12-02	2022-04-02	$800	1
254	565471	52F04J181	Brooks and Heronry Lake Area	2019-12-02	2022-04-02	$800	1
255	565470	52F04J164	Brooks Lake Area	2019-12-02	2022-04-02	$800	1
256	565469	52F04J163	Brooks Lake Area	2019-12-02	2022-04-02	$800	1
257	565468	52F04J162	Brooks Lake Area	2019-12-02	2022-04-02	$800	1
258	565467	52F04J161	Brooks and Heronry Lake Areas	2019-12-02	2022-04-02	$800	1
259	565466	52F04K200	Brooks and Heronry Lake Areas	2019-12-02	2022-04-02	$800	1
260	565465	52F04K199	Heronry Lake Area	2019-12-02	2022-04-02	$800	1
261	565464	52F04K198	Heronry Lake Area	2019-12-02	2022-04-02	$800	1
262	565463	52F04K180	Brooks and Heronry Lake Areas	2019-12-02	2022-04-02	$800	1
263	565462	52F04K179	Heronry Lake Area	2019-12-02	2022-04-02	$800	1
264	565461	52F04K178	Heronry Lake Area	2019-12-02	2022-04-02	$800	1
265	539388		Heronry Lake Area	2019-01-16	2022-01-16	$800	1
Note: Claim 539388 was not included in the earlier NI43-101 Report.							
	Total					$112,000	265 units
		In this area of Ontario unit cells range from 21.037 ha to 21.073 ha. So, the above 264 units would be an area of approximately 5,579 ha.					
		The claims in italics have been given an extension to allow application of a VTEM survey (now completed) so an additional $400.00/claim assessment is required for these claims this year.					
		The green highlighted claims cover the area of the geophysical survey and the interpretstion report as well as the area of applied work.					
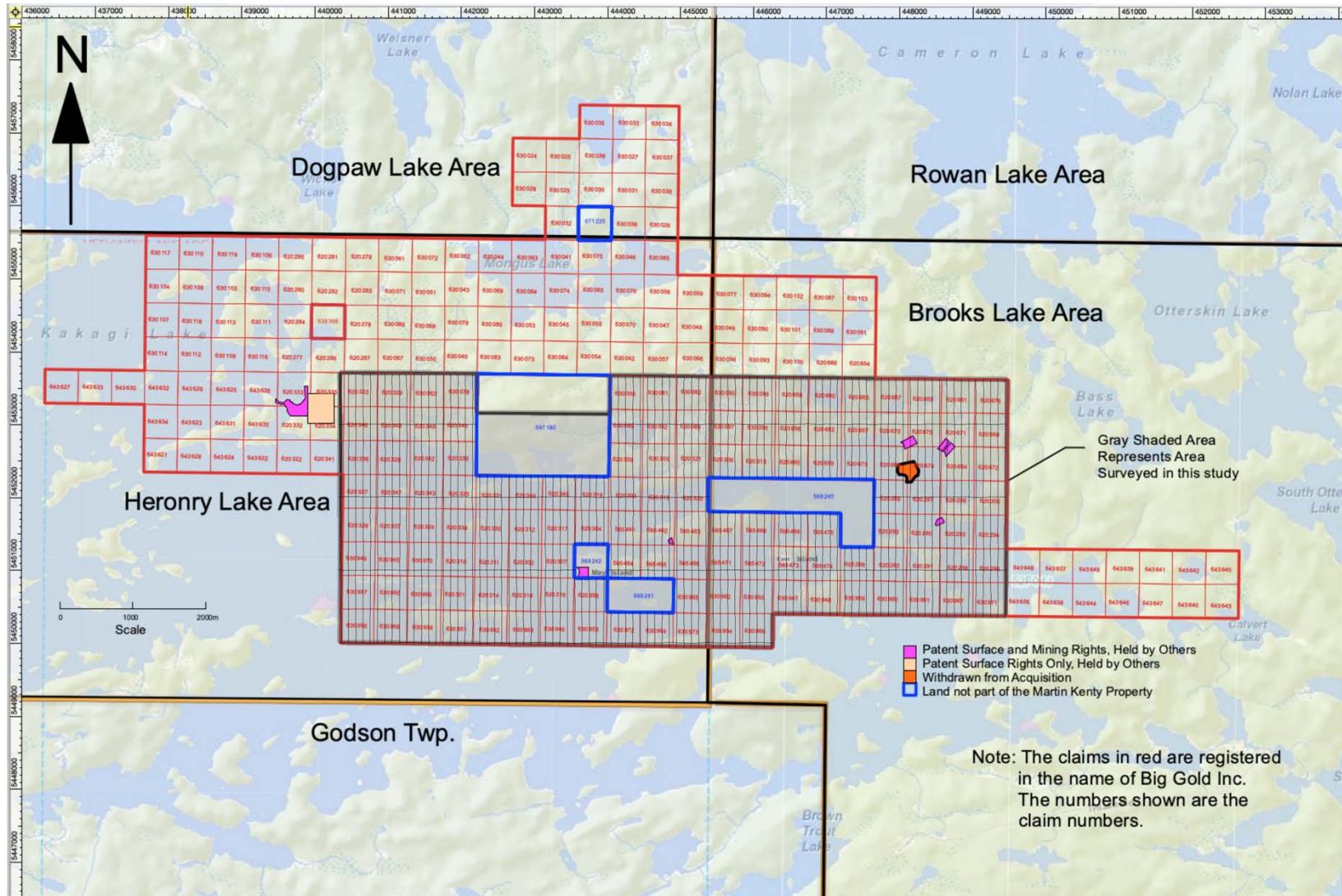
Figure 3. Martin Kenty Property Claims *(outlined in red) showing the gray shaded area of the Geotech VTEM survey with the fight lines shown over the property. – Kenora Mining Division, Ontario - information from MLAS NAD 83 Zone 15U.*

Figure 3a. Martin Kenty Property Claims and Cell numbers over which the survey was flown and assessment applied (area filled in red) – *Kenora Mining Division, Ontario - information from MLAS NAD 83 Zone 15. See gray shaded area in Figure 3 for the location and scale information.*

Item 5: Accessibility, Climate, Local Resources, Infrastructure and Physiography

The property is located in the Mining District of Kenora about halfway between the communities of Kenora and Fort Francis.

Access to the Property is by boat on Kakagi Lake or trails along the northeast and east of the property from Cameron Road. Numerous private tourist lodges with boat launches are located along the west side of Kakagi Lake. Road access to the lodges is by the paved Highway 71 which skirts the west side of Kakagi Lake. Kakagi and other lakes in the area offer additional access. In winter these frozen lakes and trails offer additional access to the Property. Nestor Falls air base offers a functional landing strip and float equipped aircraft operate from Kakabitchiwan Lake. Figures 1, 2 and 3 show the area of the Property.

The temperature in the area varies from -44°C in winter to +36° in the summer. Freeze-up begins in late November and break-up occurs in mid to late April. Various types of exploration work can be undertaken year-round. Average temperature for Kenora is shown in Figure 4 below. Extreme temperatures are also shown on this figure for possible field operational safety considerations (ie: propane can freeze at -40° and summer heat can reduce work efficiency). Some variation for this site is possible as Figure 4 is based on Kenora which is located 104 km northwest of the site.

Vegetation consists of white and red pine and spruce on the higher ground with spruce birch and poplar in the lower areas with some local areas of tag alders, cedar and tamarack.

The maximum relief on the Property is roughly 420m above sea level in the area northeast of Mongus Lake and the lowest elevation along the lakeshore of Kakagi Lake is 340m above sea level. The topography is hummocky to moderately rugged with generally low rounded outcrop ridges separated by glacial debris and interconnected lakes. Locally prominent cliff faces in excess of 30 metres are associated with fault structures. The watershed flows west into Lake of the Woods and the Winnipeg River system, ultimately draining into Hudson Bay via the Nelson River.

Tourism, forestry, and mining are the main industries in the area. The Town of Kenora is 104 road-kilometers to the northwest with a population of 15,096 (Statistics Canada, 2016), while Fort Francis located has a population of 7,739 and is located 105 road-kilometres to the southwest. The Kenora-Fort Francis area has a long mining history, and several mines and exploration projects are presently active. Mining personnel, equipment, and supplies are readily available in Ontario within numerous communities including Thunder Bay, Timmins, Kirkland Lake, and Sudbury. There is sufficient water and land within the Property boundaries to carry out exploration programs and develop and operate a mine and milling complex.

Electricity to supply a mining operation is available from high voltage power lines along highway 71, about 7 km to the west of the Property.

Temperature:	Jan	Feb	Mar	Apr	May	Jun	Jul	Aug	Sep	Oct	Nov	Dec	Year	Code
Daily Average (°C)	-17.3	-12.9	-5.6	3.6	11.8	16.7	19.5	18.2	11.9	5.1	-4.9	-14.1	2.7	A
Standard Deviation	3.7	3.8	2.8	2.5	2.3	1.8	1.5	1.8	1.6	1.6	2.9	3.8	1.1	A
Daily Maximum (°C)	-12.6	-7.9	-0.5	9	17.4	21.8	24.4	23.1	16.4	8.9	-1.5	-9.9	7.4	A
Daily Minimum (°C)	-22	-17.8	-10.6	-1.8	6.2	11.6	14.5	13.3	7.4	1.3	-8.2	-18.3	-2	A
Extreme Maximum (°C)	8.3	8.8	23.3	30.6	35.4	35.6	**35.8**	35	34.6	26.7	19.4	9.4		
Date (yyyy/dd)	1942/23	2000/23	1946/27	1952/30	1986/29	1995/17	**1983/14**	1955/18	1983/02	1943/08	1975/05	1941/03		
Extreme Minimum (°C)	**-43.9**	-41.4	-36.1	-27.2	-12.2	-0.6	3.9	1.1	-6.7	-13.9	-31.3	-38.3		
Date (yyyy/dd)	**1943/20**	1996/02	1962/01	1954/02	1958/01	1969/13	1972/02	1938/28+	1965/25	1951/31	1985/28	1967/31		
Precipitation:														
Rainfall (mm)	0.4	2.7	6.9	19.8	63	107.7	95.3	85.8	80.2	42.7	9.3	0.6	514.4	A
Snowfall (cm)	28	17.9	22.3	13.6	1.5	0.1	0	0	0.8	11.4	35.2	27.4	158.2	A
Precipitation (mm)	26.1	19.3	27.7	32.7	64.3	107.8	95.3	85.8	81.2	53.7	42.3	25.7	661.8	A
Average Snow Depth (cm)	37	43	30	6	0	0	0	0	0	0	9	22	12	A
Median Snow Depth (cm)	37	44	30	4	0	0	0	0	0	0	8	23	12	A
Snow Depth at Month-end (cm)	43	41	19	0	0	0	0	0	0	1	16	29	12	A
Extreme Daily Rainfall (mm)	4.2	16.2	19.8	33.3	49.3	121.4	**153.5**	92.5	108	46.5	21.3	29.7		
Date (yyyy/dd)	1997/01	2000/26	1960/28	1974/21	1991/22	1999/25	**1993/27**	1972/20	1981/06	1940/04	1944/07	1951/03		
Extreme Daily Snowfall (cm)	24.6	26.9	33.8	**36.3**	20.6	1.4	0	0	30	26.2	32.8	22.8		
Date (yyyy/dd)	1975/11	1955/20	1966/04	**1957/10**	1970/15	1998/01	1939/01+	1938/26+	1964/26	1970/09	1977/09	1984/16		
Extreme Daily Precipitation (mm)	24.6	26.9	26.9	36.3	49.3	121.4	**153.5**	92.5	108	46.5	32.8	37.1		
Date (yyyy/dd)	1975/11	1955/20	1966/04	1957/10	1991/22	1999/25	**1993/27**	1972/20	1981/06	1940/04	1977/09	1951/03		
Extreme Snow Depth (cm)	102	117	**145**	84	23	1	0	0	20	20	66	91		
Date (yyyy/dd)	1966/17+	1962/16+	**1966/05+**	1962/01	1966/02	1997/27	1955/01+	1955/01+	1964/27	2001/26	1965/28+	1965/31		

Data courtesy of **Environment Canada**

***Figure 4: Average Temperature and Precipitation Information for Kenora** from Environment Canada. Note that Code A indicates no more than 3 consecutive or 5 missing years between 1971 and 2000.*

Item 6: History

Exploration work in the area was carried out for gold in the late 1800s. Numerous gold deposits were discovered at that time and two short lived mines were developed, the Gold Panner Mine on Caviar lake in 1899 and the Flint Lake Mine on Flint lake in 1901, both outside of the Property. All subsequent economic activity

has been concerned with gold properties except for relatively recent interest in base metal mineralisation possibly associated with the mafic to ultramafic sills and the felsic metavolcanics.

Exploration in the area of the Martin Kenty Property began in 1944 when Noranda Exploration Company Limited undertook an x-ray diamond drilling program to test a gold showing discovered by Noranda prospectors, Roy Martin and Jack Kenty on East Island in August of 1944. This being the current Martin F.M. Occurrence.

The gold bearing zone was trenched and 6 x-ray holes drilled (see drill hole location plan East island). In addition to the X-ray drilling 3 trenches gave the following favorable assays:
Trench No. 1 0.30 oz. Au over 11.5 feet (10.29 g/t over 3.51 m.)
Trench No. 2 0.16 oz. Au over 14 feet   (5.49 g/t over 4.27 m.)
Trench No. 3 0.15 oz. Au over 18 feet   (5.14 g/t over 5.49 m.)

Assay returns from the drilling were substantially lower. Core recovery averaged only 50% and it was debatable whether the drilling gave representative results.

Note: The above grade and tonnage of <u>The Kakagi Lake Shear</u> are considered historic and the qualified person of this report has been unable to verify the information and that the information is not necessarily indicative of the mineralization on the property that is the subject of the technical report; furthermore a qualified person has not done sufficient work to classify the historical estimate as current mineral resources or mineral reserves; and the issuer is not treating the historical estimate as current mineral resources or mineral reserves.

In 1973 the area was mapped by the Ontario Department of Mines and two samples taken from a rusty schist zone on Hay Island, about 5000 feet (1524m) west of the original discovery, returned values of 0.04 oz/ton (1.37 g/t) Au and 0.34 oz/ton (34.29 g/t). Au.

Note: The above grade and tonnage of <u>The Kakagi Lake Shear</u> are considered historic and the qualified person of this report has been unable to verify the information and that the information is not necessarily indicative of the mineralization on the property that is the subject of the technical report; furthermore a qualified person has not done sufficient work to classify the historical estimate as current mineral resources or mineral reserves; and the issuer is not treating the historical estimate as current mineral resources or mineral reserves.

In 1974 the property was optioned by Roy Martin to a joint venture consisting of Noranda, Newconex and Tombill Mines. Geological mapping was carried out during the summer of 1974. Geophysical surveys and a diamond drilling programme was completed during February and March 1975. Seven holes, totaling 2016 feet (615m)

were drilled; six of these at the East Island showings and one at the Hay Island occurrence.

In February and March of 1983 Barrier Reef Resources drilled seven holes totalling 3877 feet (1181.7m) along an east-west trending zone 6500 feet (1981m) in length which included Hay Island, East Island and the intervening lake bottom. Numerous geophysical surveys were undertaken during this time as well as outlined in both Sections 6.1 and 6.2.

A survey was carried out to detail the Topography of the lake bottom and to recover lake sediment samples which were analyzed for gold and arsenic of the lake bottom and to recover lake sediment samples which were analysed for gold and arsenic.

For further information pertaining to previous work, refer to the report by McCormick 1974. Additional further information from the Ontario Mineral Inventory (OMI) and the assessment files is discussed in Items 6.1 and 6.2.

Note: The above grade and tonnage of <u>The Kakagi Lake Shear</u> are considered historic and the qualified person of this report has been unable to verify the information and that the information is not necessarily indicative of the mineralization on the property that is the subject of the technical report; furthermore a qualified person has not done sufficient work to classify the historical estimate as current mineral resources or mineral reserves; and the issuer is not treating the historical estimate as current mineral resources or mineral reserves.

6.1: History from OMI Ontario Mineral Inventory Martin Kenty Property

The 5 known mineralized occurrences that occur on the Property are: the Martin F.M. Occurrence, Au; the Kakagi Lake Occurrence, Au, Ag (secondary); the Roy Martin East Occurrence, Au; the Mongus Lake Occurrence, A; and the Mongus Lake North, Ni**.** See section 7.3 for some further historical information on these properties.

6.2: History from MNDM Reports and Assessment Files Martin Kenty Property

Note: in the references listed below the terms "AFRI File" and AFRO ID" refer to the assessment report's identification numbers for the files as found in the MNDM's Assessment File Research Image Database (AFRI) retrieved from http://www.geologyontario.mndm.gov.on.ca.

Due to the large number of reports submitted for assessment in the MNDM's Assessment File Research Image Database many of which are airborne geophysics reports or only partly cover Martin Kenty's Property; they have not all been listed in the "References" (Item 26 of this report). The author has examined the reports and believe that the pertinent information is presented in this Report.

The following Figures 5-11 and the following Table 7 (11 pages) relate to the filed historic assessment work registered with MNDMNRF on their AFRI database.
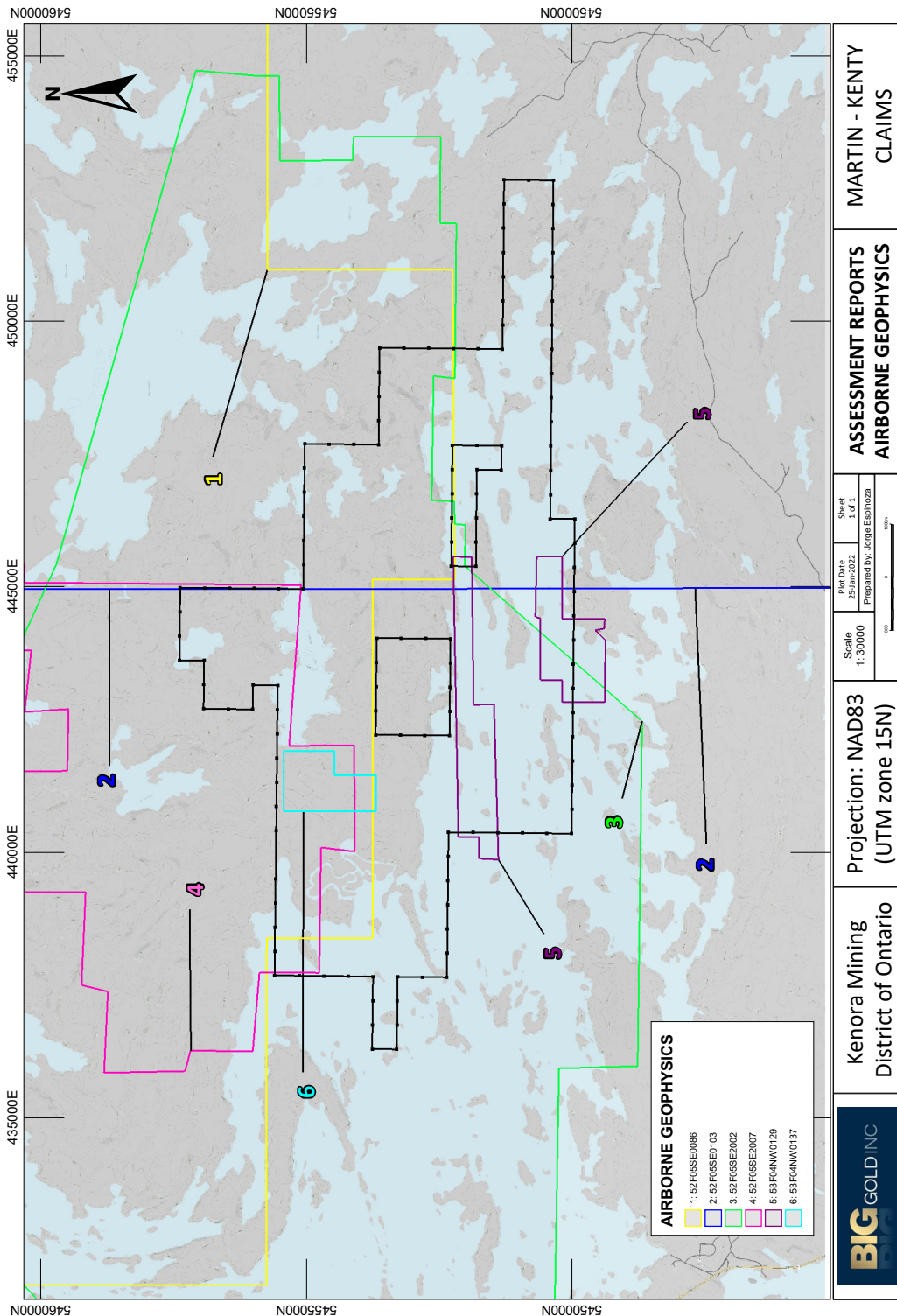

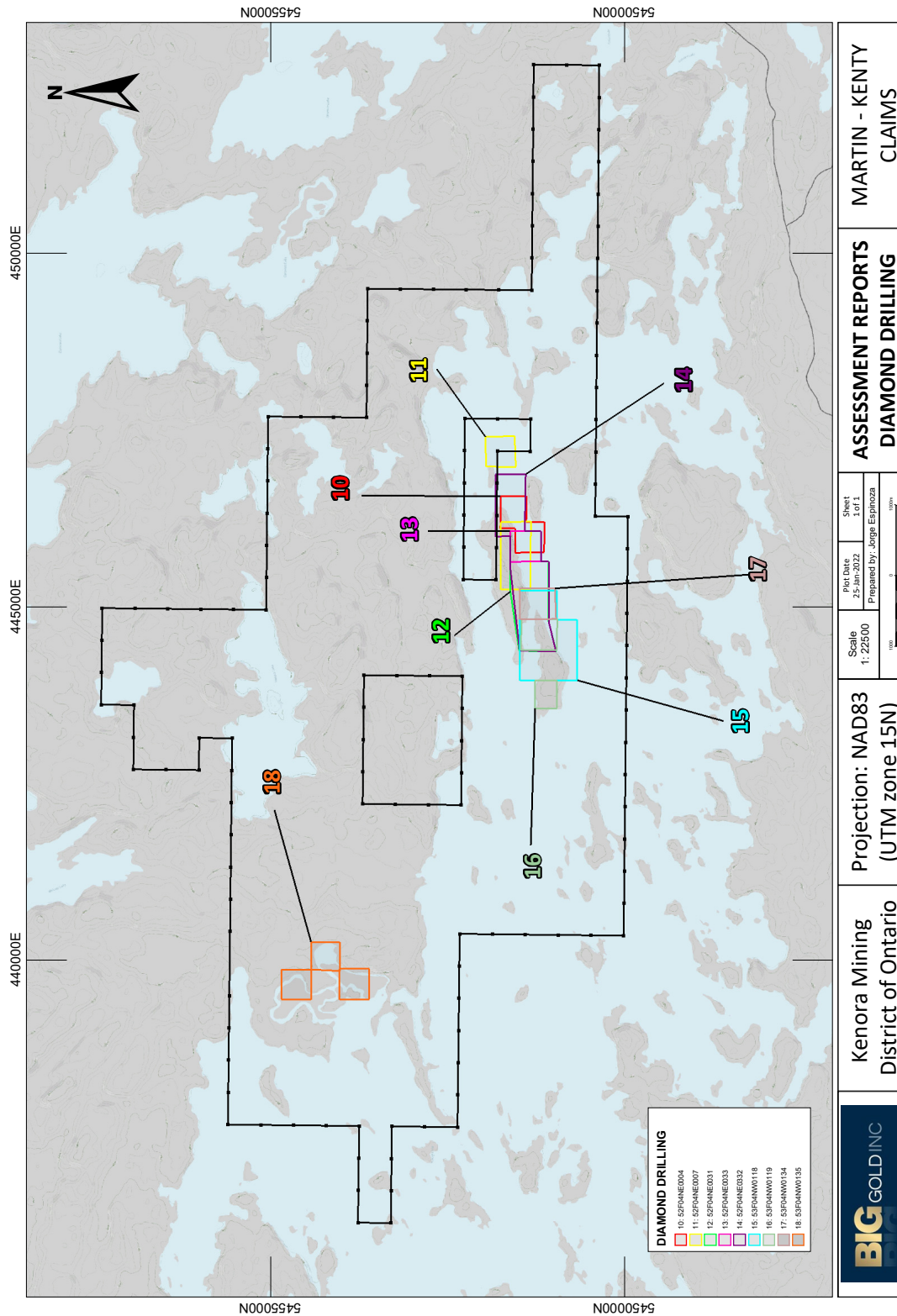***Figure 5: Outline of Airborne Geophysical Work*** *from MNDMNRF Geology Ontario's OGS Earth Assessment files.*

Big Gold Inc.

Martin Kenty Property

Figure 6: Outline of Diamond Drilling Work from MNDMNRF Geology Ontario's OGS Earth Assessment files.

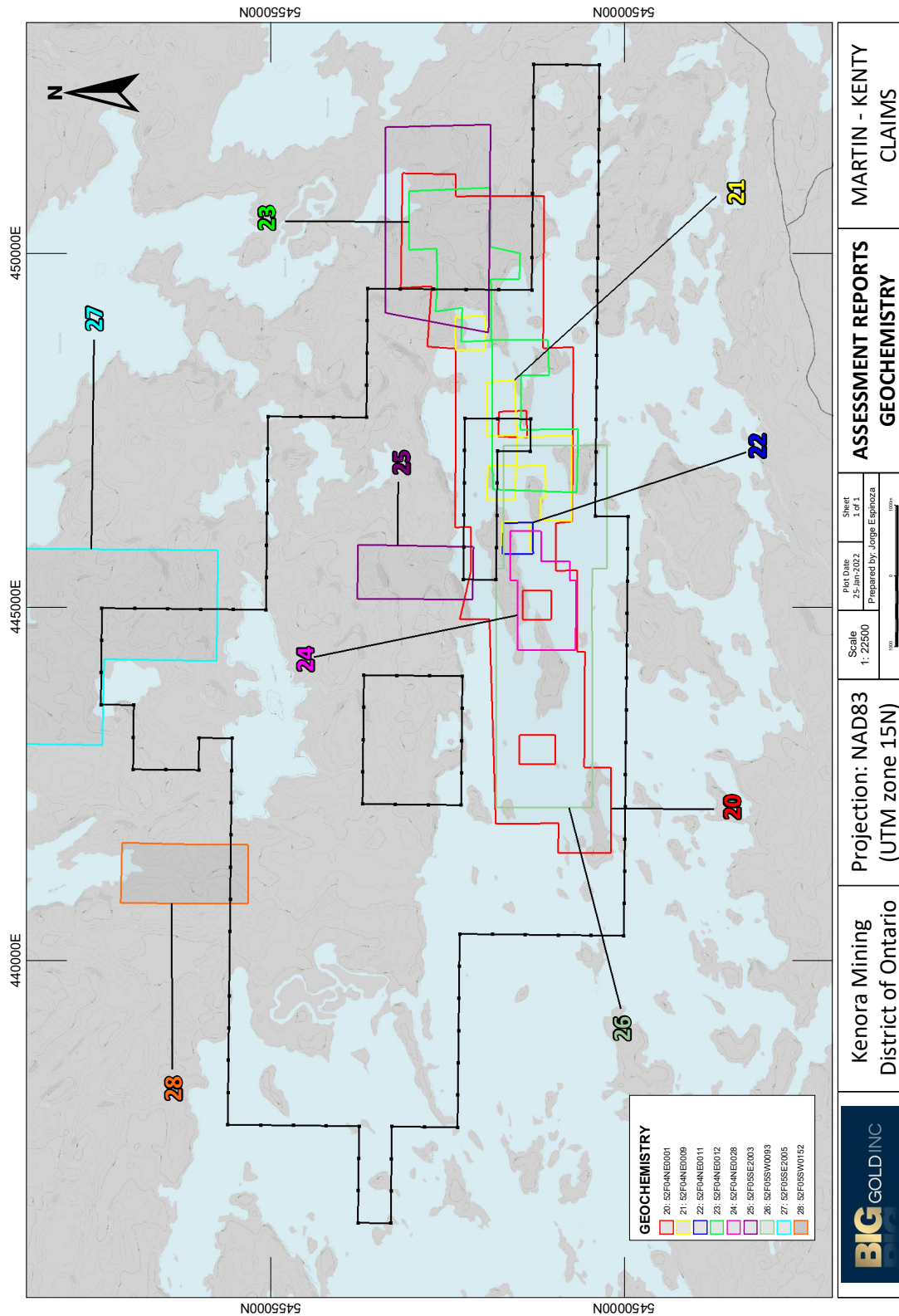February 2022   29   Bedrock Research Corp.

Figure 7: Outline of Geochemical Work *from MNDMNRF Geology Ontario's OGS Earth Assessment files.*
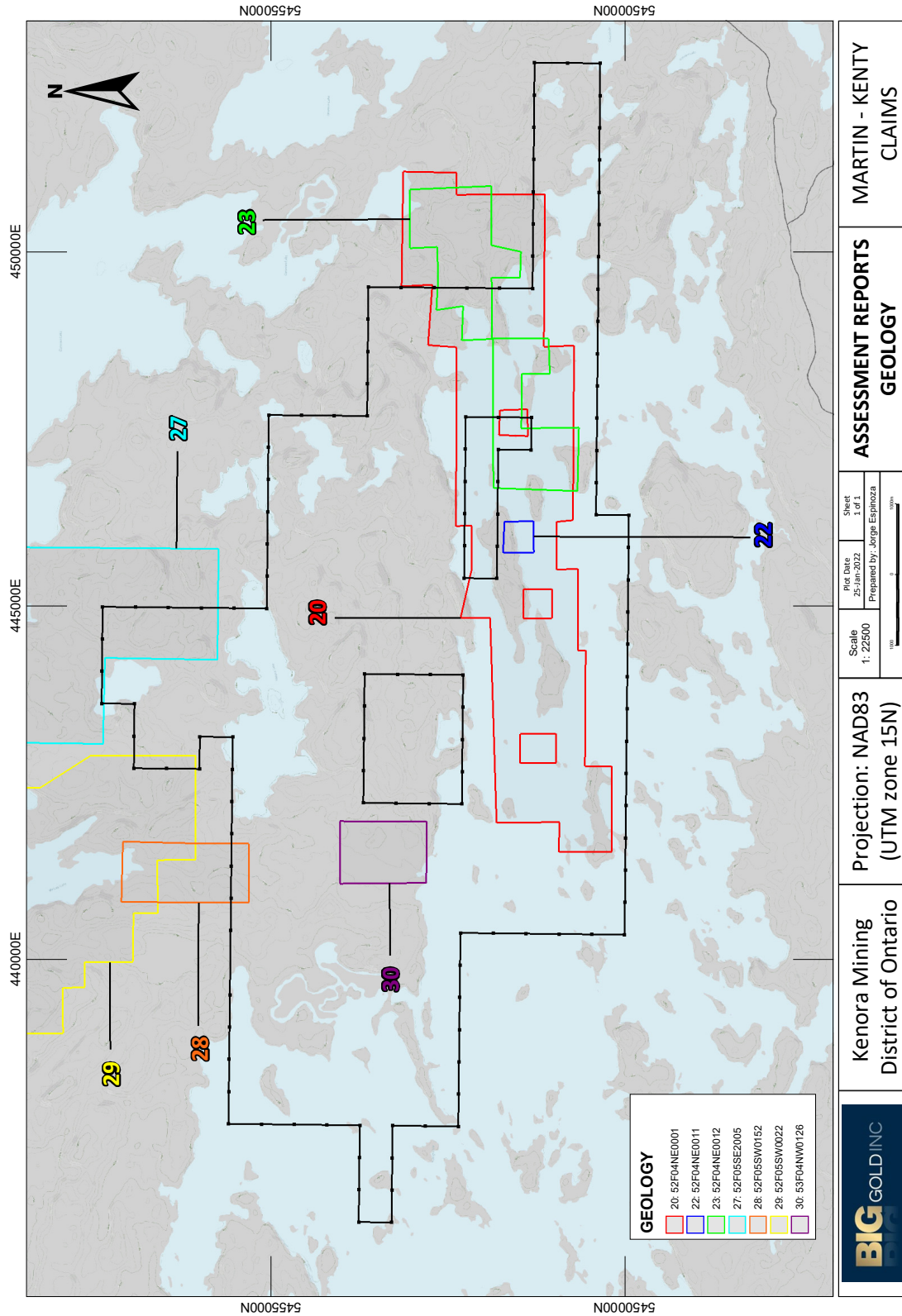
Figure 8: Outline of Geological Work from MNDMNRF Geology Ontario's OGS Earth Assessment files.
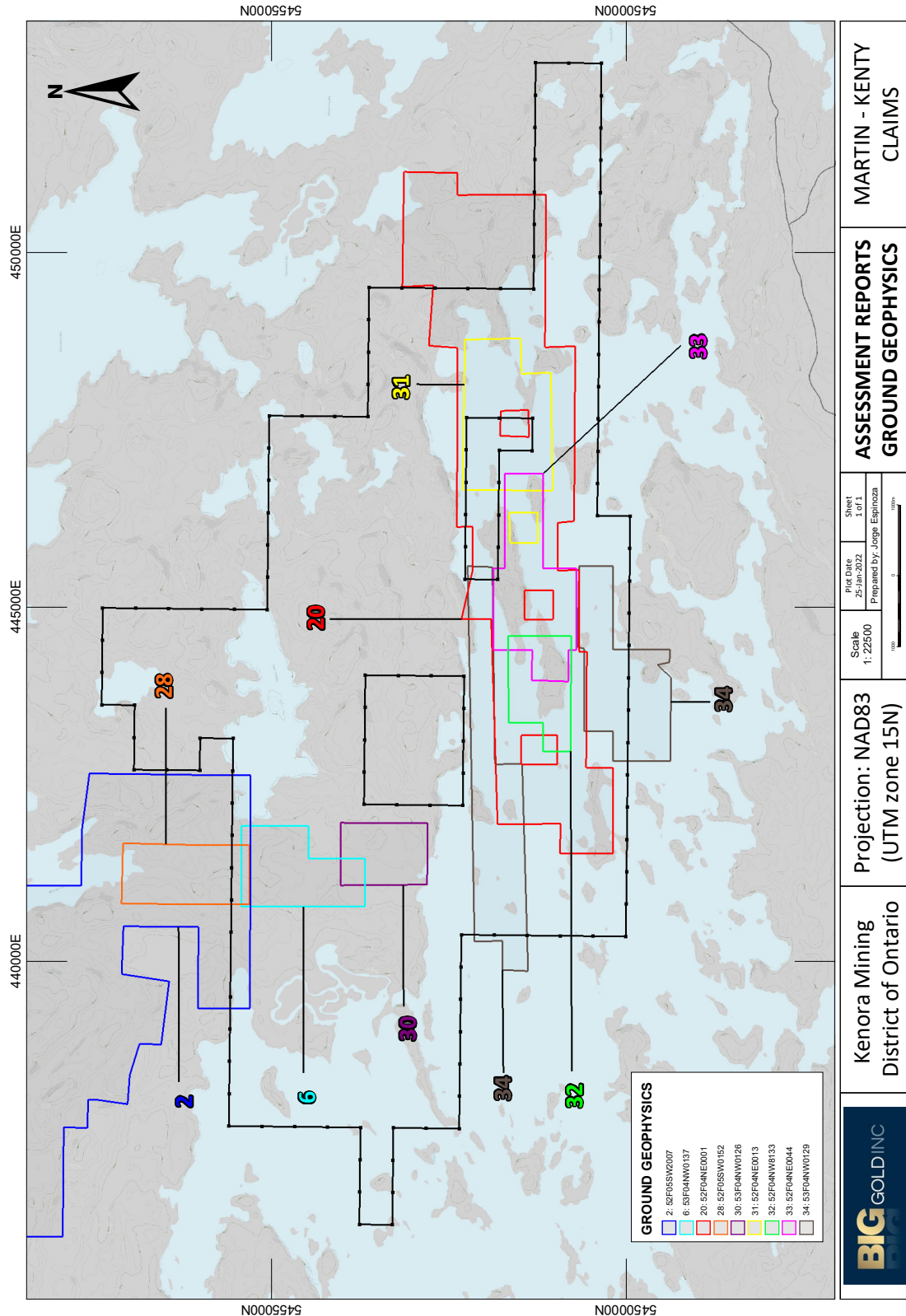
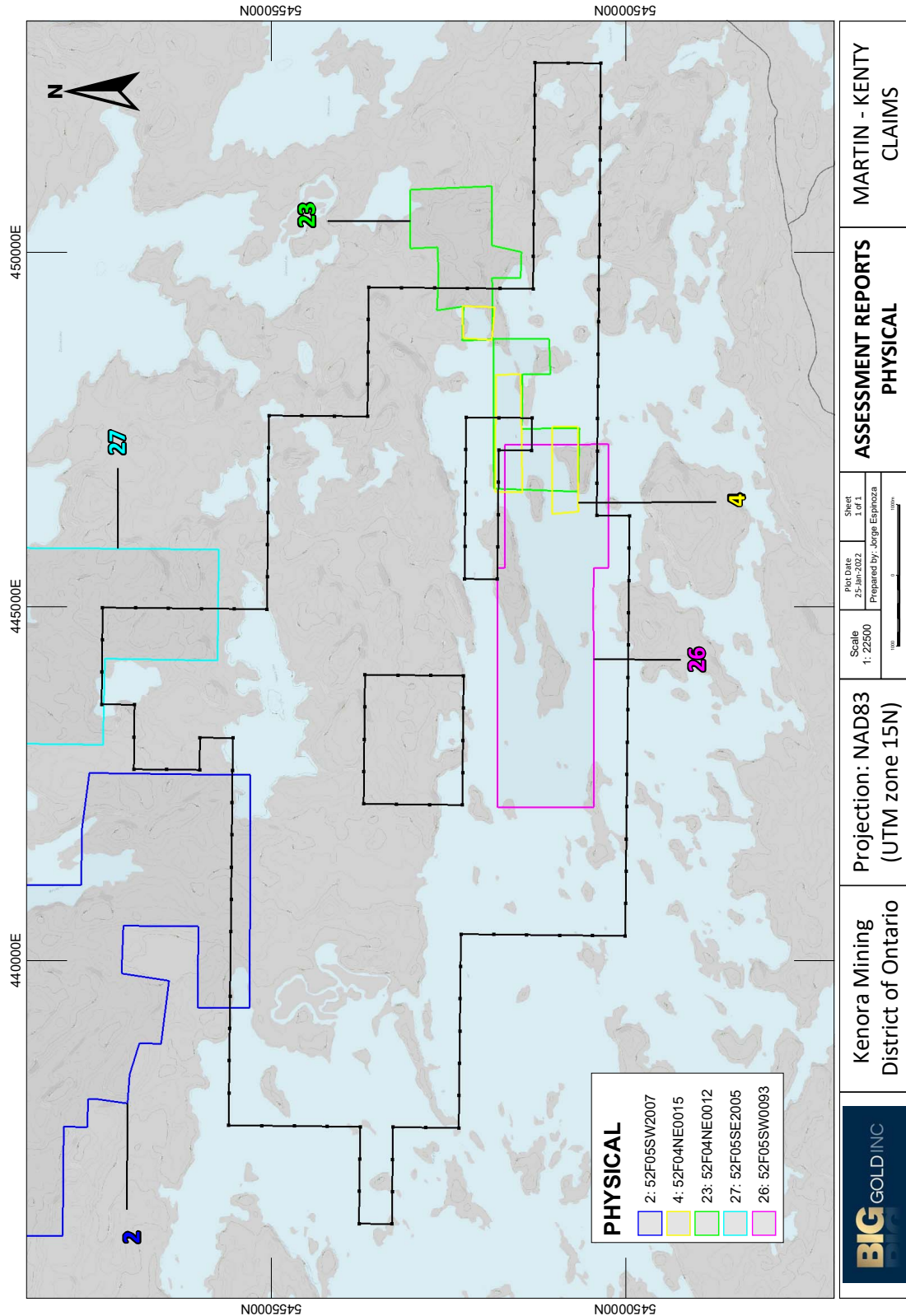**Figure 9: Outline of Ground Geophysical Work** *from MNDMNRF Geology Ontario's OGS Earth Assessment files.*

Figure 10: Outline of Physical Work *from MNDMNRF Geology Ontario's OGS Earth Assessment files.*
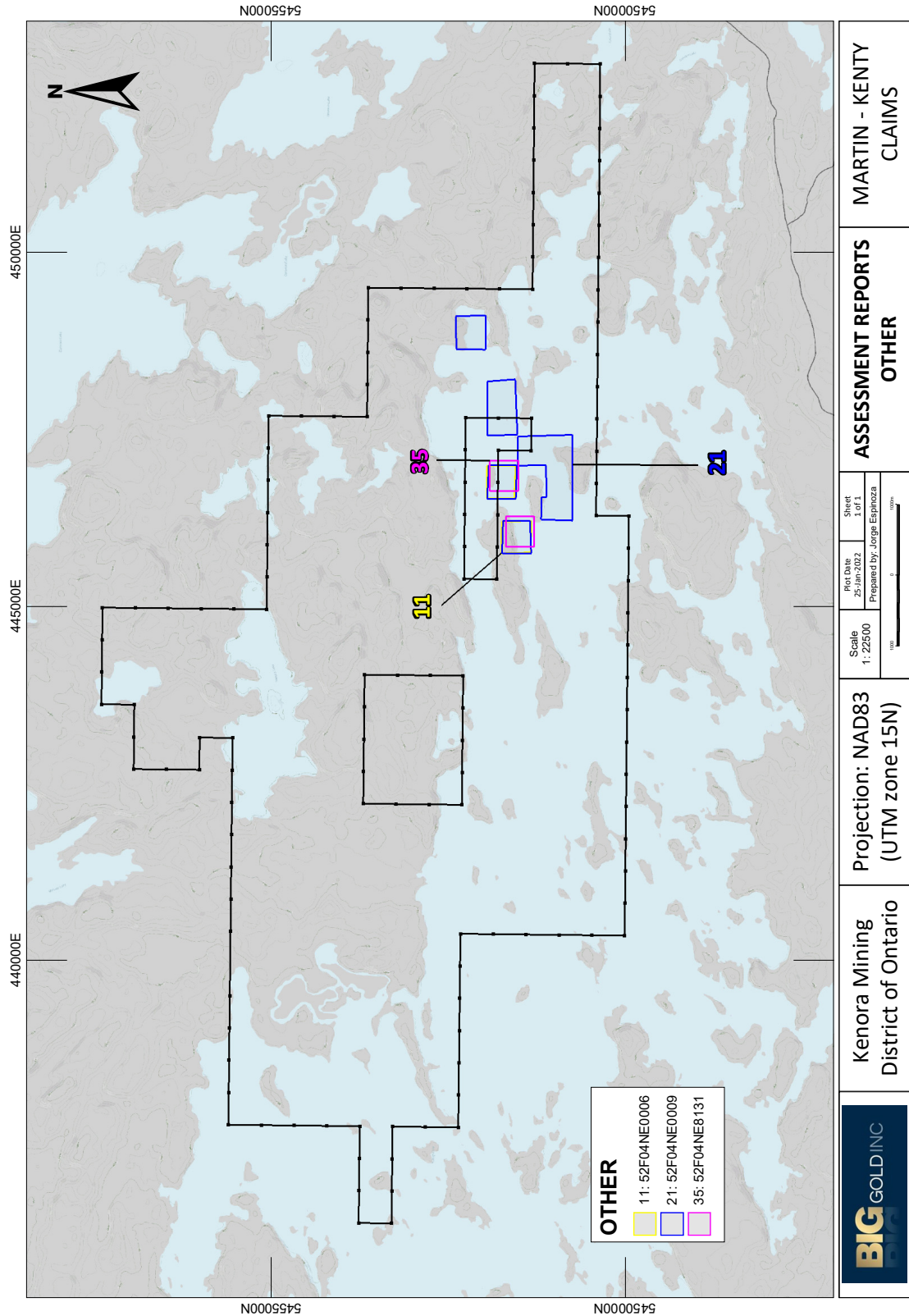
Figure 11: Outline of Other Work from MNDMNRF Geology Ontario's OGS Earth Assessment files.

Insert Assmnt Rpt List pg 1 **Table 3**

Insert Assmnt Rpt List pg 2 Table 3

Insert Assmnt Rpt List pg 3 Table 3
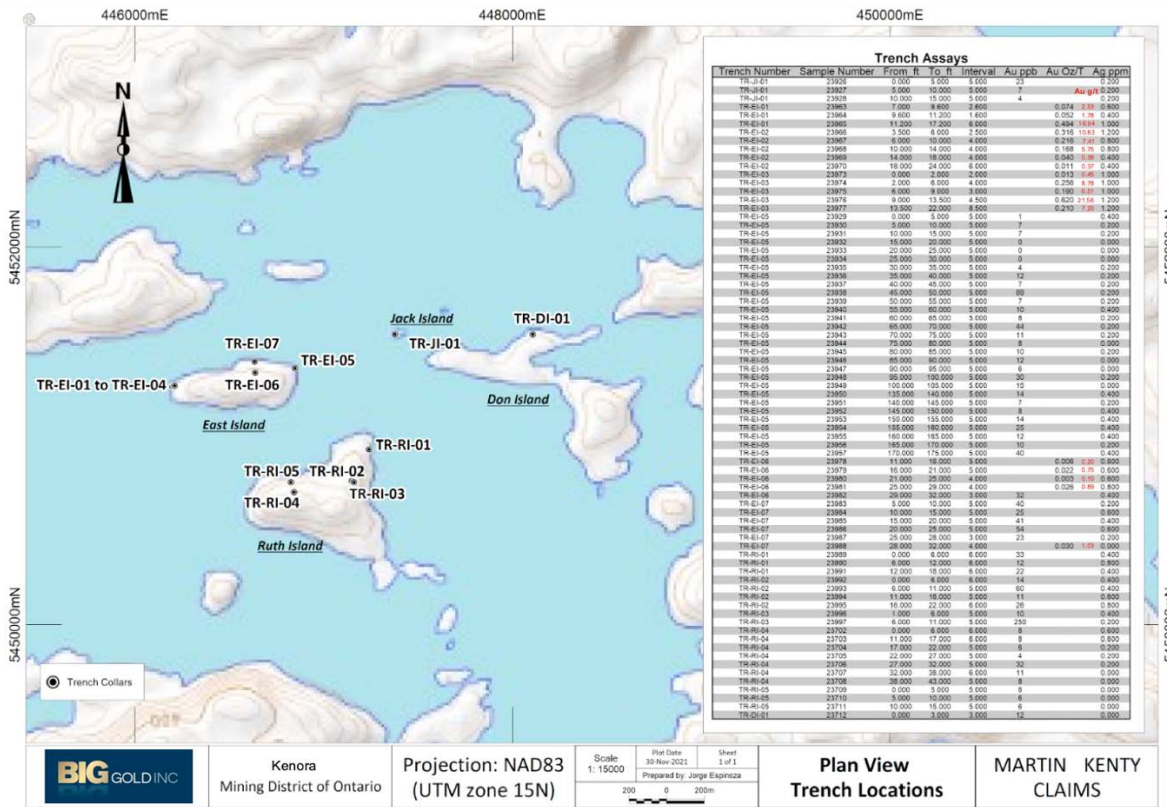
Insert Assmnt Rpt List pg 4 Table 3

Figure 12: SE Kakagi Lake Historic trench sampling locations prepared by BG from collected and consolidated records from the AFRI files of Table 7 above, primarily AFRI # 52F04NE0012. Assay values above 0.1 g/t Au shown in red.
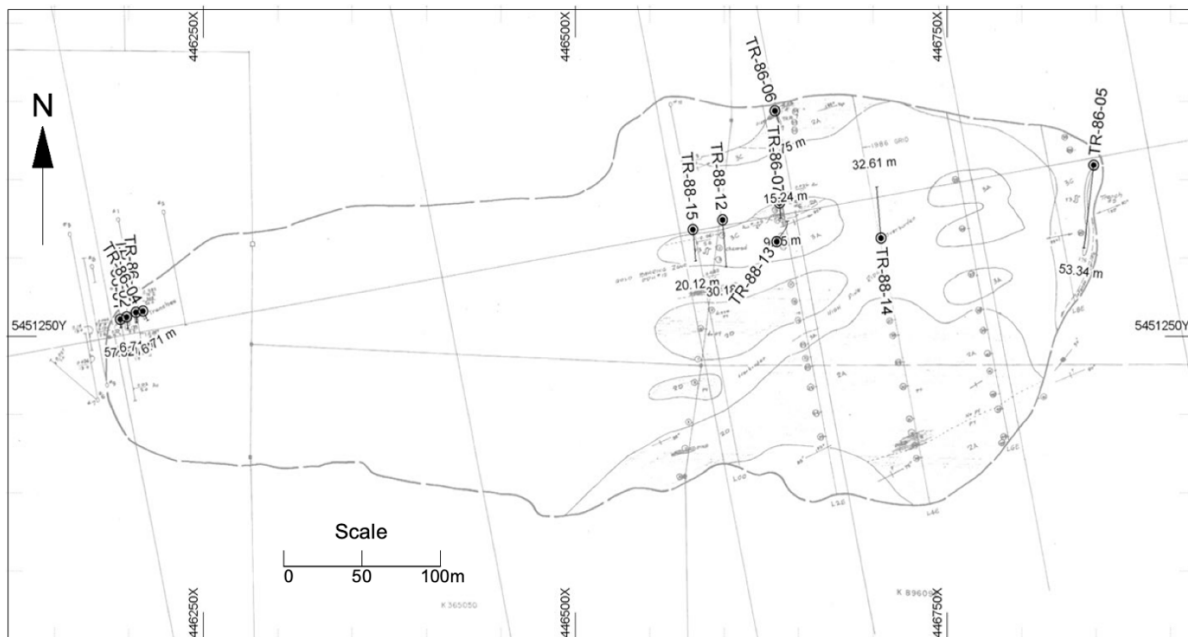

Figure 13: Historic trench sampling and drill hole locations on East Island in Kakagi Lake. Modified from Source: Blais, R.M. 1987 AFRI 52F04NE0012 Geol Map of East Island with DDH, Trenching and Assay data, 1987.

The drill holes shown above in Figure 13 have been drilled on the Property by several parties as listed in Table 7. Many of these holes totaling were drilled for gold in the area around East and Hay islands as shown in Figure 14. An additional three holes totaling 1,835 feet (559m) were drilled in in 1969 by Canadian Nickel Co.[1] in the area of Peninsula Bay in the northwest of the property. Diorite, gabbro and peridotite were noted in that drill program with a minor graphitic shear noted at one contact with the volcanic rocks.

A geophysical interpretation was also undertaken in 1997 for Hornby Bay Exploration as shown in Figure 16 below. Of interest is a discontinuous east-west conductor located along the north shore of Kakagi Lake in mafic to ultramafic rocks. The area was classified into various magnetic domains I-V and various conductors shown as C. A more detailed breakdown is given in the report by Jagodis, Francis L. AFRI 52F05SE2002.

---

[1] Canadian Nickel Co. Ltd. 1969, AFRI 53F04NW0135
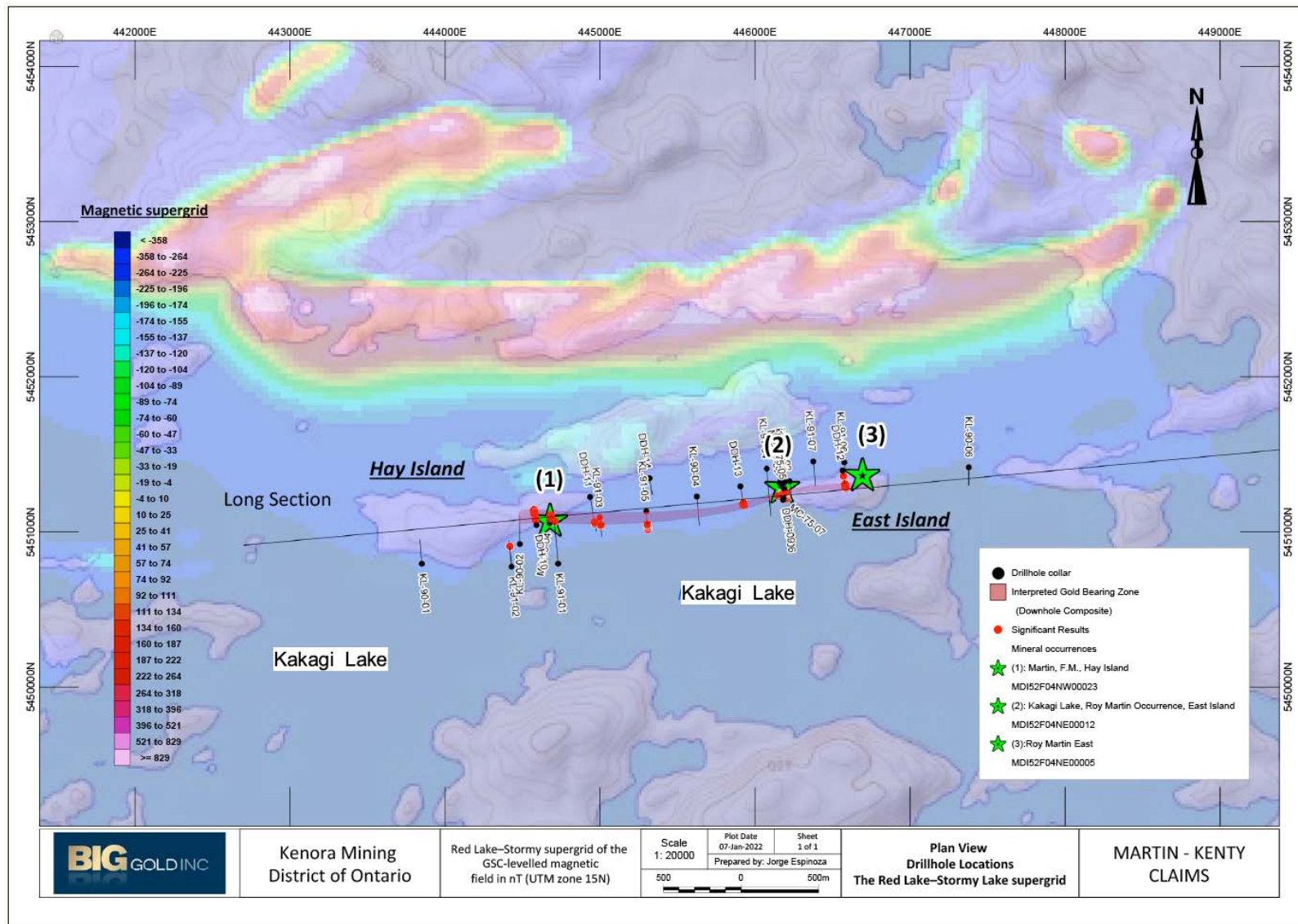
Figure 14: Historic drill hole locations on Hay and East Island areas in Kakagi Lake showing the 3 OMI Au occurrences along the auriferrous Kakagi Lake Shear zone.

Figure 15:Drill Section of the Kakagi Lake Shear looking to the north. *Source: Big Gold corporate files from consolidation of AFRI file data*

Figure 16: Historic Geophysical Interpretation. *Note conductors in gabbroic or peridotitic rocks and also in the northwest in volcanic rocks.* **Red outline shows the Martin Kenty Property.** *Source: Jagodits, Francis L. 1998, AFRI 52F05SE20*

Item 7: Geological Setting and Mineralization

7.1 Regional Geology

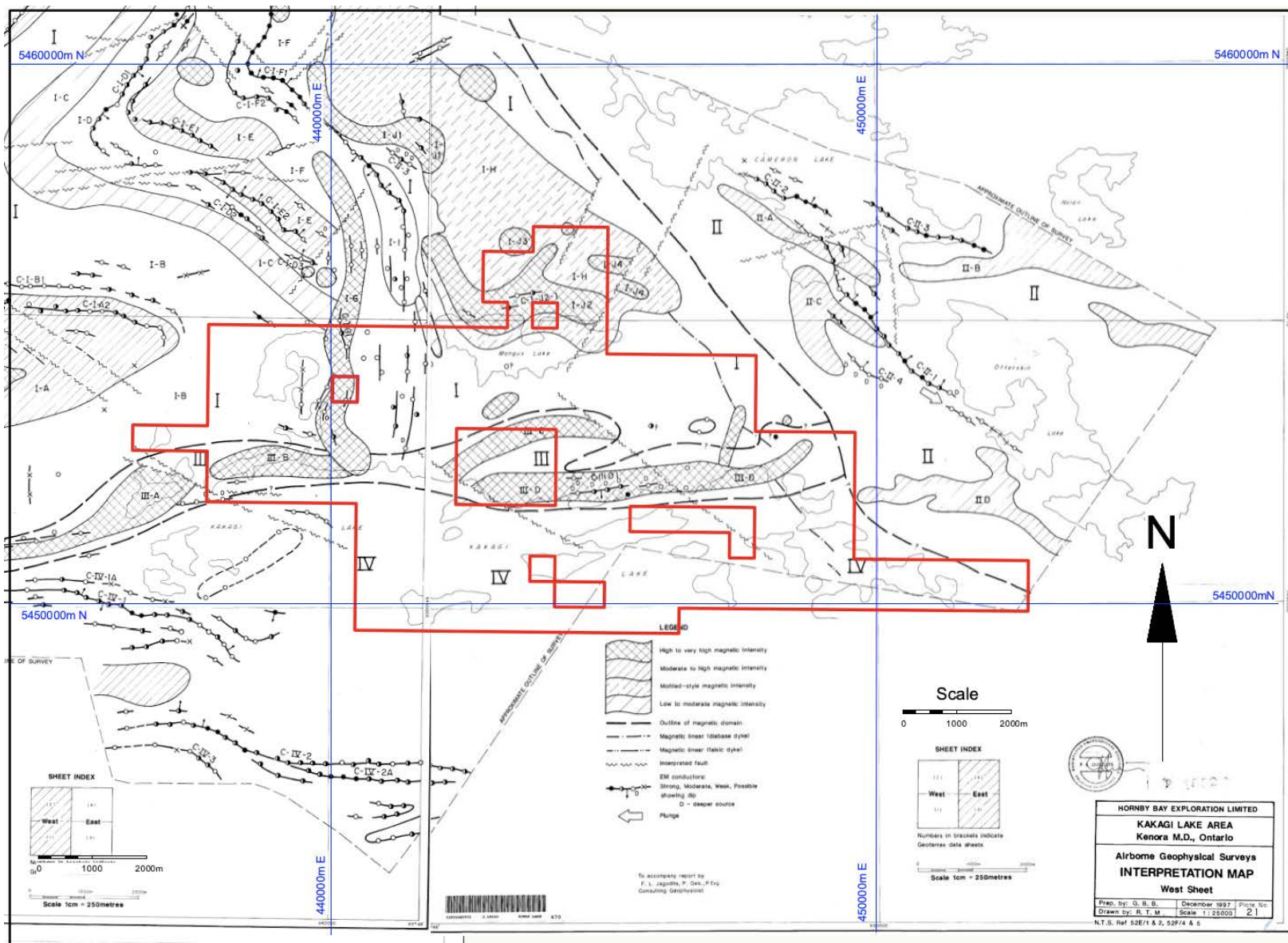**Geology Comments**

The Property is located within Kakagi-Rowan Lakes greenstone belt, located on the western end of the Wabigoon Subprovince within the Superior Province of the Canadian Shield. The Wabigoon Subprovince is a granite-greenstone terrain between the gneissic terrains of the Quetico Subprovince to the South and the Winnipeg River Subprovince to the north. The lithologies in the study area are steeply dipping, Early Precambrian mafic metavolcanics overlain by a complex of intermediate to felsic metavolcanics, intruded by differentiated mafic to ultramafic sills, and have been folded into a major anticline and syncline with east-northeast trending vertical axial planes. These folds are truncated by a major west-northwest trending fault with right-handed movement. The main foliation developed is schistosity in zones of shearing. All bedrock in the area is Early Precambrian (Archean) age except for a northwest trending diabase dike. Glacial stria indicates an ice flow direction from the northeast.

The following description of the geological setting is taken from, Raoul, Allen J., AFRI # 20000000079.

"*The geologic setting of the Property lies within the Wabigoon structural sub-province of the Superior Province. Major fault structures, the Pipestone-Cameron Lake deformation zone and the Manitou Stretch deformation zone subdivide the greenstone belt into distinct geological domains. These large individual domains are characterized by complex assemblages of mafic and felsic volcanic rocks and minor sedimentary rocks that are intruded by subvolcanic intrusives and granitic batholiths.*

Widespread intense alteration associated with the major deformation zones and associated secondary structures and alteration associated with complex centers of felsic volcanism are prime areas for gold mineralization. Numerous gold showings and occurrences are associated with these features within the project area. In addition to shear zone hosted gold deposits associated with major regional carbonate alteration zones; the Property is prospective for shear zone hosted, Bousquet and Hemlo type gold mineralization. The property has potential for volcanic hosted massive sulphide mineralization and PGE mineralization associated with mafic - ultramafic intrusive rocks."
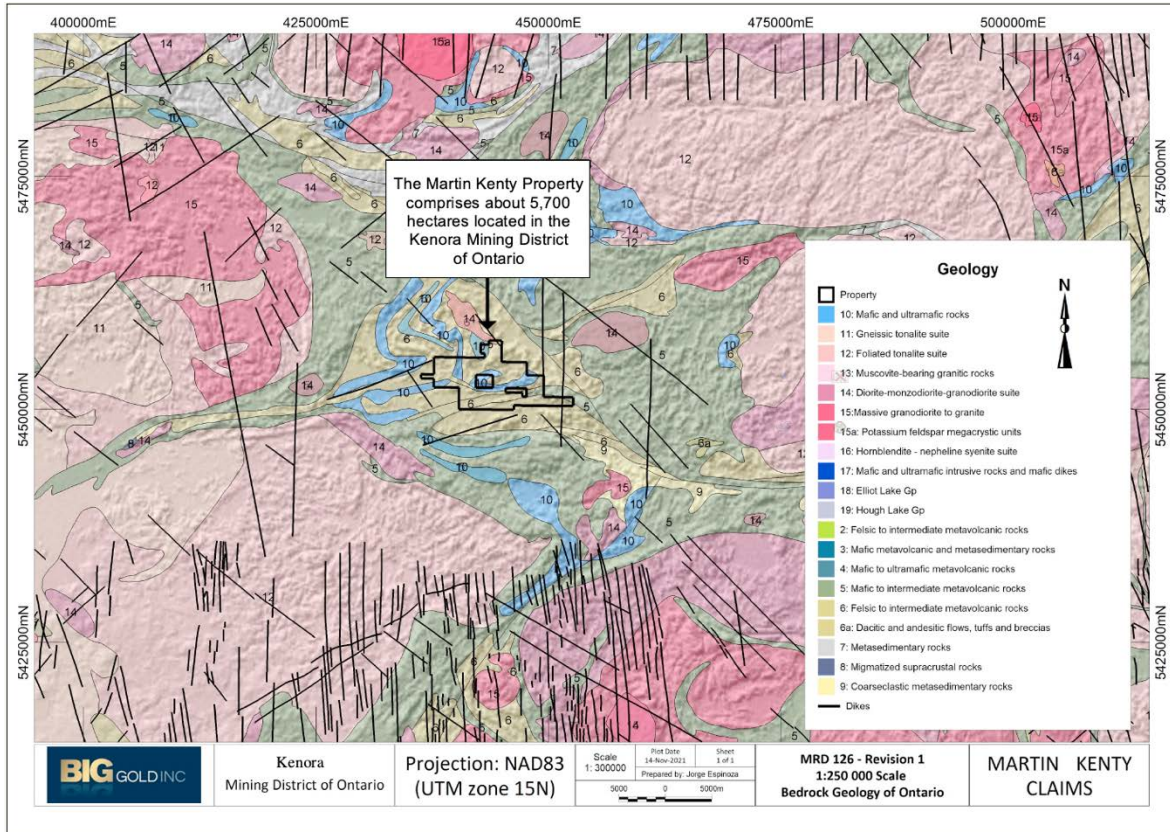
Figure 17: Regional Geology showing the Kakagi-Rowan Lakes Greenstone Belt and structural elements with the Property outlined in black. Basemap source: Ontario Geological Survey 2011 MRD 126.
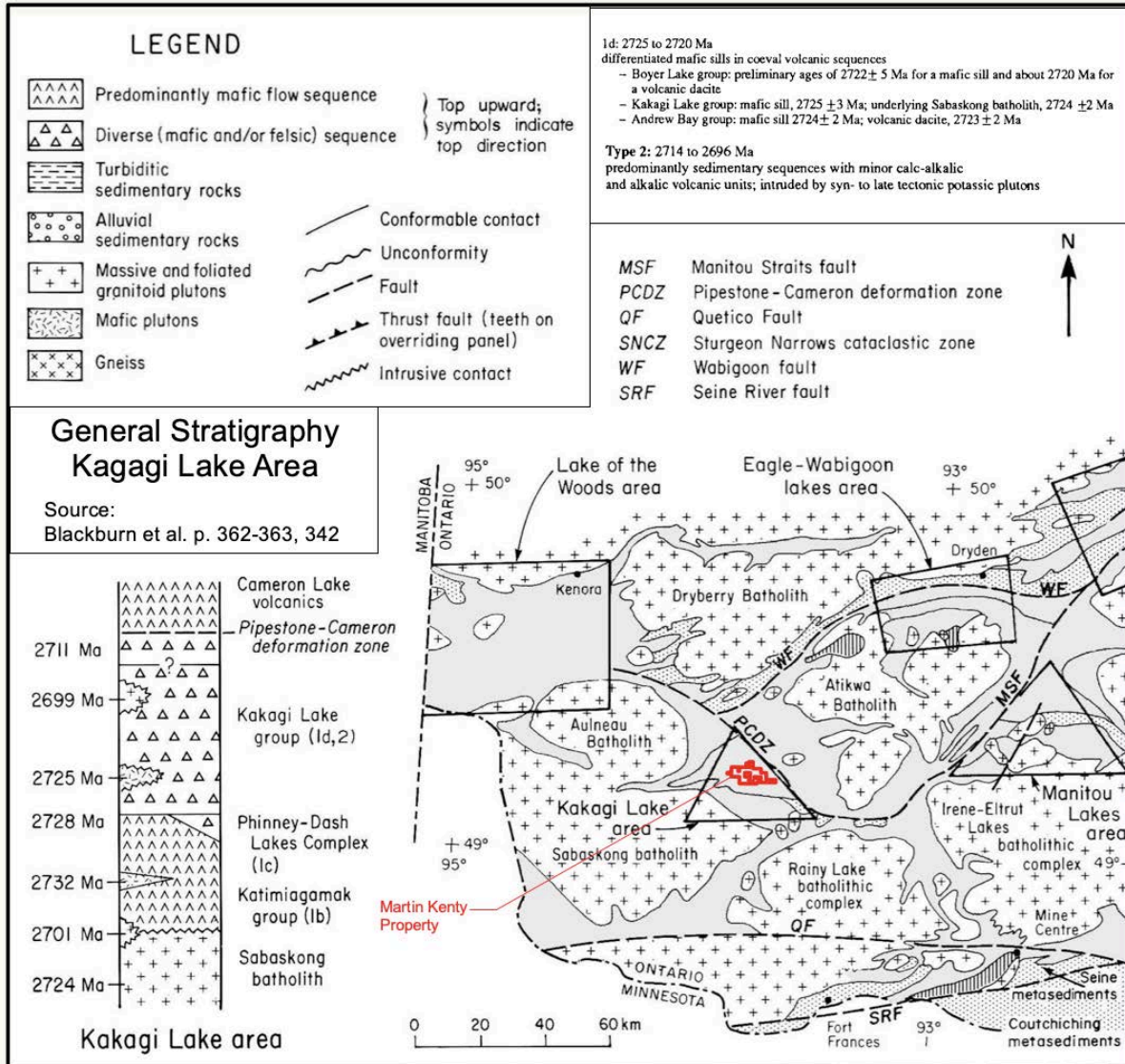
Figure 18: General Stratigraphy of the Kakagi Lake Area with the Property outlined in red.

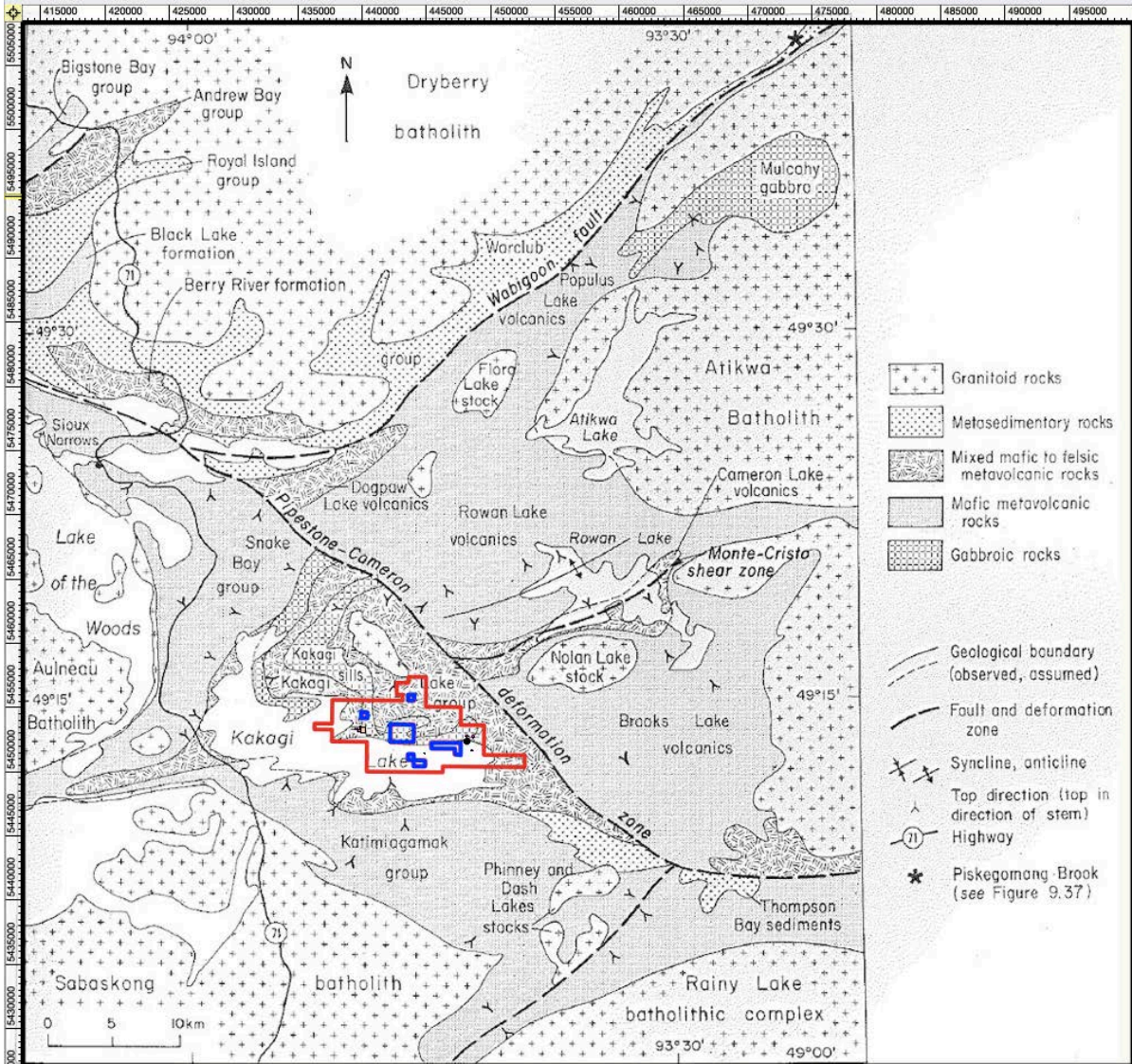***Figure 19: Geology of the Kakagi Lake Area*** *showing the Kakagi-Rowan Lakes Greenstone Belt and structural elements with the Property outlined in red. Blue areas are claims held by others. Basemap source:* Blackburn C.E., et al.1991.
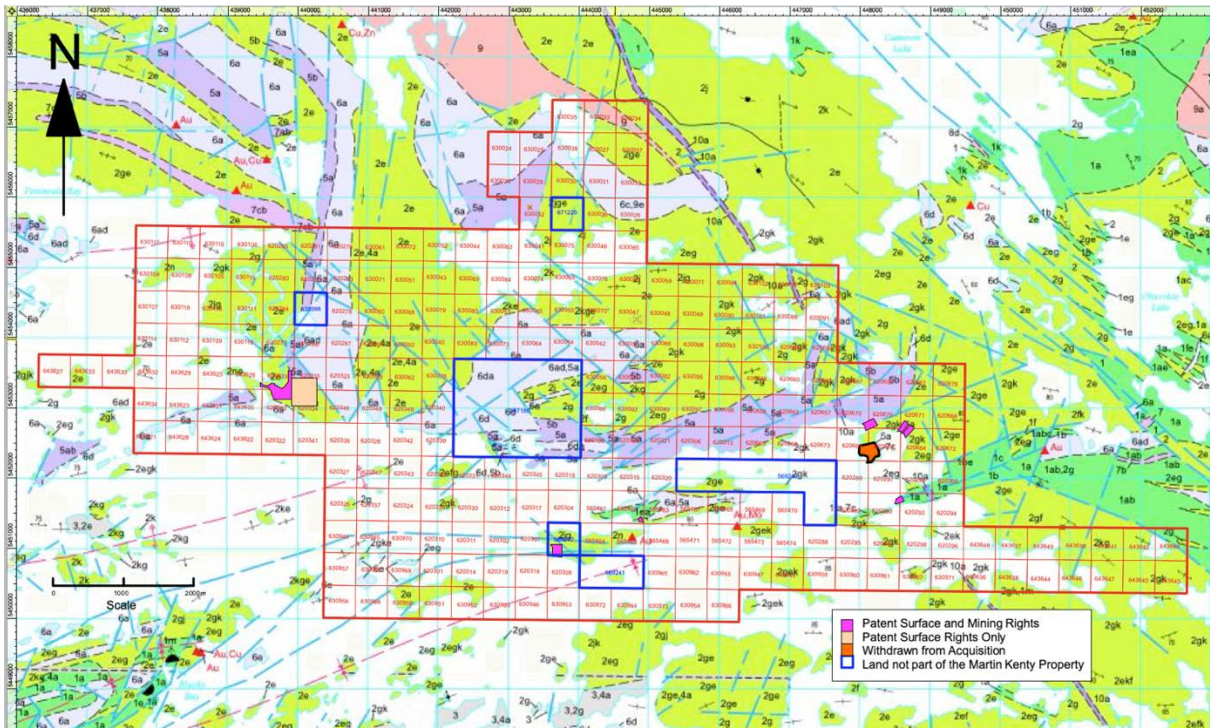
Figure 20: Local Geology Overlain with the Property - *see legend in Figure 20a - Source Johns, G.W., 2007.*

LEGEND[a]

PHANEROZOIC

CENOZOIC

QUATERNARY

PLEISTOCENE AND RECENT
Glacial, glacial-fluvial, swamp, lake, and stream deposits

UNCONFORMITY

PRECAMBRIAN

LATE PRECAMBRIAN

10 **Mafic Intrusive Rocks**
10a Diabase
10b Diorite

INTRUSIVE CONTACT

EARLY PRECAMBRIAN (ARCHEAN)

9 **Porphyritic Intermediate to Felsic Intrusive Rocks**
9a Syenite, monzonite
9b Porphyritic hornblende monzodiorite (K-feldspar phenocrysts)
9c Altered granite
9e Diorite

INTRUSIVE CONTACT

8 **Intermediate to Felsic Intrusive Rocks**
8a Granodiorite
8b Quartz-phyric granodiorite
8c Hornblende granodiorite
8d Tonalite
8e Quartz monzonite
8f Porphyritic granodiorite (K-feldspar phenocrysts)

INTRUSIVE CONTACT

7 **Metamorphosed Felsic to Intermediate Intrusive Rocks**
7a Feldspar porphyry
7b Quartz-feldspar porphyry, feldspar-quartz porphyry
7c Quartz porphyry

INTRUSIVE CONTACT

6 **Metamorphosed Mafic Intrusive Rocks**
6a Gabbro (may in part be extrusive)
6b Diorite
6c Coarse-grained porphyritic gabbro (hornblende phenocrysts)
6d Leucocratic gabbro
6e Anorthosite gabbro

INTRUSIVE CONTACT

5 **Metamorphosed Ultramafic Intrusive Rocks**
5a Peridotite
5b Pyroxenite/hornblendite

INTRUSIVE CONTACT

METAVOLCANIC AND METASEDIMENTARY ROCKS

4 **Chemical Metasedimentary Rocks**
4a Hematite/limonite ironstone
4b Graphitic shales

3 **Clastic Metasedimentary Rocks**
3a Feldspathic wacke
3b Quartz-feldspar wacke
3d Feldspathic arenite
3e Argillite
3g Biotite-feldspar schist

2 **Intermediate to Felsic Metavolcanic Rocks[b]**
2e Tuff
2f Quartz-feldspar tuff
2g Lapilli tuff
2h Pyroclastic breccia
2j Tuff breccia
2k Lapillistone
2n Schistose/gneissose

1 **Mafic to Intermediate Metavolcanic Rocks**
1a Fine-grained massive flow
1b Medium-grained massive flow (may in part be intrusive)
1c Porphyritic flow (plagioclase feldspar phenocrysts)
1d Porphyritic flow (large plagioclase feldspar phenocrysts, "Leopard Rock")
1e Pillowed flow
1f Amygdaloidal flow
1g Autoclastic breccia
1h Pillow breccia
1j Epidotized mafic flow
1k Schistose mafic flow
1m Amphibolite
1n Amphibolite gneiss

[a] This is a field legend and may change as a result of subsequent laboratory investigations.
[b] The order of units so designated does not imply relative stratigraphic position.
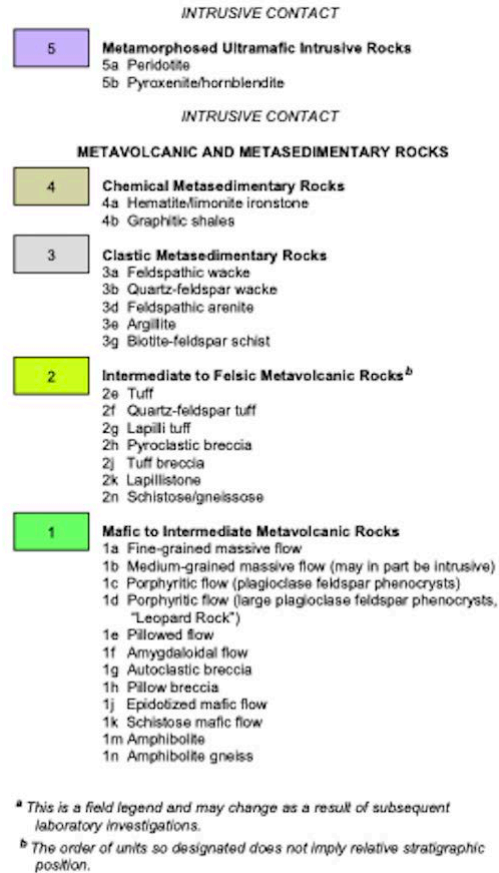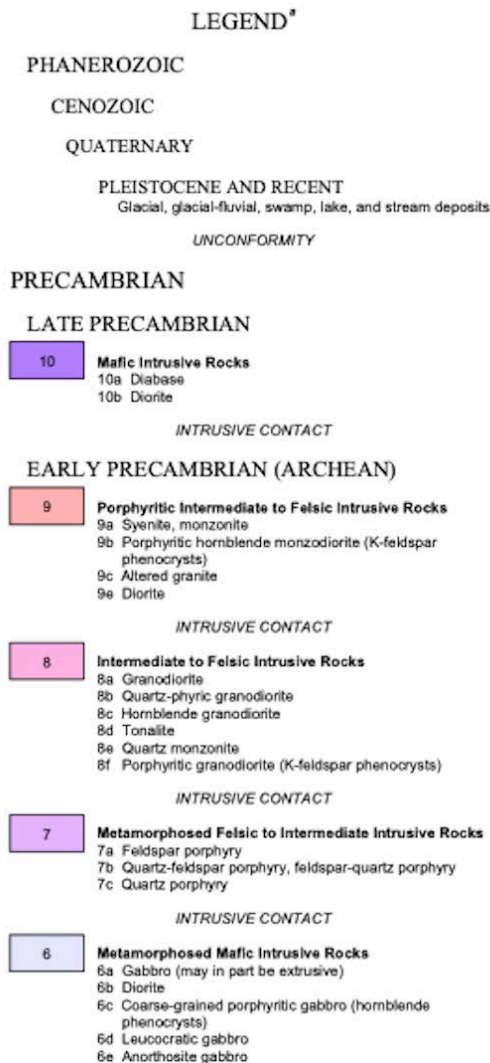
Figure 20a: Map Legend for Figure 17 *from Johns, G.W. 2007*

7.2 Property Geology and Mineralization

The lithologies in the study area are steeply dipping, Early Precambrian mafic metavolcanics overlain by a complex of intermediate to felsic metavolcanics, intruded by differentiated mafic to ultramafic sills, and have been folded into a major anticline and syncline with east-northeast trending vertical axial planes. These folds are truncated by a major west-northwest trending fault with right-handed movement. the main foliation developed is schistosity in zones of shearing. All bedrock in the area is Early Precambrian (Archean) age except for a northwest trending diabase dike. Glacial stria indicates an ice flow direction from the northeast.

The 4 earlier published geological map sheets that cover the claims and surrounding area are: Cedartree Lake, Map 2319, 1"=1/2 mile; Kakagi Lake, Map 2447, 1"=1/2 mile; Schistose Lake, Map 2421, 1"=1/2 mile; and Rowan Lake Area, P.831, 1"=1/4 mile (northeast of the claims). All maps are within the Kenora Mining

Division. A later 5th compilation map, P3594 Kakagi Rowland Lake Area (see Figure 20) was prepared over the area in 2007. All maps are within the Kenora Mining Division.

The following text is a description of the local geology extracted from Jagodits, Francis L., 1998, AFRI 52F05SE 2002.

"*The Property covers an Archean volcanic complex centered around Kakagi Lake. This complex is composed of a complete mafic-felsic volcanic cycle which was initiated by a vast effusion of massive, pillowed and plagioclase-phyric mafic volcanic flows intruded by synvolcanic gabbro sills. Together these early mafic sequences are referred to as the Snake Bay formation. The Snake Bay formation, to the east off the property, is unconformably overlain by an equally thick succession of intermediate to felsic pyroclastic rocks estimated to be in the order of over 3 kilometers. Intrusive into the pyroclastics are cosanginous, differentiated ultramafic to gabbroic sills referred to as the Kakagi Lake sills. Together, these two distinct rock units form the Kakagi Lake group.*

The Kakagi Lake group consists of pyroclastic rocks and was deposited by long lived intermediate volcanic centres. It has been subdivided into 5 formations which in order of decreasing age are: the South Kakagi Lake formation (not exposed on the property), the East Kakagi Lake formation (not on property), the Emm Bay formation, the Cedartree Lake formation and the Stephen Lake formation (also not exposed on the within survey area option).

The Emm Bay formation is the most extensive and volcanogenically most complex formation in the Kakagi Lake group. Most of the formation is composed of interbedded heterolithic, matrix supported lapilli tuff to pyroclastic breccia debris flows and monolithic, matrix supported, lapilli tuff to breccia pyroclastic flows.

The Cedartree Lake formation overlies the Emm Bay formation. It is composed entirely of distal plus epiclastic facies deposits. These units consist of predominantly fine pyroclastic rocks with minor interbedded coarse deposits. A member of the Cedartree Lake formation consisting of thick to thin bedded arenite, wacke, chert and fine ash flow deposits occurs in the eastern Cedartree area.

The latter part of the volcanic cycle is represented by thin units of Volcanogenic sediments (Siltstone and graces) and by felsic and partially bedded ash flows. As is typical for other Archean terranes, the supracrustal volcanics and sediments are intruded by quartz porphyry dykes and plugs and by late diabase dykes. The majority of the felsic dykes are found associated with the lower mafic meta-volcanics while the diabase dykes cut across the entire stratigraphic package. The entire Complex is bounded to the west by the Aulnean Batholith, to the south by the Sabaskong Batholith and to the northeast by the regional Pipestone-Cameron Lake Fault" (Pitman, 1997).

Mineral occurrences of gold have been documented on the Ontario Mineral Inventory (OMI) database for this Property with base metal occurrences to the north and beyond the Property. Detailed geological maps showing these sites on the Property can be found on Ontario government Geological Maps M2421, M2447, M2319 and P831. Figure 21 also shows some of these occurrences. Figure 14 shows the 3 gold occurrences along the Kakagi Lake Shear.
.

Known mineralization on the property relates to gold mineralization along east-west shears and anomalous nickel associated with mafic and ultramafic sills of the Kakagi Lake group. An unknown style of gold mineralization with reported visible gold in the area of Peninsula Bay was not located.

Five occurrences, described below, are shown in the Ontario Mineral Inventory (OMI) records of the MNDMNRF within the Martin Kenty Property. These are:

1. Martin F.M. Occurrence, Au
  OMI Number: MDI52F04NW00023; **Other Deposit Names:** F.M. Martin - 1974, Hay Island - 1973

2. Kakagi Lake Occurrence, Au, Ag (secondary)
OMI Number: MDI52F04NE00012; **Other Deposit Names**: Kakagi Lake - 1944, Roy Martin Occurrence - 1944, East Island - 1944

3. Roy Martin East Occurrence, Au
  OMI Number: MDI52F04NE00005; **Other Deposit Names:** Roy Martin East – 1944.

4. Mongus Lake Ocurrence, Au
 OMI Number: MDI52F04NW00021 **Other Deposit Names:** Mongus Lake - 1983

5. Mongus Lake North, Ni
 OMI Number: MDI000000002082 **Other Deposit Names:** Mongus Lake North - 2010
Status: DISCRETIONARY OCCURRENCE

The first 3 of these occurrences occur along the Kakagi ake Sheae and are shown in Figure 14.

Further details on these occurrences are described below.

Photo 1: Kakagi Lake Shear *striking 85° along the south shoreline of Hay Island in the area of the Martin F.M. Occurrence showing steeply dipping rusty and sericitic schist.*

1. F.M. Martin Occurrence, Au

Work Undertaken

1973: the area was mapped by the Ontario Department of Mines and samples were taken.

1974: Property was optioned by R. Martin to a joint venture consisting of Noranda, Newconex, and Tombill Mines. Geological mapping was conducted.

1975: the joint venture conducted geophysical surveys and drilled 7 DDH totalling 614.5m. One of these DDH was on Hay Island.

1982-3: Barrier Reef Resources Ltd. drilled 7 DDH totalling 1181.7m along East and Hay Islands, and conducted a lake bottom sediment survey. Some of this work was within the F.M. Martin Occurrence. See Item 6 of this report for further details on the past work done and the assessment AFRI work files on file with MNDMF namely: 53F04NW0118, 53F04NW0119, 53F04NW0134, 52F04NE0031, 52F05SW0093 and 52F04NE0028. See also Item 9.1 and 12 for work undertaken by the Issuer.

Lithology and Mineralization

The host rock in the area consists of east-west steeply dipping felsic and intermediate metavolcanics. Mineralization occurs along a sericitized and silicified east-west schist (The Kakagi Lake Shear) often associated with pyrite. A quartz feldspar porphyry dyke was also noted in some areas along the shear.

ODM Map P.921 sidenotes (Kaye, L. 1974) gives a statement of this occurrence that states:

"*Two of the author's grab samples taken from a strong vertically dipping rusty schist zone exposed on the southeastern shore of the island near the East Central boundary of the map area, (FM Martin claim) were analyzed by the Ministry Research Branch Ontario Division of Mines and yielded 0.34 ounce and 0.04 ounce gold per ton respectively (11.66 and 1.37g/t Au). The schist zone which is about 15 feet (4.6 meters) wide and is traced for 150 feet (45.7 meters) strikes generally N 85° E and lies within a broad zone of shearing that is in the hinge of Blacky Bay Syncline. In the light of current interest in large-tonnage, low-grade gold deposits (this gold occurrence is extremely interesting) and strong shear and schist zones that are associated with fold and fault structures in the map area merit further investigation*".

Note: The above grade and tonnage of <u>The F.M. Martin Occurrence</u> is considered historic and the qualified person of this report has been unable to verify the information and that the information is not necessarily indicative of the mineralization on the property that is the subject of the technical report; furthermore a qualified person has not done sufficient work to classify the historical estimate as current mineral resources or mineral reserves; and the issuer is not treating the historical estimate as current mineral resources or mineral reserves.

In addition to the above, past diamond drill results described in Item 6 and Figure 14 revealed: DDH LK-91-01 assayed 638 ppb Au (0.64 g/t) from 361.5-362.5 ft (110.19-110.49m) (AFRI 53F04NW0118), DDH MC 75-4 assayed 0.21 opt (7.2 g/t) from 231-236 ft (70.41m) (AFRI 53F04NW0134), and Barrier's DDH-4 assayed 2414 ppb (2.41 g/t) over 14 ft (2.27m) (AFRI 52F04NE0031).

Two additional prospecting sampling campaigns by BG were undertaken in this area by BG. This work will be submitted in a separate assessment report later.

Photo 2: Old trench at the west end of Hay Island at the Kakagi Lake Au Occurrence.

2. Kakagi Lake Occurrence, Au, Ag (secondary)

Work Undertaken

1944: Gold was discovered on the west end of East Island by Noranda prospectors. Trenching and sampling was conducted.

1974: the property was optioned by Roy Martin to a joint venture consisting of Noranda, Newconex, and Tombill Mines. The JV conducted geological mapping.

1975: the joint venture conducted geological surveys and drilled 7 DDH totalling 614.5 m (6 of the holes were on the East Island showings).

1983: Barrier Reef Resources drilled 7 DDH totalling 1181.7 m across Hay Island, East Island, and the intervening lake bottom. A lake bottom survey was carried out to detail the topography and recover lake sediment samples.

1986: Laramide Resources Ltd. conducted trenching and sampling.

1987: Laramide conducted magnetometer, VLF-EM, and IP surveys.

1990: Rio Algom and Laramide Resources drilled 1 DDH totalling 310 m.

See Item 6 of this report for further details on the past work done and the assessment AFRI work files on file with MNDMF namely: 52F04NE0012, 52F04NE0031, 52F04NE0007, 52F04NE0033, 52F04NE0011, 52F04NE0044, 52F05SW0093, 52F04NE0006. See also Items 9.1 and 12 for work undertaken by the Issuer.

Lithology and Mineralization

The lithology and mineralization of the Kakagi Lake Occurrence was very similar to that of the F.M. Martin Occurrence, both being along the Kakagi Lake Shear.

Oct 27, 2017 - Grab samples from west end of East Island returned up 0.62 opt Au (21.126 g/t) quoted from Assessment File 52F04NE 0012, trench TR-86-03, sample 23976, R.M. Blais 1987 (see figure 18 of this report, trench 3 is located near trenches 1, 2, and 4).

Oct 27, 2017 – OMI MDI15F04NE00012 (Therese Pettigrew) - Three trenches from 1944 were reported as follows: Trench No. 1: 0.30 opt (10.29 g/t) Au over 11.5 ft (3.50m); Trench No. 2: 0.16 opt (5.49 g/t) Au over 14 ft (4.27m); Trench No. 3: 0.15 opt (5.14 g/t) Au over 18 ft (5.49m). Mapping by the OGS has outlined a strong zone of shearing and deformation extending from Hay Island, through East Island to the mainland, a distance of about 3 miles that includes the known gold showings. DDH MC 75-3 intersected the zone 70 ft west of the No. 1 trench and 200 ft below the surface. The zone yielded 0.33 opt (11.31 g/t) Au over 5 ft (1.5m). A zone of pyrite mineralization is located beneath the western end of East Island. Pyrite occurs in the tuffaceous matrix of slightly siliceous intermediate to felsic lapilli tuffs in the form of medium to coarse grains 1 to 3 mm in diameter, and as very finely disseminated grains. The pyrite comprises from 5 to 20% of the rock and averages 10%. Concentrations of pyrite are found along the outer boundaries of lapilli fragments and as isolated aggregates. The fragments contain little or no pyrite. The pyrite-rich zone extends for at least 240 feet (73.15m) near surface on the west end of East Island. The zone strikes 080° and dips 80° to 85° to the north. The gold-bearing zone lies within the pyrite-rich zone and has a strike length of 150 ft, terminating at the end of the island and pinching out to the east along with the pyrite-rich zone. Partial alteration of the rocks occurs in the form of sericitization, carbonatization, and minor silicification and chloritization. Sericitization is the most common occurring as films of sericitic minerals along foliation planes and paper-thin sericitic partings parallel to the local foliation. Narrow quartz and quartz-carbonate veins occur at random intersecting all rock types. They average 1 to 4cm in width and exhibit no preferred orientation. Carbonate content varies from trace amounts to 30%. The veins are typically barren of sulfides. Locally, inclusions of country rock within the veins carry minor pyrite. Barrier Reef's 1982-83 drill program outlined a more or less continuous zone with an average true thickness of 100 feet (30.5 m) and an average gold concentration of 300 ppb along a strike length of 6500 ft (1981.2 m). The gold-bearing unit is a near vertical bed of felsic to rhyolitic lapilli tuff containing up to 2% banded and disseminated pyrite (AFRI 52F04NE0031). Edwards (1980) collected 5 chip samples from Trench #2. The samples returned assays ranging from trace up to 0.47 opt (16.15 g/t) Au and 0.22 opt (7.54g/t) Ag.

Note: The above grade and tonnage of <u>Kakagi Lake Occurrence</u> is considered historic and the qualified person of this report has been unable to verify the information and that the information is not necessarily indicative of the

mineralization on the property that is the subject of the technical report; furthermore a qualified person has not done sufficient work to classify the historical estimate as current mineral resources or mineral reserves; and the issuer is not treating the historical estimate as current mineral resources or mineral reserves.

3. Roy Martin East Occurrence, Au

Work Undertaken

Work undertaken on this occurrence was in concert with the work undertaken on the Kakagi Lake Occurrence described above.

See Item 6 of this report for further details on the past work done and the assessment AFRI work files on file with MNDMF namely: 52F04NE0012, 52F04NE0332, 52F04NE0015, 52F04NE0004, 52F04NE0031, 52F04NE0011, 52F05NE0044, 52F04NE O-3, 52F04NW S-1, and 52F04NW S-2. See also Items 9.1 and 12 for work undertaken by the Issuer.

Lithology and Mineralization

The lithology of this occurrence consists of sheared felsic & intermediate volcanics occurring along the Kagagi Lake Shear.

10/27/2017 (T Pettigrew) - The best assay in Trench #6 was 754 ppb (0.754 g/t) Au over 5 ft (1.52m) (AFRI 52F04NE0012). DDH 12 from Barrier Reef Resources 1983 drill program assayed 1120 ppb (1.12 g/t) Au over 5 ft (1.52m) from 165-170 ft, 2100 ppb Au over 5 ft from 395-400 ft, and 2800 ppb Au over 5 ft (1.52m) from 485-490 ft (50.30-149.35m) AFRI 52F04NE0332). The highest assay from Rio Algom's DDH KL-91-06 was 357 ppb (0.357 g/t) Au from 71.5-72.6 m (AFRI 52F04NE0004). See figures 13, 14 and 15 for the locations of the above work.

Note: The above grade and tonnage of <u>**Roy Martin East Occurrence**</u> **is considered historic and the qualified person of this report has been unable to verify the information and that the information is not necessarily indicative of the mineralization on the property that is the subject of the technical report; furthermore a qualified person has not done sufficient work to classify the historical estimate as current mineral resources or mineral reserves; and the issuer is not treating the historical estimate as current mineral resources or mineral reserves.**

Photo 3: Rusty gossan boulder *with up to 40% interstitial pyrite in brecciated silicified intermediate volcanics.*
Peninsula Bay Area believed to be near the Mongus Lake Au, Cu discretionary occurrence.

4. <u>Mongus Lake Occurrence Au, Cu</u>

Work Undertaken

1969: Canadian Nickel Company Ltd. drilled several holes in the area of Peninsula Bay located at the west side of the property. This work is described in AFRI work file 53F04NW0135.

Lithology and Mineralization

Two locations are given for this discretionary occurrence, one, a surface site (the Mongus Lake Occurrence), and another in drill core (the Burnt Occurrence).

Lithology Comments
10/27/2017 (T Pettigrew) - Ferguson et al. (1971) MDC013, p.240:
describe the surface showing as felsic metavolcanics intruded by diorite and cut by quartz veins striking east and dipping N70°E with some pyrite, chalcopyrite and visible gold. The surface showing is labeled as the Mongus Lake Gold Occurrence.

Mineralization Comments
10/27/2017 (T Pettigrew) - Beard and Garratt (1976) MDC016, p.11, 26: describe the mineralization as pyrite, chalcopyrite and visible gold. Diamond drilling in hole 32875 indicated relatively high-grade assays over narrow widths. The diamond drill hole is labelled the Burnt Occurrence. It is also described as being located about ½ mile N of Kakagi Lake and 1 mile W of Mongus Lake.

Note: Some confusion exists on the location of this site. The OMI reference relates the gold to a later 3 hole drill program (OMI #53F04NW0135), specifically Hole DDH 32875, drilled in 1969. No logs were found on this hole. Note the OMI locate and drill hole 32875 do not match. The original locate from MDC 013, is: Lat 49° 00', Long. 93°45' while the OMI locate is: Lat 49° 14' 25.64", Long -93° 49' 16.92". Unfortunately, during the author's site visit, despite finding a gossanous zone with very low Au values, the original site was not located. It should be noted that the casing was pulled after drilling. Figure 21 shows the location of this occurrence.

5. Mongus Lake North, Ni

2010: Metalore Resources Ltd. conducted prospecting and sampling as described in AFRI 20000007673.

Lithology Comments
May 04, 2017 (C RAVNAAS) - Pyroxenite - Coarse grained, beige gray weathered, dark gray fresh, no noticeable sulfides (Kenora AF 52F05SW, LLLL-10, 2.49609, Metalore Resources ltd., pg.9).

Mineralization Comments
May 04, 2017 (C RAVNAAS) - Metalore grab sample 262265 assayed 939ppm (.094%) Ni (Kenora AF 52F05SW, LLLL-10, 2.49609, Metalore Resources Ltd., pg.16)

Note: Most of this assessment work (AFRI 20000007673) occurred to the north of the Property and was not shown in the AFRI historic work of this report, however a single grab sample collected to the north of Monger Lake (and currently within the Property) was the justification for this discretionary occurrence. It should be noted that serpentine, a frequent alteration product of olivine rich rocks, can contain up to 0.36% Ni. Figure 21 shows the location of this occurrence.
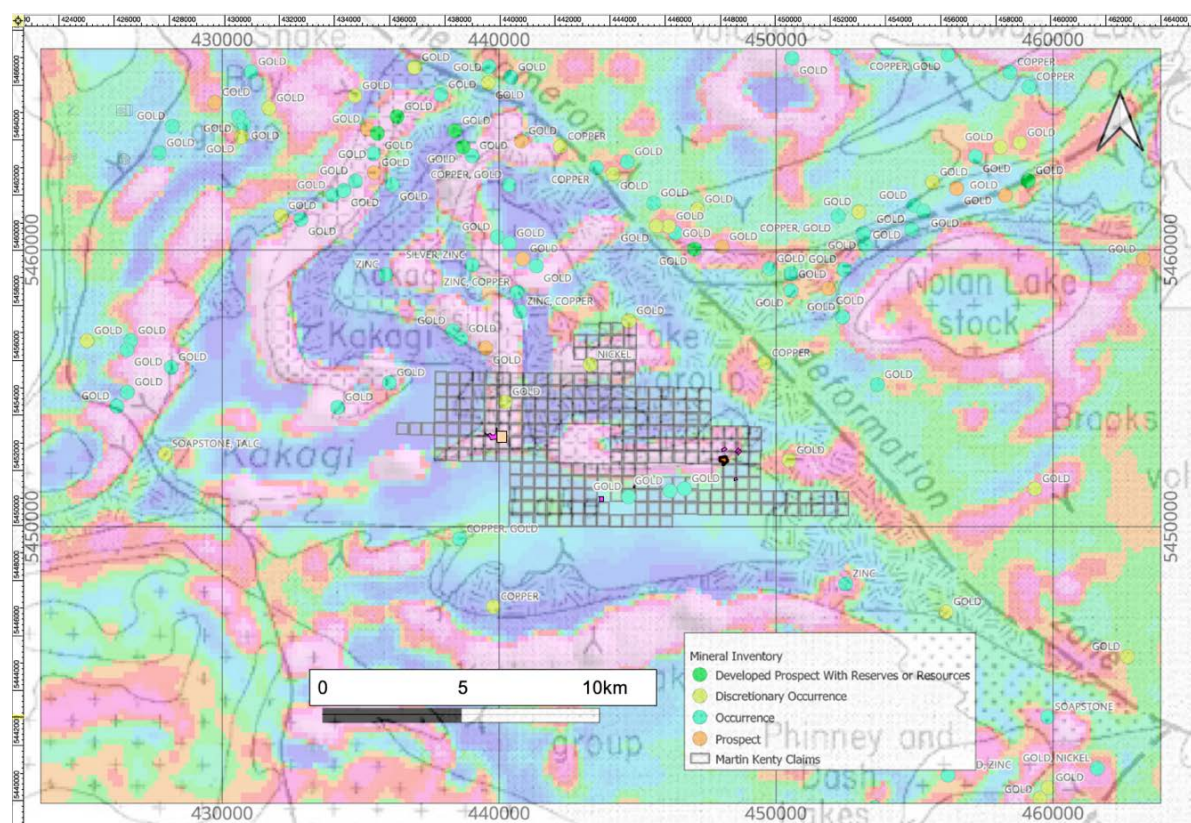
Figure 21: Ontario Mineral Inventory Locations by Commodity showing the Kakagi-Rowan Lakes Greenstone Belt and structural elements with the Property outlined, overlain with 1st Derivative magnetometer survey data. Note the occurrences of gold showings along structural elements and along the intrusive contacts. Basemap sources: Geology: Blackburn C.E., et al.1991, 1st derivative magnetics: OGS 2117, magnetic supergrids.

Item 8 Deposit Types

Gold mineralization is the primary commodity sought on this property, followed by possible Cu, Zn volcanogenic massive sulphides (VMS), nickel and potential PGM mineralization. See Figure 21 for the distribution of various occurrences on the property and in the area.

8.1 Gold Mineralization

For a review of the grades and distribution of gold on the Property see Item 7.2.

Mineral deposit circular MDC 016 (Beard, R. et al.) recommends, on page 4, the following 5 geological settings for gold prospecting in the Kenora-Fort Frances area.

1. Areas of high-level granitic intrusives genetically related to felsic volcanism. These intrusives are typically quartz and/or feldspar porphyries. Narrow sills of porphyry are of special interest, as are relatively small stocks within or closely associated with volcanic belts. Larger granitic batholiths not genetically related to volcanic belts are usually of little interest.

2. Felsic pyroclastic horizons, especially very fine-grained felsic tuffs.

3. Sericite and carbonate bearing shear zones containing gold mineralisation remobilized into favorable structures often associated with pyrite.

4. Narrow horizons of volcano-chemical sediments (sulphides, chert, carbonate, graphite) within felsic to intermediate volcanic sequences.

5. Mafic meta-volcanics containing significant quartz carbonate veins.

The gold mineralization is believed to be a late emplacement event and introduced during the Neoarchean time between the ages of 2716 +/- 2 Ma and 2709 +/- 2 Ma and at relatively the same time across extremely large areas of the Superior Province (Breakhouse, G. 1991, p.368).

In the area of the Property a major east-west shear across several islands (the Kakagi Lake Shear Zone) hosts gold mineralization along the geologic setting of number 3 above.

Downie, Ian, 1990 (AFRI # 52F04NE0001) on page 5 discusses this gold mineralized east-west shear across Hay and East Islands in Kakagi Lake and states:

"The "unit" is interpreted as being deformed by easterly striking, major isoclinal folding. A strong foliation (interpreted as shearing) is imposed and faulting is quite common.

The ODM interprets the foliation/shearing as indicative of a "deformation zone" which can be interpreted as a branch or splay stemming from the Cameron Lake Fault Zone. It is shown to extend eastward from Rowan Lake to Lake of the Woods. The known values associated with the deformation zone attracted the attention of RAE.

Geological investigations by the writer, H. Klatt, R. van Ingen, and detailed investigation by K. Kivi suggested that the sequence of immediate interest is not strongly sheared: Thin section work (J. Balinski of GEOPROCESS) reveals that primary fabric and grain are clearly evident. Alteration is most probably due to chemical processes rather than the action of strong, structural forces.

A previously unrecognised quartz diorite to leucocratic diorite runs parallel to the zone along most of its length. The horizon of main interest is composed of intermediate to felsic tuffs, and there is some thought that the "felsics" are in some, and even large measure, silicified intermediate rocks.

Some of the rock is quartz porphyritic and feldspar porphyry is seen.

Silicification is prevalent and sericite nearly ubiquitous. Pyrite is common and concentrations thought to be coeval with silicification. Pervasive silicification with

strong pyritization and tourmalinization are present at the west of East Island-the zone of best gold values. Iron carbonate (ferrous dolomite) is common.

Some gold values are noted at the contact of volcanic rocks with quartz-diorite which are locally intruded by differentiated basic to ultrabasic sills. All units are strongly affected by large scale east-trending tight isoclinal folds which plunge north to northeast. Shearing is common and faulting is widespread. Volcanics are found on the West part of the large island immediately north of Hay Island. In addition, similar rocks occur in an east to north-easterly trend band near the East End of the property. Areas of metamorphose mafic to ultramafic intrusive rocks are found on the island north of Hay Island. Shearing is common on the property. Recent mapping by the Ontario department of Mines has outlined a strong zone of shearing and deformation extending from Hay Island through East Island to the mainland, a distance of about 3 miles. The presently known gold showing lies on claim number K 896127. A fourth showing is located on strike approximately 4 miles West of the Bay Island occurrence and vicinity of Blacky Bay on Chase Point Peninsula. Associated with the shear zone and gold showings are a series of felsic quartz and feldspar porphyry sills. These sills appear intermittently along the shear zone and are metamorphosed to about the same degree as their volcanic host rocks.

The 1983 drilling program carried out by Barrier Reef Resources Ltd. of Vancouver, B.C. explored an east-west shear zone with a strike length of 6500 feet across a maximum width of 1000 feet. This shear zone contains a gold bearing zone that appears to be a bed of volcanic-sedimentary material identified principally by its gold and pyrite content. Most of the gold bearing zone is covered by lake water and the geological interpretation is based on drill core from this program the new 44 claim group explored by Laramide Resources Ltd. only covers the east half (3000 feet) of previous 1983 strike length. The 3000 foot strength length includes diamond drill holes 1, 2, 3, 5, 6, 7, 9, 12 and 13. For complete details of the 1983 drill program, refer to the summary report dated April 20th 1983 by R M Blais P.Eng. filed at Kenora Ontario.

The explored area is underlain by an assemblage of Archean volcaniclastic rocks. Low grade metamorphism has produced textures ranging from weak foliation with stretched fragments to strongly foliated schist band. The average strike is N 85 degrees east with dips of 85 degrees N to 90 degrees. The isoclinal fold platter pattern is not well known so the local stratigraphy top and bottom has not been determined.

The volcanic sequence is divided into two general parts: a group of mafic to intermediate volcanics (intermediate group) to the north and a group of felsic to intermediate metavolcanic (felsic groups) to the south. Textural and compositional variations of these units were detailed when logging the core. These variations are more prevalent in the felsic units.

Within the Felsic group, adjacent to the Intermediate group contact, is located a <u>gold bearing zone</u> approximately 200 feet in average width. The richest part of this zone carries <u>300 ppb gold over an average width of 100 feet</u> it is composed of felsic

to rhyolitic clastic material sparsely flecked with fuchsite mica and up to 25% banded and disseminated pyrite.

Bands of Quartz Sericite Schist (QSS) locally divide the Felsic group and intermediate groups. The shist band appears to be structurally controlled and partly overprints itself on the gold bearing unit.

An apparently concordant sill which has been called quartz feldspar porphyry QFP appears intermittently along the gold bearing zone. It has a coarse granitic texture, composed of K-feldspar quartz and hornblende. It is well altered and can only be seen plainly in hole #9. Elsewhere it is broken down by metamorphism to quartz-sericite schist with a spotted amphibole texture noted in the drill log as "remnant QFP."

The purpose of the 1986 summer exploration program and the 1987 winter geophysical service was to further explore and define this shear and gold bearing zone and related parallel zones along its strike length from East Island to the first service is showing at Roy Lake".

Other varieties of gold mineralization are discussed in Item 22, Adjacent Properties. It is possible some of these other styles of gold mineralization may also be found on the Martin Kenty Property.

8.2 Volcanogenic Massive Sulphide (VMS) Mineralization

No known VMS occurrences have, at this time, been found on the Martin Kent Property, however The Weisner Lake Cu-Zn occurrence is located just to the north of the Property. Similar volcanic host rocks exist on the property and from the Geophysical interpretation of Hornby Bay Exploration Limited (see Figure 16) several conductors in this area exist on the Property.

A general description of VMS mineralization is described below.

"Volcanogenic massive sulfide VMS deposits also known as volcanic associated, volcanic hosted and volcano sedimentary hosted massive sulfide deposits are major sources of zinc, copper, lead, silver and gold and significant sources for cobalt, tin, selenium manganese, cadmium, Indium, bismuth, tellurium, gallium and germanium. They typically occur as lenses of polymetallic massive sulfide that form at or near the seafloor in submarine volcanic environments, and are classified according to base metal content, gold content or host rock lithology. As of 2007, there are close to 350 known VMS deposits in Canada and over 800 known worldwide. Historically they account for 27% of Canada's copper production, 49% of zinc, 20% of its lead, 40% of its silver and 3% of its gold. They are discovered in submarine volcanic terrains that range in age from 3.4 Ga to actively forming deposits in modern seafloor environments. The most common feature among all types of VMS deposits is that they are formed in extensional tectonic settings, including both oceanic sea floor spreading and arc environments. Most ancient VMS deposits that are still preserved in the geological record formed mainly in

oceanic and continental nascent-arc, rifted arc, and back-arc settings. Primitive bimodal mafic volcanic-dominated oceanic rifted arc and bimodal felsic-dominated siliciclastic continental back-arc terranes contain some of the world's most economically important VMS districts. Most but not all, significant VMS mining districts are defined by deposit clusters formed within rifts or calderas. Their clustering is further attributed to a common heat source that triggers large-scale subsea floor fluid convection systems. These subvolcanic intrusions may also supply metals to the VMS hydrothermal system through magmatic devolatilization as a result of large-scale fluid flow. VMS mining districts are commonly characterized by extensive semi-conformable zones of hydrothermal alteration that intensifies into zones of discordant alteration in the intermediate footwall and hanging wall of individual deposits. VMS camps can be further characterized by the presence of thin but areally extensive, units of ferruginous chemical sediment formed from exhalation of fluids and distribution of hydrothermal particulates." (Galley, Alan G., et al, 2007, pg. 141-161).

8.3 Nickel PGM Mineralization

The presence of gabbroic and ultramafic rocks of the Kakagi Group offer the potential for hosting both nickel, copper and PGM mineralization. The Mongus Lake North Ni Occurrence with anomalous nickel illustrates this.

Figures 22 - 25 show images of anomalous elements of platinum, nickel, gold and palladium in a lake sediment study conducted over the area of the Property and surrounding area. (Dyer et al. 2006)

The presence of 2 clusters of Ni anomalous lakes, one centered on Cedartree Lake, the other in the Wicks/Weisner Lake area; the latter includes the highest Ni value of the survey (150 ppm) at site 1459. Despite the lack of known nickel occurrences on the Property according to the Ontario Mineral Inventory (OMI) (OGS 2004), the lake sediment geochemistry in association with the presence of gabbroic rocks suggests good potential for Ni mineralization. (Dyer et al.2006 p. 14) The Kenbridge nickel mine of Tartisan Nickel Corp. located 12.5km to the North and outside of the Property is an example of a significant accumulation of nickel and copper in these rocks.

Additional anomalous lake sediment values for platinum, gold and palladium along with nickel show a correlation with the gabbro and ultramafic rocks.

Figure 26 shows a large gravity anomaly surrounding the Property. This suggests a large volume of heavy rocks suggestive of mafic and ultramafic rocks. Both potential source rocks for nickel, copper and PGMs. This large anomaly could represent an intrusive with the capacity to hold significant amounts of nickel or PGMs.
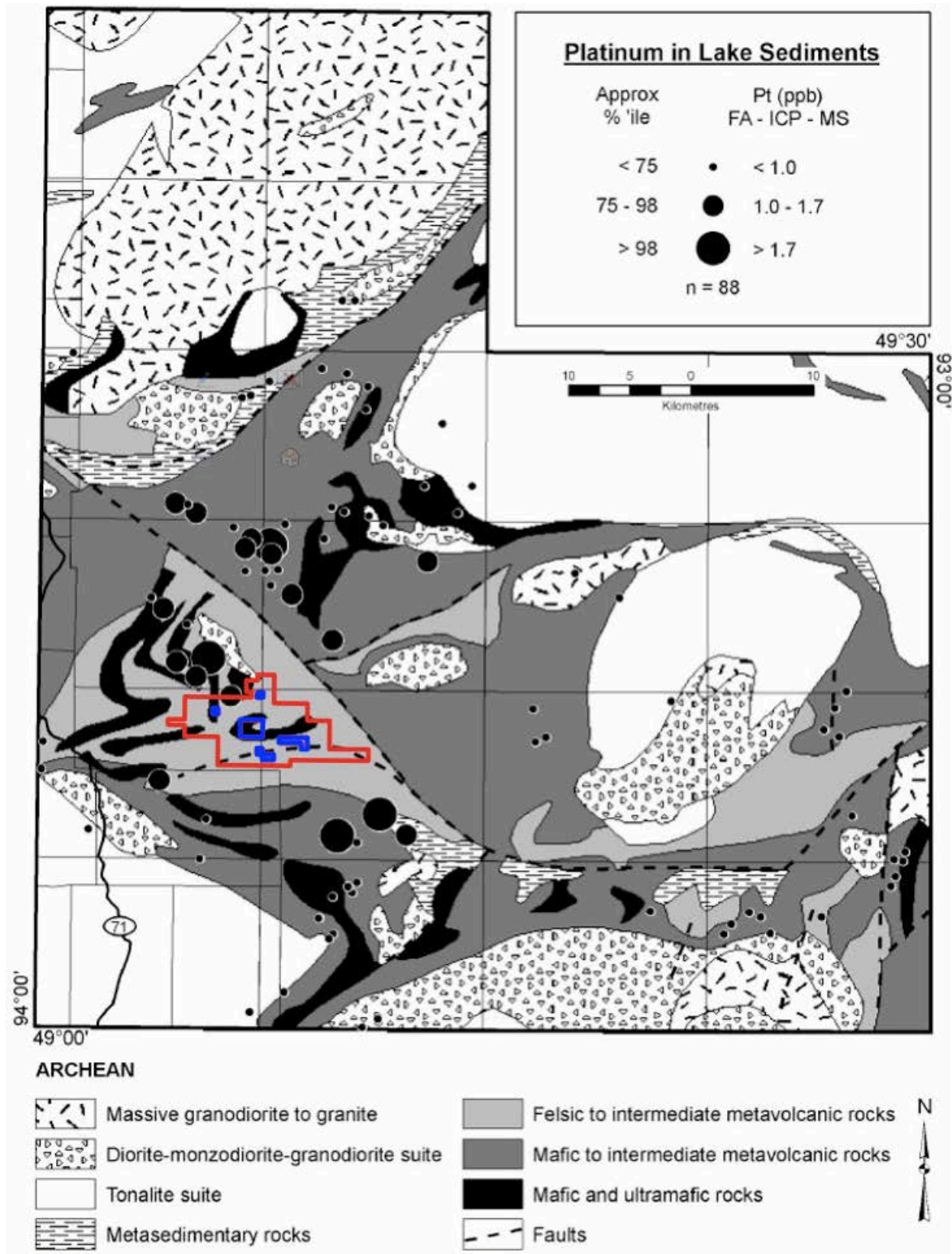
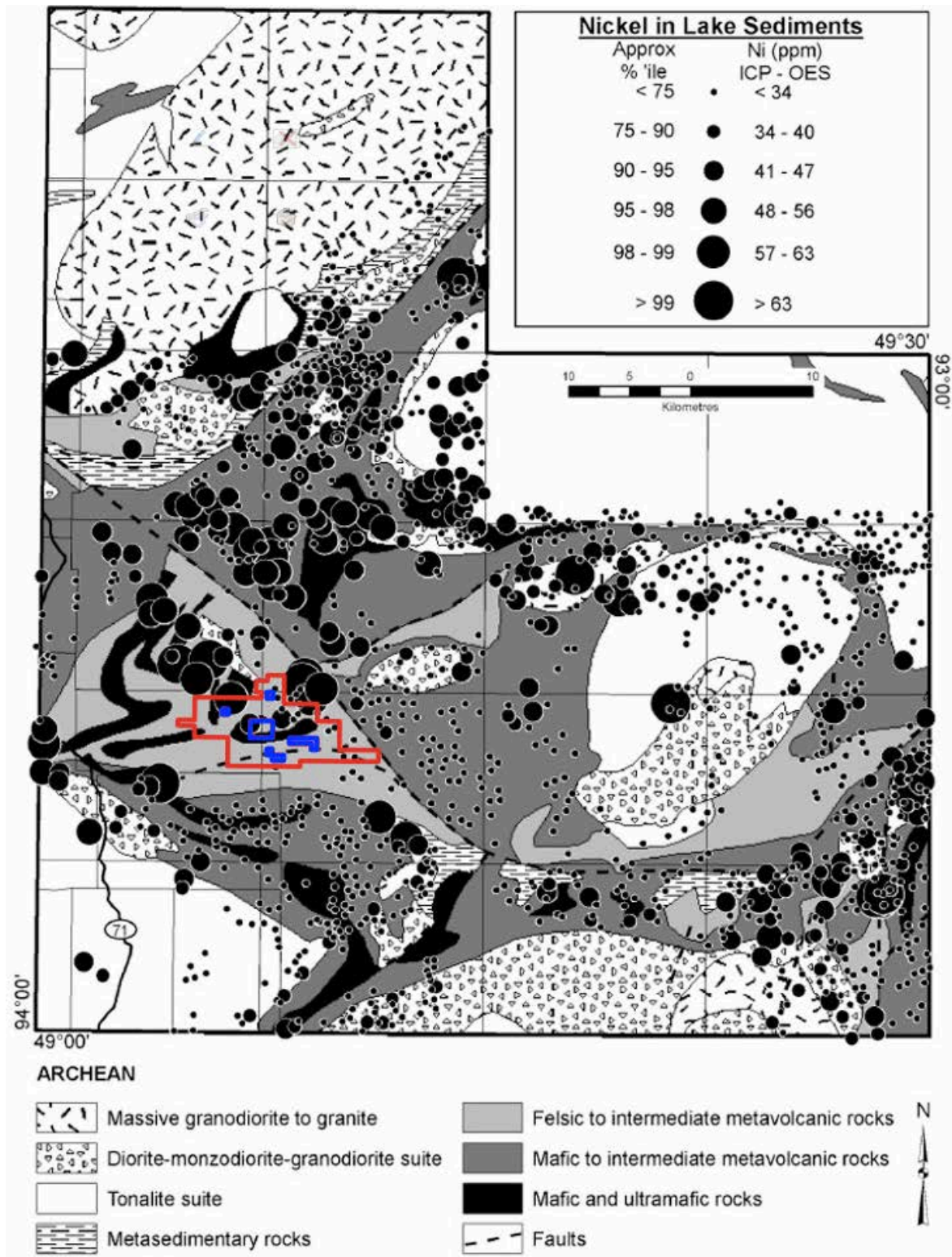**Figure 22: Platinum in Lake Sediments** *Source: Dyer et al. OFR 6188 (2006?)*

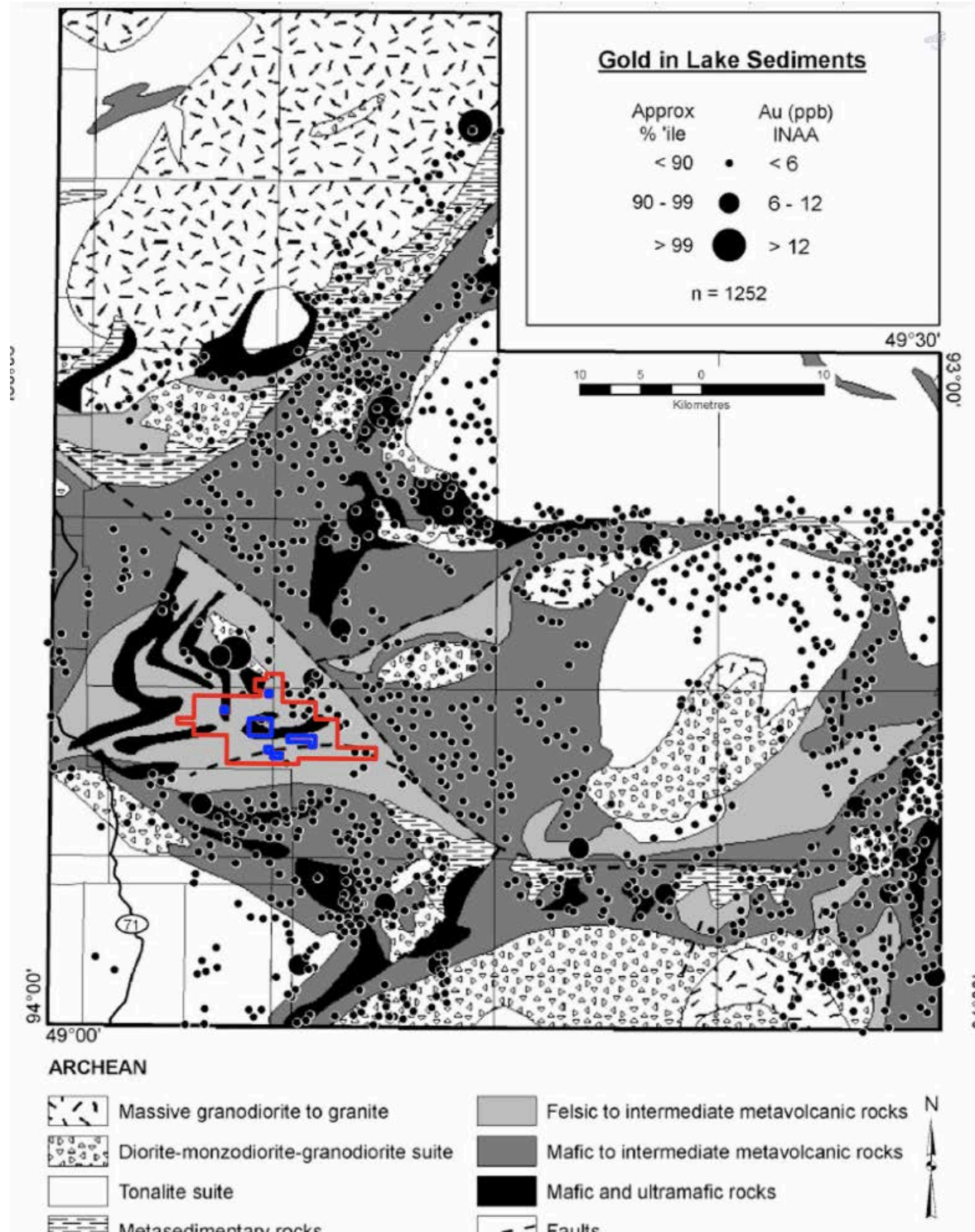***Figure 23: Nickel in Lake Sediments*** *Source: Dyer et al. OFR 6188 (2006?)*

Figure 24: Gold in Lake Sediments Source: Dyer et al. OFR 6188 (2006?)
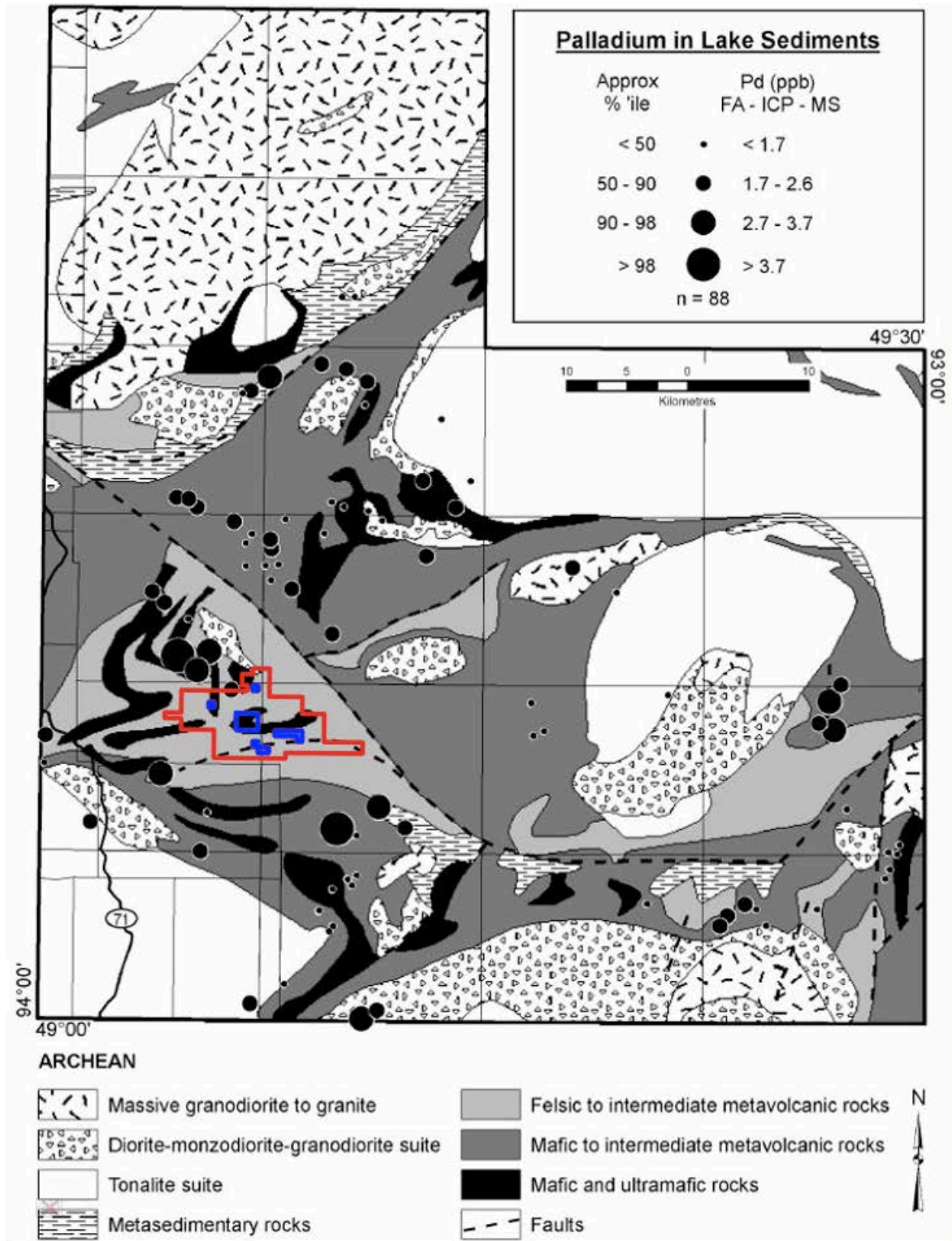
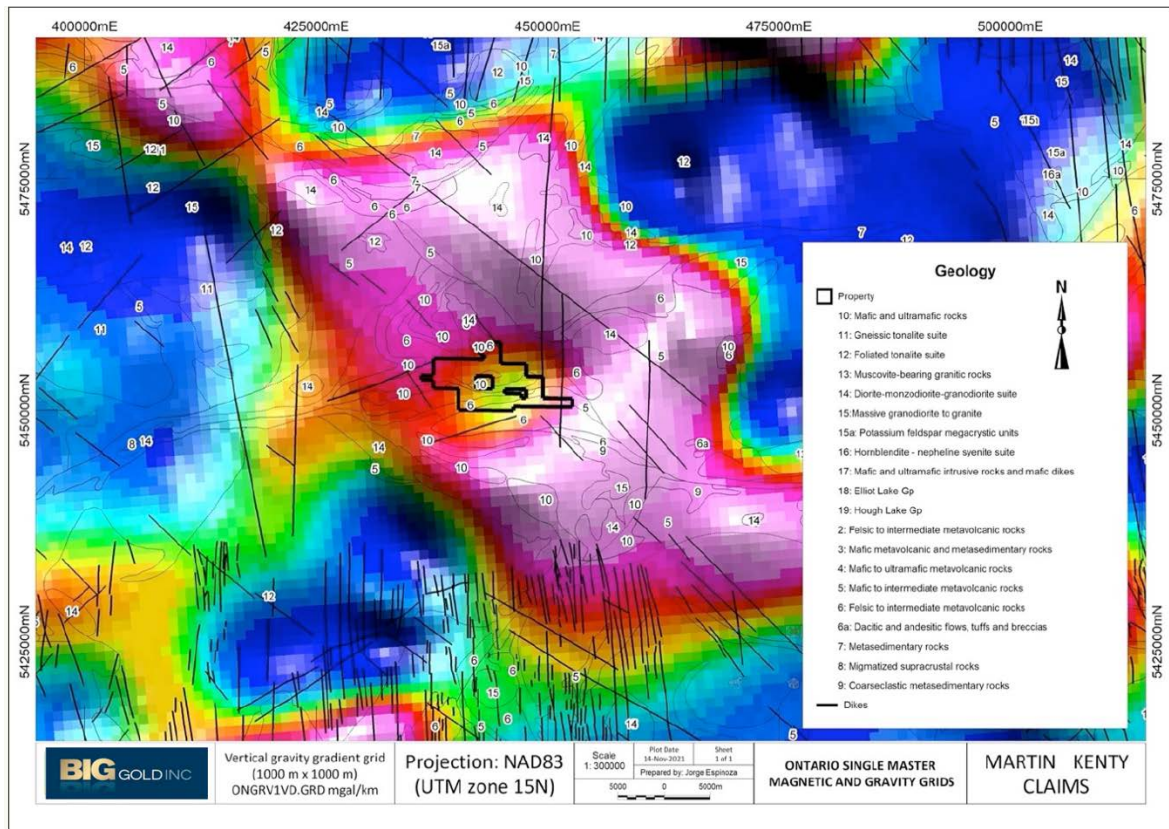**Figure 25: Palladium in Lake Sediments** Source: Dyer et al. OFR 6188 (2006?)

Figure 26: Vertical Gravity Map illustrating a very large area underlain with high density rocks, possibly gabbro and peridotite, potential suitable hosts to Ni, PGE mineralization.

Item 9: Exploration

Exploration by BG since its acquisition of the property has included:
1) May 19, 2021: a cursory prospecting examination,
2) July 12 -18, 2021: a prospecting field site visit by the author,
3) Oct. 7- Dec. 2021: a helicopter Geotech VTEM and magnetometer survey,
4) Jan 24, 2022, a 3D inversion of the geophysical data undertaken by Douglas H. Pitcher and his team at Technoimaging, Salt Lake City Utah.

9.1 Initial Prospecting Examination

During the May 19, 2021 prospecting examination of the Property, prospectors D. McKinnon and C. Johnson visited: the Martin F. M. Occurrence, the Kakagi Lake Occurrence, and the Roy Martin East Occurrence. An attempt to locate the discretionary Mongus Lake Occurrence was unsuccessful.

A subsequent report of this assessment work will be submitted at a later date.

9.2 Prospecting Field Site Visit

A field site visit was also undertaken by the author and his assistant C. Johnson from July 12-20, 2021. The details of that visit will also be discussed under a later subsequent assessment submission.

9.3 VTEM and Magnetometer Survey

A VTEM Plus and horizontal magnetic gradiometer helicopter survey was conducted by Geotech Inc. over part of the Martin Kenty Property near Nestor Falls Ontario from October 7th to October 27th 2021. The information presented was from the December 2021 Geotech Report.

Principal geophysical sensors included a versatile time domain electromagnetic (VTEM™ Plus) system and a horizontal magnetic gradiometer with two cesium sensors. Ancillary equipment included a GPS navigation system and a radar altimeter. A total of 365 line-kilometres of geophysical data were acquired during the survey.

In-field data quality assurance and preliminary processing were carried out daily during the acquisition phase. Preliminary and final data processing, including generation of final digital data and map products were undertaken from the office of Geotech Ltd. in Aurora, Ontario.

The preliminary processed survey results were presented as the following maps:

- Electromagnetic stacked profiles of the B-field Z Component
- Electromagnetic stacked profiles of dB/dt Z Component
- B-Field Z Component Channel grid
- dB/dt Z Component Channel grid
- Fraser Filtered X Component Channel grid
- Total Magnetic Intensity (TMI)
- Magnetic Total Horizontal Gradient
- Magnetic Tilt Angle Derivative
- Calculated Time Constant (Tau) with Calculated Vertical Derivative of TMI contours
- Calculated Vertical Gradient (CVG) of the total magnetic Intensity (TMI)
- Resistivity Depth Images (RDI) sections, depth-slices, and voxel are presented.

Digital data included electromagnetic and magnetic products, plus ancillary data including the waveform.

The survey report describes the procedures for data acquisition, equipment used, processing, image presentation and the specifications for the digital data set.

The survey area is located approximately 13 km northeast of Nestor Falls, ON

Figure 27: Survey area location map on Google Earth.

The Martin Kenty project was flown in the south to north (N 0° E azimuth) direction with traverse line spacings of 100 metres, as depicted in Figure 27 and 28. Tie lines were flown perpendicular to traverse lines at 1000-meter line spacing. For more detailed information on the flight spacings and directions, see Table 5.

Figure 28: Martin Kenty Project Flight Paths over a Google Earth Image.

Table 5: Flight Survey Specifications

Survey block	Line spacing(m)	Area (km^2)	Planned[1] Line-km	Actual Line-km	Flight direction	Line numbers
Martin Kenty Project	Traverse: 100	34	351	365	N0°E / N180°E	L1000 – L1910
	Tie: 1000				N90°E / N270°E	T2000 – T2030
	Total	34	351	365		

Final results of this survey were released on December 2021.

A total magnetic intensity map is shown below. In addition, a Magnetic Tilt Angle Derivative and a dB/dt Z-Component Calculated Time Constant (Tau) map are also displayed below. The complete report is contained in Appendix 1.
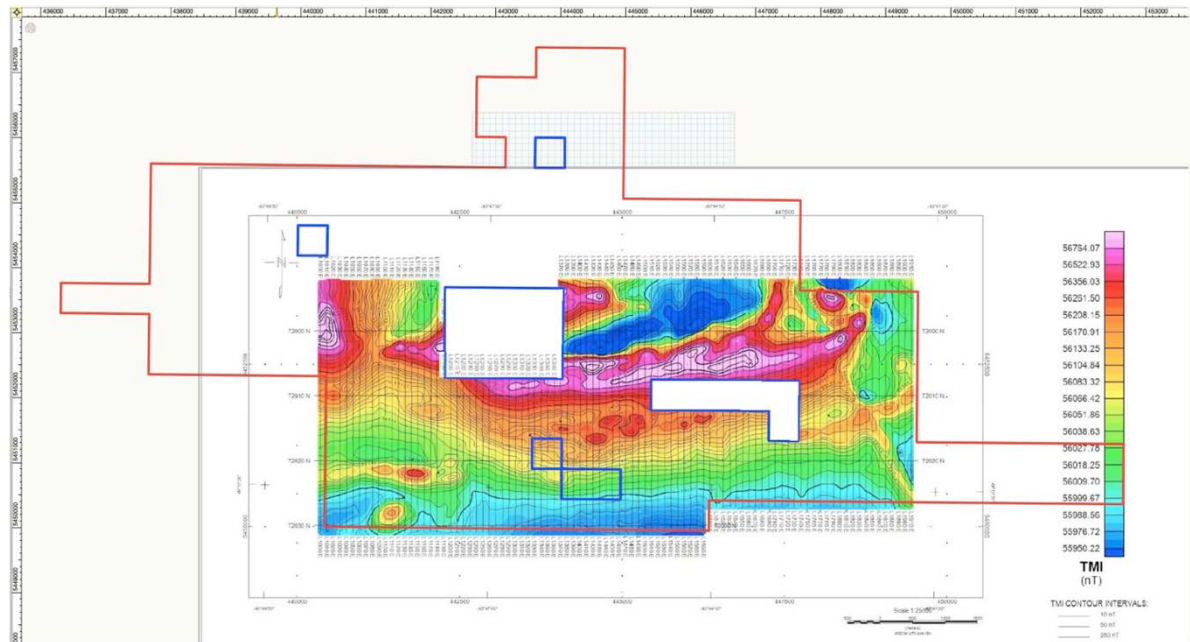
Figure 29: Total Magnetic Intensity (TMI) colour image and contours, showing claim fabric outlined in red. Source Geotech Report December 2021. Co-ordinates are shown in NAD 83 Zone 15N.
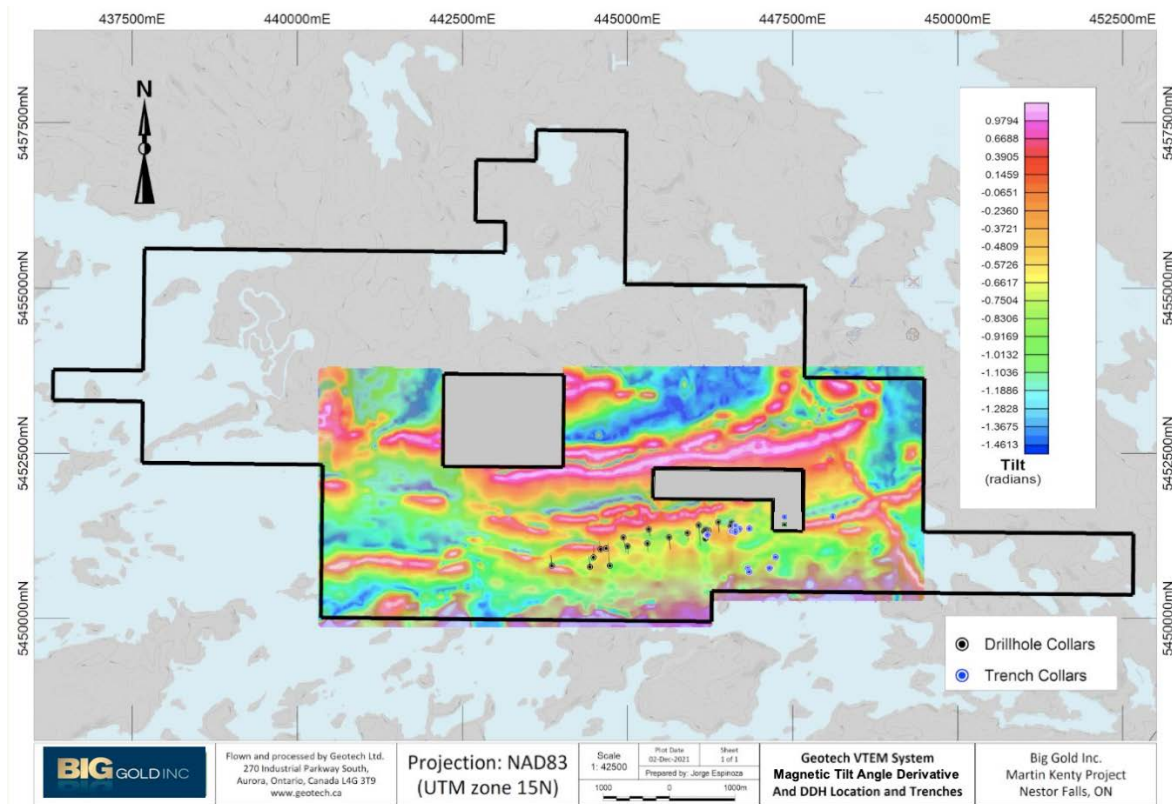
Figure 30: Magnetic Tilt Angle Derivative *showing DDH and trench locations with the Property outline in black. Source: Geotech Report December 2021. Co-ordinates are shown in NAD 83 Zone 15N*
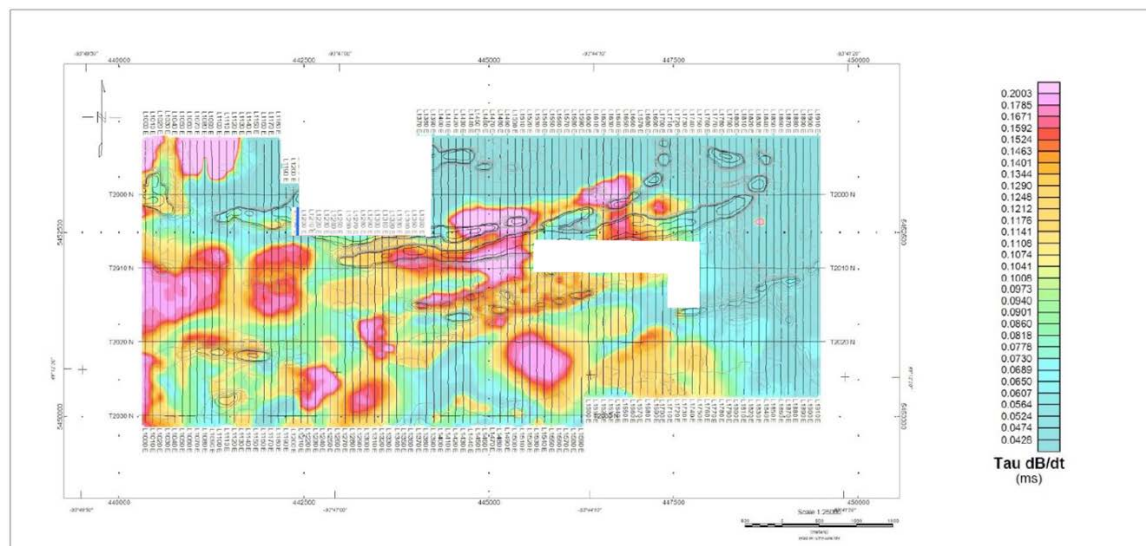
Figure 31: dB/dt Z-Component Calculated Time Constant (Tau) *with Calculated Vertical Gradient (CVG) contours. See Figure 30 above for Property outline. Source Geotech Report December 2021. Co-ordinates are shown in NAD 83 Zone 15N*

Geophysical Data Interpretation
Information acquired from Geotech Report December 2021 - Conclusions and Recommendation

"*Based on the geophysical results obtained, a number of geophysical anomalies have been identified across the Martin Kenty project survey area. Magnetically, the block is active, with a measured range of >2,800nT, and features on a long (>6km), oval-shaped, EW to ENE trending magnetic high unit in the northern half of the block, with pronounced negative response in the center that suggests magnetic remanence. Magnetic derivatives highlight the banded nature of this magnetic high unit, as well as thinner, weaker paralleling lineaments in the southern half of the block. Electromagnetically, the survey area features a number of discrete, short to medium strike length (>0.5-1km), generally EW to ENE trending conductors with weak to moderate conductivities. Maximum dB_z/dt EM TAU decay time constants fall in the 0.2-0.8 msec range. The most conductive features tend to occur in the northern half of the block, including along the main magnetic high trend. Elsewhere, conductors tend to occur in non-magnetic rocks, including conductive bodies in the southern half that occur within the near-surface and are dominantly flat-lying, potentially relating to lake-bottom sediments. The eastern and northern parts of the block host resistive rocks. The relationship between the EM conductors and magnetics is highlighted the EM TAU decay constant image with magnetic CVG contour map (Appendix C) and the RDI resistivity-depth image sections (Appendix G). Based on RDI results, apparent resistivities range from as low as approx. 15-30 ohm-m and also reach highs of approx. 4500 ohm-m. The estimated depth of the top of the anomalous zones is between approximately near surface and 50m depths, and maximum depths of investigation (DOI) vary from ~425m to >550m.*

The Martin Kenty Project lies in the Kenora/Rainy River mining district and is prospective for massive-sulphide hosted gold mineralization (www.biggold.ca/martin-kenty-project/). As a result, both the EM and magnetic results are likely to be of exploration interest. We recommend that EM anomaly picking be performed along with Maxwell EM plate modeling of major anomalies of interest. 1D EM inversions will prove useful in determining the thickness and depth extent of flat- lying conductive units. CET-type magnetic lineament analysis and 3D MVI magnetic inversions will be useful for mapping structure, alteration, and lithology in 2D-3D space across the block. We recommend that more advanced, integrated interpretation be performed on these geophysical data and these results further evaluated against the known geology for future targeting."

9.4 3D Inversion of Geotech's VTEM and Total Magnetic Intensity Data

As a follow up to the recommendations of the Geotech survey report, the VTEM and TMI data collected from the Geotech Survey was further evaluated by Technoimaging of Salt Lake City for Big Gold Inc. This analysis is described below (taken from page 4 of their report – see Appendix 2):

"The VTEM dB/dt data were successfully inverted into 3D conductivity and chargeability voxel models. The TMI data were inverted into both 3D magnetic susceptibility models and 3D magnetization vector (remanent magnetization) models. All four types of inverse models have been provided to Big Gold in the form of 3D voxel files. Several conductive anomalies and separate chargeable anomalies have been imaged, which can be achieved with TechnoImaging's patented inversion methods.

*Processed TMI data were independently fit to **Glass Earth**® magnetic susceptibility and magnetization vector models. TechnoImaging's 3D magnetization vector inversion method is sensitive to both induced and remanent magnetization, whereas traditional magnetic susceptibility inversion methods are sensitive to induced magnetization only. Many features of interest have been brought into focus in the magnetization vector model that are less apparent in the susceptibility model.*

Deliverables include 3D conductivity and chargeability models, 3D magnetic susceptibility models and 3D magnetization vector models in UBC mesh/model format, conductivity, chargeability, and magnetic properties, and this final report.

A list of deliverables is provided below:

1)   *3D volume of conductivity derived from AEM data*

2)   *3D volume of chargeability derived from AEM data*

3)   *3D volume of magnetic susceptibility derived from TMI data*

4)   *3D volume of magnetization vector derived from TMI data*

5)   *Final report in PDF format"*

A significant part of the survey was covered with water and conductive lake sediments. Consequently, the resolution below the conductive lakes is not as good as below islands because the conductive sediments mask the deeper material. Figure 32 illustrates the lake bottom sediment effect as well as the location of 2 conductors C1 and C2 found as a result of this analysis.
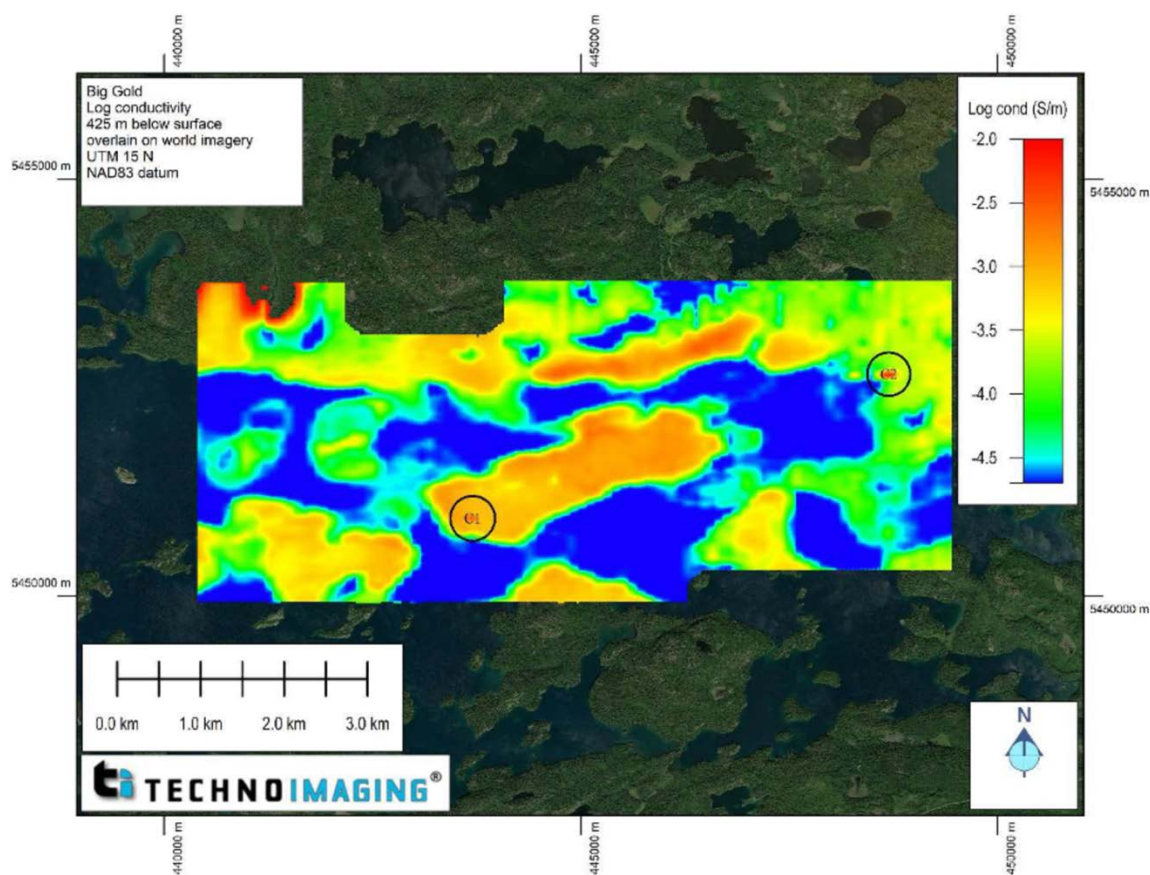
Figure 32: Conductivity Inversion Results *at a depth of 425 m below the surface. The veryresistive areas (cool colors) are likely not well imaged due to the conductive lake bottom sediments shielding deeper material. These results are plotted on a compressed color scale to bring out details. Conductive targets C1 and C2 are shown by the black circles.These are well-confined conductors and could correspond to gold/silver or nickel deposits.*

Figures 33 and 34 below show the conductive anomalies C1 and C2 shown in detail, respectively. Both vertical planes of conductivity, plus isosurfaces at a constant conductivity are shown in the Figures. Figure 33 shows the body C1 with an isosurface at 0.002 S/m, and Figure 34 shows the body C2 with a surface of 0.001 S/m. The geometry of the bodies can be clearly seen in these Figures. However, these are single line anomalies, and extracting detailed geometries and conductivities cannot be done with a single flight line response. If these are of economic interest, tighter flight line spacing or ground follow-up would be needed to better describe these targets.
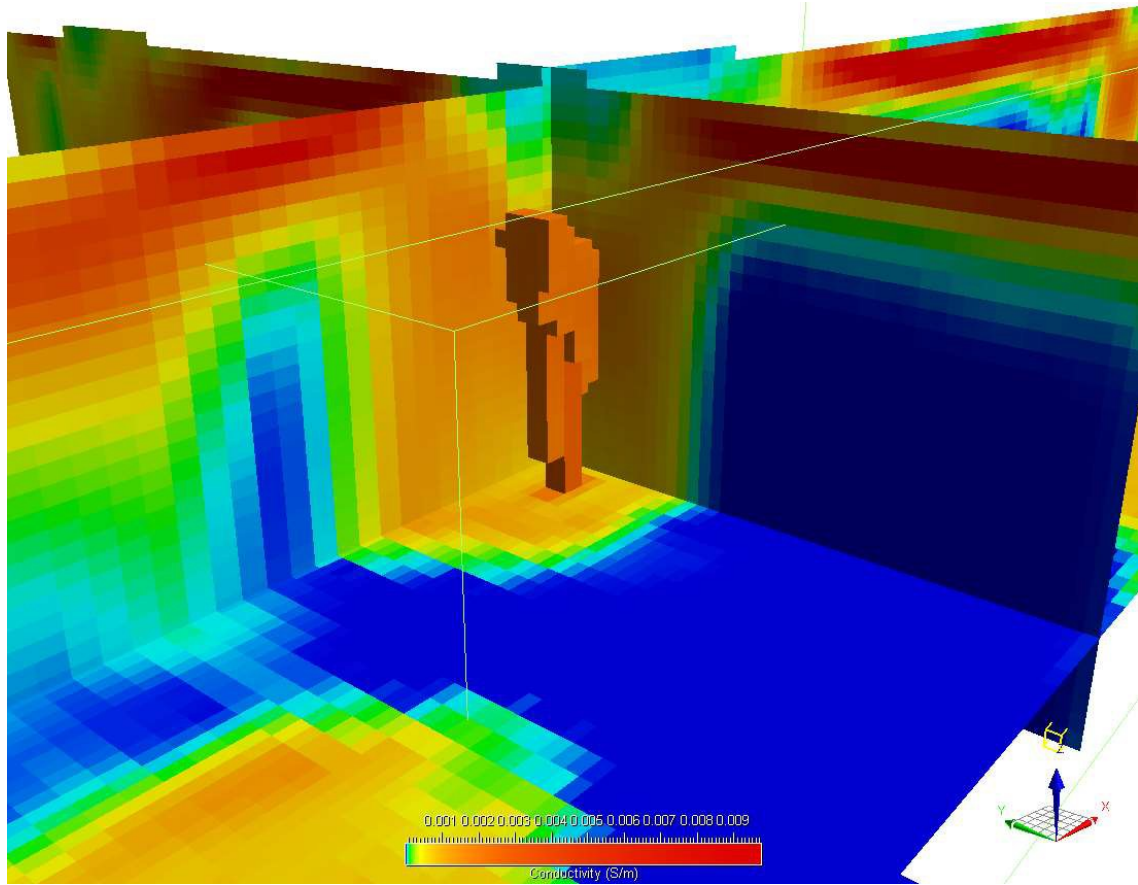
Figure 33: Detail of body C1 looking northeast. *The isosurface is shown at 0.002 S/m. The body is about 400 m in depth extent and 200 m depth-to-top. The full section depth extent isabout 600 m. The vertical exaggeration is 1.5.*
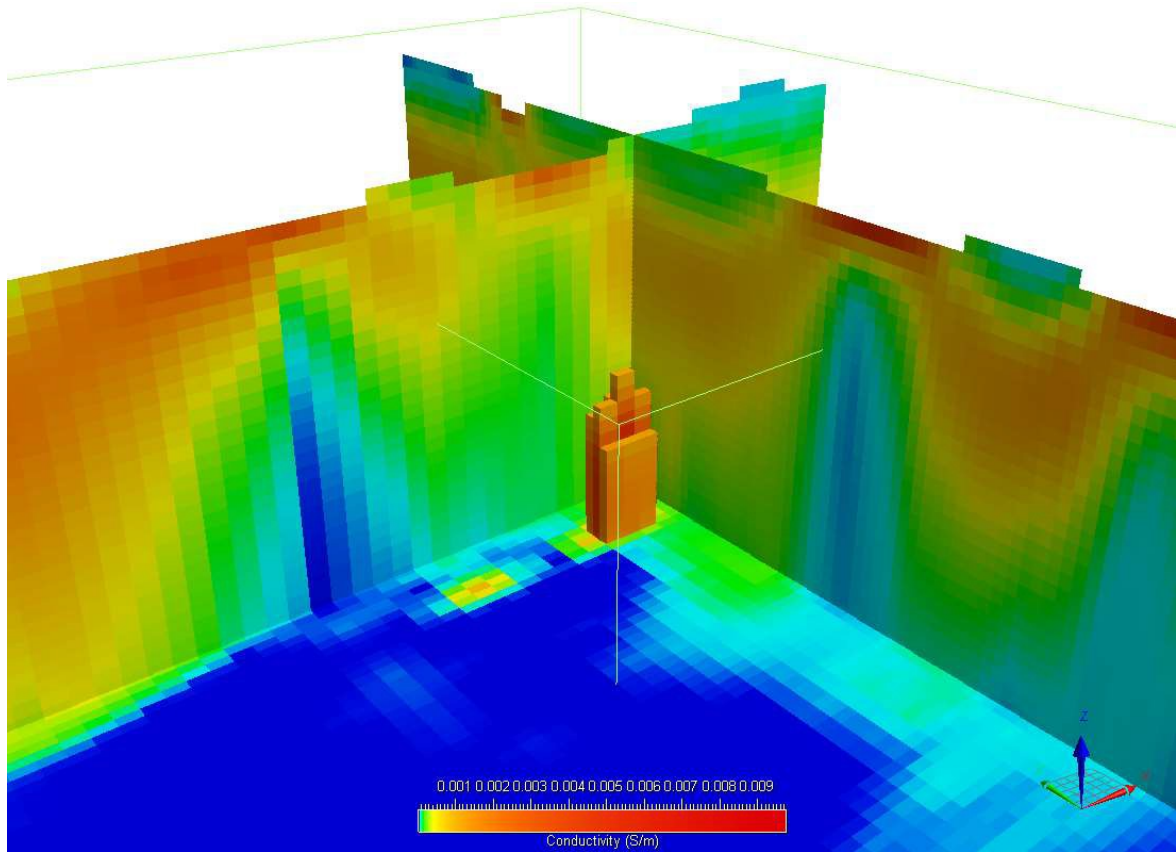
Figure 34: Detail of body C2 looking northeast. The isosurface is shown at 0.001 S/m. The body is about 300 m in depth extent and 300 m below depth-to-top. The full section depth extentis about 600 m. The vertical exaggeration is 1.5
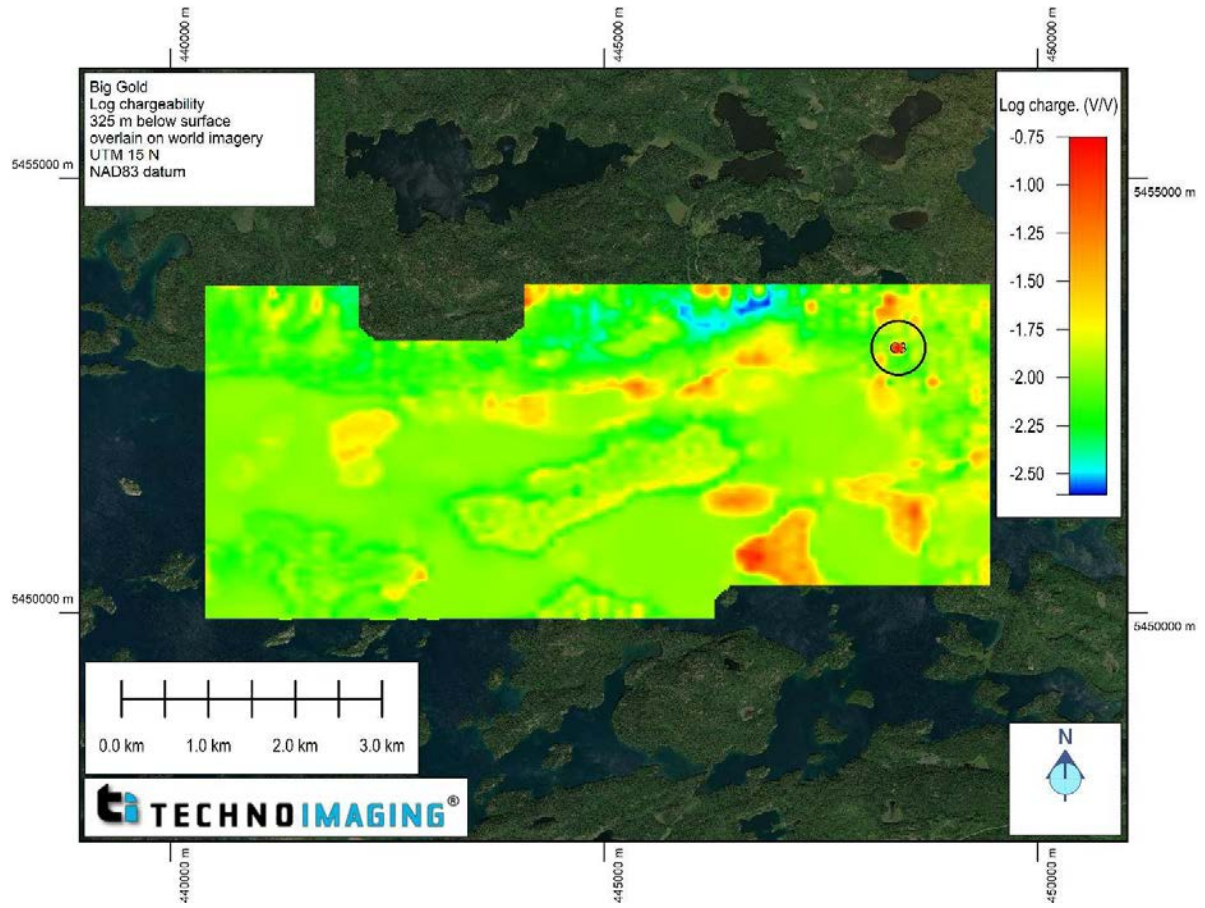
Figure 35: Chargeability at a depth of 325 m *overlain on satellite imagery. The correlation between the lakes and the chargeability anomalies is apparent. However, anomaly C3 at 448400 mE and 5453050 mN show chargeability that is not associated with a lake. This anomaly is indicated by the black circle.*
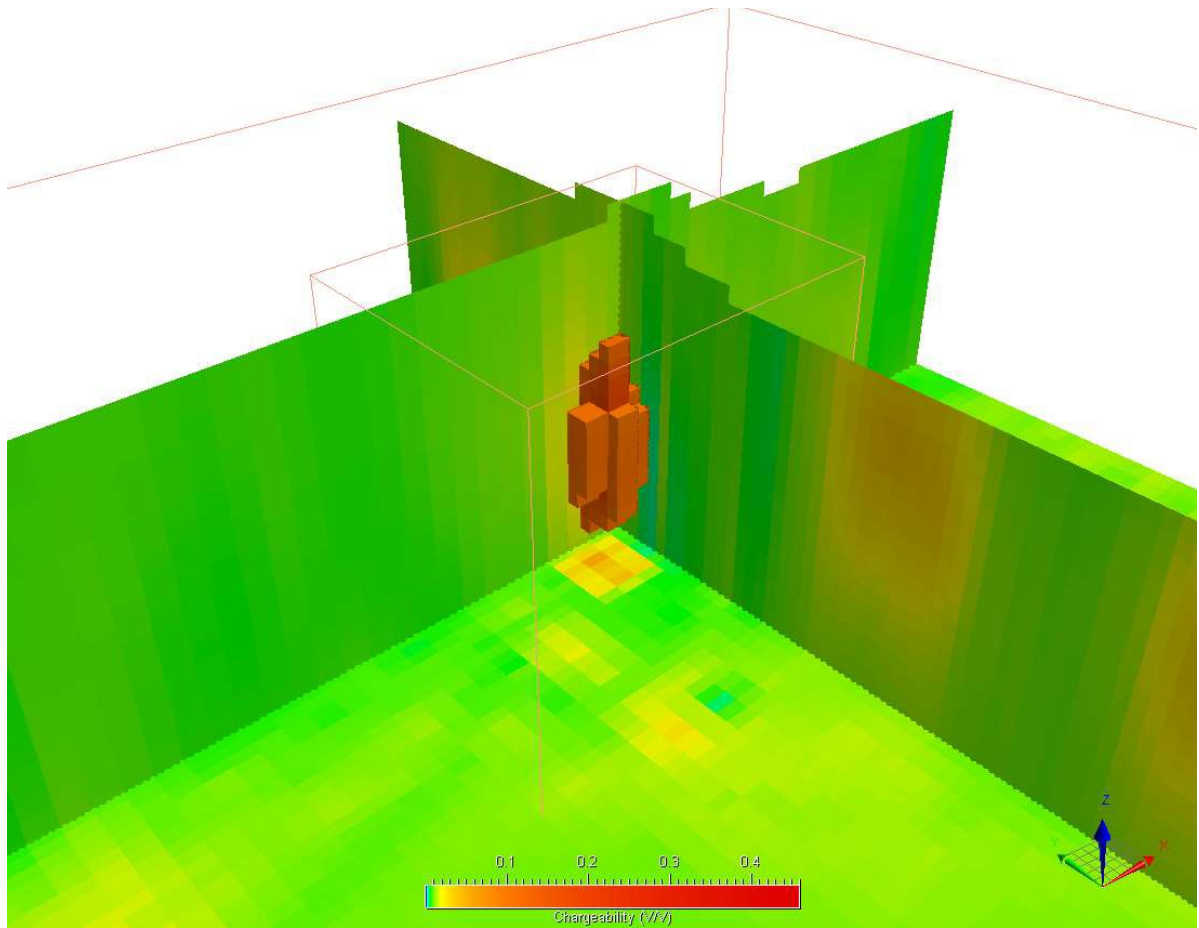
Figure 36: Chargeability anomaly C3 isosurface *shown at a cutoff of 0.1 V/V. The anomaly is roughly 300 meters in depth extent and 200 meters depth-to-top. Vertical exaggeration is 1.5.*
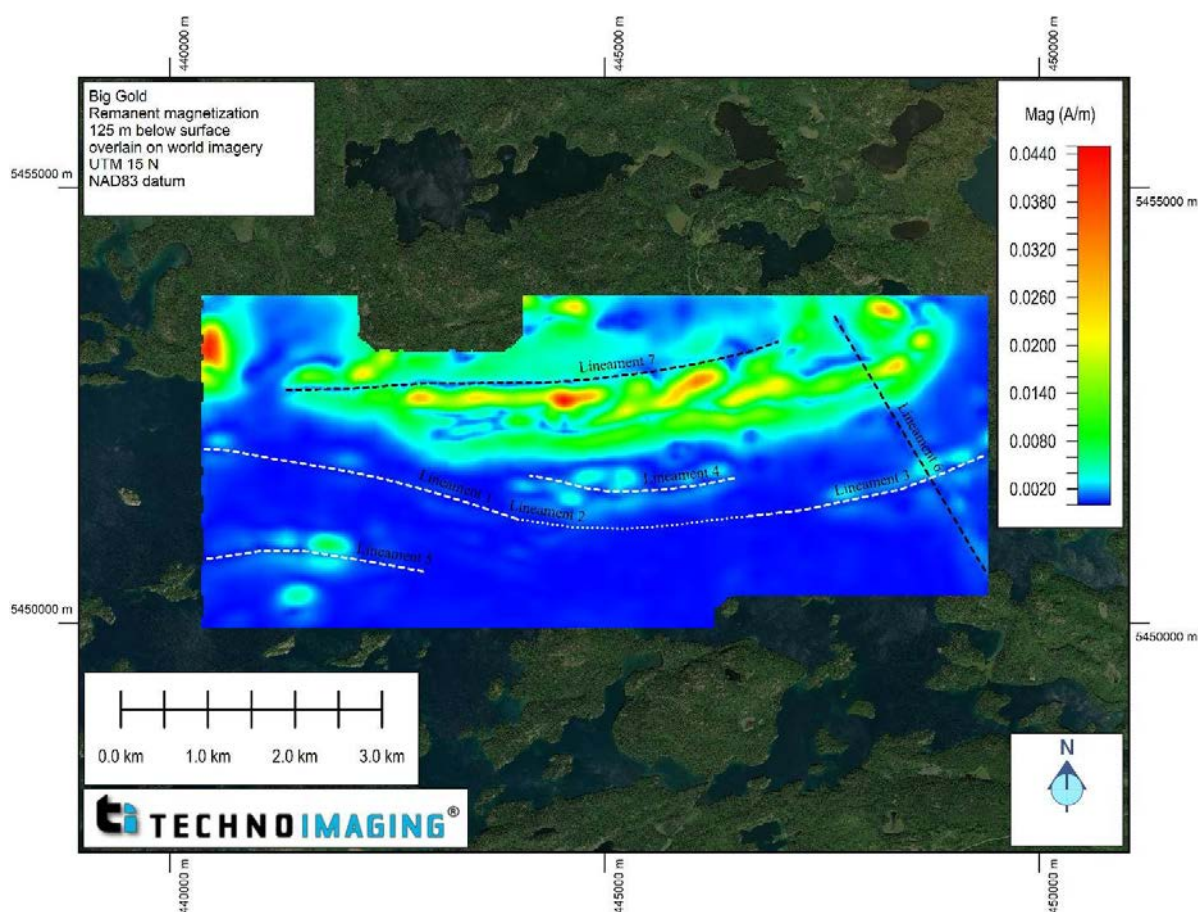
Figure 37: Horizontal section of the amplitude of the remanent component of the magnetization vector *at 125 m below the surface. Interpreted lineaments of interest are shown. Lineaments 1,3,4,5 (white dashed lines) are on-trend or parallel to high gold intercepts from drillholes shown by lineament 2 (white dotted line). These lineaments are all of interest. N-S trending lineament 6 is a diabase dike. E-W trending lineament 7 (black dashed line) is an ultramafic/intermediate-felsic contact. The ultramafics are characterized by a high magnetic response and a prominent fold in evident in the north.*

The interpretive report concludes:

"This report provides a brief geological and geophysical setting for the Martin Kenty Project Area work by TechnoImaging. In addition, it documents the data collection methods and gives an overview of the theoretical processing applied to the data to generate 3D models.

The field data collection was of high quality, and three-dimensional conductivity, chargeability, susceptibility, and magnetic vector property models have been produced from the provided field data. The results correlate well with the known geology in the area. Several examples of potential targets have been suggested based on our understanding of the area, and an abbreviated summary is listed below:

- *Lineaments 1,3,4,5 in the 3D remanent component of the magnetization vector are of interest. They are parallel to or adjoining the shear zone with high gold intercepts from drilling.*

- *Although the airborne-based chargeability highlights lake bottom sediments in*

the project area, there are other chargeability anomalies, i.e., chargeability anomaly C3, in other areas that warrant further investigation for gold and disseminated sulphide mineralization.

- *Conductive anomalies C1 and C2, as well as chargeability anomaly C3, warrant follow-up.*
  The geometries of these suggest nickel deposits, Barnes and Mungall (2018).

The inclusion of remanence in the TMI data interpretation and chargeability in the AEM data were instrumental in developing the above targets. These state-of-the-art techniques are standard in TechnoImaging's algorithms and interpretations.

This report provides a high-level overview of what we see in the results, and it gives ideas on how to view and integrate the 3D models and suggestions on how to perform the interpretation of the data. These models are rich with information, but a full interpretation of the geophysics requires a detailed geological understanding of the area and knowledge to build and test geological models. TechnoImaging would be pleased to help direct these initial efforts in collaboration with staff geologists and geophysicists.

The full interpretive report is found in Appendix 2.

Item 10: Adjacent Properties

Note that the properties mentioned in this section are not located on the Property that is the subject of this technical report. Numerous other mineral occurrences outside the Martin Kenty Property exist in the Kakagi Lake Greenstone Belt, some of which have shafts and adits, but only those determined by the OMI database as being developed or past producing prospects are described below under the headings of each commodity.

Gold Properties

Two significant gold mines exist in the area around the Martin Kenty property. These being the Rainy River Gold Mine and the Hammond Reef Gold Mine, both within the Western Wabigoon Subprovince. In addition, 7 other developed gold properties (as defined in the OMI database) exist within a 20km radius of the Martin Kenty Property.
These being:

1. The Cameron Lake Deposit - OMI record MDI52B14NW0003,
2. The Monte Cristo Property - OMI record MDI52F05SE00013,
3. The Maybrun Mine - OMI record MDI52F05NE00008,
4. The East Cedartree Lake Property - OMI record MDI52F05SW00142,
5. The Dubenski Gold Prospect - OMI record MDI52F05SW00013,
6. The Dogpaw Lake Property - OMI record MDI52F05SW00012, and
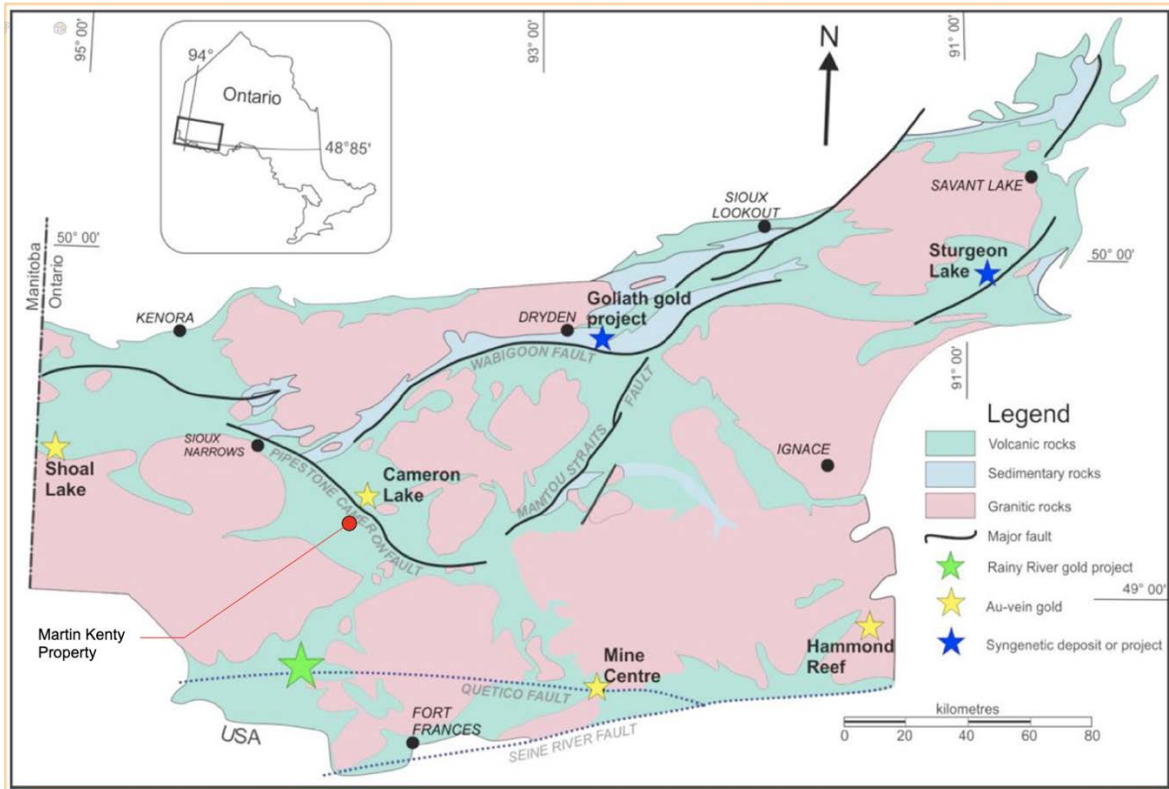7. The Angel Hill Gold Zone - OMI record MDI52F05SW00140.

Figure 38: Simplified geological map with location of significant Au deposits and prospects in the Western Wabigoon. Pelletier 2016 p. 20.
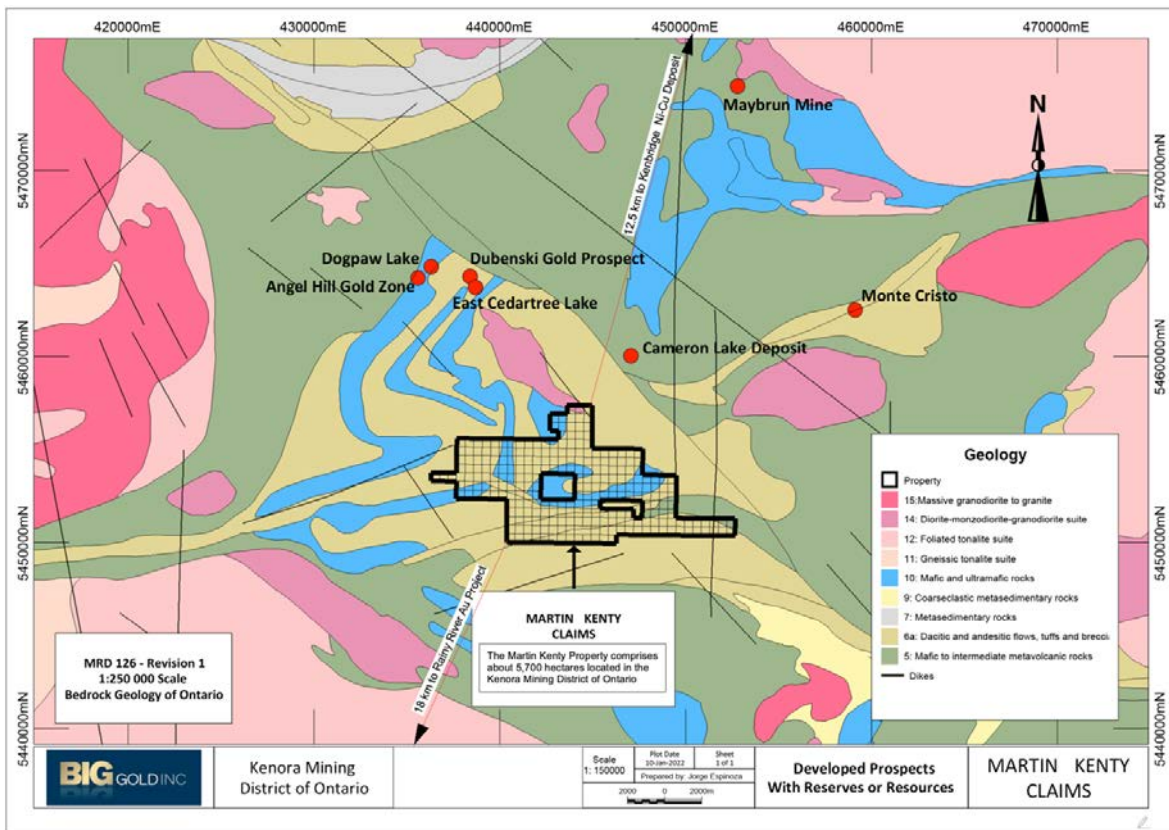

Figure 39: Adjacent Au Properties Map and showing the Kenbridge Ni Property.

Item 11: Interpretation and Conclusions

A 2 day preliminary prospecting program was undertaken by BG in May with 31 samples collected from both the Kagagi Lake Shear on Hay and East Island and the Peninsula Bay area. A second field site visit was undertaken on the Property in July 2022. This work will be discussed in a forthcoming assessment submission. The Kakagi Lake Shear was confirmed to consist of an east west shear of sericitzed, slightly silicified metavolcanics, with the protolith being felsic to intermediate volcanics although diorite and quartz feldspar porphyry was also noted.

Further work on the mineralization of the Kakagi Lake Shear on East and Hay Islands is warranted to define diamond drill targets.

An attempt to find the discretionary Mongus Lake Au, Cu occurrence was attempted in the area of Peninsula Bay. This was unsuccessful as its location was not well defined, however a gossanous zone of pyritiferrous silicified metavolcanic rocks were encountered about 100 meters to the west of a north-south gabbroic content. Overburden and limited time prevented a more definitive examination of this mineralization.

A further examination of this area is warranted, both to find the Mongus Lake Au, Cu discretionary occurrence and also to investigate the gabbro in the area for possible copper nickel mineralization. An IP survey is planned for this area which should help to define further targets for evaluation.

A helicopter VTEM and gradient magnetometer survey was conducted by Geotech in the fall of 2021 (see Item 9.3). This survey was flown over the area of the Kagagi Lake Shear gold mineralization. The magnetometer information from this survey helped to define and confirm the lithology of the area, especially of the gabbroic sills. The VTEM survey helped to define some conductors that may be important for mineralization, so a further 3D modeling was done on the data.

The 3D inversion modelling of the geophysical data was analyzed by Technoimaging (see Item 9.4) whose final report was delivered on January 24, 2022. This report created a series of maps produced from 3D voxels populated with various rock properties such as total magnetic field, magnetic susceptibility, magnetic remanence, conductivity, chargeability and various X, Y Z dB/dt component data as well as an inverted induced polarization model (GEMTIP model). This remanent magnetism was very useful in showing possible structural elements such as a large-scale structure believed to be a fold structure of a possible mafic sill. The axis of this "possible fold" appears offset but parallel to the strike of the Kagagi Lake Shear. The data from this study needs further evaluation especially regarding the drill data, surface mapping, and in the comparison with the anomalies found with the historic geophysical survey of Hornby Bay (see Figure 16).

Evaluation of the chargeability has defined 3 discrete conductive anomalies some of these may be along the same strike as the Kagagi Lake Shear Zone. Another interesting anomaly occurs in the northwest of the survey area.

In addition to the work done on this Property, information on adjacent properties also describes mineralization models that can be applicable to this Property. The VMS Weisner Lake Cu-Zn occurrence is located just to the north of the Property should be investigated for continuity on the Property as the volcanics with associated conductors extend into the Property.

Another style of gold mineralization noted off the Property is The Maybrun copper-gold deposit (Setterfield et al., 1983), This deposit is hosted in mafic volcanics close to the Pipestone-Cameron deformation zone and is the only interpreted syngenetic gold deposit documented in the Wabigoon. Sulphides in inter-pillow space and fractures of mafic volcanics grade at 1.12 wt.% Cu and 1 g/t Au on average. The presence of mafic volcanic sills on the property and the numerous intersecting lineaments mapped on the Property may provide a similar style of gold mineralization on the Property.

Finally, the presence of significant nickel mineralization at the nearby Kenbridge Mine in gabbroic rocks of similar age to those on the Property should be considered.

An earlier lake sediment study[2] was also taken in the area on and around the Martin Kenty Property. This study did not show any anomalous gold, but the high nickel values were noted in areas of mafic-ultramafic rocks. The highest reading of the study area was 1459 ppb Ni collected about 1.4 km northwest of Wicks Lake, about 2km north of the Property. Anomalous Platinum and Palladium were also noted associated with these mafic to ultramafic sills.

---

[2] Dyer, R.D et al. 2006

Item 12: Recommendations

A 2 phase $350,000 2-year exploration program is proposed consisting of:

Phase 1: Year 1 - $150,000 for localized compilation, prospecting/geological mapping, line-cutting/IP and initial diamond drilling and a

Phase 2: Year 2 – $200,000 primarily for more diamond drilling

Phase 1: Year 1 Program

A significant amount of work has been undertaken on this Property by previous operators. This data is primarily found in the assessment files, some of the older data is of very poor quality, unreadable and even missing. In many cases this data extends over areas much larger than the current Property. It would be of value to retrieve and tabulate all this data on a clean interactive georeferenced database providing target locations to be reviewed in the field and provide direction for the exploration program. While this was done for this report some details were missing. Concurrent to this, prospecting can commence to field locate and verify known occurrences and examinations of selected new or potential anomalies. This work should include the 3D modelling of Technoimaging and the potential surface projection of these anomalies as well as areas with similar geology and structure to other known mineral occurrences in the area. This consolidation will also assist locating potential outcrops and diamond drill holes.
An initial prospecting program should focus on:

1) following up on compilation of the previous work done on the islands in Kakagi Lake and the production of a tentative 3D mineralization model, examination of the potential for gold occurrences with sampling along the eastward extension of the Kakagi Lake Shear and their relationship to the east-west shearing in the area as shown on OGS map P1000 is warranted as detailed below:

The Kakagi Lake Shear should be further examined by preparing a 3D model of the past drilling based on grade, alteration, lithology, and structure. This information should be combined with:
a) the 3D inversion model completed of the geophysical data
b) further mapping and sampling of the older trenches that should be cleaned out, extended and resampled
c) try to obtain the original core and have it relogged and correlate the surface mapping, alteration, and mineralization
d) add further information from an IP survey over the area to define areas of chargeability and resistivity.
e) with the combined data of the above several drill site should be located for drilling and extensions of mineralization especially on the mainland,

2) reviewing and locating the C1, C2 and C3 conductive anomalies of the 3D interpretation. The location of conductor C3 located east of Kakagi Lake is

interesting and may have some relationship with the Kakagi Lake Shear which trends in that direction.

3) seeking out and examining the on-surface projection of conductors and magnetic remanent anomalies locate along the north shore and observe any lithology, structure or alteration to explain them as a conductive anomaly was noted 300 metres below surface. Of particular interest is the possible E-W plunging fold (or fault or shear plane?) of an ultramafic sill as shown on the cross line magnetic remanent voxel model. This fold may be critical to the structure of the auriferous east-west shear to the south and locating possible other auriferous shears.

4) examining the gabbroic rocks for potential Ni and PGM mineralization concentrating on the gabbro to gabbronorite and peridotite contacts and those gabbroic bodies with talc aureole rims around their perimeter as noted in the Kenbridge Nickel Deposit.

5) examining an east-west pegmatitic band within gabbroic rocks that has been mapped north of Kakagi Lake. PGM rich pegmatitic rocks have been associated with PGM mineralization in the River Valley Area east of Sudbury Ontario and notably in the Lac Des Isles PGM mine which occurs in the Central Wabigoon subprovince. map across the sills and collect some samples for potential PGMs

6) examining the contact areas of both gabbroic and felsic intrusions adjacent to the host metavolcanics and metasediments in the area, especially in the vicinity of structural elements (shown on existing maps) of lineaments, shearing, fold axis and potential dilation zones, along with mineralization and alteration associated with potential gold or VMS mineralization, especially in the north of the Property.

7) examining mafic rocks for potential Maybrun-Style "syngenetic" gold mineralization possibly associated with iron carbonate selvage around pillows.

8) examining known areas of quartz feldspar and quartz porphyry's noted on the property. One of these sites being in the vicinity of Peninsula Bay.

9) undertakng a lakeshore examination of all shears on the property confirming the rock type and plot the shears dip & strike, noting any alterations and collection of samples for assay.

Assaying, followed up with petrological work, when warranted, is recommended in the course of prospecting and geological mapping

Ground geophysics should be completed to determine the extent and attitude of known targets to help refine trenching and diamond drilling locations. Undertaking of line cutting followed up with localized IP surveys and magnetometer surveys in areas of potential Au mineralization is recommended prior to drilling.

An initial 250 metre diamond drill program would focus on testing the blind (overburden, swamp and lake covered) targets defined in previous studies and new

geophysical work, including forthcoming IP work, on the Property.

This integrated exploration program will allow the determination of the potential of the various targets and allow for scoping and focus of further exploration.

Phase 2: Year 2 Program

Based on positive results of Phase 1, a Phase 2 Program will be undertaken to follow up on areas of merit as outlined in the proposed expense budget as shown below. Some stripping may also be undertaken if warranted.

Item 12.1 Proposed Budget

Table 11: Proposed Budget

Activity Phase 1	Estimate
Compilation and VTEM Target Modeling for site visits	10,000.00
Local Prospecting and Sampling (2 people) (all inclusive) 10 days @ $1,500 / day	15,000.00
Local Geological Mapping and Sampling (2 people) (all inclusive) 10 days @ $2,000 / day	20,000.00
Local Geophysics IP and Linecutting)	40,000.00
Analysis and Petrology	5,000.00
Preliminary Diamond Drilling (all inclusive) 250 metres @ $200 / metre	50,000.00
Contingencies	10,000.00
TOTAL	**$150,000.00**

Activity Phase 2	Estimate
Local Prospecting and Sampling (2 people) (all inclusive) 5 days @ $1,500 / day	7,500.00
Local Geological Mapping and Sampling (2 people) (all inclusive) 5 days @ $2,000 / day	10,000.00
Analysis and Petrology	20,000.00
Diamond Drilling (all inclusive) 750 metres @ $200 / metre	150,000.00
Contingencies	12,500.00
TOTAL	**$200,000.00**

Item 26: References

Note: in the references listed below the terms "AFRI File" and AFRO ID" refer to the assessment report's identification numbers for the files as found in the MNDM's Assessment File Research Image Database (AFRI) retrieved from http://www.geologyontario.mndm.gov.on.ca.

Due to the large number of reports submitted for assessment in the MNDM's Assessment File Research Image Database many of which are airborne geophysics reports or only partly cover the Martin Kenty Property, they have not all been listed in this "References" section (Item 26). The author has examined the reports and believe that the pertinent information is presented in this Report.

Adams, Glen W., 1975, AFRI file:52F04NE0031, Summary Report Diamond Drilling Program Martin Option-Crow Lake Joint Venture, Kenora Mining Division.

Barnes, S. J. and Mungall, J. E. (2018), Blade-shaped dikes and nickel sulfide deposits: A model for the emplacement of ore-bearing small intrusions: Economic Geology, v. 113, no. 3, pp. 789– 798.

Beard, R. C., Garratt G. L., 1976, Gold Deposits of the Kenora-Fort Frances Area, district of Kenora and Rainy River, Publication Number MDC16.

Bidwell, G. E., 1990, Quetico (Reconnaissance) Project, OMIP Program No. OM90-094, Bulk Till Sampling Program, Thunder Bay and Kenora Mining Divisions.

Blackburn C.E., Johns G.W., Ayer J A and Davis D.W., 1991.Wabigoon Subprovince; in Geology of Ontario, Ontario Geological Survey, Special Volume 4, Part 1, p.303-382.

Canadian Nickel Co. Ltd., 1969. AFRI file: 54F04NW0135 Diamond Drilling Report, Heronry Lake.

Chastko, L. C., 1985, AFRI file: 52F05SE0078, VLF-EM Magnetometer Survey, Cameron Lake Property, Lear Oil & Gas Corporation, Rowan Lake Area.

Crukor, D., Gignac, L-P., Dagbert, M., 2011, NI 43-101 Technical Report on the Hammond Reef Gold Property; Atikokan Area, Ontario, SGS Canada Inc.

Davis J. C., and Marin, J. A. 1976, Geology of the Cedartree Lake Area, District of Kenora Ontario Division of Mines, GR134, 52 pages, accompanied by Map 2319 (coloured), Geol. Ser., Scale 1:31,680 or 1 Inch to 1/2 Mile. Geology 1971.

Davis J. C., and Marin, J. A. 1972, Cedartree Lake Area, District of Kenora, Ontario Dept. Mines and Northern Affairs, Prelim. Map P.731, Geol. Ser., Scale 1 Inch to 1/4 Mile. Geology 1971.

Davis J. C., Pryslak, A.P., 1963-1965, Map 2115 Kenora-Fort Frances Sheet, Geological Compilation, Kenora, Rainy River Districts, Scale 1:253,440 or 1 Inch to 4 Miles.

Dyer, R. D., Ravnaas, C., Felix, V. E., Russell, D. F., Kakagi Lake Area Lake Sediment Geochemical Survey, Northwestern Ontario, Ontario Geological Survey, Open File Report 6188.

Edwards, G., 1980, Schistose Lake, Ontario Geological Survey Report 194, 67p. accompanied by Map 2421, Precambrian Geology Series, Scale 1:31,680 or 1 inch to ½ mile. Geology 1974.

Ferguson, S. A., Groen, H. A., Haynes, R., 1971, Gold Deposits of Ontario: Part 1, Districts of Algoma, Cochrane, Kenora, Rainy River, and Thunder Bay: Ontario Division of Mines MRC13, 315 pages, reprinted 1982.

Frances Resources Ltd., 1983. AFRI file: 52F04NE0332, Diamond Drilling Report, Brooks Lake Area.

Frances Resources Ltd. & Blais, Ron and Associates, 1986. AFRI 52F04NE8131, Geology, Trenching and Assays showing DDH's.

Goodwin, A.M., 1970. Archean Volcanic Studies in the Lake of the Woods – Manitou Lake-Wabigoon Region Western Ontario, Open File Report 5042, Ontario Department of Mines Geological Branch.

Hudak, G.J. (2005) Field trip 10 – Mattabi/Sturgeon Lake historic VMS camp.

Proceedings of the 61st annual meeting of the Institute on Lake Superior Geology (Dryden, Ontario, May 21-22, 2015), p. 116-151.

Jagodits, Francis L., 1998,Report on Airborne GEOTEM Transient Domain Electromagnetic-Magnetic Survey, Kakagi Lake Project, for Hornby Bay Exploration Ltd., AFRI 52F05SE2002.

Johns, G.W. 2007, Precambrian geology, Kakagi-Rowan Lakes Area; Ontario Geological Survey, Preliminary Map P.3594, scale 1:50,000

Kaye, L., 1974. Crow Lake Area (Heronry Lake Area) Eastern Part, District of Kenora, Ontario Div. Mines, Prelim. Map P.921, Geol. Se., scale 1 inch to ¼ mile. Geology 1973.

Laramide Resources Ltd. / Rio Algom Exporation Inc. 1990. AFRI file: 52F04NE0007, Diamond Drilling Report, Brooks Lake Area.

Laramide Resources Ltd. 1987. AFRI file: 52F04NE0015, Physical Work, Drill and Blast Trench Report, Brooks Lake Area.

MacCormack, L.V., 1974, Report on Geological Survey of Roy Martin claim group Kakagi (Crow) Lake, Kenora Mining Division, Newconex Canadian Exploration Limited, Company Report.

McPhie, J., Doyle, M., Allen, R. L., and Allen, R. (1993) Volcanic Textures: A Guide to the Interpretation of Textures in Volcanic Rocks. Centre for Ore Deposit and Exploration Studies, University of Tasmania. Hobart, Australia. 198 p.

Morton, R.L., and Franklin, J.M. (1987) Two-fold classification of Archean volcanic-associated massive sulfide deposits. Economic Geology 82 : 1057-1063.

Noranda Exploration Co. Ltd., 1975. AFRI file: 52F04NE0033, Diamond Drilling Report, Brooks Lake Area

Noranda Exploration Co. Ltd., 1975. AFRI file: 53F04NW0134, Diamond Drilling Report, Heronry Lake Area.

Ontario Geological Survey 2011. 1:250,000 Scale Bedrock Geology of Ontario, Miscellaneous Release Data, MRD126 - Rev. 1

Ontario Geological Survey 2017. Ontario airborne geophysical surveys, magnetic data, grid data (ASCII and Geosoft® formats), magnetic supergrids; Ontario Geological Survey, Geophysical Data Set 1037—Revised. ISBN 978-1-4868-0293-7 (DVD) ISBN 978-1-4868-0294-4 (zip).

Pelletier, Mireille, 2016, The Rainy River Gold Deposit, Wabigoon Subprovince, Western Ontario: Style, Geometry, Timing and Structural Controls on Ore Distribution and Grades.

Pitman, P., 1997.Geological Report, Kakagi Lake Project, (Northwest Ontario). NTS 52E/1, 52F4,5M 16R., PWO Consulting Company, prepared for Hornby Bay Exploration Ltd.

Raoul, Allen J., 2008, Pipestone Property Airborne Geophysical Assessment Report, NTS Sheets 52F/4 and 52F/5, April 4, 2008, AFRI # 20000000079.

Reading, K.L., 1998, 1997-19-98 Kakagi Lake Recon Report - A Prospecting Reconnaissance Report on Hornby Bay's Kakagi Lake Property in the Kenora District of Ontario, prepared for Hornby Bay Exploration Ltd. AFRI # 52F05SE2003.

Rio Algom Exploration Inc., 1991. AFRI file: 52F04NE0004, Diamond Drilling Report, Brooks Lake Area.

Rio Algom Exploration Inc., 1990. AFRI file: 53F04NW0119, Diamond Drilling Report, Heronry Lake Area.

Setterfield, T., Watkinson, D.H., and Thurston, P.C. (1983) Quench-textured, pillowed metabasalts and copper mineralization, Maybrun mine, northwestern Ontario. CIM Bulletin, November 1983, p. 69-74.

Zhdanov, Michael, January 24, 2022, Three-dimensional Inversion VTEM Electromagnetic and TMI data Martin Kent Project Area, Nestor Falls Northwestern Ontario, Canada, prepared for Big Gold Inc.

Item 14: Certificate of Qualifications

CERTIFICATE OF AUTHOR – ROBERT G. KOMARECHKA

I, Robert G. Komarechka P.Geo, (PGO No.1150), P.Geo. (APEGA No. M39059), of 545 Granite Street, Sudbury, Ontario, do hereby certify with respect to 'The Assessment Report on the Martin Kenty Property (The Property) in Dogpan, Heronry Lake and Brooks Lake Area, Kenora Mining Division, Ontario, Canada", (the "Assessment Report") with a revised date of June 2022, and an original signature date of February 25, 2022, prepared for Big Gold Inc., that:

1. I am an independent consulting professional geoscientist operating under the name of Bedrock Research Corp. with an office located at 545 Granite Street, Sudbury, Ontario, Canada, P3C 2P4.
2. I graduated from Laurentian University in Sudbury with a B.Sc. (1978) with a major in Geology and have practiced my profession for 41 years since graduation with government, academia, and the private sector with both major and junior companies. During this time, I have been involved in oil and gas exploration, wellsite geology, mineral exploration, mineral property acquisitions and evaluations, drill program management, field crew supervision and mine management. Commodities have included gold, silver, platinum group metals, base metals, uranium, diamonds, lithium, graphite, industrial minerals, dimension stone, aggregate and high purity silica. This work has been conducted in most provinces of Canada, United States (Montana, Arizona, Nevada, Idaho, Kentucky, and Maine), Mexico, Peru, and Spain.
3. I am a registered practicing professional member in good standing with the Association of Professional Engineers and Geoscientists of Alberta (APEGA) since 1985 with P.Geol. membership number M39059.
4. I am a registered practicing professional member in good standing with the Geoscientists of Ontario (PGO) since 2004 with P.Geo. membership number 1150.
5. I am a registered Fellow in good standing of the Canadian Gemmological Association since graduation as a Gemmologist in 1990.
6. I personally examined and studied the literature of government and corporate reports on the Property of Big Gold Inc., I am familiar with the project area and have visited the property from November 14 and 16, 2021.
7. I have knowledge of the geology and mineralization in this general area having recently completed, last year, a Technical Report on the Kenora U Property located 60 km north of the Martin Kenty Property in addition to a Technical Report on this property
8. I have had no prior or subsequent involvement with the property that is the subject of the Technical Report.
9. I am not aware of any material fact or material change with respect to the subject matter of the Technical Report that is not reflected in the Technical Report, the omission to disclose which makes the Technical Report misleading.
10. I am independent of the issuer applying all of the tests in section 1.5 of National Instrument 43-101. I do not own, directly or indirectly, nor am I under an agreement, arrangement or understanding or expect to acquire any securities of Big Gold Inc. or any affiliated entity of the Company. I hold no interest, directly or indirectly, in the mineral properties that are the

subject of the forgoing report or in any adjacent mineral properties nor do I expect to receive any direct or indirect interest in the Property.

11. I have read the definition of "qualified person" set out in National Instrument 43-101/Regulation 43-101 ("NI 43-101") and certify that by reason of my education, affiliation with a professional association (as defined in NI 43-101) and past relevant work experience, I fulfill the requirements to be a qualified person for the purposes of NI 43-101 on this Assessment Report.

12. I am responsible for the preparation of all Sections of "The Assessment Report"

Originally signed this 25 day of February 2022 in Sudbury, Ontario, Canada

_____

Robert G. Komarechka, P.Geo., (PGO No. 1150)

Effective Date: February 25, 2022
Signed Date: February 25, 2022
Revision Date: June, 2022

Appendices

Appendix 1

VTEM Survey Report of Geotech

VTEM™ Plus

REPORT ON A HELICOPTER-BORNE VERSATILE TIME
DOMAIN ELECTROMAGNETIC (VTEM™ Plus) AND HORIZONTAL
MAGNETIC GRADIOMETER GEOPHYSICAL SURVEY

December 2021

PROJECT: MARTIN KENTY PROJECT
LOCATION: NESTOR FALLS, ON
FOR: BIG GOLD INC.
SURVEY FLOWN: OCTOBER 2021
PROJECT: GL210091

TABLE OF CONTENTS

LIST OF FIGURES

Project GL210091
VTEM™ Plus Report on Airborne Geophysical
Survey for Big Gold Inc.

1

LIST OF TABLES

APPENDICES

Project GL210091
VTEM™ Plus Report on Airborne Geophysical
Survey for Big Gold Inc.

2

GEOTECH
AIRBORNE GEOPHYSICAL SURVEYS

EXECUTIVE SUMMARY

MARTIN KENTY PROJECT
NESTOR FALLS, ON

Between October 7th and October 27th, 2021, Geotech Ltd. carried out a helicopter-borne geophysical survey over Martin Kenty Project near Nestor Falls, ON.

Principal geophysical sensors included a versatile time domain electromagnetic (VTEM™ Plus) system and a horizontal magnetic gradiometer with two caesium sensors. Ancillary equipment included a GPS navigation system and a radar altimeter. A total of 365 line-kilometres of geophysical data were acquired during the survey.

In-field data quality assurance and preliminary processing were carried out on a daily basis during the acquisition phase. Preliminary and final data processing, including generation of final digital data and map products were undertaken from the office of Geotech Ltd. in Aurora, Ontario.

The preliminary processed survey results are presented as the following maps:

- Electromagnetic stacked profiles of the B-field Z Component
- Electromagnetic stacked profiles of dB/dt Z Component
- B-Field Z Component Channel grid
- dB/dt Z Component Channel grid
- Fraser Filtered X Component Channel grid
- Total Magnetic Intensity (TMI)
- Calculated Time Constant (Tau) with Calculated Vertical Derivative of TMI contours
- Calculated Vertical Gradient (CVG) of Total Magnetic Intensity (TMI)
- Total Magnetic Horizontal Gradient (TotHG)
- Magnetic Tilt-Angle Derivative (TiltDrv)
- Resistivity Depth Imaging (RDI) sections and depth-slices are presented.

Digital data include all electromagnetic and magnetic products, plus ancillary data including the waveform.

The survey report describes the procedures for data acquisition, equipment used, processing, image presentation and the specifications for the digital data set.

Project GL210091
VTEM™ Plus Report on Airborne Geophysical
Survey for Big Gold Inc.

3

GEOTECH
AIRBORNE GEOPHYSICAL SURVEYS

1. INTRODUCTION

1.1 GENERAL CONSIDERATIONS

Geotech Ltd. performed a helicopter-borne geophysical survey over the Martin Kenty Project near Nestor Falls, ON (Figure 1 & Figure 2).

Gary Handley represented Big Gold Inc. during the data acquisition and data processing phases of this project.

The geophysical surveys consisted of helicopter borne EM using the versatile time-domain electromagnetic (VTEM™) plus system with Full-Waveform processing. Measurements consisted of Vertical (Z) and In-line Horizontal (X & Y) components of the EM fields using an induction coil and a horizontal magnetic gradiometer using two caesium magnetometers. A total of 365 line-km of geophysical data were acquired during the survey.

The crew was based out of Nestor Falls, ON (Figure 2) for the acquisition phase of the survey. Survey flying occurred on October 17th to October 25th, 2021.

Data quality control and quality assurance, and preliminary data processing were carried out on a daily basis during the acquisition phase of the project. Final data processing followed immediately after the end of the survey. Final reporting, data presentation and archiving was completed in December 2021.

Figure 1: Survey location

Project GL210091
VTEM™ Plus Report on Airborne Geophysical
Survey for Big Gold Inc.

4

1.2   SURVEY AND SYSTEM SPECIFICATIONS

The survey area is located approximately 13km northeast of Nestor Falls, ON (Figure 2).

Figure 2: Survey area location map on Google Earth.

The Martin Kenty Project was flown in a south to north (N 0° E azimuth) direction with traverse line spacings of 100 metres, as depicted in Figure 3. Tie lines were flown perpendicular to traverse lines at 1000m line spacing. For more detailed information on the flight spacings and directions, see Table 1.

1.3   TOPOGRAPHIC RELIEF AND CULTURAL FEATURES

Topographically, the survey area exhibits relief with elevations ranging from 331 to 422 metres over an area of 34 square kilometres (Figure 3).

There are visible signs of culture such as roads, within the Martin Kenty Project area.

Figure 3: Martin Kenty Project flight paths over a Google Earth Image.

Project GL210091
VTEM™ Plus Report on Airborne Geophysical
Survey for Big Gold Inc.

6
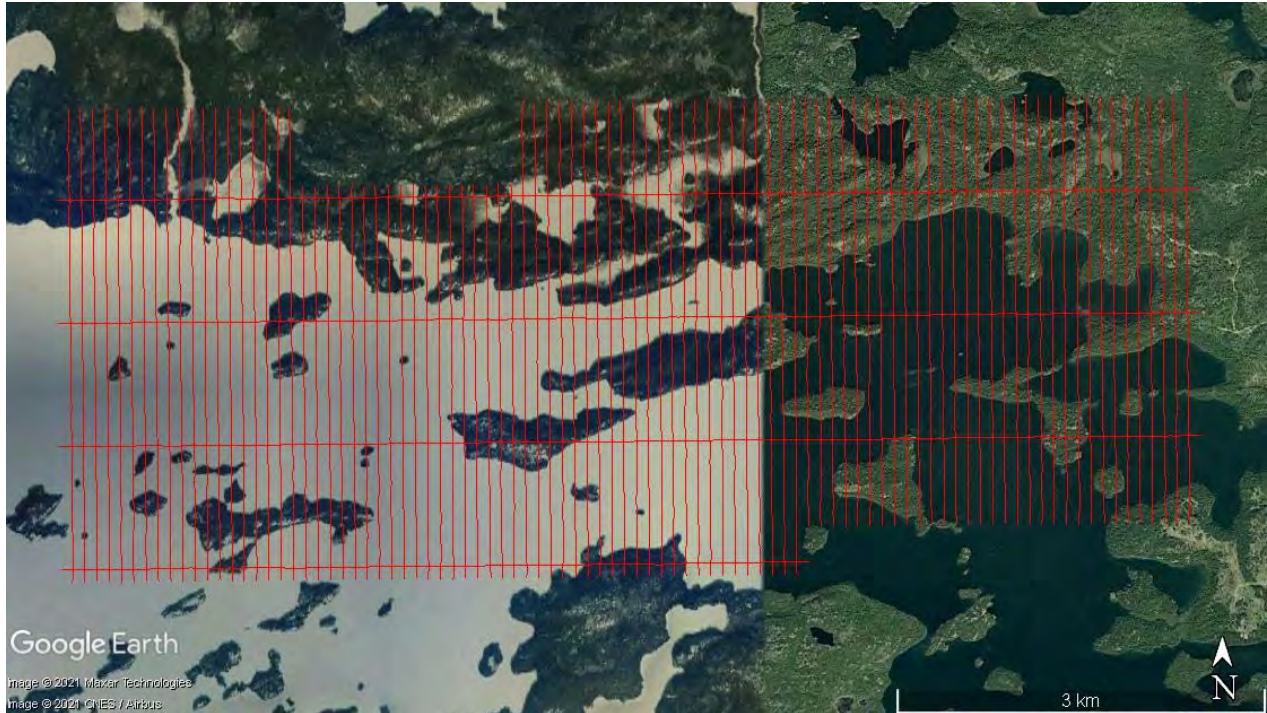
2. DATA ACQUISITION

2.1 SURVEY AREA

The survey area (see Figure 3 and Appendix A) and general flight specifications are as follows:

Table 1: Survey Specifications

Survey block	Line spacing (m)	Area (km²)	Planned Line-Km	Actual Line-km	Flight direction	Line numbers
Martin Kenty	Traverse: 100	34	351	365	N 0° E / N 180° E	L1000 – L1910
	Tie: 1000				N 90° E / N 270° E	T2000 – T2030
Total		34	351	365		

Survey area boundaries co-ordinates are provided in Appendix B.

2.2 SURVEY OPERATIONS

Survey operations were based out of Nestor Falls, ON (see Figure 2). The following table shows the timing of the flying.

Date	Comments
07-Oct	Mobilization
08-Oct	Start system assembly
09-Oct	Heli installation, set up base stations, continue loop assembly
10-Oct	Reconnaissance flight
11-Oct	Continue loop assembly
12-Oct	Continue loop assembly
13-Oct	Complete loop assembly
14-Oct	Weather day
15-Oct	Weather day
16-Oct	System tests
17-Oct	Production flight - 351 km flown
18-Oct	System calibrations
19-Oct	QC of data collected. 116km of data accepted
20-Oct	Production flight, troubleshoot Z-component noise
21-Oct	Test flights
22-Oct	Crew change
23-Oct	Weather day
24-Oct	Production flight - 99 km flown
25-Oct	Production flight - 136 km flown
26-Oct	Client review of data
27-Oct	Demobilization

Project GL210091
VTEM™ Plus Report on Airborne Geophysical
Survey for Big Gold Inc.

7

GEOTECH
AIRBORNE GEOPHYSICAL SURVEYS

2.3   FLIGHT SPECIFICATIONS

During the survey, the helicopter was maintained at a mean altitude of 76 metres above the ground with an average survey speed of 85 km/hour. This allowed for an actual average Transmitter-receiver loop terrain clearance of 40 metres and a magnetic sensor clearance of 50 metres.

The on-board operator was responsible for monitoring the system integrity. He also maintained a detailed flight log during the survey, tracking the times of the flight as well as any unusual geophysical or topographic features.

On return of the aircrew to the base camp the survey data was transferred from a compact flash card (PCMCIA) to the data processing computer. The data were then uploaded via ftp to the Geotech office in Aurora for daily quality assurance and quality control by qualified personnel.

2.4   AIRCRAFT AND EQUIPMENT

2.4.1   SURVEY AIRCRAFT

The survey was flown using Eurocopter Aerospatiale (A-Star) 350 B3 helicopters, registration C-GTEQ. The helicopter is owned and operated by Geotech Aviation Ltd. Installation of the geophysical and ancillary equipment was carried out by a Geotech Ltd. crew.

2.4.2   ELECTROMAGNETIC SYSTEM

The electromagnetic system was a Geotech Time Domain EM (VTEM™ Plus) full receiver-waveform streamed data recorded system. The "full waveform VTEM system" uses the streamed half-cycle recording of transmitter and receiver waveforms to obtain a complete system response calibration throughout the entire survey flight. VTEM with the serial number 10 had been used for the survey. The VTEM™ transmitter current waveform is shown diagrammatically in Figure 4.

The VTEM™ Receiver and transmitter coils were in concentric-coplanar and Z-direction oriented configuration. The receiver system for the project also included coincident-coaxial X&Y-direction coils to measure the in-line and cross-line dB/dt and calculate B-Field responses. The Transmitter-receiver loop was towed at a mean distance of thirty-six (36) metres below the aircraft as shown in Figure 5.
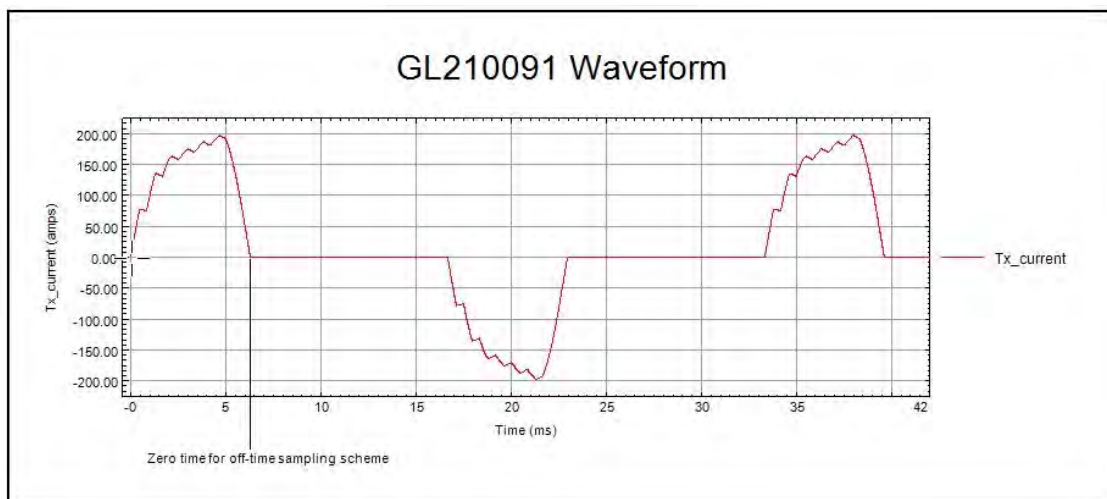
Project GL210091
VTEM™ Plus Report on Airborne Geophysical
Survey for Big Gold Inc.

8

The VTEM™ decay sampling scheme is shown in Table 2 below. Forty-three-time measurement gates were used for the final data processing in the range from 0.021 to 8.083 msec. Zero time for the off-time sampling scheme is equal to the current pulse width and is defined as the time near the end of the turn-off ramp where the dI/dt waveform falls to 1/2 of its peak value.

Table 2: Off-Time Decay Sampling Scheme

VTEM™ Decay Sampling Scheme				
Index	Start	End	Middle	Width
Milliseconds				
4	0.018	0.023	0.021	0.005
5	0.023	0.029	0.026	0.005
6	0.029	0.034	0.031	0.005
7	0.034	0.039	0.036	0.005
8	0.039	0.045	0.042	0.006
9	0.045	0.051	0.048	0.007
10	0.051	0.059	0.055	0.008
11	0.059	0.068	0.063	0.009
12	0.068	0.078	0.073	0.010
13	0.078	0.090	0.083	0.012
14	0.090	0.103	0.096	0.013
15	0.103	0.118	0.110	0.015
16	0.118	0.136	0.126	0.018
17	0.136	0.156	0.145	0.020
18	0.156	0.179	0.167	0.023
19	0.179	0.206	0.192	0.027
20	0.206	0.236	0.220	0.030
21	0.236	0.271	0.253	0.035
22	0.271	0.312	0.290	0.040
23	0.312	0.358	0.333	0.046
24	0.358	0.411	0.383	0.053
25	0.411	0.472	0.440	0.061
26	0.472	0.543	0.505	0.070
27	0.543	0.623	0.580	0.081
28	0.623	0.716	0.667	0.093
29	0.716	0.823	0.766	0.107
30	0.823	0.945	0.880	0.122
31	0.945	1.086	1.010	0.141
32	1.086	1.247	1.161	0.161
33	1.247	1.432	1.333	0.185
34	1.432	1.646	1.531	0.214
35	1.646	1.891	1.760	0.245
36	1.891	2.172	2.021	0.281

Project GL210091
VTEM™ Plus Report on Airborne Geophysical
Survey for Big Gold Inc.

9

VTEM™ Decay Sampling Scheme				
Index	Start	End	Middle	Width
Milliseconds				
37	2.172	2.495	2.323	0.323
38	2.495	2.865	2.667	0.370
39	2.865	3.292	3.063	0.427
40	3.292	3.781	3.521	0.490
41	3.781	4.341	4.042	0.560
42	4.341	4.987	4.641	0.646
43	4.987	5.729	5.333	0.742
44	5.729	6.581	6.125	0.852
45	6.581	7.560	7.036	0.979
46	7.560	8.685	8.083	1.125

Z Component: 4-46 time gates
X Component: 20-46 time gates
Y Component: 20-46 time gates

Table 3: VTEM™ System Specifications

Transmitter	Receiver
- Transmitter loop diameter: 26 m - Number of turns: 4 - Effective Transmitter loop area: 2123.7 m^2 - Transmitter base frequency: 30 Hz - Peak current: 197.5 A - Pulse width: 6.28 ms - Waveform shape: Bi-polar trapezoid - Peak dipole moment: 419,434 nIA - Average transmitter-receiver loop terrain clearance: 40 metres	- X -Coil diameter: 0.32 m - Number of turns: 245 - Effective coil area: 19.69 m^2 - Y -Coil diameter: 0.32 m - Number of turns: 245 - Effective coil area: 19.69 m^2 - Z-Coil diameter: 1.2 m - Number of turns: 100 - Effective coil area: 113.04 m^2

Project GL210091
VTEM™ Plus Report on Airborne Geophysical
Survey for Big Gold Inc.

10

GEOTECH
AIRBORNE GEOPHYSICAL SURVEYS
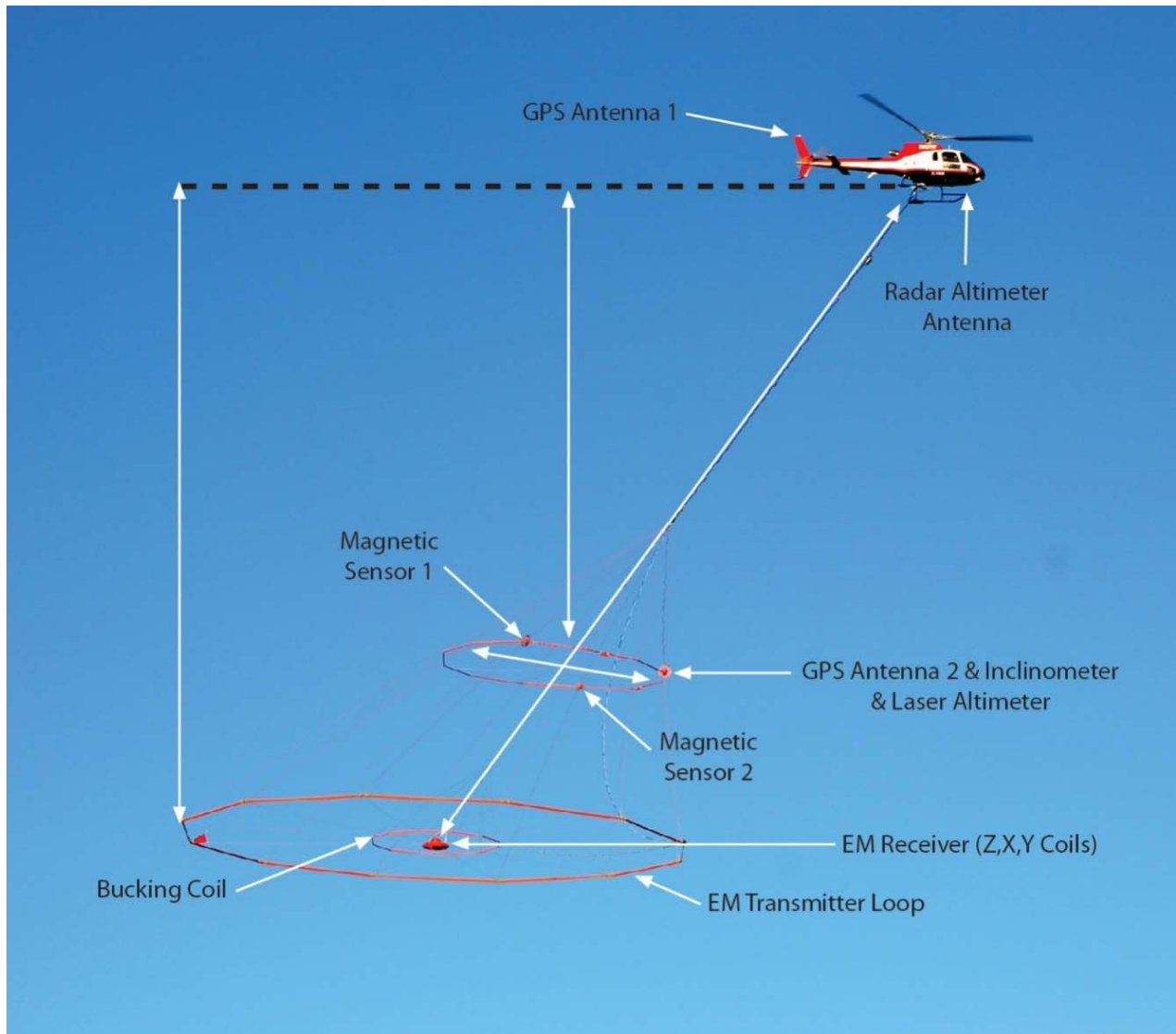
Figure 5: VTEM™plus System Configuration.

2.4.3 FULL WAVEFORM VTEM™ SENSOR CALIBRATION

The calibration is performed on the complete VTEM™ system installed in and connected to the helicopter, using special calibration equipment. This calibration takes place on the ground at the start of the project prior to surveying.

The procedure takes half-cycle files acquired and calculates a calibration file consisting of a single stacked half-cycle waveform. The purpose of the stacking is to attenuate natural and man-made magnetic signals, leaving only the response to the calibration signal.

This calibration allows the transfer function between the EM receiver and data acquisition system and the transfer function between the current monitor and data acquisition system to be determined. These calibration results are then used in VTEM full waveform processing.

Project GL210091
VTEM™ Plus Report on Airborne Geophysical
Survey for Big Gold Inc.

11

2.4.4 HORIZONTAL MAGNETIC GRADIOMETER

The horizontal magnetic gradiometer consists of two Geometrics split-beam field magnetic sensors with a sampling interval of 0.1 seconds. These sensors are mounted 12.5 metres apart on a separate loop, 10 metres above the Transmitter-receiver loop. A GPS antenna and Gyro Inclinometer is installed on the separate loop to accurately record the tilt and position of the magnetic gradiometer sensors.

2.4.5 RADAR ALTIMETER

A Terra TRA 3000/TRI 40 radar altimeter was used to record terrain clearance. The antenna was mounted beneath the bubble of the helicopter cockpit (Figure 5).

2.4.6 GPS NAVIGATION SYSTEM

The navigation system used was a Geotech PC104 based navigation system utilizing a NovAtel's WAAS(Wide Area Augmentation System) enabled GPS receiver, Geotech navigate software, a full screen display with controls in front of the pilot to direct the flight and a NovAtel GPS antenna mounted on the helicopter tail (Figure 5). As many as 11 GPS and two WAAS satellites may be monitored at any one time. The positional accuracy or circular error probability (CEP) is 1.8 m, with WAAS active, it is 1.0 m. The coordinates of the survey area were set-up prior to the survey and the information was fed into the airborne navigation system. The second GPS antenna is installed on the additional magnetic loop together with Gyro Inclinometer.

2.4.7 DIGITAL ACQUISITION SYSTEM

A Geotech data acquisition system recorded the digital survey data on an internal compact flash card. Data is displayed on an LCD screen as traces to allow the operator to monitor the integrity of the system. The data type and sampling interval as provided in Table 4.

Table 4: Acquisition Sampling Rates

Data Type	Sampling
TDEM	0.1 sec
Magnetometer	0.1 sec
GPS Position	0.2 sec
Radar Altimeter	0.2 sec
Inclinometer	0.1 sec

Project GL210091
VTEM™ Plus Report on Airborne Geophysical
Survey for Big Gold Inc.

12

2.5 BASE STATION

A combined magnetometer/GPS base station was utilized on this project. A Geometrics Caesium vapour magnetometer was used as a magnetic sensor with a sensitivity of 0.001 nT. The base station was recording the magnetic field together with the GPS time at 1 Hz on a base station computer.

The base station magnetometer sensor was installed in a secured location away from electric transmission lines and moving ferrous objects such as motor vehicles. The base station data were backed-up to the data processing computer at the end of each survey day.

Project GL210091
VTEM™ Plus Report on Airborne Geophysical
Survey for Big Gold Inc.

13

3. PERSONNEL

The following Geotech Ltd. personnel were involved in the project.

FIELD:

Project Manager: Steven Cargnello (Office)

Data QC: Matthew Johnston

Crew chief: Paul Taylor
Ben Kodisang

Operator: Lyle Bilberry

The survey pilot and the mechanical engineer were employed directly by the helicopter operator – Geotech Aviation Ltd.

Pilot: Brent Jewel

Mechanical Engineer: n/a

OFFICE:

Preliminary Data Processing: Matthew Johnston

Final Data Processing: TaiChyi Shei

Data QA/QC: Emily Data
Jean Legault

Reporting/Mapping: Emily Data
Jean Legault

Processing and Interpretation phases were carried out under the supervision of Emily Data & Jean M. Legault, Chief Geophysicist. The customer relations were looked after by Paolo Berardelli.

Project GL210091
VTEM™ Plus Report on Airborne Geophysical
Survey for Big Gold Inc.

14

GEOTECH
AIRBORNE GEOPHYSICAL SURVEYS

4.   DATA PROCESSING AND PRESENTATION

Data compilation and processing were carried out by the application of Geosoft OASIS Montaj and programs proprietary to Geotech Ltd.

4.1 FLIGHT PATH

The flight path, recorded by the acquisition program as WGS 84 latitude/longitude, was converted into the WGS84 Datum, UTM Zone 15N coordinate system in Oasis Montaj.

The flight path was drawn using linear interpolation between x, y positions from the navigation system. Positions are updated every second and expressed as UTM easting's (x) and UTM northing's (y).

4.2 ELECTROMAGNETIC DATA

The Full Waveform EM specific data processing operations included:

- Half cycle stacking (performed at time of acquisition).
- System response correction.
- Parasitic and drift removal.

A three-stage digital filtering process was used to reject major sferic events and to reduce noise levels. Local sferic activity can produce sharp, large amplitude events that cannot be removed by conventional filtering procedures. Smoothing or stacking will reduce their amplitude but leave a broader residual response that can be confused with geological phenomena. To avoid this possibility, a computer algorithm searches out and rejects the major sferic events.

The signal to noise ratio was further improved by the application of a low pass linear digital filter. This filter has zero phase shift which prevents any lag or peak displacement from occurring, and it suppresses only variations with a wavelength less than about 1 second or 15 metres. This filter is a symmetrical 1 sec linear filter.

The results are presented as stacked profiles of EM voltages for the time gates, in linear - logarithmic scale for the B-field Z component and dB/dt responses in the Z and X components. B-field Z component time channels recorded at 0.880 milliseconds after the termination of the impulse is also presented as a colour image. Calculated Time Constant (TAU) with Calculated Vertical Derivative contours is presented in Appendix C. Resistivity Depth Image (RDI) is also presented in Appendix G.

VTEM™ has three receiver coil orientations. Z-axis coil is oriented parallel to the transmitter coil axis, and both are horizontal to the ground. The X-axis coil is oriented parallel to the ground and along the line-of-flight. The Y-axis coil is oriented parallel to the ground and across the line-of-flight. The combination of the X, Y, and Z coils configuration provides information on the position, depth, dip, and thickness of a conductor. Generalized modeling results of VTEM data are shown in Appendix D.

Project GL210091
VTEM™ Plus Report on Airborne Geophysical
Survey for Big Gold Inc.

15

GEOTECH
AIRBORNE GEOPHYSICAL SURVEYS

In general X-component data produce cross-over type anomalies: from "+ to – "in flight direction of flight for "thin" sub vertical targets and from "- to +" in direction of flight for "thick" targets. Z component data produce double peak type anomalies for "thin" sub vertical targets and single peak for "thick" targets. The limits and change-over of "thin-thick" depends on dimensions of a TEM system (Appendix D, Figure D-16).

Because of X component polarity is under line-of-flight, convolution Fraser Filter (Figure 6) is applied to X component data to represent axes of conductors in the form of grid map. In this case positive FF anomalies always correspond to "plus-to-minus" X data crossovers independent of the flight direction.
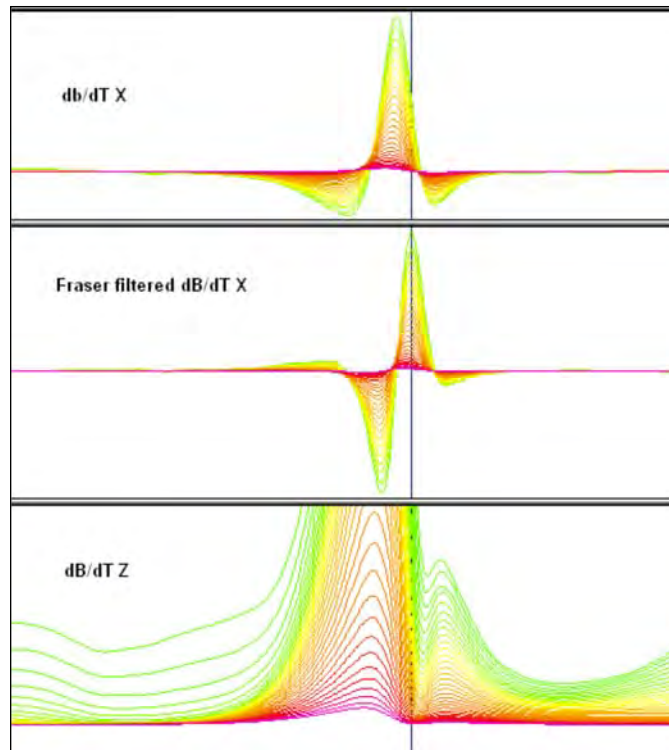
Figure 6: Z, X and Fraser filtered X (FFx) components for "thin" target.

Project GL210091
VTEM™ Plus Report on Airborne Geophysical
Survey for Big Gold Inc.

16

GEOTECH
AIRBORNE GEOPHYSICAL SURVEYS

4.3 HORIZONTAL MAGNETIC GRADIOMETER DATA

The horizontal gradients data from the VTEM™ Plus are measured by two magnetometers 12.5 m apart on an independent bird mounted 10m above the VTEM™ loop. A GPS and a Gyro Inclinometer help to determine the positions and orientations of the magnetometers. The data from the two magnetometers are corrected for position and orientation variations, as well as for the diurnal variations using the base station data.

The position of the centre of the horizontal magnetic gradiometer bird is calculated from the GPS utilizing in-house processing tool in Geosoft. Following that total magnetic intensity is calculated at the center of the bird by calculating the mean values from both sensors. In addition to the total intensity advanced processing is done to calculate the in-line and crossline (or lateral) horizontal gradient which enhance the understanding of magnetic targets. The in-line (longitudinal) horizontal gradient is calculated from the difference of two consecutive total magnetic field readings divided by the distance along the flight line direction, while the crossline (lateral) horizontal magnetic gradient is calculated from the difference in the magnetic readings from both magnetic sensors divided by their horizontal separation.

Two advanced magnetic derivative products, the total horizontal derivative (THDR), and tilt angle derivative and are also created. The total horizontal derivative or gradient is defined as:

THDR = sqrt (Hx*Hx+Hy*Hy), where Hx and Hy are crossline and in-line horizontal gradients.

The tilt angle derivative (TDR) is defined as:

TDR = arctan (Vz/THDR), where THDR is the total horizontal derivative, and Vz is the vertical derivative.

Measured crossline gradients can help to enhance crossline linear features during gridding.

Project GL210091
VTEM™ Plus Report on Airborne Geophysical
Survey for Big Gold Inc.

17

5. DELIVERABLES

5.1 SURVEY REPORT

The survey report describes the data acquisition, processing, and final presentation of the survey results. The survey report is provided in two paper copies and digitally in PDF format.

5.2 MAPS

Final maps were produced at scale of 1:10,000 for best representation of the survey size and line spacing. The coordinate/projection system used was WGS84 Datum, UTM Zone 15N. All maps show the flight path trace and topographic data; latitude and longitude are also noted on maps.

The results of the survey are presented as EM profiles, a late-time gate gridded EM channel, and a colour magnetic TMI contour map.

- Maps at 1:10,000 in Geosoft MAP format, as follows:

GL210091_10k_dBdt:	dB/dt profiles Z Component, Time Gates 0.220 – 7.036 ms in linear – logarithmic scale.
GL210091_10k_BField:	B-field profiles Z Component, Time Gates 0.220 – 7.036 ms in linear – logarithmic scale.
GL210091_10k_BFz30:	B-field Z Component Channel 30, Time Gate 0.880 ms colour image.
GL210091_10k_SFz30:	VTEM dB/dt Z Component Channel 30, Time Gate 0.880 ms colour image
GL210091_10k_SFxFF25:	Fraser Filtered dB/dt X Component Channel 25, Time Gate 0.440 ms colour image.
GL210091_10k_TauSF:	dB/dt Calculated Time Constant (Tau) with Calculated Vertical Derivative contours
GL210091_10k_TMI:	Total Magnetic Intensity (TMI) colour image and contours.
GL210091_10k_CVG:	Calculated Vertical Derivative (nT/m)
GL210091_10k_TotHG:	Magnetic Total Horizontal Gradient (nT/m)
GL210091_10k_TiltDrv:	Magnetic Tilt derivative (radians)

- Maps are also presented in PDF format.

- The topographic data base was derived from 1:250,000 CANVEC data. Background shading is from ASTER GDEM (https://gdex.cr.usgs.gov/gdex). Inset data derived from the Geocommunities (www.geocomm.com)

- A Google Earth file *GL210091_BigGold.kmz* showing the flight path of the block is included. Free versions of Google Earth software from: http://earth.google.com/download-earth.html

Project GL210091
VTEM™ Plus Report on Airborne Geophysical
Survey for Big Gold Inc.

18

GEOTECH
AIRBORNE GEOPHYSICAL SURVEYS

5.3 DIGITAL DATA

Two copies of the data and maps on DVD were prepared to accompany the report. Each DVD contains a digital file of the line data in GDB Geosoft Montaj format as well as the maps in Geosoft Montaj Map and PDF format.

- DVD structure.

    Data   contains databases, grids and maps, as described below.
    Report   contains a copy of the report and appendices in PDF format.

Databases in Geosoft GDB format, containing the channels listed in Table 5.

Table 5: Geosoft GDB Data Format

Channel name	Units	Description
X	metres	Easting WGS84 Zone 15N
Y	metres	Northing WGS84 Zone 15N
Longitude	Decimal Degrees	WGS84 Longitude data
Latitude	Decimal Degrees	WGS84 Latitude data
Z	metres	GPS antenna elevation
Zb	metres	EM bird elevation
Radar	metres	Helicopter terrain clearance from radar altimeter
Radarb	metres	Calculated EM transmitter-receiver loop terrain clearance from radar altimeter
DEM	metres	Digital Elevation Model
Gtime	Seconds of the day	GPS time
Mag1L	nT	Measured Total Magnetic field data (left sensor)
Mag1R	nT	Measured Total Magnetic field data (right sensor)
Basemag	nT	Magnetic diurnal variation data
Mag2LZ	nT	Z corrected (w.r.t. loop center) and diurnal corrected magnetic field left mag
Mag2RZ	nT	Z corrected (w.r.t. loop center) and diurnal corrected magnetic field right mag
TMI2	nT	Calculated from diurnal corrected total magnetic field intensity of the centre of the loop
TMI3	nT	Microleveled total magnetic field intensity of the centre of the loop
Hginline		Calculated in-line gradient
Hgcxline		Measured cross-line gradient
CVG	nT/m	Calculated Magnetic Vertical Gradient of TMI
SFz[4]	pV/(A*m4)	Z dB/dt 0.021 millisecond time channel
SFz[5]	pV/(A*m4)	Z dB/dt 0.026 millisecond time channel
SFz[6]	pV/(A*m^4)	Z dB/dt 0.031 millisecond time channel
SFz[7]	pV/(A*m^4)	Z dB/dt 0.036 millisecond time channel
SFz[8]	pV/(A*m^4)	Z dB/dt 0.042 millisecond time channel
SFz[9]	pV/(A*m^4)	Z dB/dt 0.048 millisecond time channel
SFz[10]	pV/(A*m^4)	Z dB/dt 0.055 millisecond time channel
SFz[11]	pV/(A*m^4)	Z dB/dt 0.063 millisecond time channel
SFz[12]	pV/(A*m^4)	Z dB/dt 0.073 millisecond time channel
SFz[13]	pV/(A*m^4)	Z dB/dt 0.083 millisecond time channel
SFz[14]	pV/(A*m^4)	Z dB/dt 0.096 millisecond time channel

Project GL210091
VTEM™ Plus Report on Airborne Geophysical
Survey for Big Gold Inc.

19

GEOTECH
AIRBORNE GEOPHYSICAL SURVEYS

Channel name	Units	Description
SFz[15]	pV/(A*m^4)	Z dB/dt 0.110 millisecond time channel
SFz[16]	pV/(A*m^4)	Z dB/dt 0.126 millisecond time channel
SFz[17]	pV/(A*m^4)	Z dB/dt 0.145millisecond time channel
SFz[18]	pV/(A*m^4)	Z dB/dt 0.167 millisecond time channel
SFz[19]	pV/(A*m^4)	Z dB/dt 0.192 millisecond time channel
SFz[20]	pV/(A*m^4)	Z dB/dt 0.220 millisecond time channel
SFz[21]	pV/(A*m^4)	Z dB/dt 0.253 millisecond time channel
SFz[22]	pV/(A*m^4)	Z dB/dt 0.290 millisecond time channel
SFz[23]	pV/(A*m^4)	Z dB/dt 0.333 millisecond time channel
SFz[24]	pV/(A*m^4)	Z dB/dt 0.383 millisecond time channel
SFz[25]	pV/(A*m^4)	Z dB/dt 0.440 millisecond time channel
SFz[26]	pV/(A*m^4)	Z dB/dt 0.505 millisecond time channel
SFz[27]	pV/(A*m^4)	Z dB/dt 0.580 millisecond time channel
SFz[28]	pV/(A*m^4)	Z dB/dt 0.667 millisecond time channel
SFz[29]	pV/(A*m^4)	Z dB/dt 0.766 millisecond time channel
SFz[30]	pV/(A*m^4)	Z dB/dt 0.880 millisecond time channel
SFz[31]	pV/(A*m^4)	Z dB/dt 1.010 millisecond time channel
SFz[32]	pV/(A*m^4)	Z dB/dt 1.161 millisecond time channel
SFz[33]	pV/(A*m^4)	Z dB/dt 1.333 millisecond time channel
SFz[34]	pV/(A*m^4)	Z dB/dt 1.531 millisecond time channel
SFz[35]	pV/(A*m^4)	Z dB/dt 1.760 millisecond time channel
SFz[36]	pV/(A*m^4)	Z dB/dt 2.021 millisecond time channel
SFz[37]	pV/(A*m^4)	Z dB/dt 2.323 millisecond time channel
SFz[38]	pV/(A*m^4)	Z dB/dt 2.667 millisecond time channel
SFz[39]	pV/(A*m^4)	Z dB/dt 3.063 millisecond time channel
SFz[40]	pV/(A*m^4)	Z dB/dt 3.521 millisecond time channel
SFz[41]	pV/(A*m^4)	Z dB/dt 4.042 millisecond time channel
SFz[42]	pV/(A*m^4)	Z dB/dt 4.641 millisecond time channel
SFz[43]	pV/(A*m^4)	Z dB/dt 5.333 millisecond time channel
SFz[44]	pV/(A*m^4)	Z dB/dt 6.125 millisecond time channel
SFz[45]	pV/(A*m^4)	Z dB/dt 7.036 millisecond time channel
SFz[46]	pV/(A*m^4)	Z dB/dt 8.083 millisecond time channel
SFx[20]	pV/(A*m^4)	X dB/dt 0.220 millisecond time channel
SFx[21]	pV/(A*m^4)	X dB/dt 0.253 millisecond time channel
SFx[22]	pV/(A*m^4)	X dB/dt 0.290 millisecond time channel
SFx[23]	pV/(A*m^4)	X dB/dt 0.333 millisecond time channel
SFx[24]	pV/(A*m^4)	X dB/dt 0.383 millisecond time channel
SFx[25]	pV/(A*m^4)	X dB/dt 0.440 millisecond time channel
SFx[26]	pV/(A*m^4)	X dB/dt 0.505 millisecond time channel
SFx[27]	pV/(A*m^4)	X dB/dt 0.580 millisecond time channel
SFx[28]	pV/(A*m^4)	X dB/dt 0.667 millisecond time channel
SFx[29]	pV/(A*m^4)	X dB/dt 0.766 millisecond time channel
SFx[30]	pV/(A*m^4)	X dB/dt 0.880 millisecond time channel
SFx[31]	pV/(A*m^4)	X dB/dt 1.010 millisecond time channel
SFx[32]	pV/(A*m^4)	X dB/dt 1.161 millisecond time channel
SFx[33]	pV/(A*m^4)	X dB/dt 1.333 millisecond time channel
SFx[34]	pV/(A*m^4)	X dB/dt 1.531 millisecond time channel
SFx[35]	pV/(A*m^4)	X dB/dt 1.760 millisecond time channel
SFx[36]	pV/(A*m^4)	X dB/dt 2.021 millisecond time channel
SFx[37]	pV/(A*m^4)	X dB/dt 2.323 millisecond time channel

Project GL210091
VTEM™ Plus Report on Airborne Geophysical
Survey for Big Gold Inc.

20

Channel name	Units	Description
SFx[38]	pV/(A*m^4)	X dB/dt 2.667 millisecond time channel
SFx[39]	pV/(A*m^4)	X dB/dt 3.063 millisecond time channel
SFx[40]	pV/(A*m^4)	X dB/dt 3.521 millisecond time channel
SFx[41]	pV/(A*m^4)	X dB/dt 4.042 millisecond time channel
SFx[42]	pV/(A*m^4)	X dB/dt 4.641 millisecond time channel
SFx[43]	pV/(A*m^4)	X dB/dt 5.333 millisecond time channel
SFx[44]	pV/(A*m^4)	X dB/dt 6.125 millisecond time channel
SFx[45]	pV/(A*m^4)	X dB/dt 7.036 millisecond time channel
SFx[46]	pV/(A*m^4)	X dB/dt 8.083 millisecond time channel
SFy	pV/(A*m^4)	Y dB/dt data for time channels 20 to 46
BFz	(pV*ms)/(A*m^4)	Z B-Field data for time channels 4 to 46
BFx	(pV*ms)/(A*m^4)	X B-Field data for time channels 20 to 46
BFy	(pV*ms)/(A*m^4)	Y B-Field data for time channels 20 to 46
SFxFF	pV/(A*m^4)	Fraser Filtered X dB/dt
NchanBF		Latest time channels of TAU calculation
TauBF	ms	Time constant B-Field
NchanSF		Latest time channels of TAU calculation
TauSF	ms	Time constant dB/dt
PLM		60 Hz power line monitor

Electromagnetic B-field and dB/dt Z component data is found in array channel format between indexes 4 – 46, and X&Y component data from 20 – 46, as described above.

- Database of the Resistivity Depth Images in Geosoft GDB format, containing the following channels:

Table 6: Geosoft Resistivity Depth Image GDB Data Format

Channel name	Units	Description
Xg	metres	Easting WGS84 Zone 15N
Yg	metres	Northing WGS84 Zone 15N
Dist	metres	Distance from the beginning of the line
Depth	metres	array channel, depth from the surface
Z	metres	array channel, depth
AppRes	Ohm-m	array channel, Apparent Resistivity
TR	metres	EM system height
Topo	metres	digital elevation model
Radarb	metres	Calculated EM transmitter-receiver loop terrain clearance from radar altimeter
SF	pV/(A*m^4)	array channel, Z dB/dT
MAG	nT	TMI data
CVG	nT/m	CVG data
DOI	metres	Depth of Investigation: a measure of VTEM depth effectiveness
PLM		60Hz Power Line Monitor

Project GL210091
VTEM™ Plus Report on Airborne Geophysical
Survey for Big Gold Inc.

21

GEOTECH
AIRBORNE GEOPHYSICAL SURVEYS

- Database of the VTEM Waveform "GL210091_Waveform.gdb" in Geosoft GDB format, containing the following channels:

Table 7: Geosoft database for the VTEM waveform

Channel name	Units	Description
Time	milliseconds	Sampling rate interval, 5.2083 microseconds
Tx_Current	amps	Output current of the transmitter

- Geosoft Resistivity Depth Image Products:

Sections:	Apparent resistivity sections along each line in .GRD and .PDF format
Slices:	Apparent resistivity slices at selected depths from 25m to depth of investigation, at an increment of 25m in .GRD and .PDF format
Voxel:	3D Voxel imaging of apparent resistivity data clipped by digital elevation and depth of investigation

- Grids in Geosoft GRD and GeoTIFF format, as follows:

BFz30:	B-Field Z Component Channel 30 (Time Gate 0.880ms)
SFxFF25:	Fraser Filtered dB/dt X Component Channel 25 (Time Gate 0.440ms)
SFz8:	dB/dt Z Component Channel 8 (Time Gate 0.042ms)
SFz30:	dB/dt Z Component Channel 30 (Time Gate 0.880ms)
SFz40:	dB/dt Z Component Channel 40 (Time Gate 3.521ms)
TauSF:	dB/dt Z Component, Calculated Time Constant (ms)
TauBF:	B-Field Z Component, Calculated Time Constant (ms)
TMI3:	Total Magnetic Intensity (nT)
CVG:	Calculated Vertical Derivative (nT/m)
Hginline:	Measured In-Line Gradient (nT/m)
Hgcxline:	Measured Cross-Line Gradient (nT/m)
TotHGrad:	Magnetic Total Horizontal Gradient (nT/m)
TiltDrv:	Magnetic Tilt derivative (radians)
DEM:	Digital Elevation Model (m)
PLM:	60 Hz Power Line Monitor

A Geosoft .GRD file has a .GI metadata file associated with it, containing grid projection information. A grid cell size of 25 metres was used.

Project GL210091
VTEM™ Plus Report on Airborne Geophysical
Survey for Big Gold Inc.

22

6.   CONCLUSIONS AND RECOMMENDATIONS
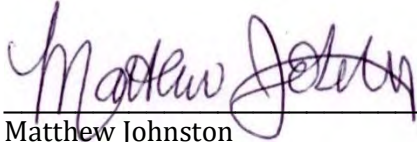
A helicopter-borne versatile time domain electromagnetic (VTEM™plus) horizontal magnetic gradiometer geophysical survey has been completed over the Martin Kenty Project near Nestor Falls, ON, on behalf of Big Gold Inc.

The total area coverage is 34km^2 and the total survey line coverage is 365 line kilometres over one survey block. The principal sensors included a Time Domain EM system, and a horizontal magnetic gradiometer system with two caesium magnetometers. Results have been presented as stacked profiles, and contour colour images at a scale of 1:10,000. A formal interpretation has not been included in this study, however RDI resistivity-depth imaging has been performed in support of the VTEM data.

Based on the geophysical results obtained, a number of geophysical anomalies have been identified across the Martin Kenty project survey area. Magnetically, the block is active, with a measured range of >2,800nT, and features on a long (>6km), oval-shaped, EW to ENE trending magnetic high unit in the northern half of the block, with pronounced negative response in the center that suggests magnetic remanence. Magnetic derivatives highlight the banded nature of this magnetic high unit, as well as thinner, weaker paralleling lineaments in the southern half of the block. Electromagnetically, the survey area features a number of discrete, short to medium strike length (>0.5-1km), generally EW to ENE trending conductors with weak to moderate conductivities. Maximum dB$_Z$/dt EM TAU decay time constants fall in the 0.2-0.8 msec range. The most conductive features tend to occur in the northern half of the block, including along the main magnetic high trend. Elsewhere, conductors tend to occur in non-magnetic rocks, including conductive bodies in the southern half that occur within the near-surface and are dominantly flat-lying, potentially relating to lake-bottom sediments. The eastern and northern parts of the block host resistive rocks. The relationship between the EM conductors and magnetics is highlighted the EM TAU decay constant image with magnetic CVG contour map (Appendix C) and the RDI resistivity-depth image sections (Appendix G). Based on RDI results, apparent resistivities range from as low as approx. 15-30 ohm-m and also reach highs of approx. 4500 ohm-m. The estimated depth of the top of the anomalous zones is between approximately near surface and 50m depths, and maximum depths of investigation (DOI) vary from ~425m to >550m.

The Martin Kenty Project lies in the Kenora/Rainy River mining district and is prospective for massive-sulphide hosted gold mineralization (www.biggold.ca/martin-kenty-project/). As a result, both the EM and magnetic results are likely to be of exploration interest. We recommend that EM anomaly picking be performed along with Maxwell EM plate modeling of major anomalies of interest. 1D EM inversions will prove useful in determining the thickness and depth extent of flat-lying conductive units. CET-type magnetic lineament analysis and 3D MVI magnetic inversions will be useful for mapping structure, alteration, and lithology in 2D-3D space across the block. We recommend that more advanced, integrated interpretation be performed on these geophysical data and these results further evaluated against the known geology for future targeting

Project GL210091
VTEM™ Plus Report on Airborne Geophysical
Survey for Big Gold Inc.

23

GEOTECH
AIRBORNE GEOPHYSICAL SURVEYS

Respectfully submitted[1,]

_____
Matthew Johnston
Geotech Ltd.

_____
TaiChyi Shei
Geotech Ltd.
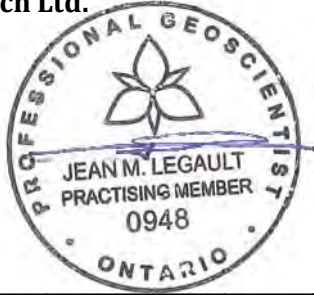
_____
Jean M. Legault, M.Sc.A, P.Eng, P.Geo
Geotech Ltd.

_____
Emily Data
Geotech Ltd.

December 2021

Project GL210091
VTEM™ Plus Report on Airborne Geophysical
Survey for Big Gold Inc.

24

GEOTECH
AIRBORNE GEOPHYSICAL SURVEYS

APPENDIX A

SURVEY AREA LOCATION MAP
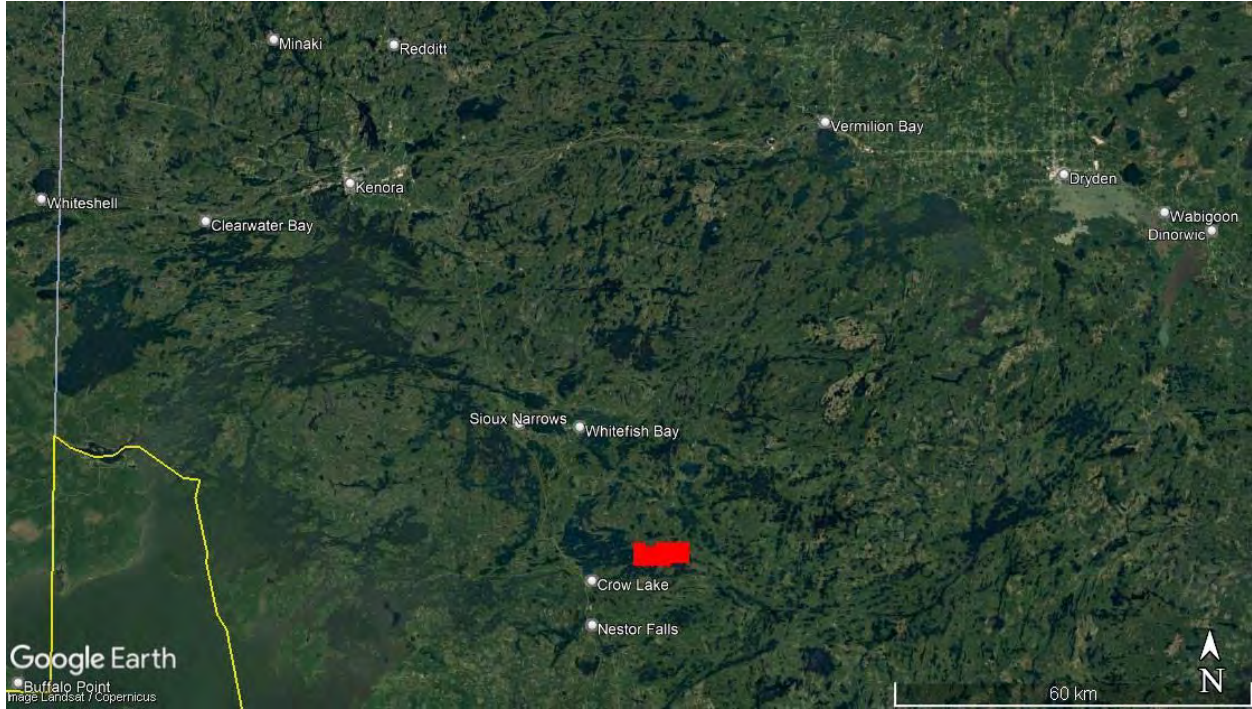
Overview of the Survey Area

Project GL210091
VTEM™ Plus Report on Airborne Geophysical
Survey for Big Gold Inc.

A1

APPENDIX B

SURVEY AREA COORDINATES
(WGS84 UTM Zone 15N)

Martin Kenty Project	
X	Y
440312	5453768
442193	5453766
442186	5453159
444012	5453161
444009	5453817
449483	5453813
449488	5450264
446288	5450262
446283	5449863
440309	5449863

Project GL210091
VTEM™ Plus Report on Airborne Geophysical
Survey for Big Gold Inc.

B1

GEOTECH
AIRBORNE GEOPHYSICAL SURVEYS

APPENDIX C - GEOPHYSICAL MAPS[1]

Z Component dB/dt profiles, Time Gates 0.220 – 7.036 ms

---
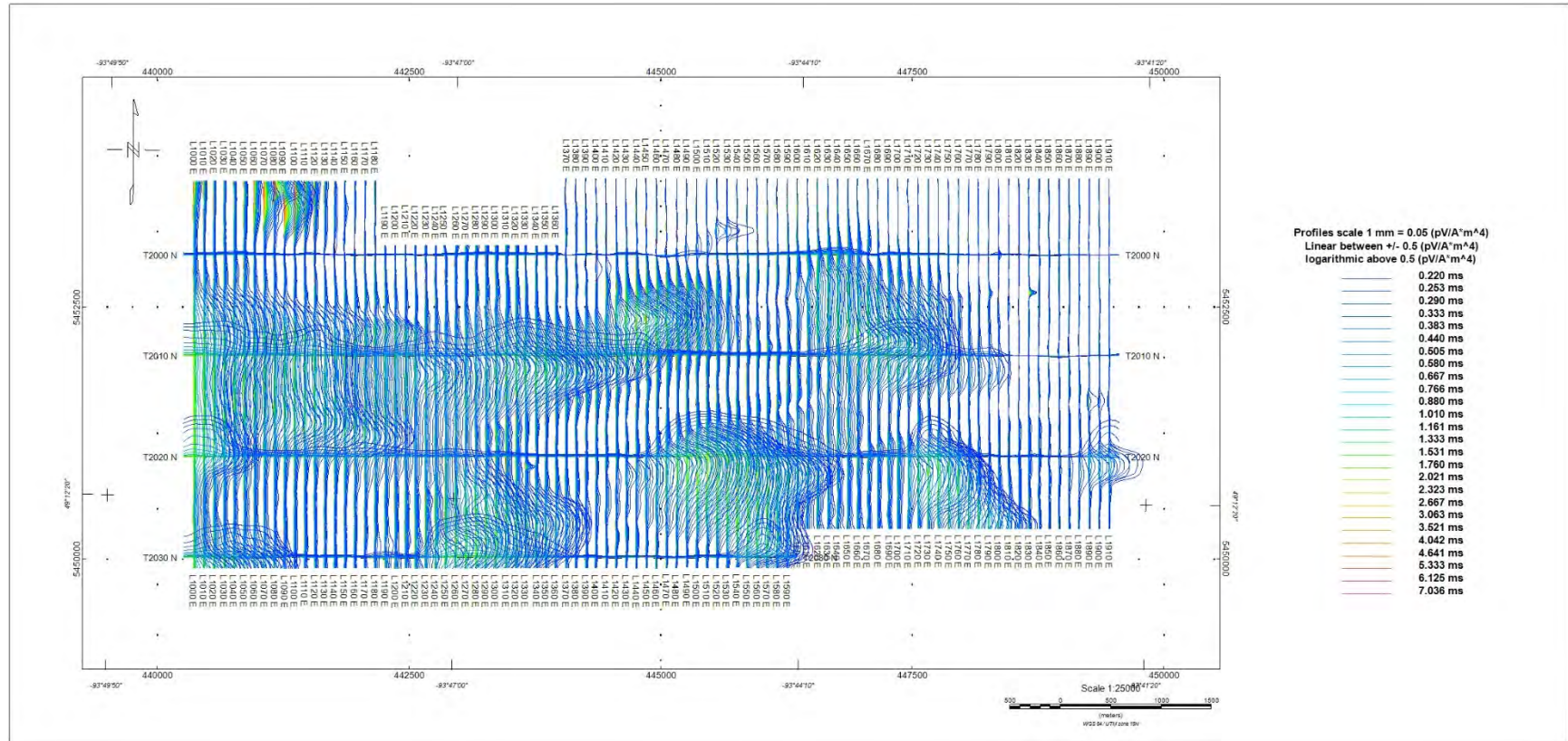
[1]Complete full size geophysical maps are also available in PDF format located in the final data maps folder.

Project GL210091
VTEM™ Plus Report on Airborne Geophysical
Survey for Big Gold Inc.

C1

GEOTECH
AIRBORNE GEOPHYSICAL SURVEYS
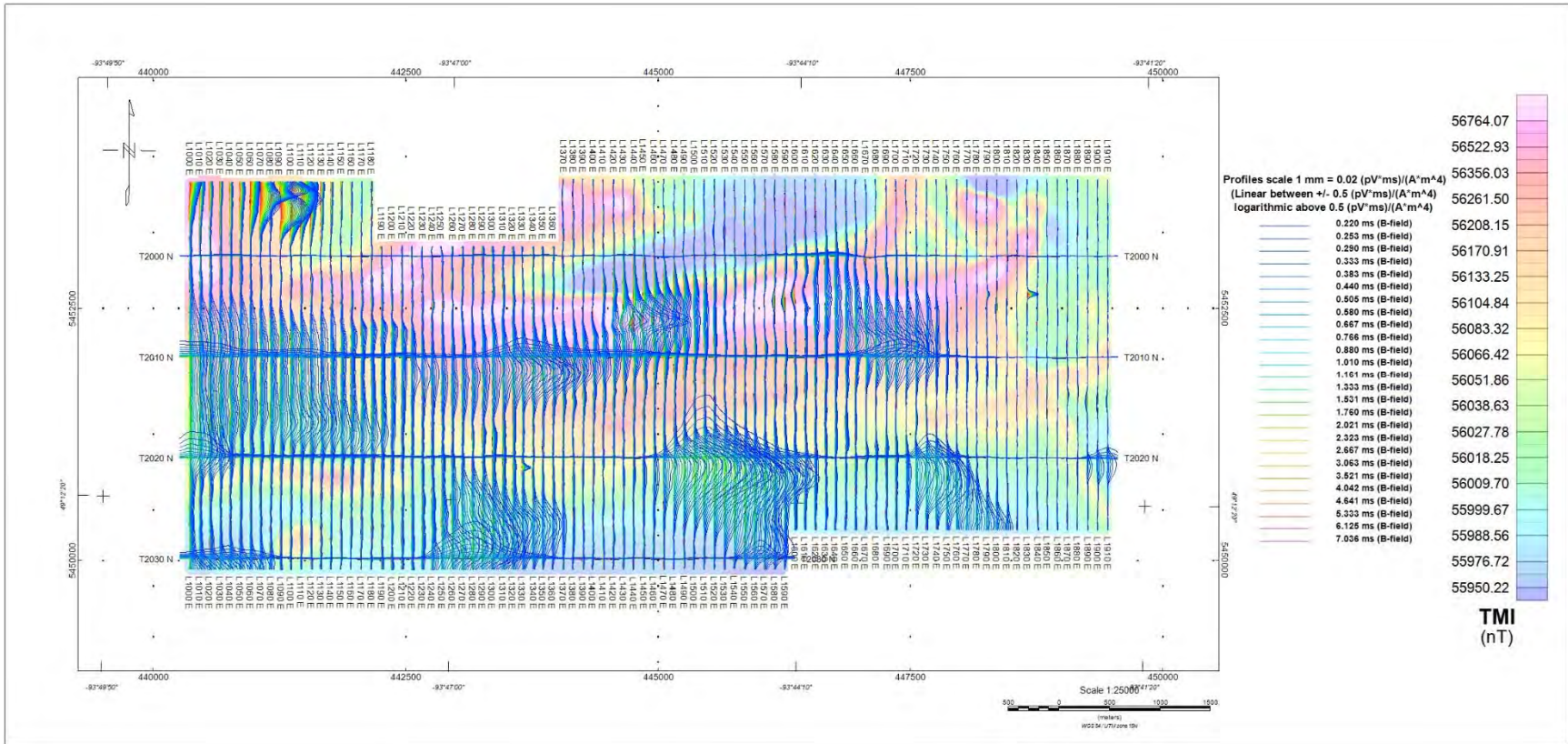
Z Component B-field profiles, Time Gates 0.220 – 7.036 ms over TMI colour image

Project GL210091
VTEM™ Plus Report on Airborne Geophysical
Survey for Big Gold Inc.

C2

GEOTECH
AIRBORNE GEOPHYSICAL SURVEYS

B-field Z Component Channel 30, Time Gate 0.880 ms colour image

Project GL210091
VTEM™ Plus Report on Airborne Geophysical
Survey for Big Gold Inc.

C3

GEOTECH
AIRBORNE GEOPHYSICAL SURVEYS

VTEM dB/dt Z Component Channel 30, Time Gate 0.880 ms colour image

Project GL210091
VTEM™ Plus Report on Airborne Geophysical
Survey for Big Gold Inc.

C4

GEOTECH
AIRBORNE GEOPHYSICAL SURVEYS

Fraser Filtered dB/dt X Component Channel 25, Time Gate 0.440 ms colour image

Project GL210091
VTEM™ Plus Report on Airborne Geophysical
Survey for Big Gold Inc.

C5

GEOTECH
AIRBORNE GEOPHYSICAL SURVEYS

dB/dt Z-Component Calculated Time Constant (Tau) with Calculated Vertical Gradient (CVG)contours

Project GL210091
VTEM™ Plus Report on Airborne Geophysical
Survey for Big Gold Inc.

GEOTECH
AIRBORNE GEOPHYSICAL SURVEYS

Total Magnetic Intensity (TMI) colour image and contours

Project GL210091
VTEM™ Plus Report on Airborne Geophysical
Survey for Big Gold Inc.

C7

GEOTECH
AIRBORNE GEOPHYSICAL SURVEYS

Magnetic Total Horizontal Gradient colour image

Project GL210091
VTEM™ Plus Report on Airborne Geophysical
Survey for Big Gold Inc.

C8
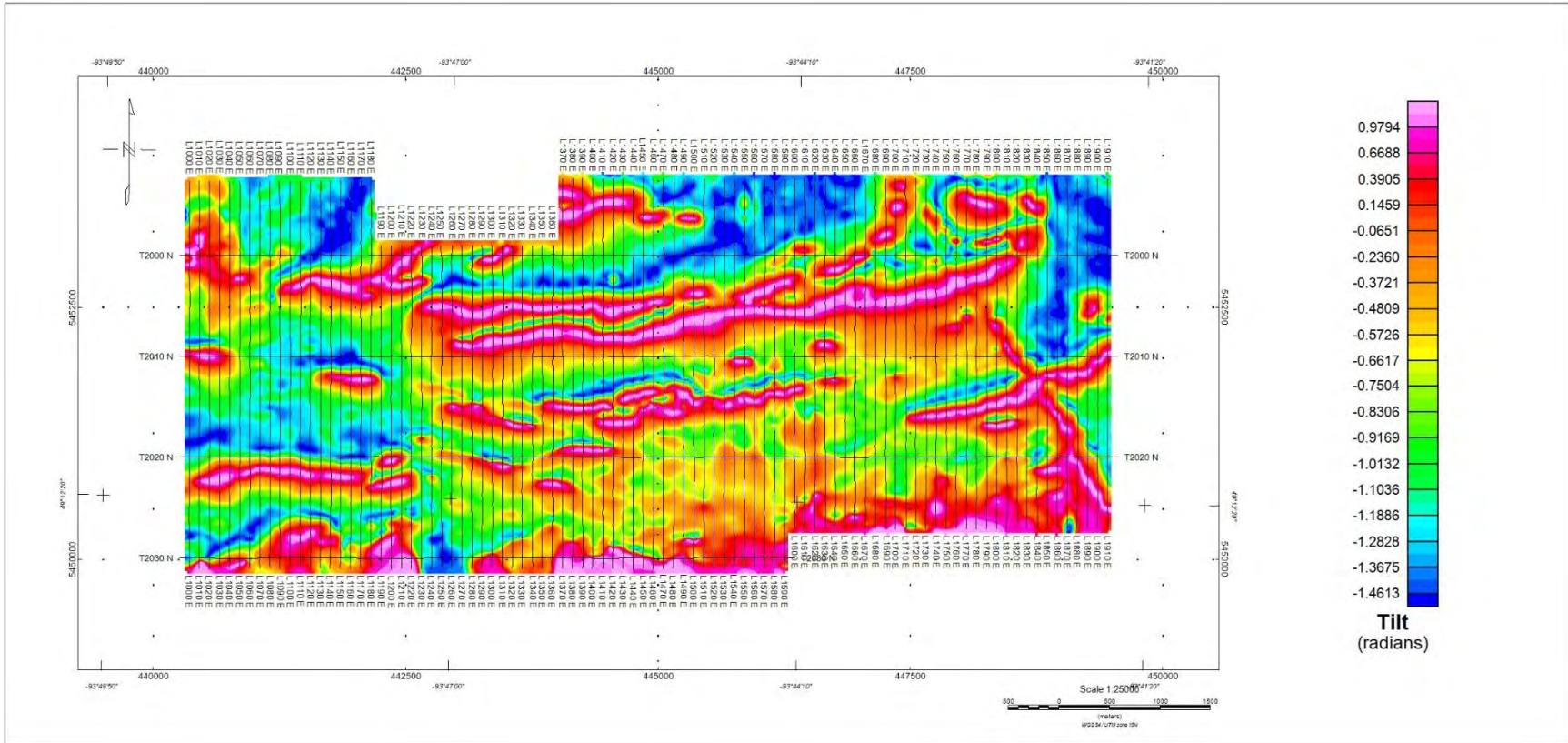
Magnetic Tilt Angle Derivative colour image

Project GL210091
VTEM™ Plus Report on Airborne Geophysical
Survey for Big Gold Inc.

C9

GEOTECH
AIRBORNE GEOPHYSICAL SURVEYS

Calculated Vertical Gradient (CVG)

Project GL210091
VTEM™ Plus Report on Airborne Geophysical
Survey for Big Gold Inc.

C10

GEOTECH
AIRBORNE GEOPHYSICAL SURVEYS
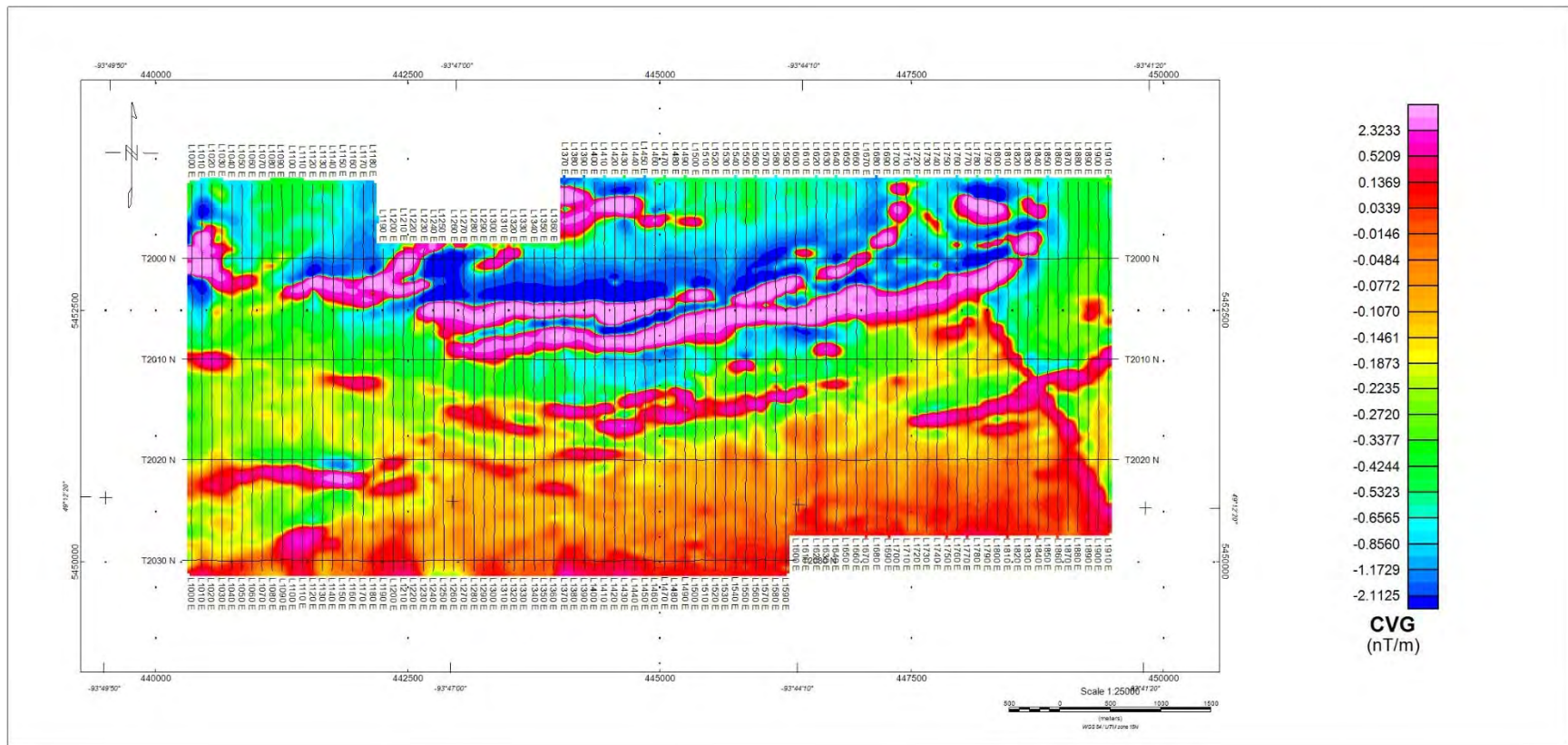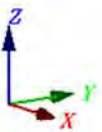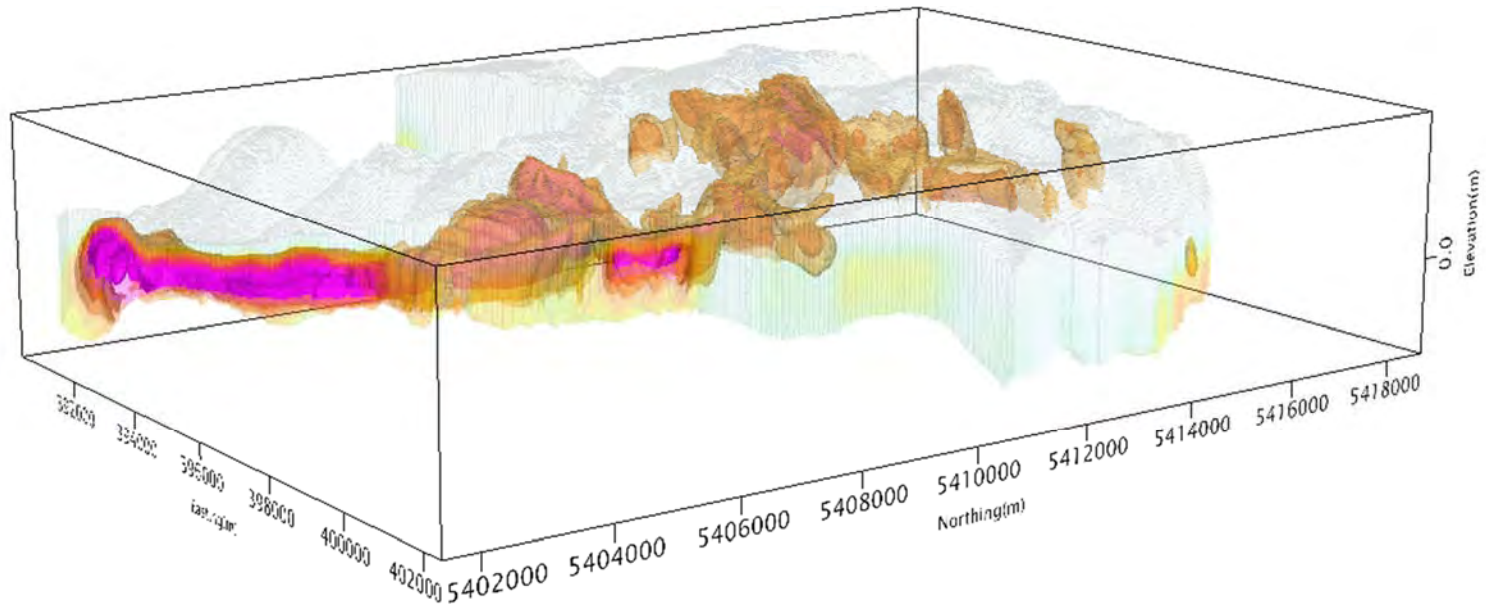
3D view of Resistivity-Depth-Image (RDI), Apparent Resistivity Voxel – Martin Kenty Project

Project GL210091
VTEM™ Plus Report on Airborne Geophysical
Survey for Big Gold Inc.

C11

APPENDIX D

GENERALIZED MODELING RESULTS OF THE VTEM SYSTEM
INTRODUCTION

The VTEM system is based on a concentric or central loop design, whereby, the receiver is positioned at the centre of a transmitter loop that produces a primary field. The wave form is a bi-polar, modified square wave with a turn-on and turn-off at each end.

During turn-on and turn-off, a time varying field is produced (dB/dt) and an electro-motive force (emf) is created as a finite impulse response. A current ring around the transmitter loop moves outward and downward as time progresses. When conductive rocks and mineralization are encountered, a secondary field is created by mutual induction and measured by the receiver at the centre of the transmitter loop.

Efficient modeling of the results can be carried out on regularly shaped geometries, thus yielding close approximations to the parameters of the measured targets. The following is a description of a series of common models made for the purpose of promoting a general understanding of the measured results.

A set of models has been produced for the Geotech VTEM™ system dB/dT Z and X components (see models D1 to D15). The Maxwell ™ modeling program (EMIT Technology Pty. Ltd. Midland, WA, AU) used to generate the following responses assumes a resistive half-space. The reader is encouraged to review these models, so as to get a general understanding of the responses as they apply to survey results. While these models do not begin to cover all possibilities, they give a general perspective on the simple and most commonly encountered anomalies.

As the plate dips and departs from the vertical position, the peaks become asymmetrical.

As the dip increases, the aspect ratio (Min/Max) decreases, and this aspect ratio can be used as an empirical guide to dip angles from near 90º to about 30º. The method is not sensitive enough where dips are less than about 30º.

Project GL210091
VTEM™ Plus Report on Airborne Geophysical
Survey for Big Gold Inc.

D1
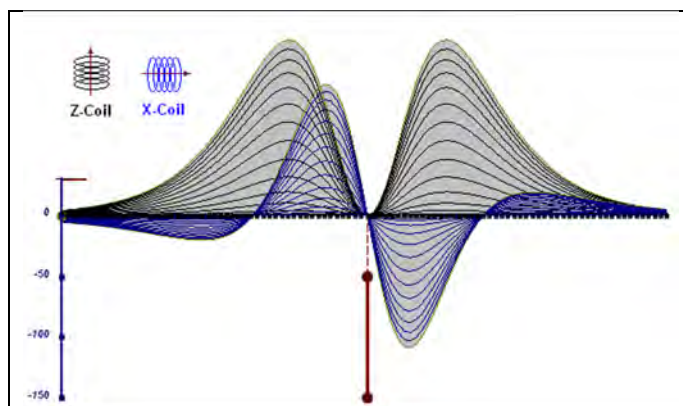
Figure D-1: vertical thin plate
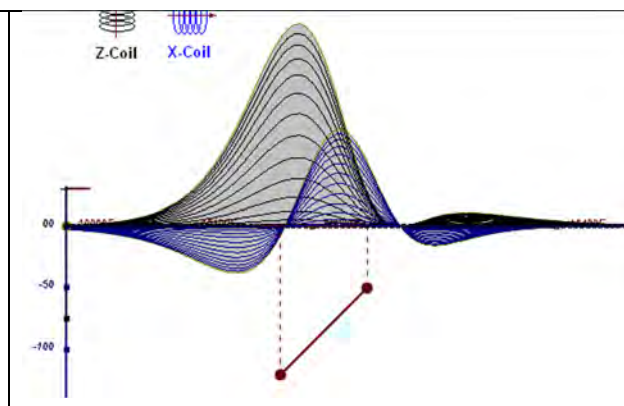
Figure D-2: inclined thin plate
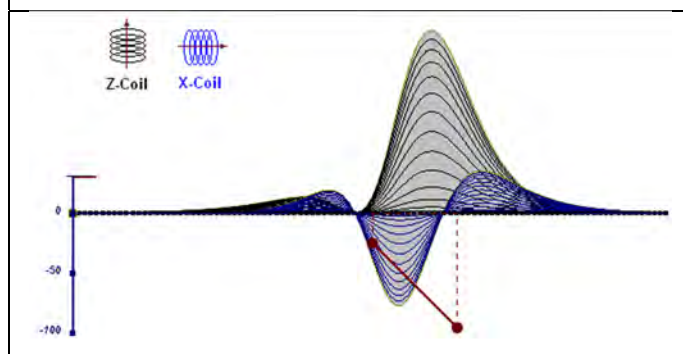
Figure D-3: inclined thin plate
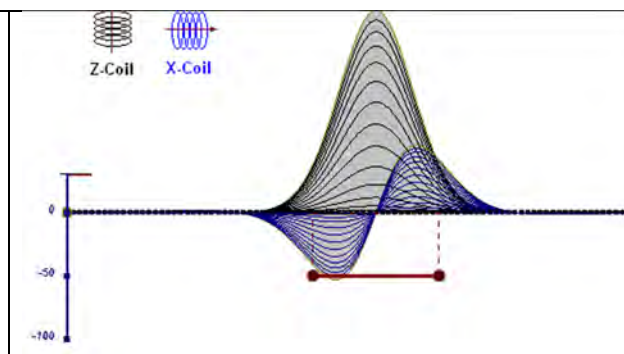
Figure D-4: horizontal thin plate
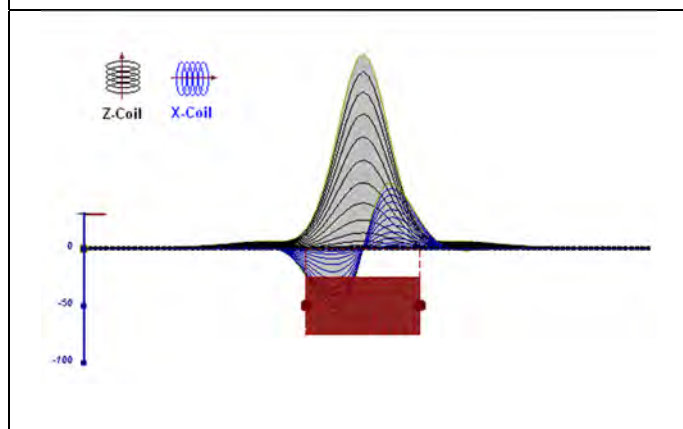
Figure D-5: horizontal thick plate (linear scale of the response)
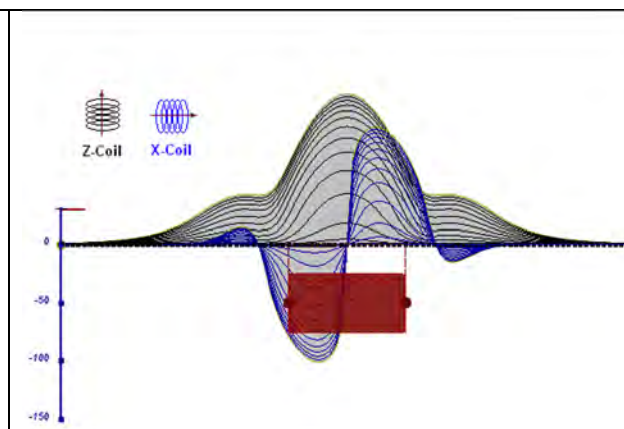
Figure D-6: horizontal thick plate (log scale of the response)

Project GL210091
VTEM™ Plus Report on Airborne Geophysical
Survey for Big Gold Inc.

D2

GEOTECH
AIRBORNE GEOPHYSICAL SURVEYS
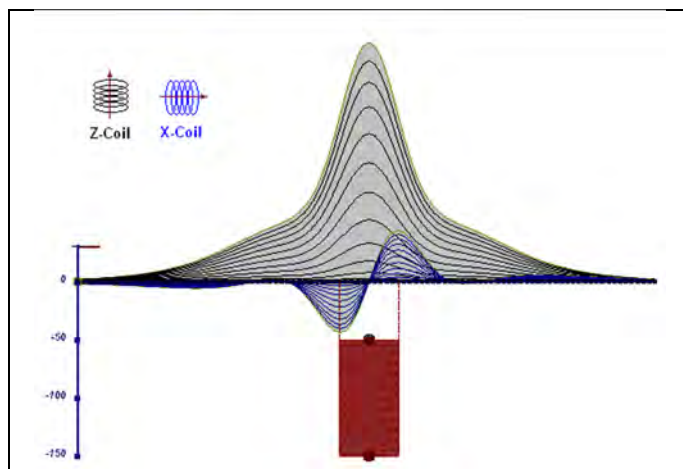
Figure D-7: vertical thick plate (linear scale of the response). 50 m depth
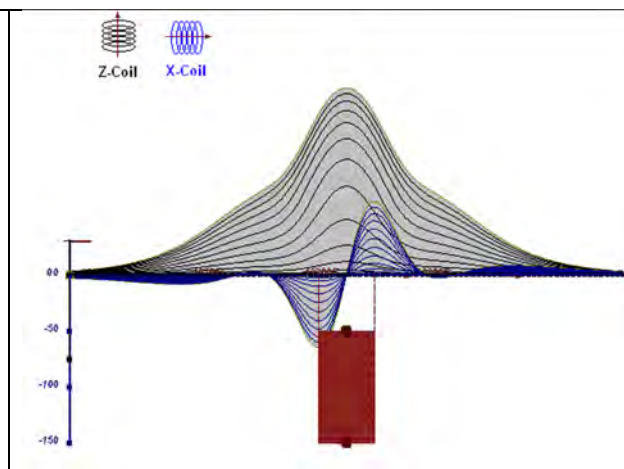
Figure D-8: vertical thick plate (log scale of the response). 50 m depth
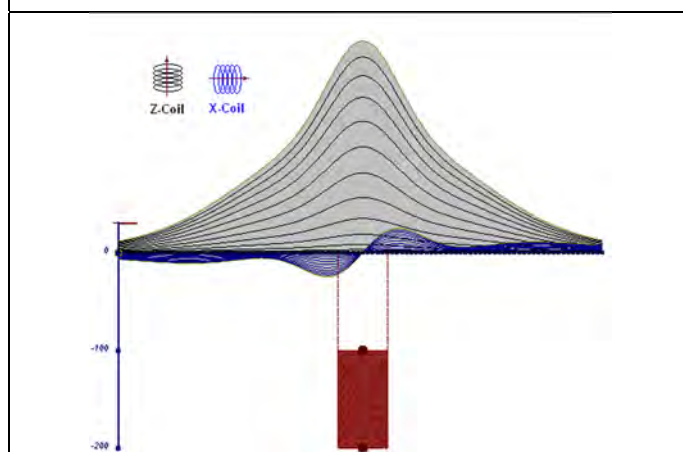
Figure D-9: vertical thick plate (linear scale of the response). 100 m depth
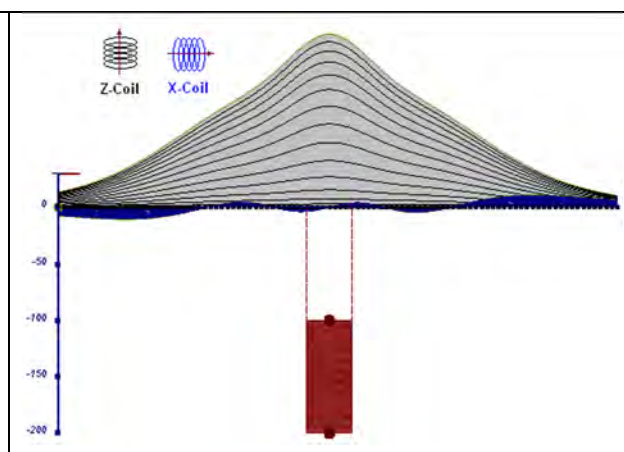
Figure D-10: vertical thick plate (linear scale of the response). Depth / horizontal thickness=2.5
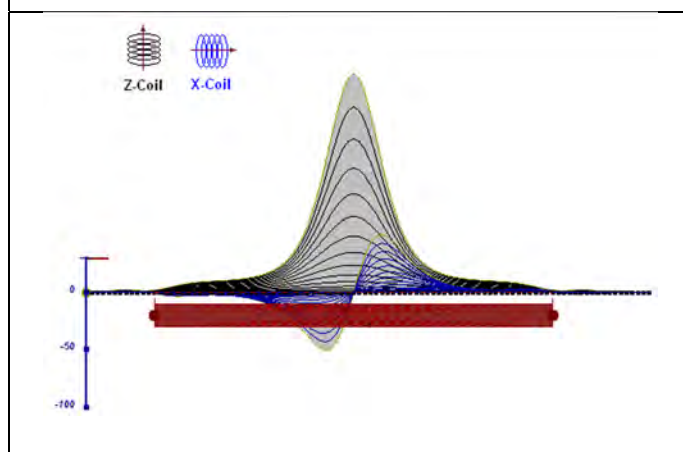
Figure D-11: horizontal thick plate (linear scale of the response)
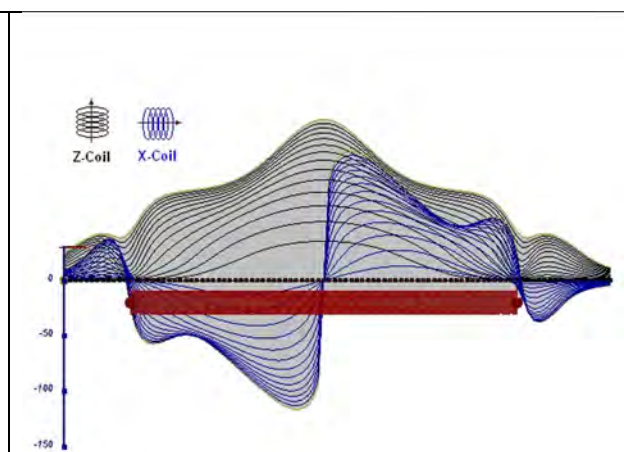
Figure D-12: horizontal thick plate (log scale of the response)

Project GL210091
VTEM™ Plus Report on Airborne Geophysical
Survey for Big Gold Inc.

D3

GEOTECH
AIRBORNE GEOPHYSICAL SURVEYS
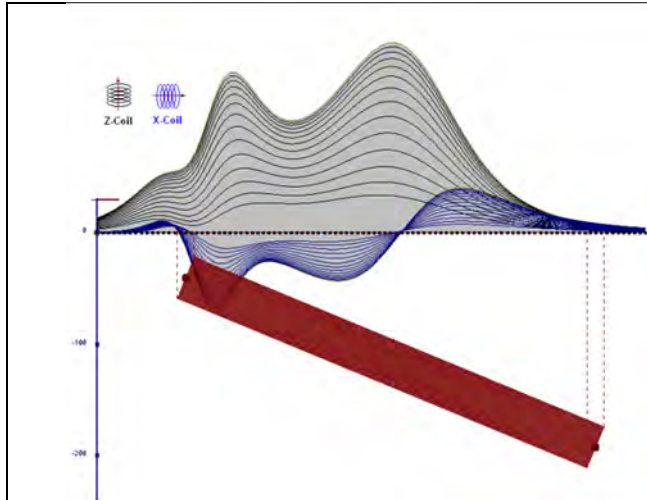
Figure D-13: inclined long thick plate
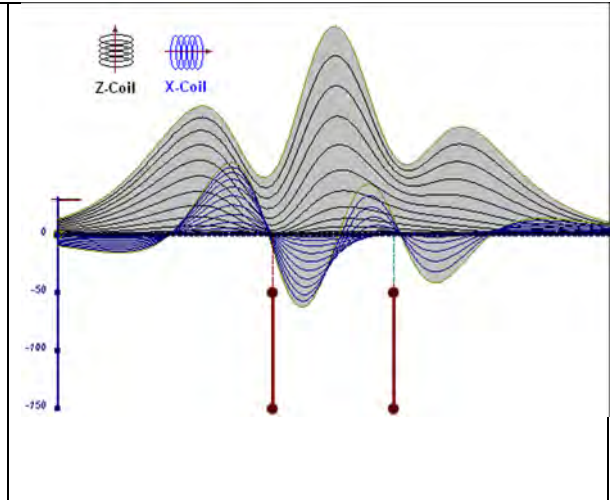
Figure D-14: two vertical thin plates
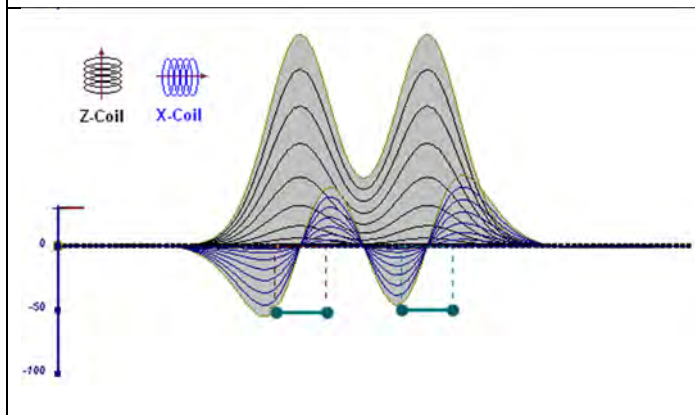
Figure D-15: two horizontal thin plates
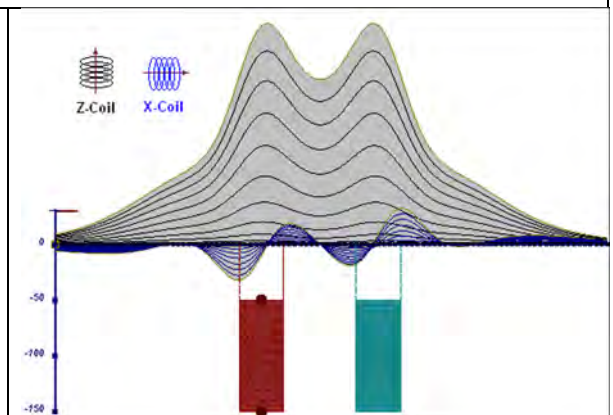
Figure D-16: two vertical thick plates

The same type of target but with different thickness, for example, creates different form of the response:
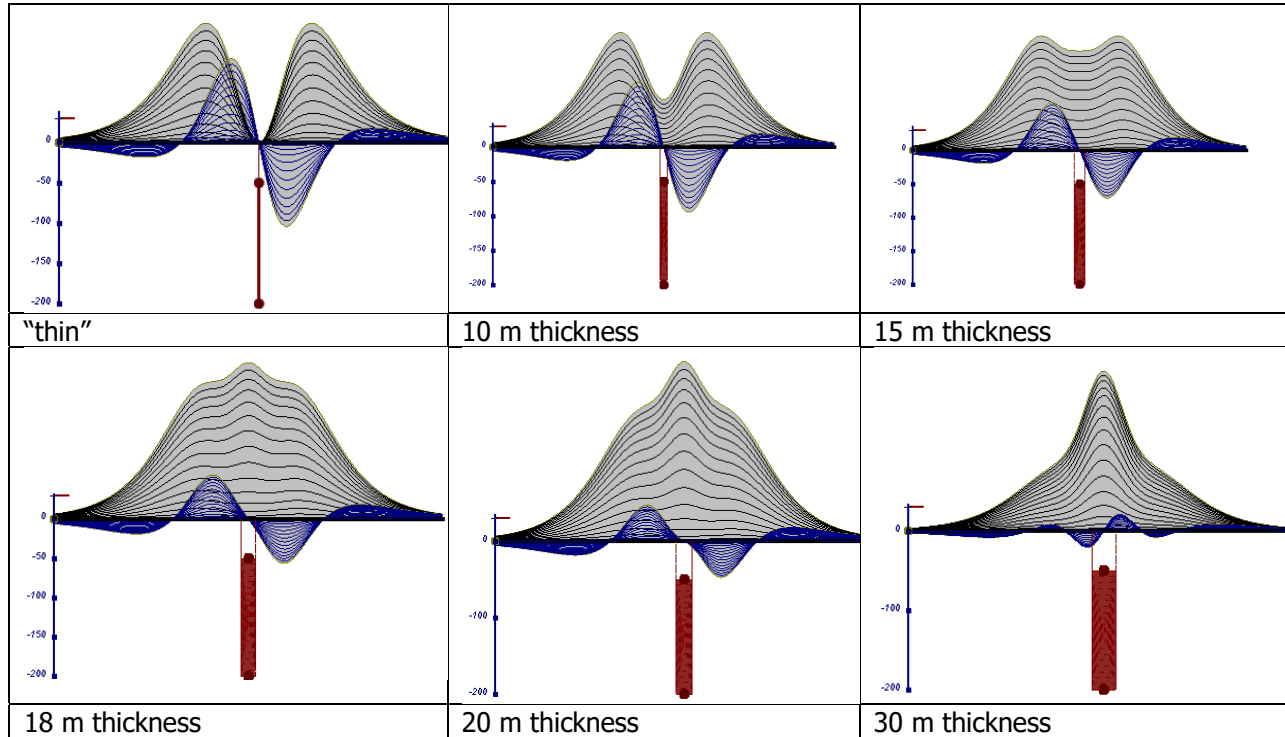
Figure E-17: Conductive vertical plate, depth 50 m, strike length 200 m, depth extends 150 m.

Geotech Ltd.

September 2010

Project GL210091
VTEM™ Plus Report on Airborne Geophysical
Survey for Big Gold Inc.

D5

APPENDIX E

EM TIME CONSTANT (TAU) ANALYSIS

Estimation of time constant parameter[1] in transient electromagnetic method is one of the steps toward the extraction of the information about conductances beneath the surface from TEM measurements.

The most reliable method to discriminate or rank conductors from overburden, background or one and other is by calculating the EM field decay time constant (TAU parameter), which directly depends on conductance despite their depth and accordingly amplitude of the response.

Theory

As established in electromagnetic theory, the magnitude of the electro-motive force (emf) induced is proportional to the time rate of change of primary magnetic field at the conductor. This emf causes eddy currents to flow in the conductor with a characteristic transient decay, whose Time Constant (Tau) is a function of the conductance of the survey target or conductivity and geometry (including dimensions) of the target. The decaying currents generate a proportional secondary magnetic field, the time rate of change of which is measured by the receiver coil as induced voltage during the Off time.

The receiver coil output voltage (e_0) is proportional to the time rate of change of the secondary magnetic field and has the form,

$$e_0 \alpha \, (1 / \tau) \, e^{-(t/\tau)}$$

> Where,
> $\tau = L/R$ is the characteristic time constant of the target (TAU)
> R = resistance
> L = inductance

From the expression, conductive targets that have small value of resistance and hence large value of τ yield signals with small initial amplitude that decays relatively slowly with progress of time. Conversely, signals from poorly conducting targets that have large resistance value and small τ, have high initial amplitude but decay rapidly with time[1](Fig. E1).
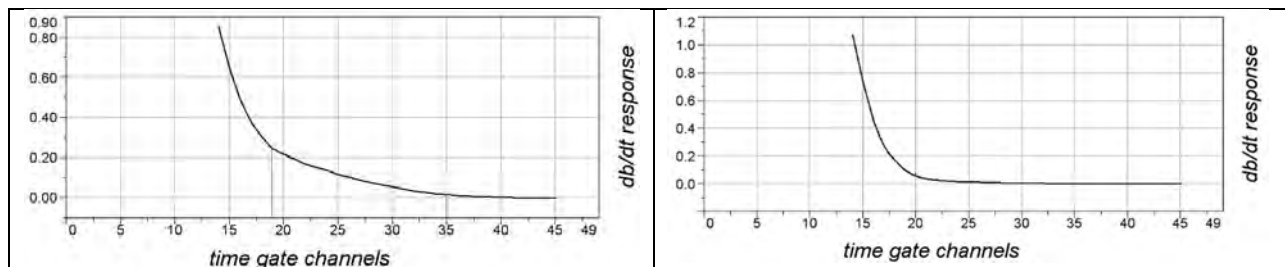
Figure E-1:Left – presence of good conductor, right – poor conductor.

---

[1]McNeill, JD, 1980, "Applications of Transient Electromagnetic Techniques", Technical Note TN-7 page 5, Geonics Limited, Mississauga, Ontario.

Project GL210091
VTEM™ Plus Report on Airborne Geophysical
Survey for Big Gold Inc.

E1

GEOTECH
AIRBORNE GEOPHYSICAL SURVEYS

EM Time Constant (Tau) Calculation

The EM Time-Constant (TAU) is a general measure of the speed of decay of the electromagnetic response and indicates the presence of eddy currents in conductive sources as well as reflecting the "conductance quality" of a source. Although TAU can be calculated using either the measured dB/dt decay or the calculated B-field decay, dB/dt is commonly preferred due to better stability (S/N) relating to signal noise. Generally, TAU calculated on base of early time response reflects both near surface overburden and poor conductors whereas, in the late ranges of time, deep and more conductive sources, respectively. For example, early time TAU distribution in an area that indicates conductive overburden is shown in Figure 2.
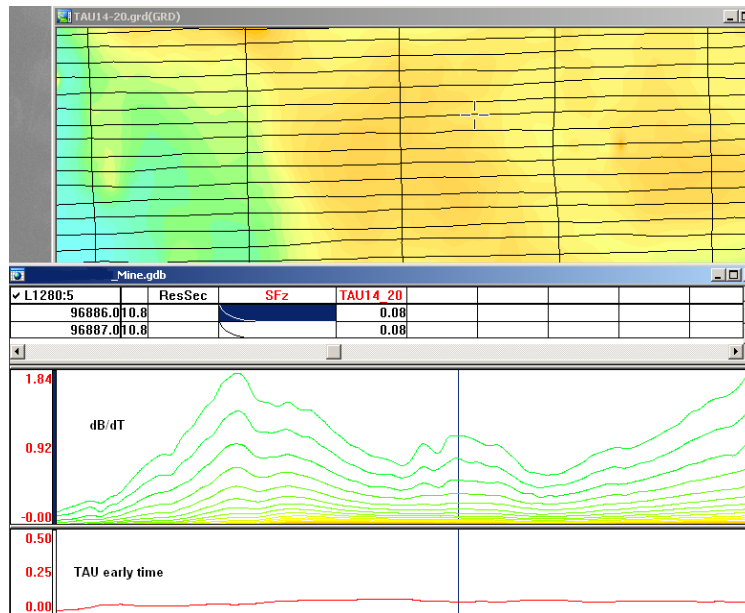
Figure E-2: Map of early time TAU. Area with overburden conductive layer and local sources.
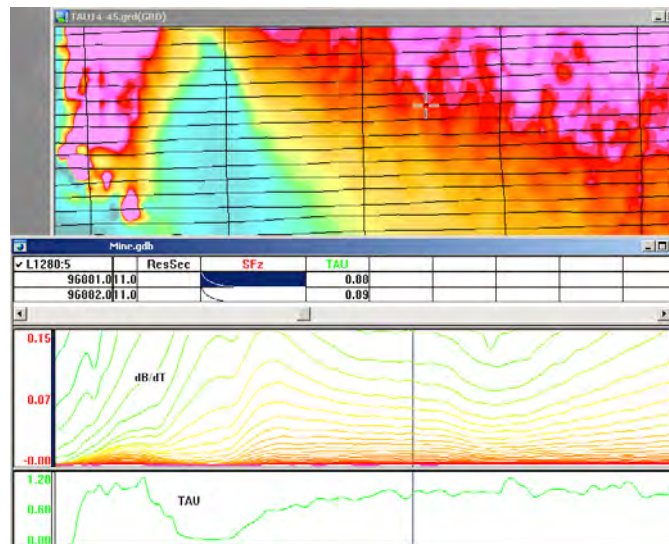
Figure E-3: Map of full-time range TAU with EM anomaly due to deep highly conductive target.

Project GL210091
VTEM™ Plus Report on Airborne Geophysical
Survey for Big Gold Inc.

E2

There are many advantages of TAU maps:

- TAU depends only on one parameter (conductance) in contrast to response magnitude.
- TAU is integral parameter, which covers time range, and all conductive zones and targets are displayed independently of their depth and conductivity on a single map.
- Very good differential resolution in complex conductive places with many sources with different conductivity.
- Signs of the presence of good conductive targets are amplified and emphasized independently of their depth and level of response accordingly.

In the example shown in Figure 4 and 5, three local targets are defined, each of them with a different depth of burial, as indicated on the resistivity depth image (RDI). All are very good conductors, but the deeper target (number 2) has a relatively weak dB/dt signal yet also features the strongest total TAU (Figure 4). This example highlights the benefit of TAU analysis in terms of an additional target discrimination tool.
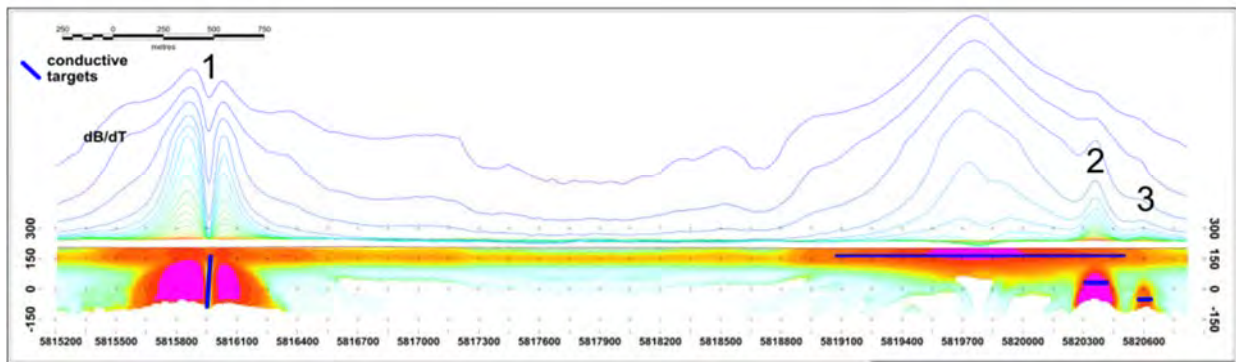
Figure E-4: dB/dt profile and RDI with different depths of targets.
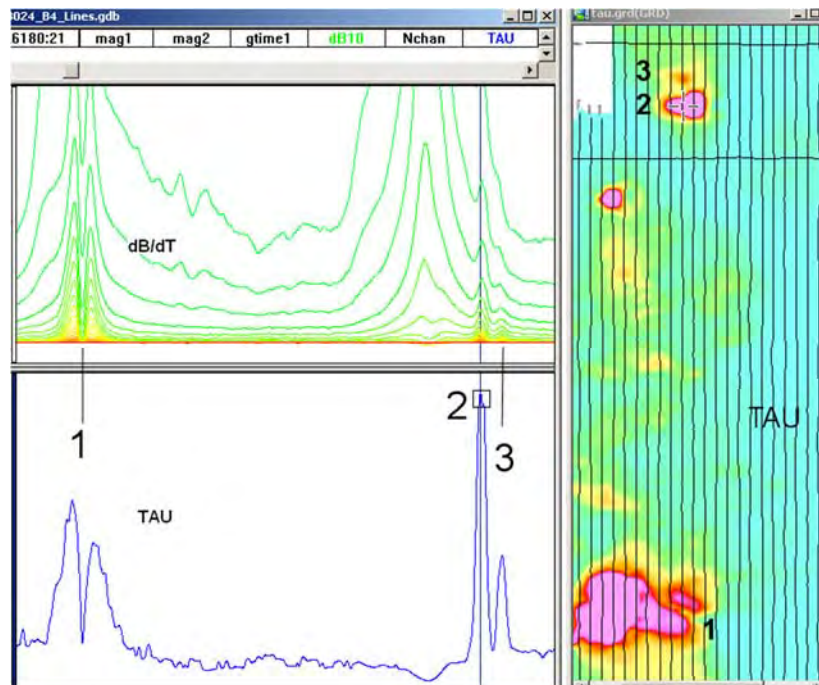
Figure E-5: Map of total TAU and dB/dt profile.

Project GL210091
VTEM™ Plus Report on Airborne Geophysical
Survey for Big Gold Inc.

E3

The EM Time Constants for dB/dt and B-field were calculated using the "sliding Tau" in-house program developed at Geotech. The principle of the calculation is based on using of time window (4 time channels) which is sliding along the curve decay and looking for latest time channels which have a response above the level of noise and decay. The EM decays are obtained from all available decay channels, starting at the latest channel. Time constants are taken from a least square fit of a straight-line (log/linear space) over the last 4 gates above a pre-set signal threshold level (Figure E6). Threshold settings are pointed in the "label" property of TAU database channels. The sliding Tau method determines that, as the amplitudes increase, the time-constant is taken at progressively later times in the EM decay. Conversely, as the amplitudes decrease, Tau is taken at progressively earlier times in the decay. If the maximum signal amplitude falls below the threshold or becomes negative for any of the 4 time gates, then Tau is not calculated and is assigned a value of "dummy" by default.
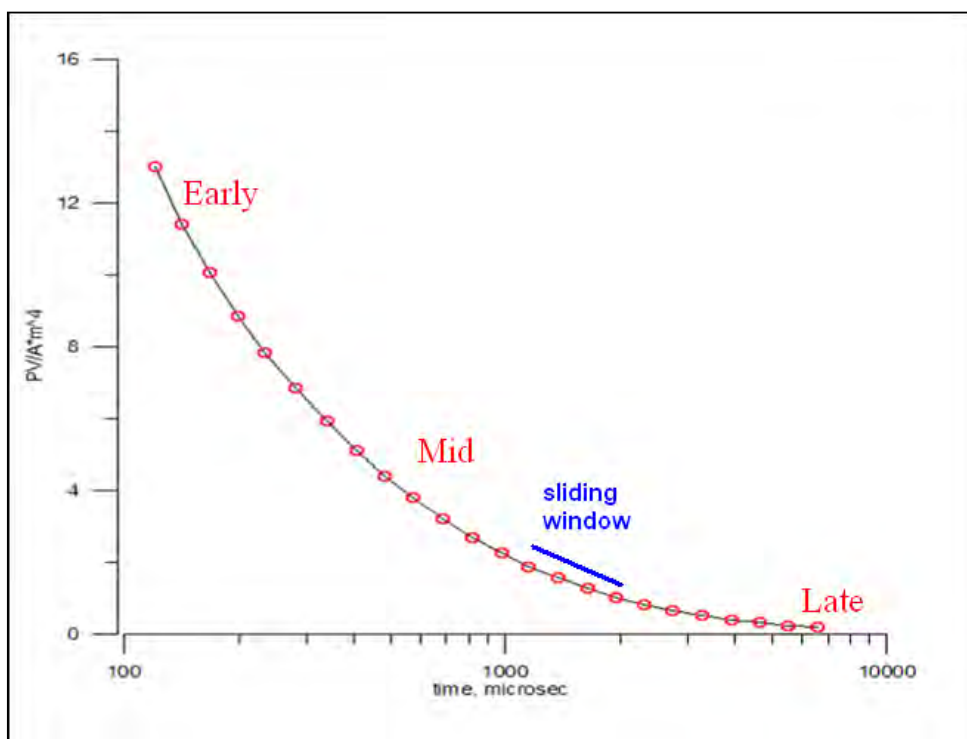
Figure E-6: Typical dB/dt decays of Vtem data

Geotech Ltd.

September 2010

Project GL210091
VTEM™ Plus Report on Airborne Geophysical
Survey for Big Gold Inc.

E4

GEOTECH
AIRBORNE GEOPHYSICAL SURVEYS

APPENDIX F

TEM RESISTIVITY DEPTH IMAGING (RDI)

Resistivity depth imaging (RDI) is technique used to rapidly convert EM profile decay data into an equivalent resistivity versus depth cross-section, by deconvolving the measured TEM data.
The used RDI algorithm of Resistivity-Depth transformation is based on scheme of the apparent resistivity transform of Meju (1998)[1] and TEM response from conductive half-space. The program is developed by Geotech Ltd. and depth calibrated based on forward plate modeling for VTEM system configuration (Fig. 1-10).

RDIs provide reasonable indications of conductor relative depth and vertical extent, as well as accurate 1D layered-earth apparent conductivity/resistivity structure across VTEM flight lines. Approximate depth of investigation of a TEM system, image of secondary field distribution in half space, effective resistivity, initial geometry and position of conductive targets is the information obtained on base of the RDIs.

Maxwell plate EM forward modeling with RDI sections from the synthetic responses (VTEM system) are presented below.
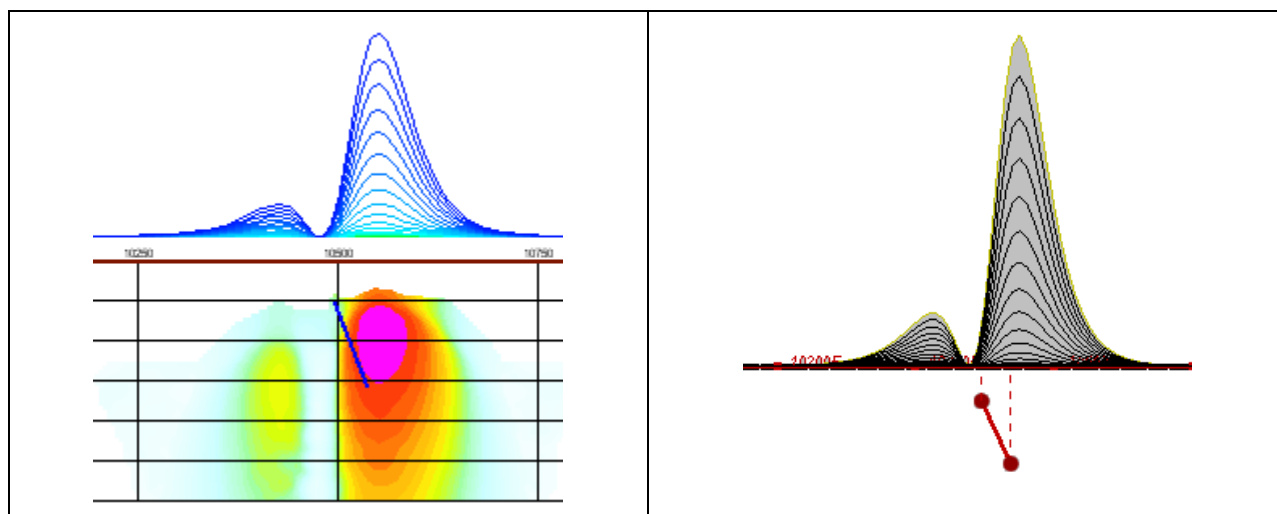
Figure F-1: Maxwell plate model and RDI from the calculated response for conductive "thin" plate (depth 50 m, dip 65 degrees, depth extend 100 m).

---

[1]Maxwell A.Meju, 1998, Short Note: A simple method of transient electromagnetic data analysis, Geophysics, **63**, 405–410.

Project GL210091
VTEM™ Plus Report on Airborne Geophysical
Survey for Big Gold Inc.

F1

GEOTECH
AIRBORNE GEOPHYSICAL SURVEYS
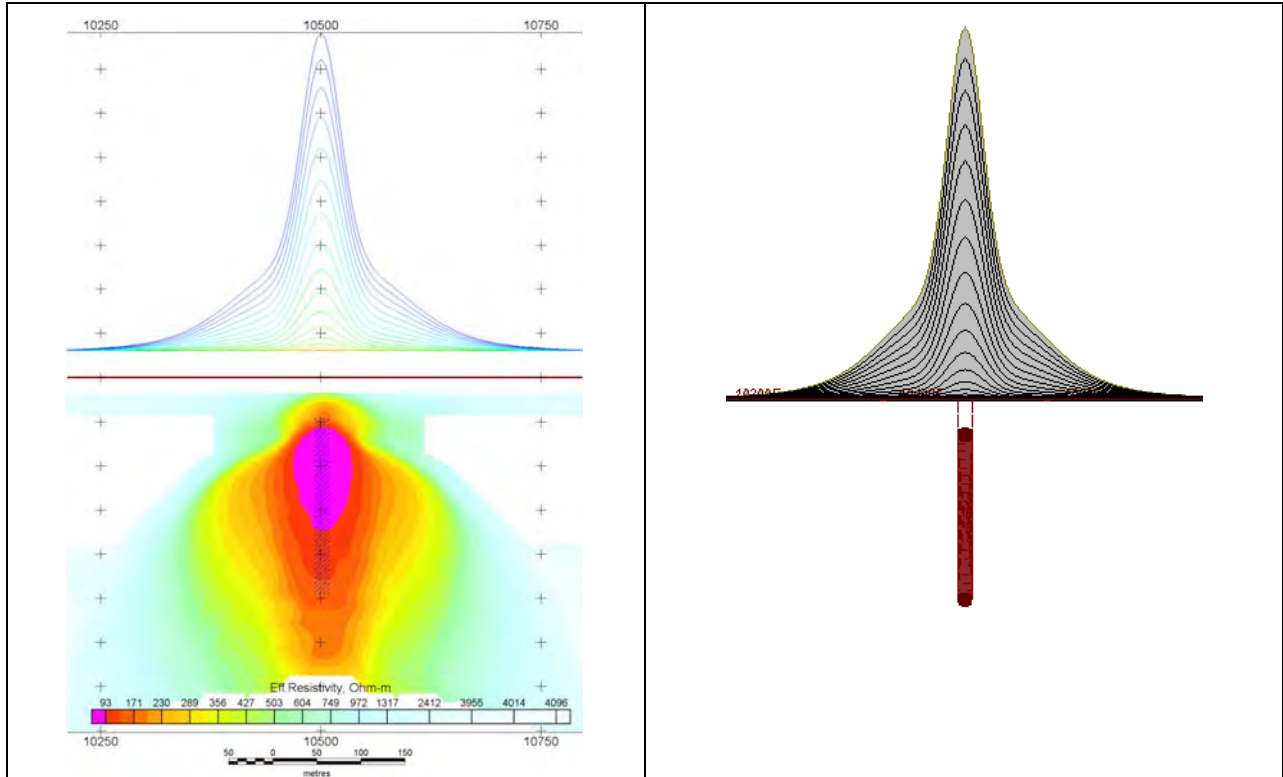
Figure F-2: Maxwell plate model and RDI from the calculated response for "thick" plate 18 m thickness, depth 50 m, depth extend 200 m).
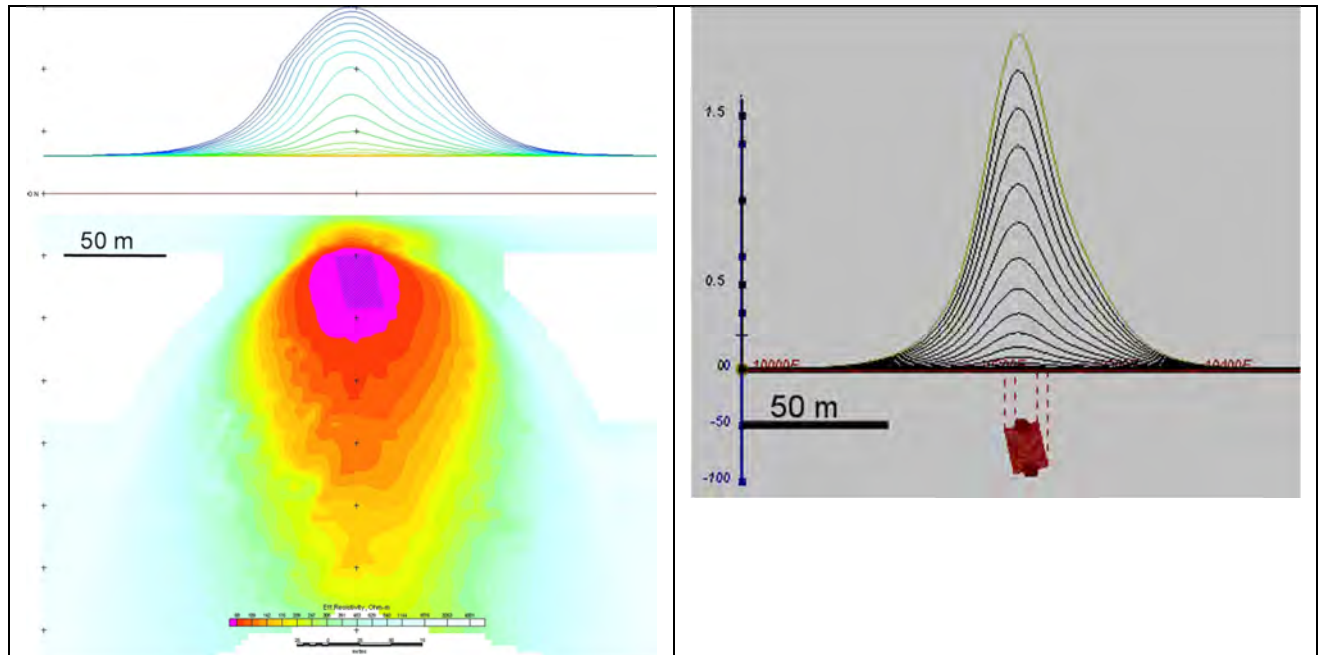
Figure F-3: Maxwell plate model and RDI from the calculated response for bulk ("thick") 100 m length, 40 m depth extend, 30 m thickness.

Project GL210091
VTEM™ Plus Report on Airborne Geophysical
Survey for Big Gold Inc.

F2
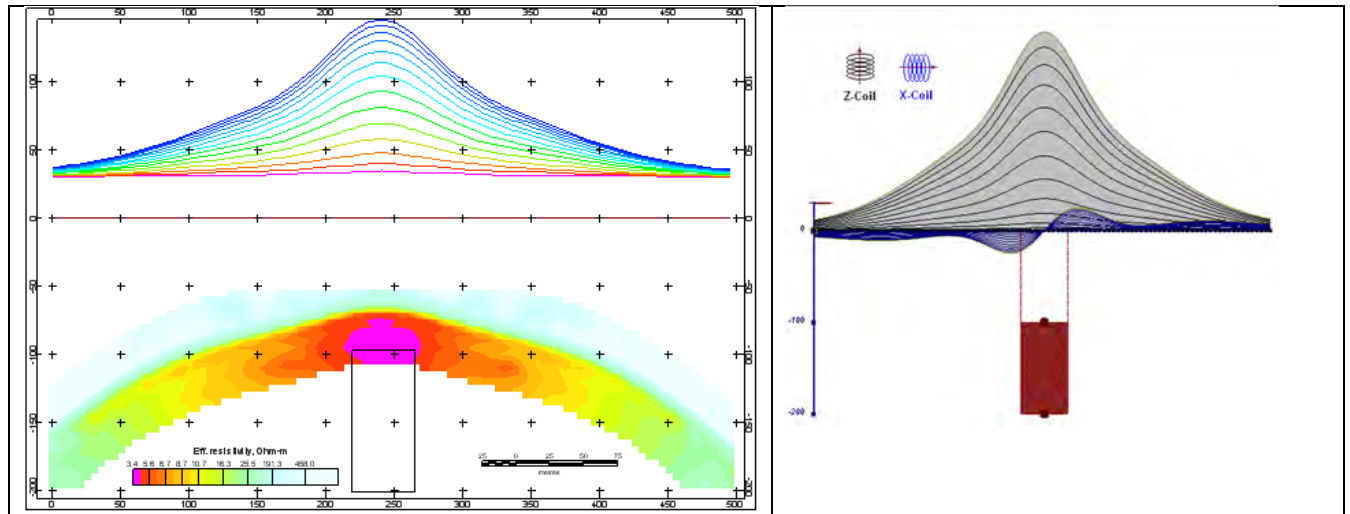
Figure F-4: Maxwell plate model and RDI from the calculated response for "thick" vertical target (depth 100 m, depth extend 100 m). 19-44 chan.
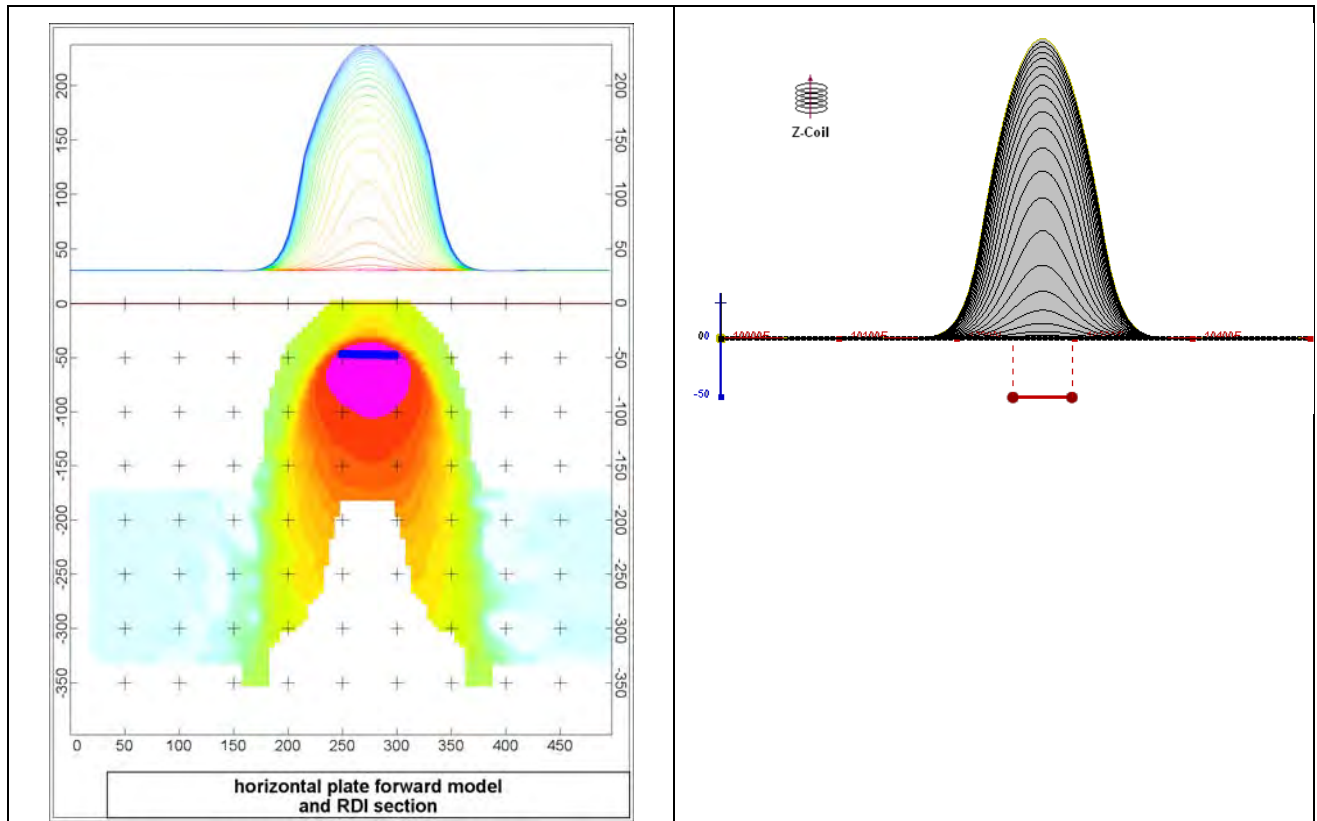
Figure F-5: Maxwell plate model and RDI from the calculated response for horizontal thin plate (depth 50 m, dim 50x100 m). 15-44 chan.

Project GL210091
VTEM™ Plus Report on Airborne Geophysical
Survey for Big Gold Inc.

F3
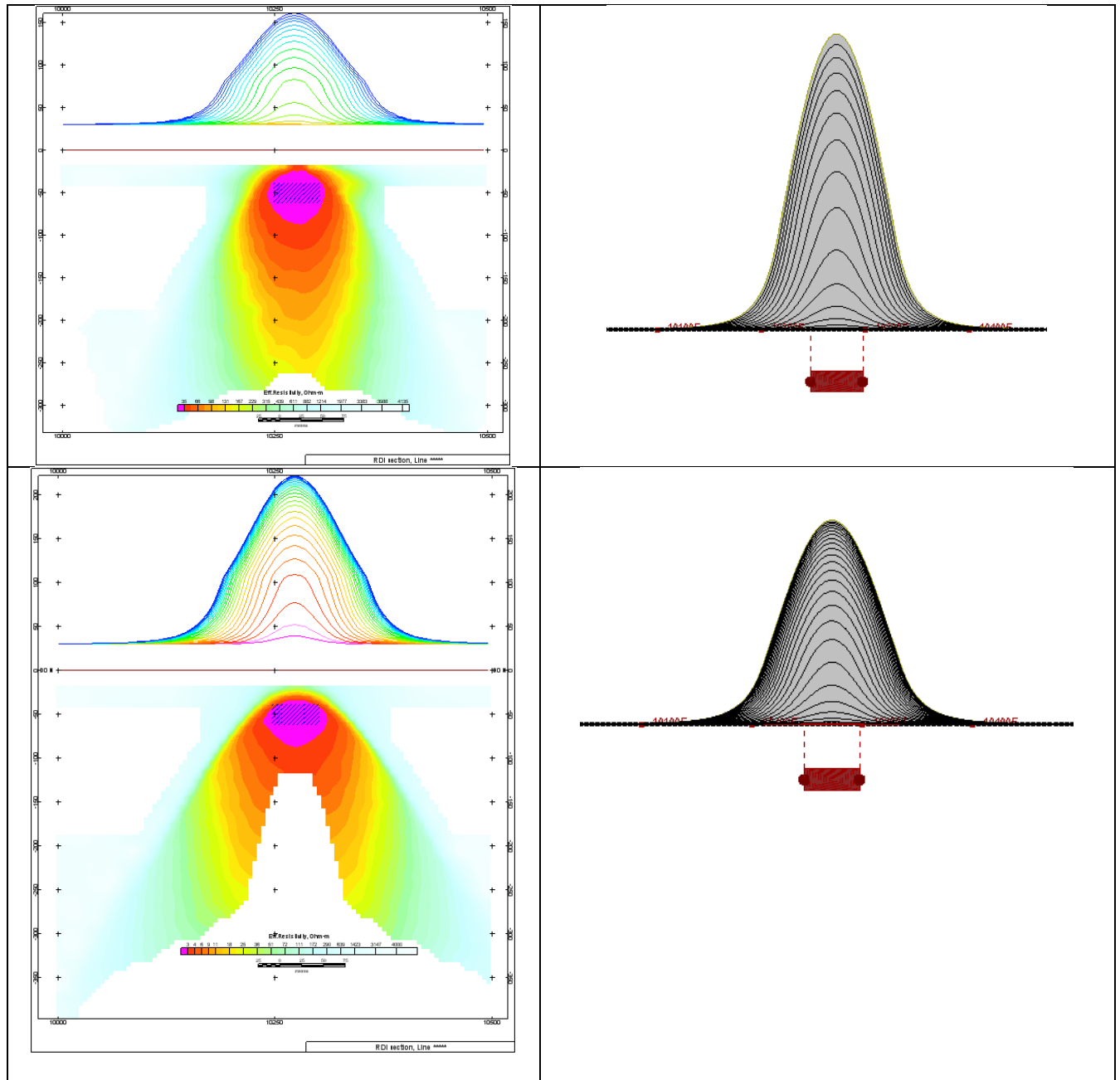
Figure F-6: Maxwell plate model and RDI from the calculated response for horizontal thick (20m) plate – less conductive (on the top), more conductive (below).

Project GL210091
VTEM™ Plus Report on Airborne Geophysical
Survey for Big Gold Inc.

F4
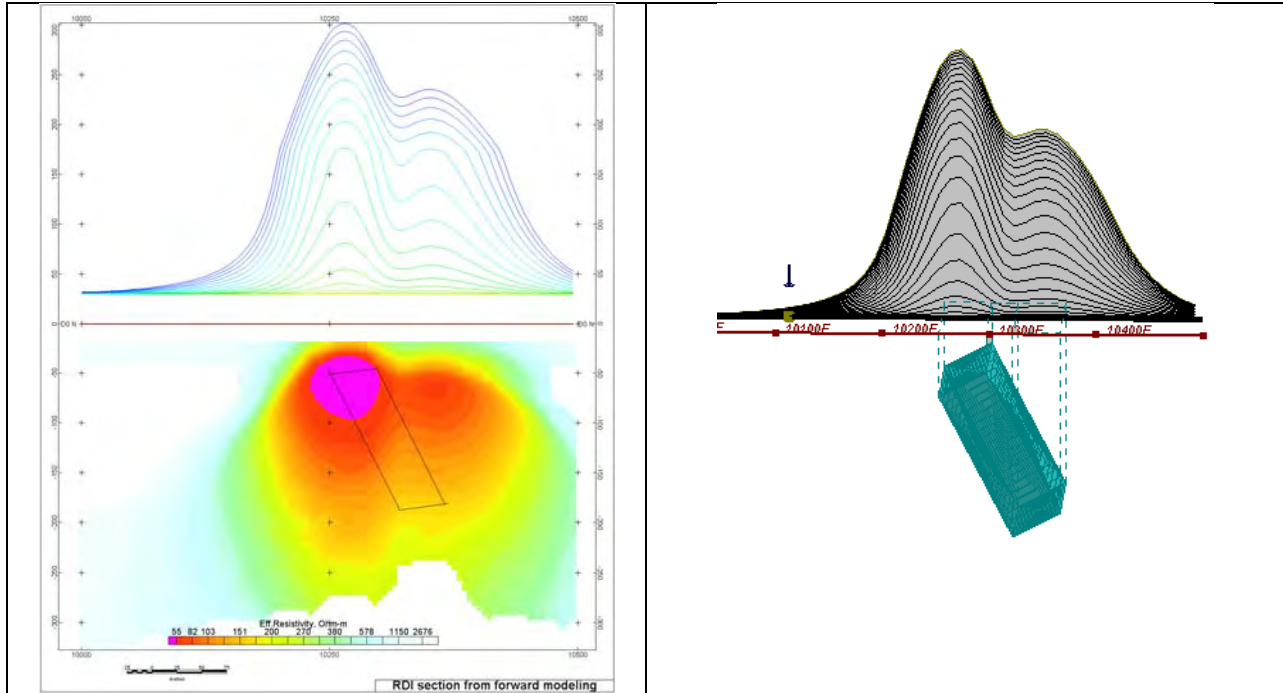
Figure F-7: Maxwell plate model and RDI from the calculated response for inclined thick (50m) plate. Depth extends 150 m, depth to the target 50 m.
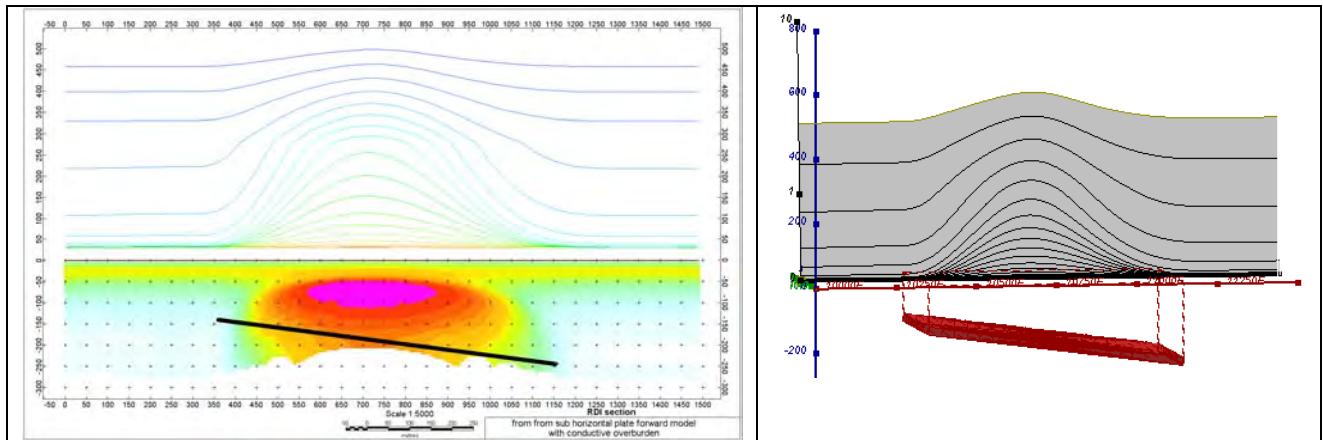
Figure F-8: Maxwell plate model and RDI from the calculated response for the long, wide and deep subhorizontal plate (depth 140 m, dim 25x500x800 m) with conductive overburden.

Project GL210091
VTEM™ Plus Report on Airborne Geophysical
Survey for Big Gold Inc.

F5
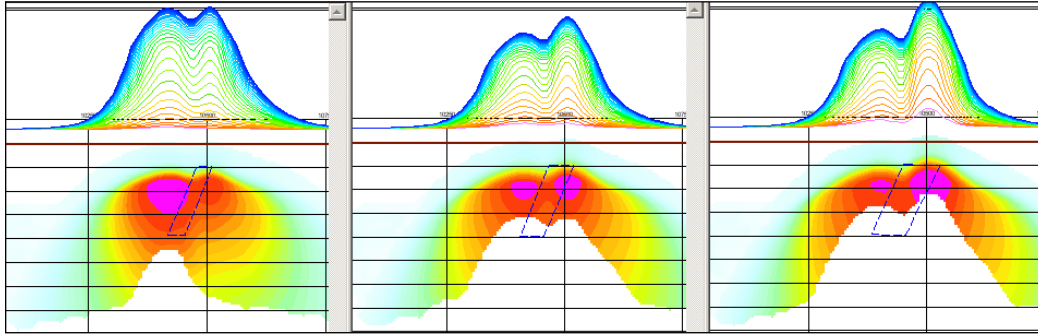
Figure F-9: Maxwell plate models and RDIs from the calculated response for "thick" dipping plates (35, 50, 75 m thickness), depth 50 m, conductivity 2.5 S/m.
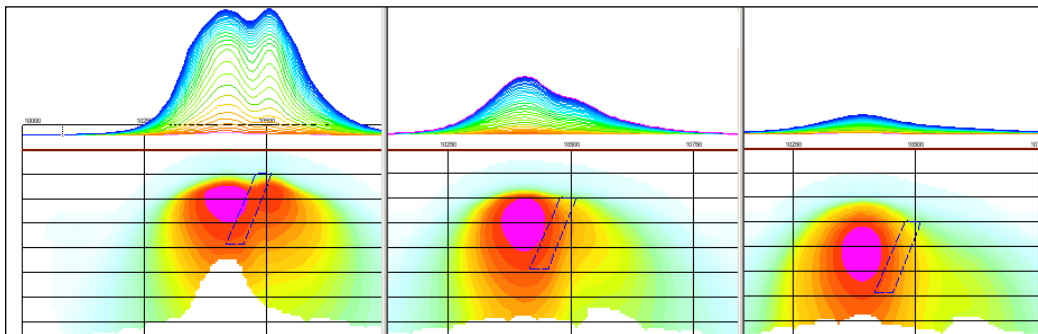
Figure F-10: Maxwell plate models and RDIs from the calculated response for "thick" (35 m thickness) dipping plate on different depth (50, 100, 150 m), conductivity 2.5 S/m.
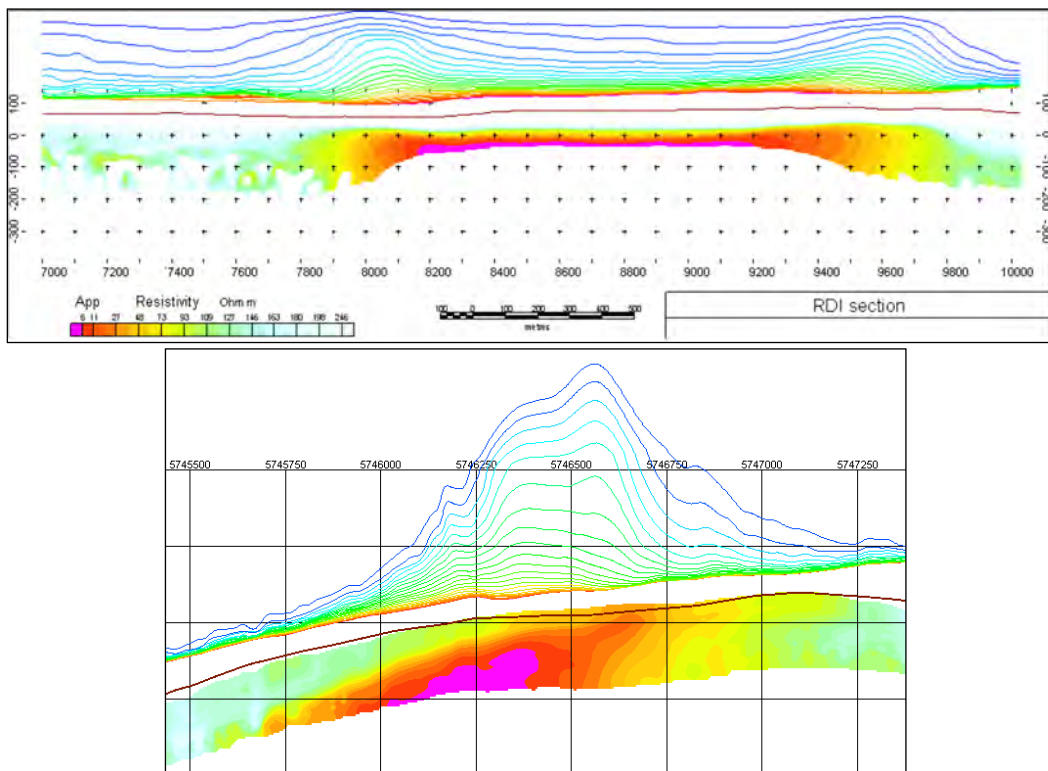
Figure F-11: RDI section for the real horizontal and slightly dipping conductive layers.

Project GL210091
VTEM™ Plus Report on Airborne Geophysical
Survey for Big Gold Inc.

F6

FORMS OF RDI PRESENTATION

PRESENTATION OF SERIES OF LINES
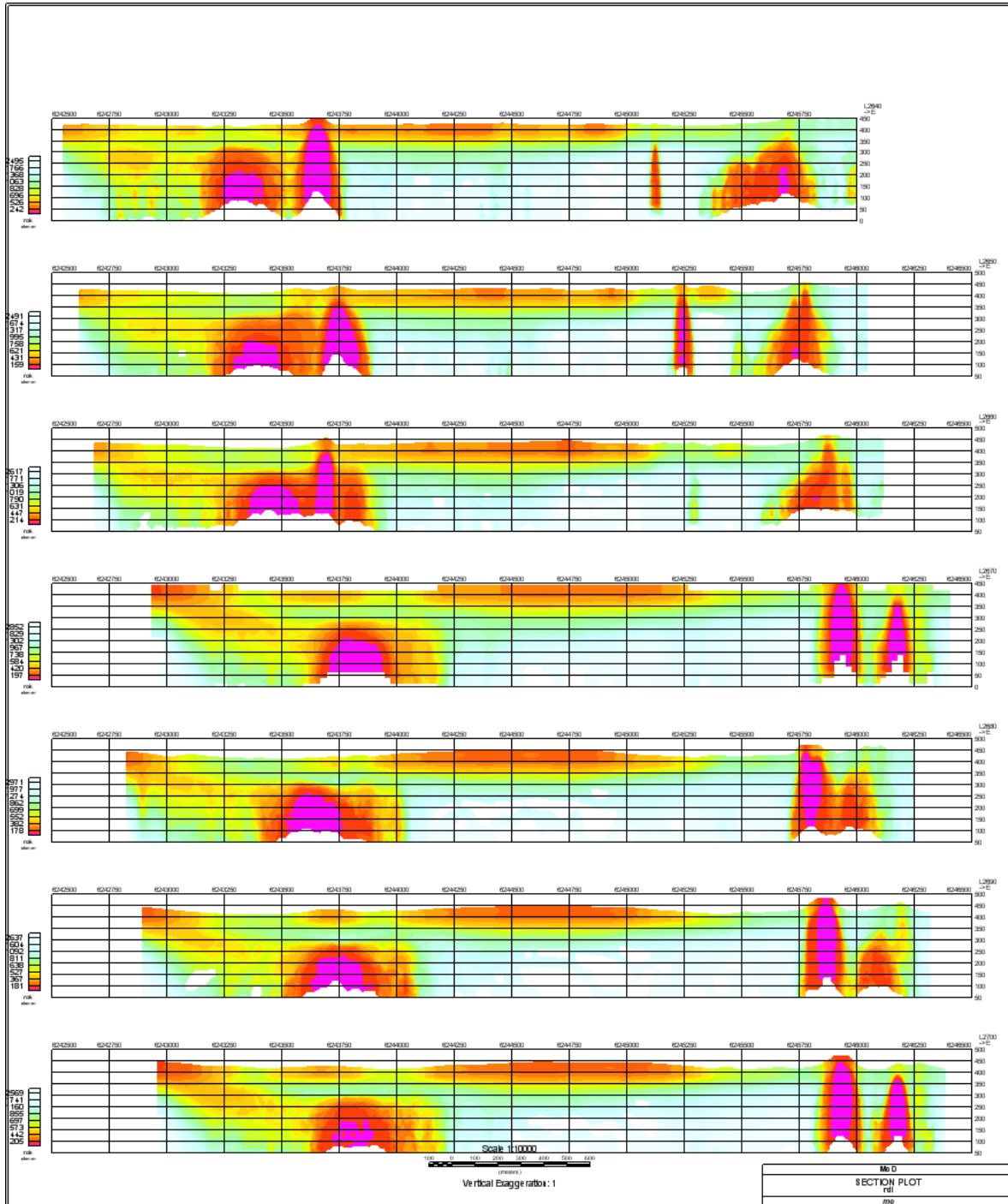
3D PRESENTATION OF RDIS
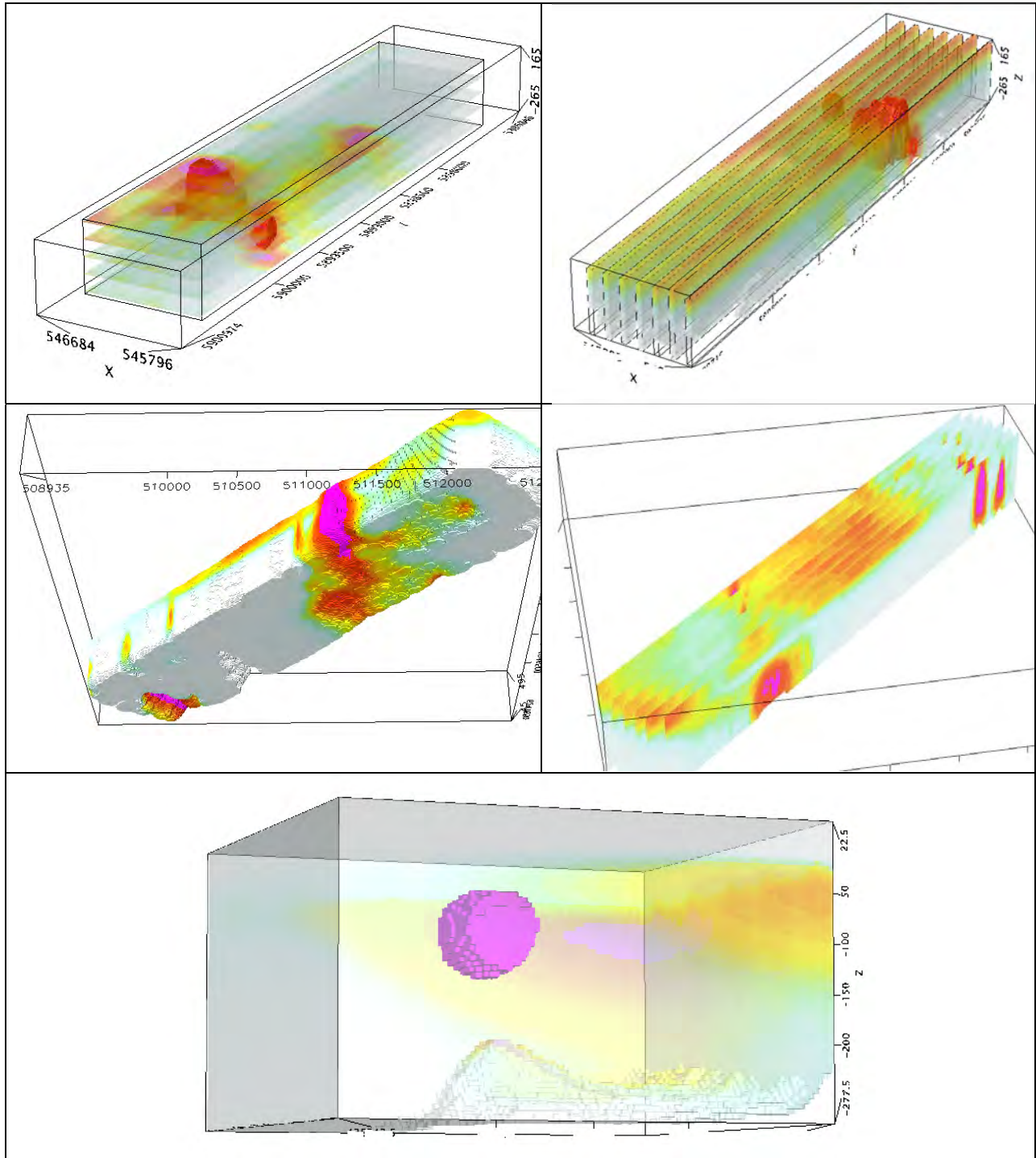
APPARENT RESISTIVITY DEPTH SLICESPLANS:

| 0 m (surface) | -100 m | -200 m |
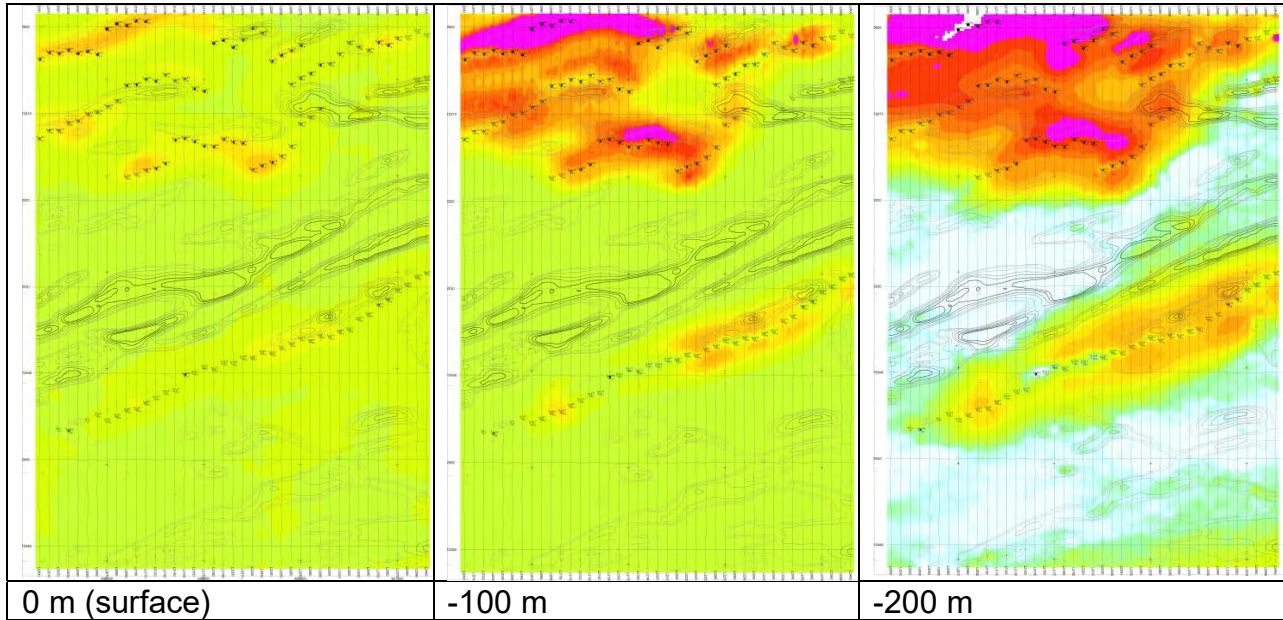
3D VIEWS OF APPARENT RESISTIVITY DEPTH SLICES:
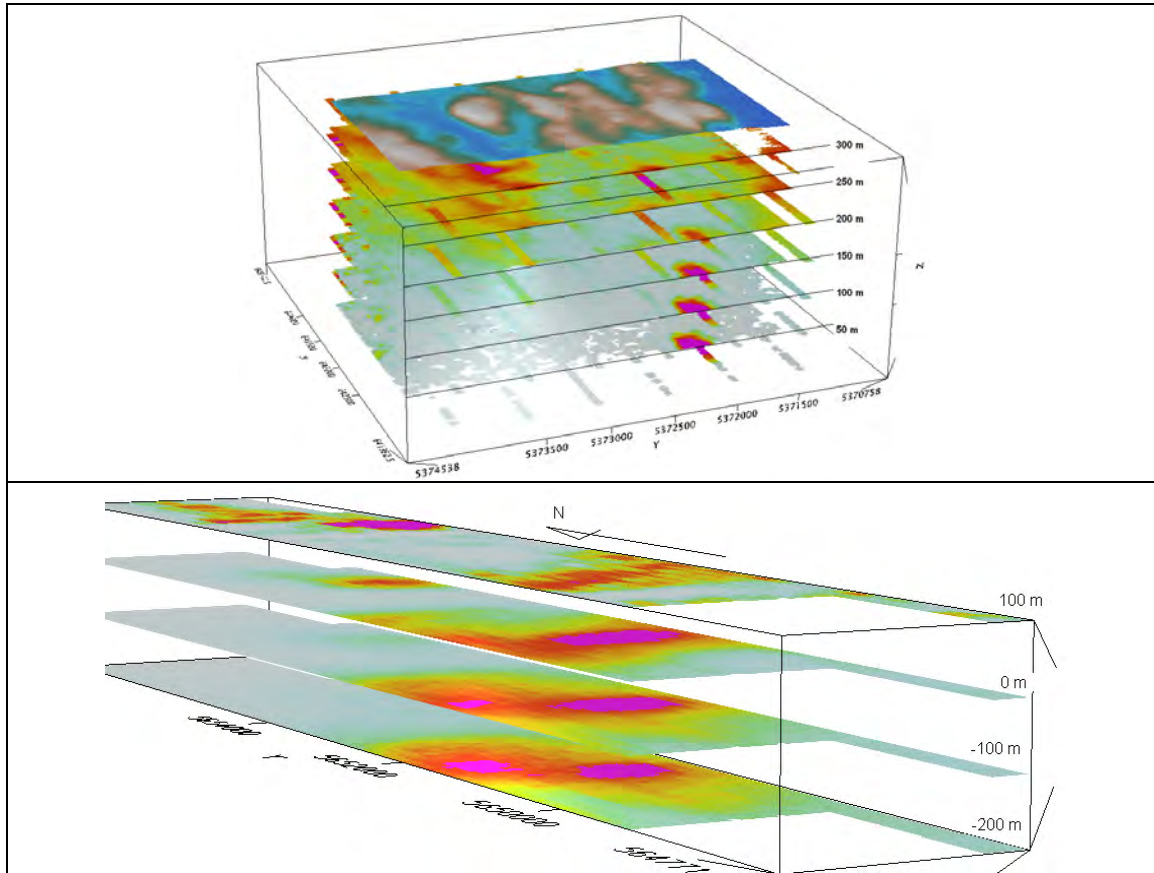
REAL BASE METAL TARGETS IN COMPARISON WITH RDIS:

RDI section of the line over Caber deposit ("thin" subvertical plate target and conductive overburden.
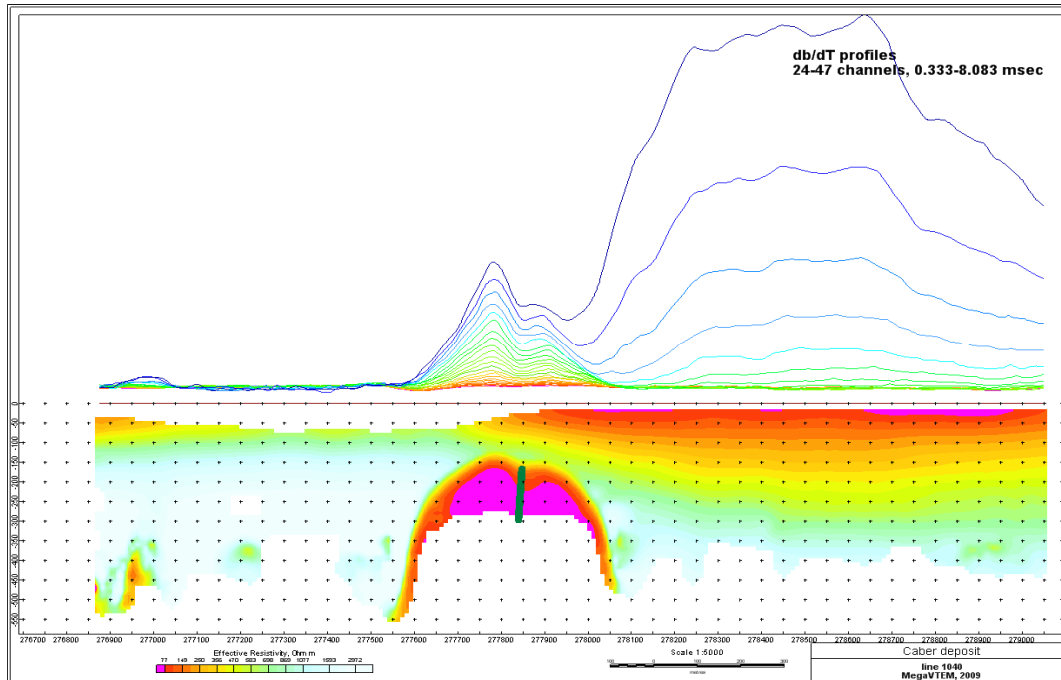
3D RDI VOXELS WITH BASE METALS ORE BODIES (MIDDLE EAST):

Project GL210091
VTEM™ Plus Report on Airborne Geophysical
Survey for Big Gold Inc.

F10

Geotech Ltd.
April 2011

Project GL210091
VTEM™ Plus Report on Airborne Geophysical
Survey for Big Gold Inc.

F11
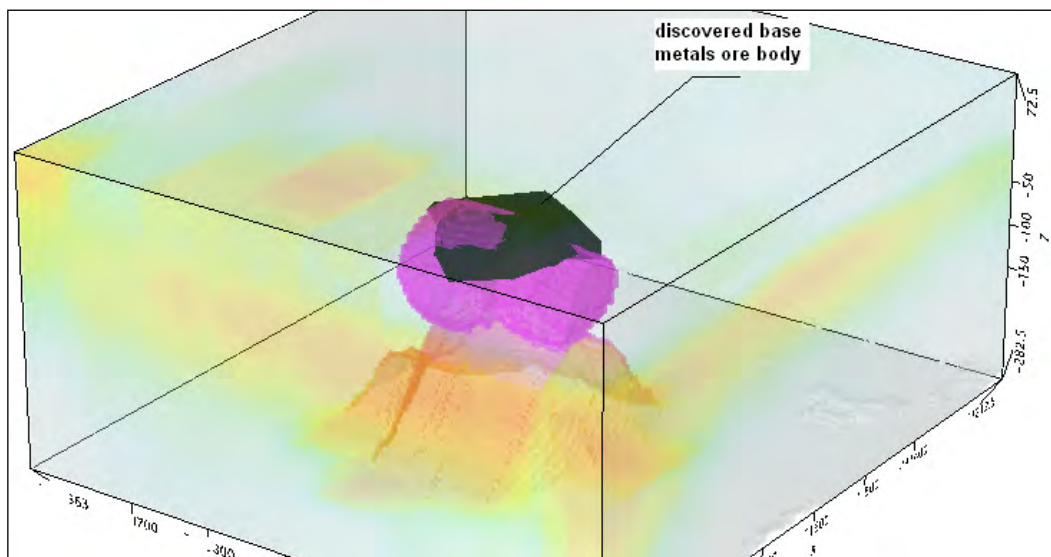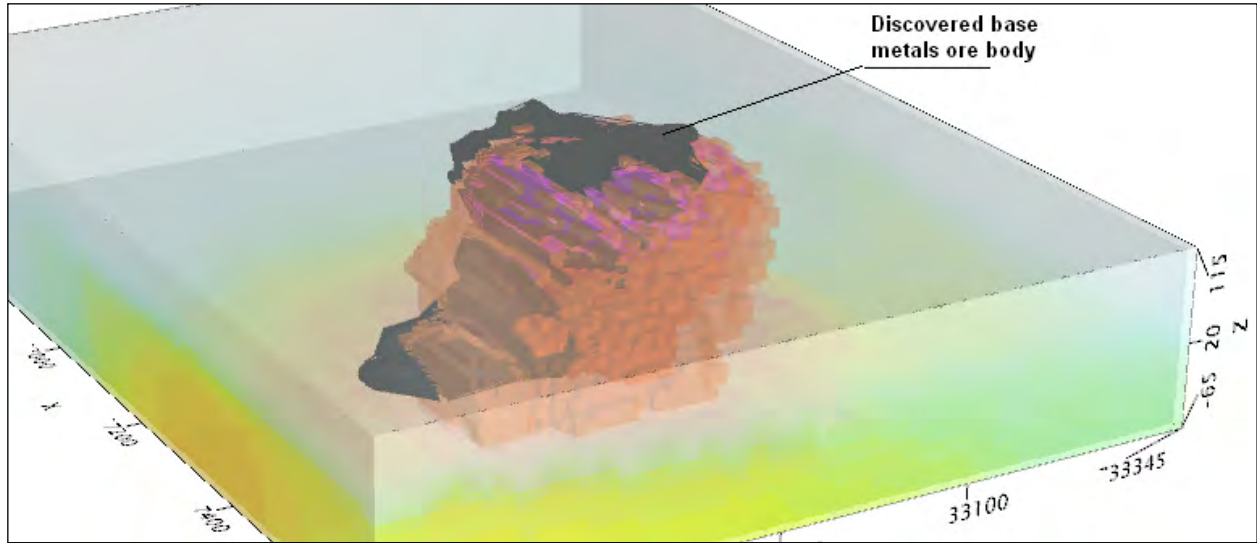
GEOTECH
AIRBORNE GEOPHYSICAL SURVEYS

APPENDIX G

RESISTIVITY DEPTH IMAGES (RDI)
Please see RDI Folder on DVD for the PDF's

Project GL210091
VTEM™ Plus Report on Airborne Geophysical
Survey for Big Gold Inc.

G1

Appendix 2

Technoimaging 3D Inversion Modelling Report of VTEM Survey

Michael Zhdanov CEO
4001 S 700 E STE 500,
Salt Lake City, UT 84107, USA
+1 801 264 6700
mzhdanov@technoimaging.com

CONFIDENTIAL

<u>Final Report</u>
Three-dimensional Inversion
VTEM Electromagnetic and TMI data
Martin Kenty Project Area, Nestor Falls
Northwestern Ontario, Canada

Prepared for

Big Gold Inc.

(BIG GOLD)

Attn: Scott Walters, President and CEO, Director
             Big Gold Inc.
             2702 – 401 Bay Street
             Toronto, Ontario M5H 2Y4, CANADA
             +1 416 567 9087
             scott@biggold.ca

January 24th, 2022

Table of Contents

1 Executive Summary

TechnoImaging has completed the final 3D inversion of 365 line-km of VTEM and Total Magnetic Intensity (TMI) data at a 100-meter line spacing over the Martin Kenty Project Area, 13 km NE of Nestor Falls in northwestern Ontario, Canada for Big Gold Inc.

The Martin Kenty Project covers approximately 4,000 hectares extending ~10 km east-west and ~6 km north-south. The Project area hosts key attributes consistent with a gold enriched system that is deep-seated and extensive. The Martin Kenty Project lies in the Kenora/Rainy River mining district and is prospective for massive-sulphide-hosted gold mineralization (www.biggold.ca/martin-kenty-project/). As a result, both the EM and magnetic data are likely to be of exploration interest.

The VTEM dB/dt data were successfully inverted into 3D conductivity and chargeability voxel models. The TMI data were inverted into both 3D magnetic susceptibility models and 3D magnetization vector (remanent magnetization) models. All four types of inverse models have been provided to Big Gold in the form of 3D voxel files. Several conductive anomalies and separate chargeable anomalies have been imaged, which can be achieved with TechnoImaging's patented inversion methods.

Processed TMI data were independently fit to **Glass Earth®** magnetic susceptibility and magnetization vector models. TechnoImaging's 3D magnetization vector inversion method is sensitive to both induced and remanent magnetization, whereas traditional magnetic susceptibility inversion methods are sensitive to induced magnetization only. Many features of interest have been brought into focus in the magnetization vector model that are less apparent in the susceptibility model.

Deliverables include 3D conductivity and chargeability models, 3D magnetic susceptibility models and 3D magnetization vector models in UBC mesh/model format, conductivity, chargeability, and magnetic properties, and this final report.

A list of deliverables is provided below:

1) 3D volume of conductivity derived from AEM data

2) 3D volume of chargeability derived from AEM data

3) 3D volume of magnetic susceptibility derived from TMI data

4) 3D volume of magnetization vector derived from TMI data

5) Final report in PDF format

2   Introduction

TechnoImaging, LLC ("TechnoImaging") inverted 365 line-km of VTEM and Total Magnetic Intensity (TMI) data to support the exploration activities of Big Gold Inc. ("Big Gold"). The data were quality controlled, processed, and inverted with TechnoImaging's proprietary software, EMVision®. This software package has a suite of codes for regularized 3D inversion of geophysical data with image focusing and sharpening to reflect geological structures better. It can transform the observed airborne EM and TMI data into 3D images of rock physical properties, thus rendering the subsurface entirely transparent – a metaphorical "Glass Earth®."

This report details the data processing and inversion workflow specific to this project. For more information on the general details and methods used, please refer to the references cited in the last section of this report.

2.1   Martin Kenty Project in the Geological and Geophysical Context

2.1.1   Geological context

Figure 1 shows a geologic map of the survey area. The red lines show the claim block perimeter, and the blue line outlines claims not currently on the property.

Past drilling indicates high gold intercepts in east-west vertical dipping shears in the volcanic units. Several of these shear lineaments are evident in the provided data. Extensions, splays, and parallel shears would be exploration targets. Figure 2 shows the area of past drilling with high gold intercepts overlain on a magnetic map and shows the trend of the east-west vertical dipping shear in the volcanics.
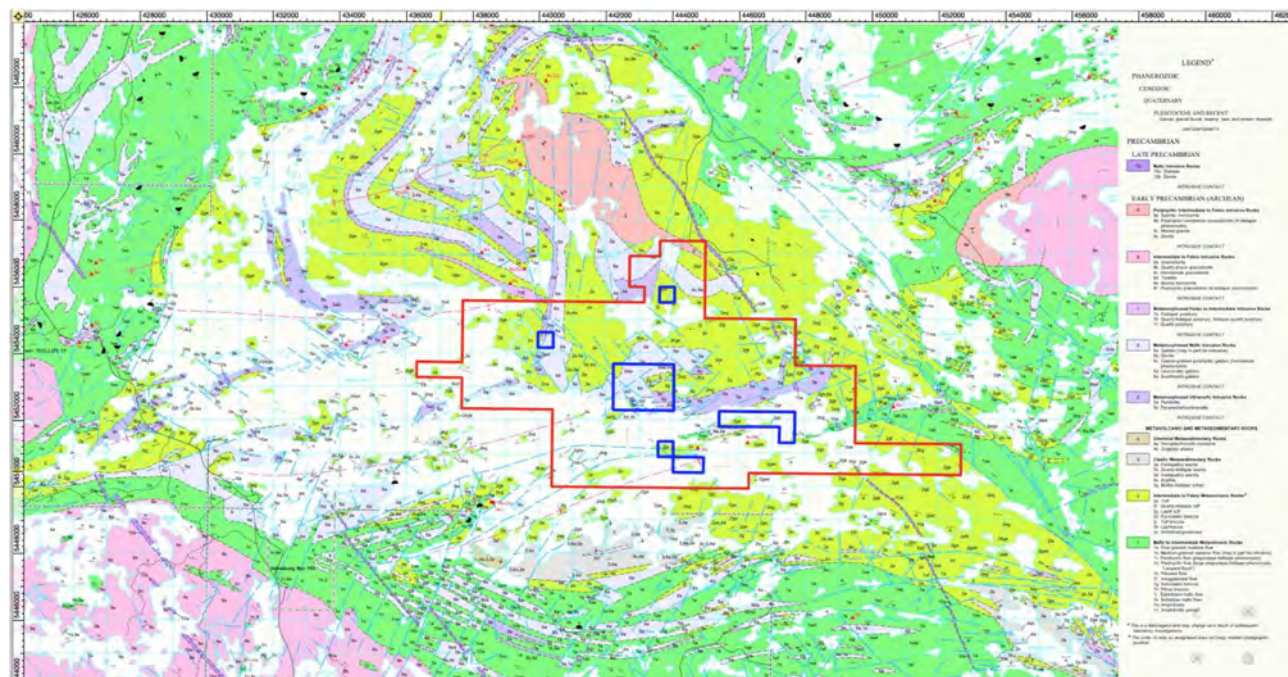
Figure 1. Regional geology from the client.
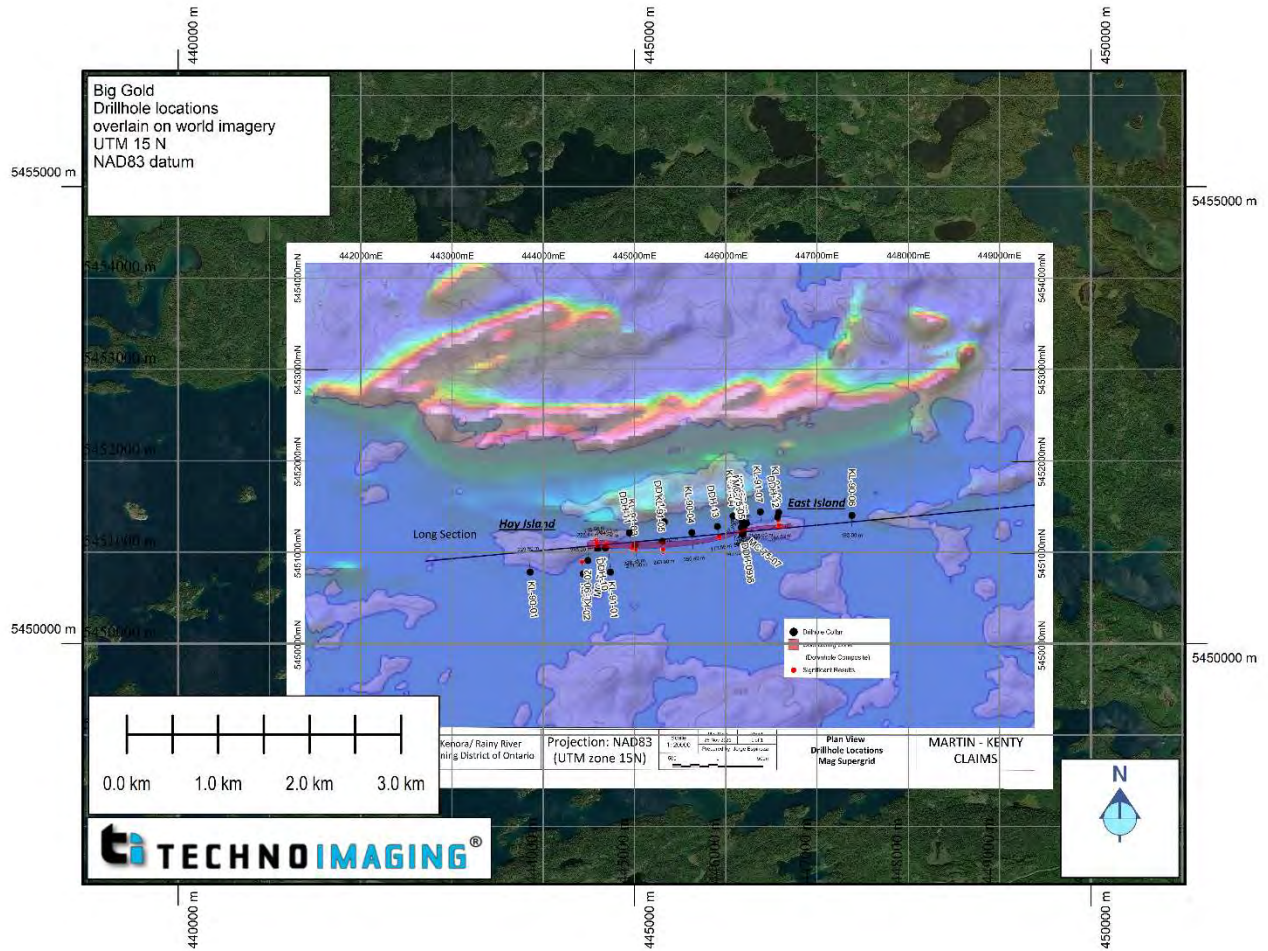
Figure 2. Map of previous drilling target overlying a magnetic map.

Locations of the 2021 sampling program are shown in Figure 3, and gold showings are listed below.

1. Roy Martin Showing

Historic trenching reported gold values of 2.8 g/t over ~1.5 meters – no follow-up

2. East Island Showing

Reported gold values across 3 trenches:

TR1: 9.3 g/ton Au over 3.5 meters

TR2: 5.0 g/ton Au over 4.3 meters

TR3: 4.7 g/ton Au over 5.5 meters

3. Hay Island Showing

Historical estimation of 109,000 tons of material grading 7.78 g/t Au*. Potential for significantly increased tonnage

4. Mongus Lake Showing

Reported pyrite, chalcopyrite, and visible gold (no Assays returned) are Located 2 km from Wicks Lake Deposit.
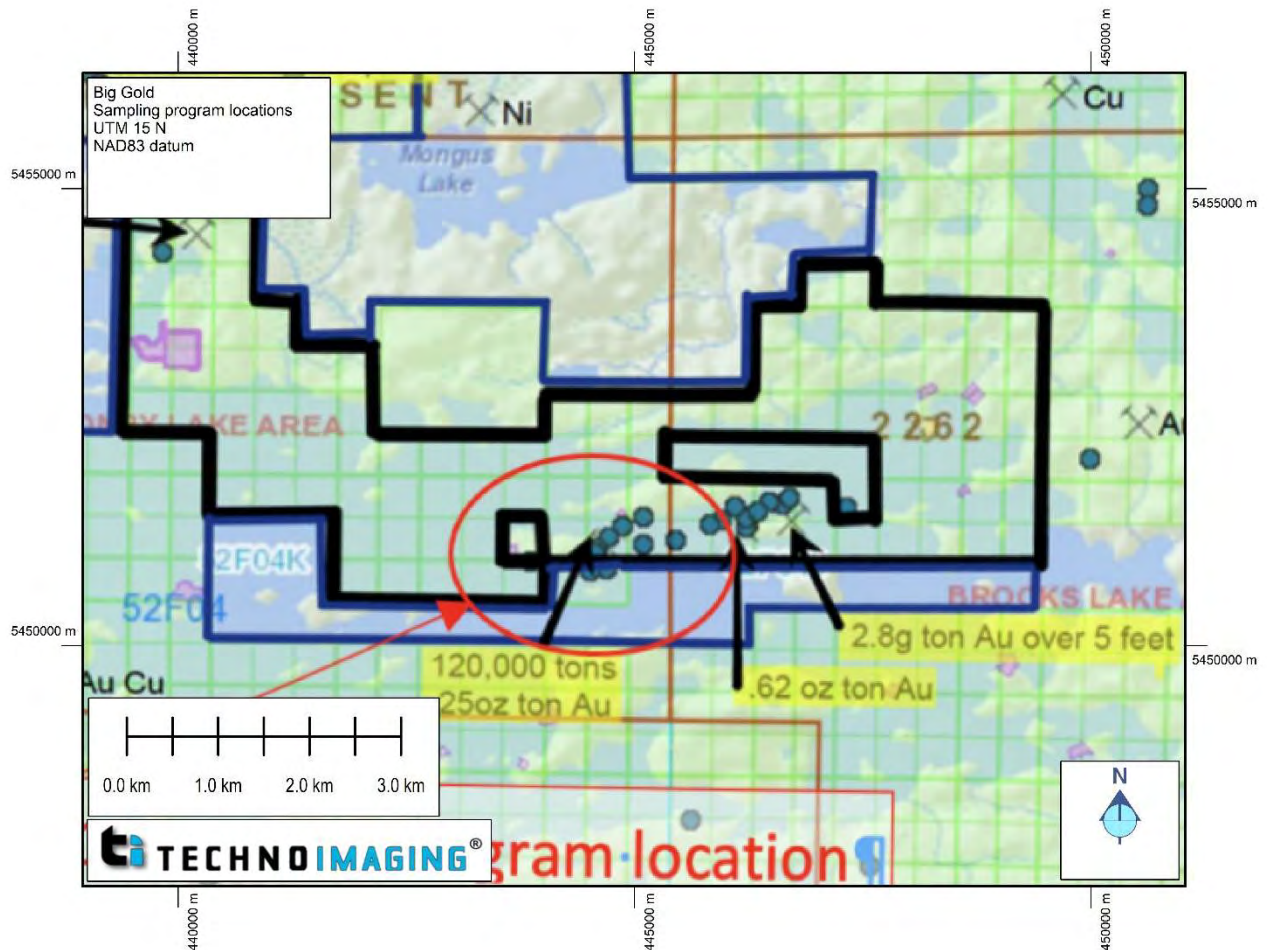
Figure 3. Staked claims and proposed staking with gold showings.

2.1.2 Geophysical context

Geotech conducted a VTEM and magnetometer helicopter survey over the Martin Kenty Property in October 2021. A total magnetic intensity map overlaying the known occurrences is shown in Figure 4. In addition, an interpretive map showing a VTEM B-Field Z Component profiles of time gates 0.051-0.059 ms are displayed along with the known occurrences on the Property in Figure 5.
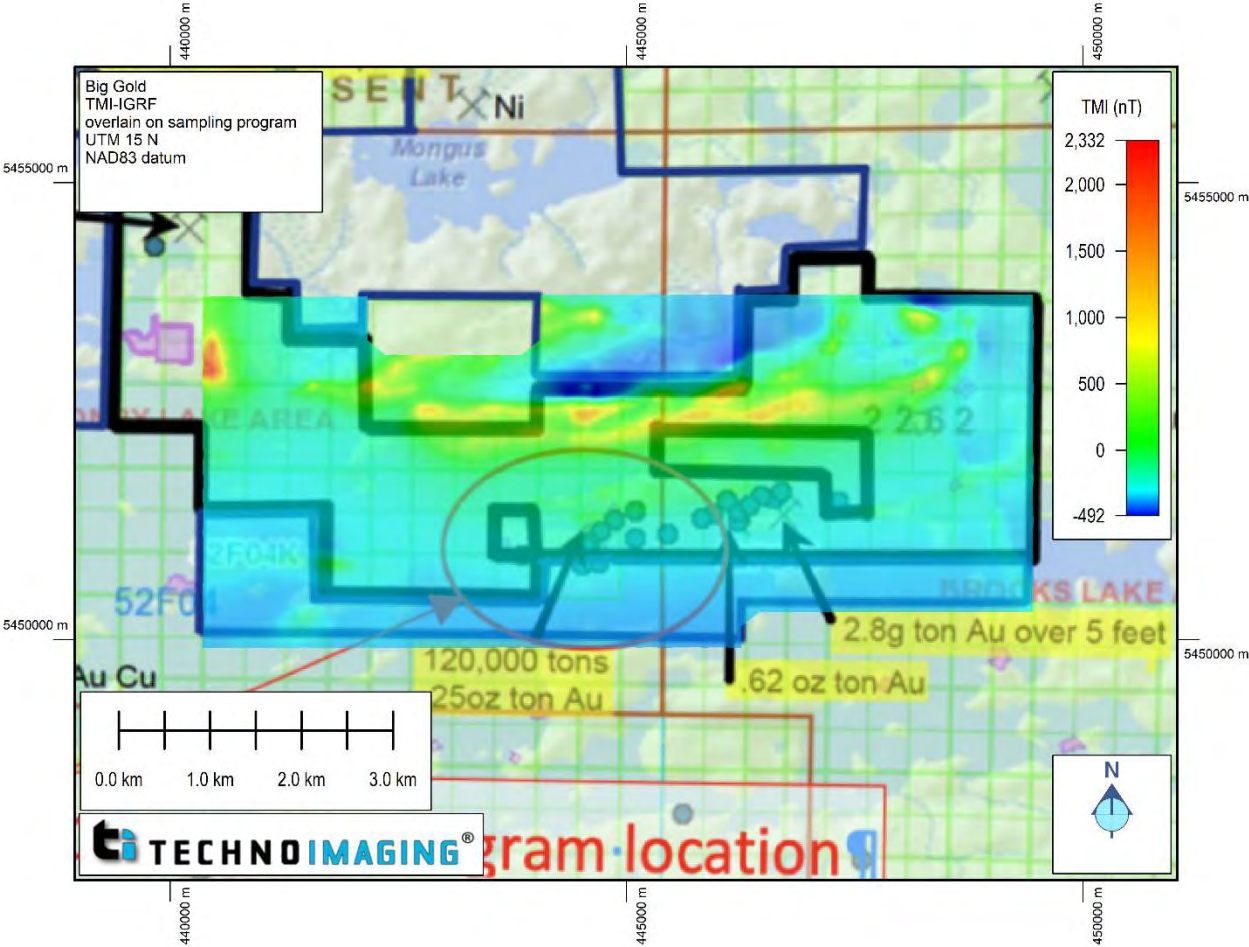
Figure 4. Geophysical map of TMI data with the main field removed (color map) overlying the known occurrences. Coordinates are shown in NAD83 Zone 15N.
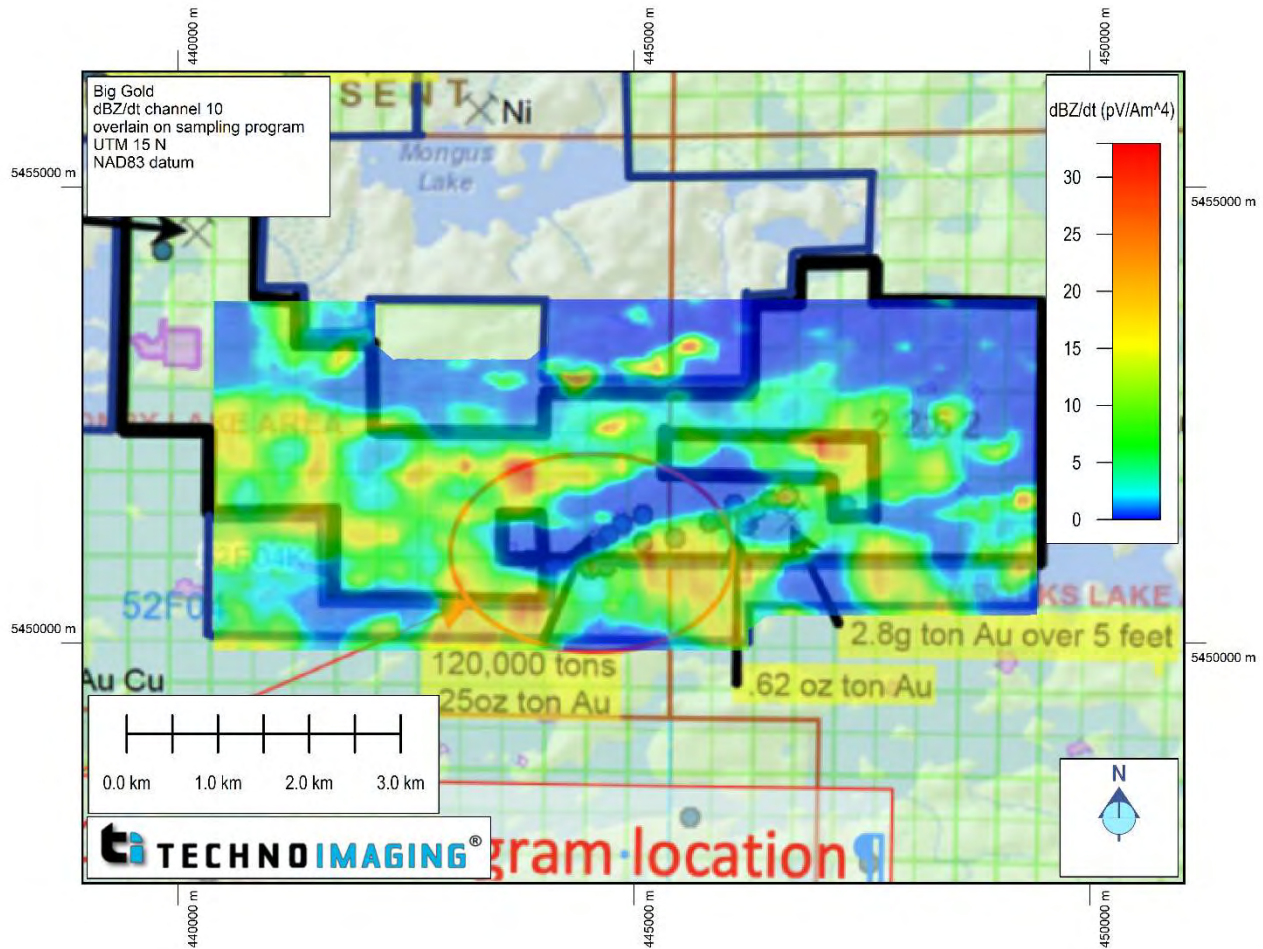
Figure 5. Geophysical map of VTEM dB/dt Z Component profile 0.055 ms (color map) is displayed along with the sampling program.

2.2 Data Provided by Big Gold to TechnoImaging

TechnoImaging received the following digital archive datasets from Big Gold that included logistics reports, a detailed description of the VTEM and TMI system, and survey specifications of the VTEM^{TM} and Horizontal Magnetic Gradient System.

- VTEM^{TM} Data

  - *GL210091_Report.pdf*: Report on a helicopter-borne Versatile *Time Domain ElectroMagnetic (VTEM™ plus) and Horizontal Magnetic Gradiometer geophysical survey*
  - *GL210091_Digital Archives: Database (.gdb), Grids (.grd & .tif), Maps(.map & .pdf), RDI's (data bases, depth slices, section grids, voxels, .pdf), waveform (.gdb)*

- Geological Data

  - *Geologic map of survey area*
  - *Map of drillholes with high gold intercepts*
  - *Map of 2021 sampling program*

2.3 Martin Kenty Project

In 2021, Geotech collected approximately 365 line-km of VTEM and TMI data at a 100 m line spacing in an N-S direction and 1 km tie lines in an E-W direction. TechnoImaging inverted the VTEM and TMI data set, covering approximately 34 square km, 13 km NE of Nestor Falls in northwestern, Ontario. Figure 6 shows the full VTEM survey outline in red and its approximate location. Figure 7 shows the VTEM survey flight path in more detail in red.

Figure 6. Martin Kenty project VTEM survey location is shown in red on a Google Earth image.
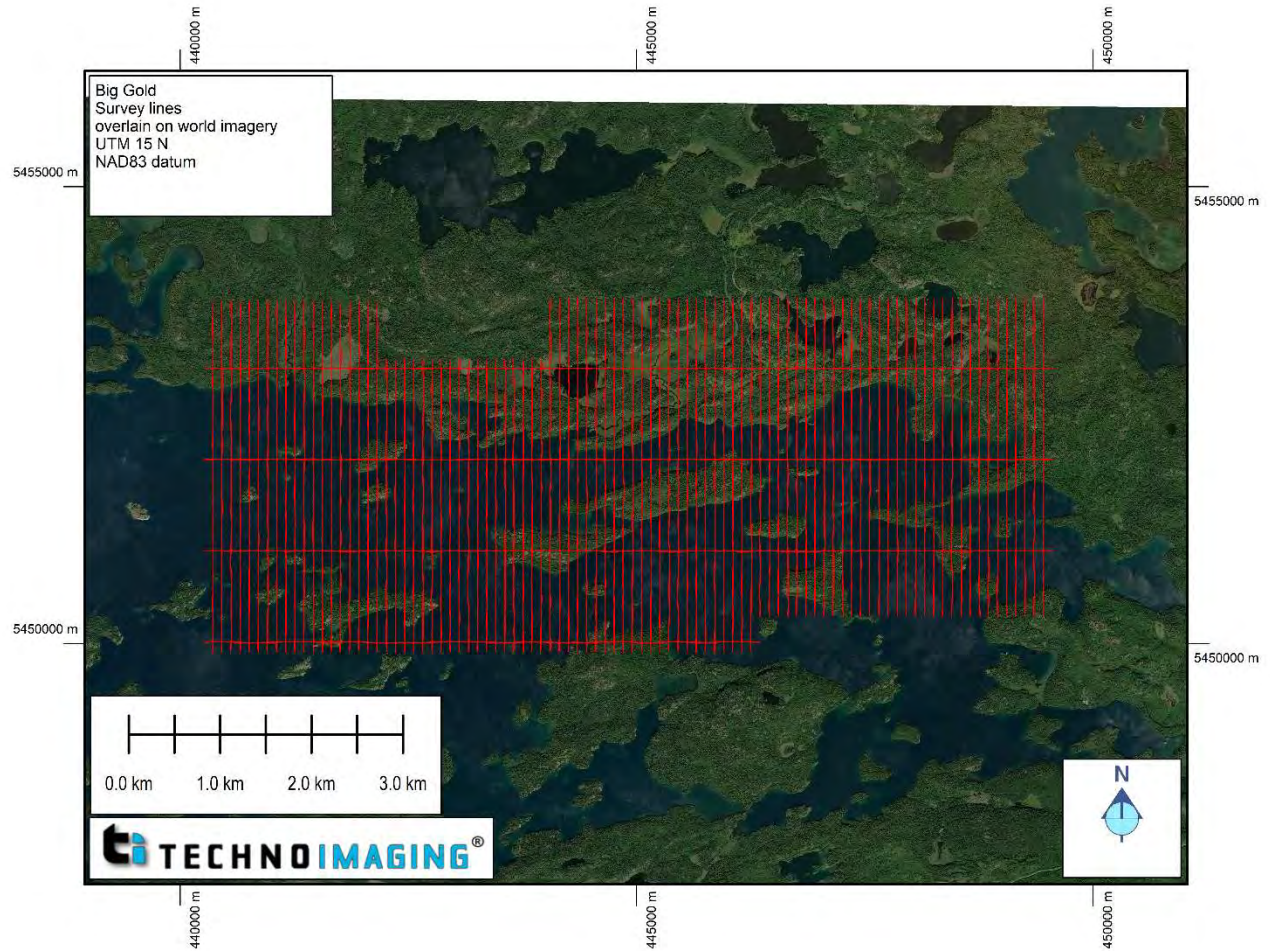
Figure 7. Martin Kenty project VTEM flight path plotted over world imagery.

3   Data Collection

The survey was flown between October 17th and October 25th, 2021, employing 100 m spaced flight lines at 000°/180° and 1 km tie lines at 090°/270° at right angles to the flight lines. The Martin Kenty area covered 365 line-km of data that were inverted in 3D. The VTEM waveform, time gates, and system geometry were taken from the geophysical survey report by Geotech "Geophysical Report on a helicopter-borne Versatile *Time Domain ElectroMagnetic (VTEM™ plus) and Horizontal Magnetic Gradiometer geophysical survey."* A photograph of the system in flight is shown in Figure 8.

3.1 VTEM™ Plus with Horizontal Crossline Magnetic Gradiometer
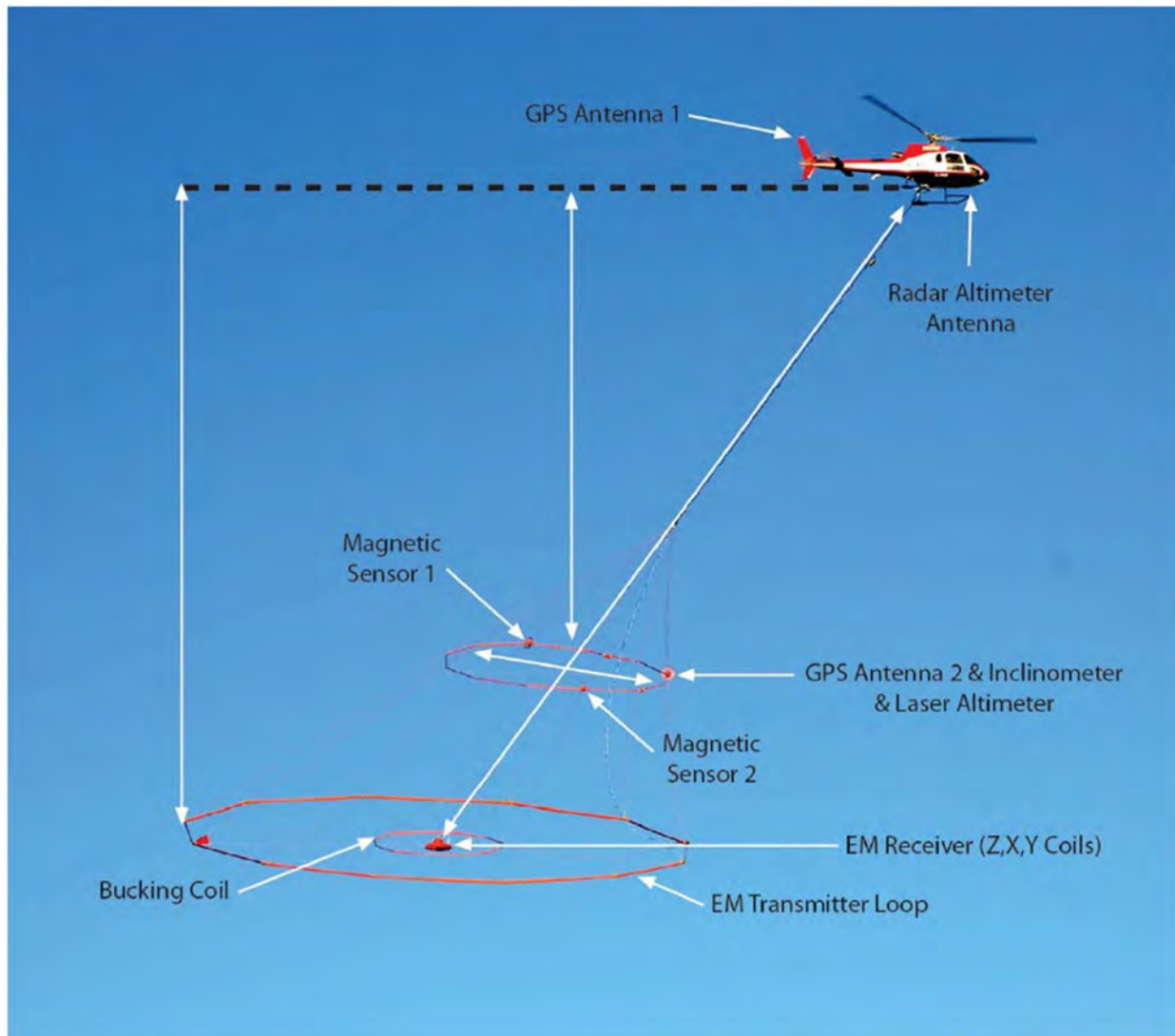
Figure 8. VTEM plus system towed beneath an AS350B3 Helicopter

During the survey, the helicopter was maintained at a mean altitude of 76 meters above the ground with an average survey speed of 85 km/hour. This allowed for an actual average transmitter-receiver loop terrain clearance of 40 meters and a magnetic sensor clearance of 50 meters. The receiver coil is located at the center of a 26 m diameter transmitter loop and is located on the same transmitter plane as the transmitter loop. The receiver measures three components of dB/dt in the horizontal (X and Y) and vertical (Z) directions. The real-time navigation GPS antenna is on the helicopter's tail boom. A radar altimeter was used to record the terrain clearance of the helicopter, and the antenna was mounted beneath the bubble of the helicopter cockpit. A second GPS antenna was attached to the front edge of the magnetic gradiometer to give positional information. An inclinometer and laser altimeter were also mounted on the magnetometer loop to give tilt information and terrain clearance, respectively.

Figure 9 shows the observed TMI data used in the inversion overlain on world imagery.
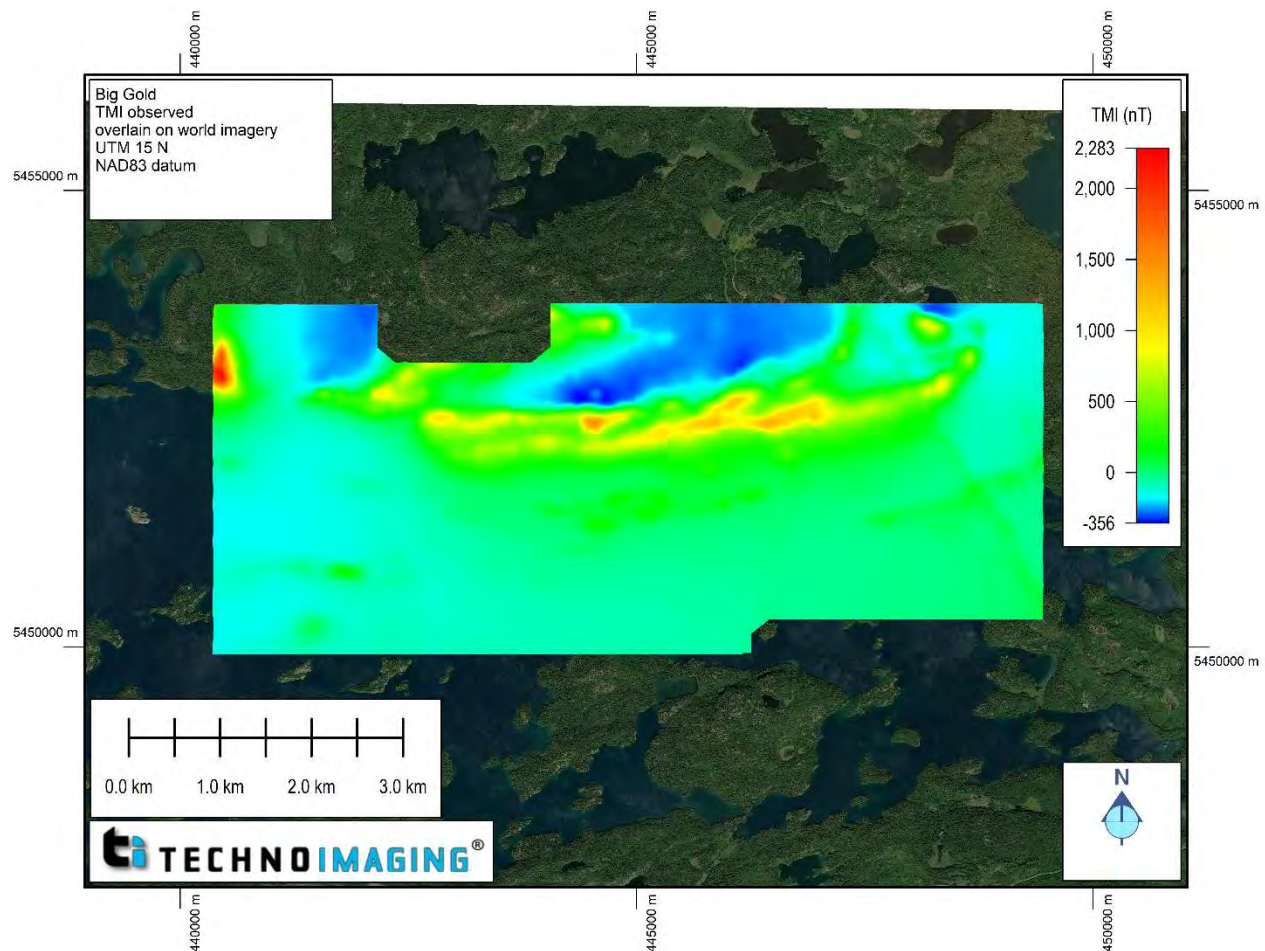
Figure 9. Martin Kenty observed TMI map after post-processing: from 2021 Geotech helicopter Survey.

3.1.1   VTEM system parameters

The electromagnetic system was a Geotech Time Domain EM (VTEM™ Plus) full receiver-waveform streamed data recorded system. The "full waveform VTEM system" uses the streamed half-cycle recording of transmitter and receiver waveforms to obtain a complete system response calibration throughout the entire survey flight. A horizontal loop transmitter produced an approximate vertical magnetic dipole for the source fields. The measured fields were vertical (Z), inline (X), and crossline (Y) dB/dt fields. The receiver is located in the center of the transmitter loop. VTEM with the serial number 10 had been used for the survey. The VTEM™ transmitter current waveform is shown diagrammatically in Figure 10. The transmitter-receiver loop was towed at a mean distance of 46 meters below the aircraft, as shown in Figure 8.
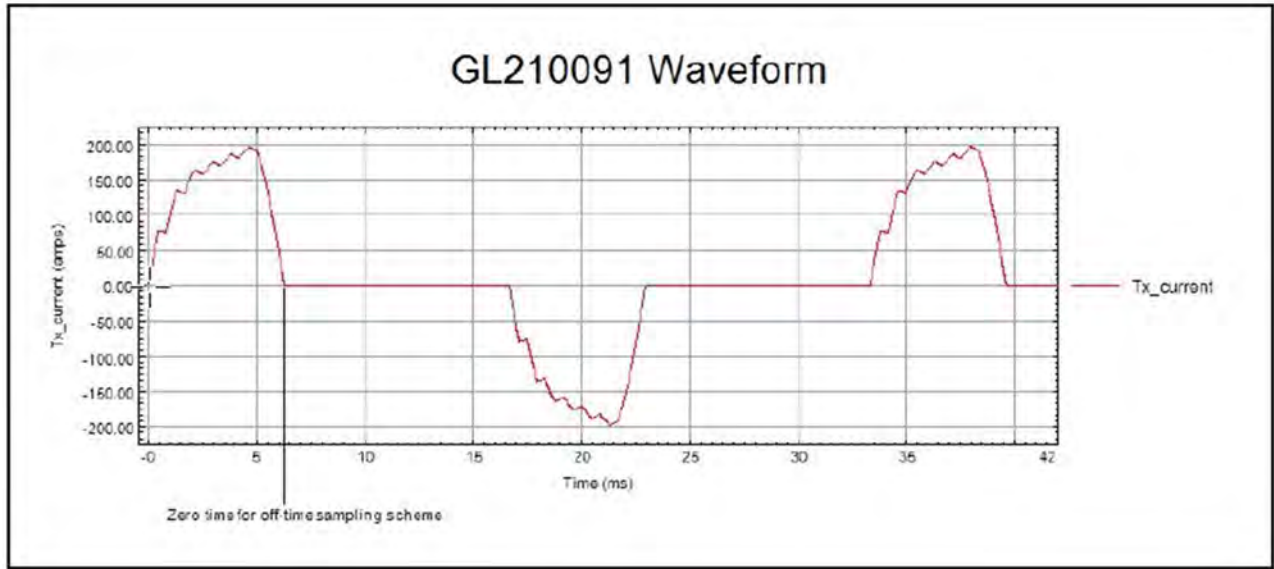
Figure 10. VTEM™ transmitter current waveform

The VTEM™ decay sampling scheme is shown in Table 1 below. Forty-three time measurement gates were archived by Geotech in the database in the range from 0.021 to 8.083 msec. Zero time for the off-time sampling scheme is equal to the current pulse width and is defined as the time near the end of the turn-off ramp where the dI/dt waveform falls to 1/2 of its peak value. This was determined to be 6.2768 ms.

Table 1. Off-Time Decay Sampling Scheme Relative to 6.2768 ms.

VTEM™ Decay Sampling Scheme				
Index	Start	End	Middle	Width
Milliseconds				
4	0.018	0.023	0.021	0.005
5	0.023	0.029	0.026	0.005
6	0.029	0.034	0.031	0.005
7	0.034	0.039	0.036	0.005
8	0.039	0.045	0.042	0.006
9	0.045	0.051	0.048	0.007
10	0.051	0.059	0.055	0.008

11	0.059	0.068	0.063	0.009
12	0.068	0.078	0.073	0.010
13	0.078	0.090	0.083	0.012
14	0.090	0.103	0.096	0.013
15	0.103	0.118	0.110	0.015
16	0.118	0.136	0.126	0.018
17	0.136	0.156	0.145	0.020
18	0.156	0.179	0.167	0.023
19	0.179	0.206	0.192	0.027
20	0.206	0.236	0.220	0.030
21	0.236	0.271	0.253	0.035
22	0.271	0.312	0.290	0.040
23	0.312	0.358	0.333	0.046
24	0.358	0.411	0.383	0.053
25	0.411	0.472	0.440	0.061
26	0.472	0.543	0.505	0.070
27	0.543	0.623	0.580	0.081
28	0.623	0.716	0.667	0.093
29	0.716	0.823	0.766	0.107
30	0.823	0.945	0.880	0.122
31	0.945	1.086	1.010	0.141
32	1.086	1.247	1.161	0.161
33	1.247	1.432	1.333	0.185
34	1.432	1.646	1.531	0.214
35	1.646	1.891	1.760	0.245
36	1.891	2.172	2.021	0.281
37	2.172	2.495	2.323	0.323

38	2.495	2.865	2.667	0.370
39	2.865	3.292	3.063	0.427
40	3.292	3.781	3.521	0.490
41	3.781	4.341	4.042	0.560
42	4.341	4.987	4.641	0.646
43	4.987	5.729	5.333	0.742
44	5.729	6.581	6.125	0.852
45	6.581	7.560	7.036	0.979
46	7.560	8.685	8.083	1.125

The Z component was measured during the time gates from 4 – 46. The X and Y component measurements started at time gate 20 and went through 46.

Figures 11 and 12 show examples of the collected data. Two vertical (Z) components channels are shown.
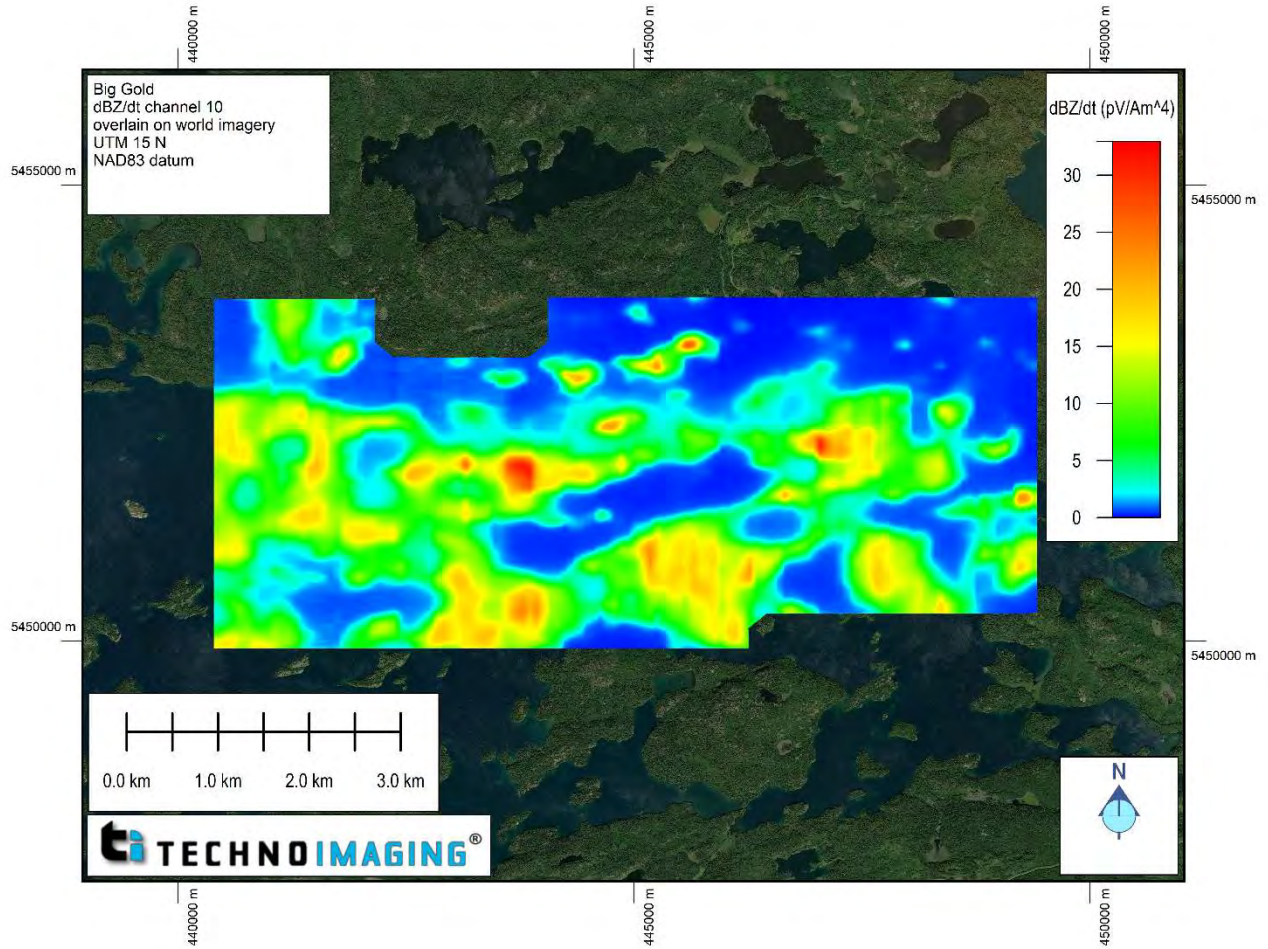
Figure 11. Martin Kenty VTEM dB/dt Z component field map channel 10. The EM data primarily respond to lake bottom sediments.
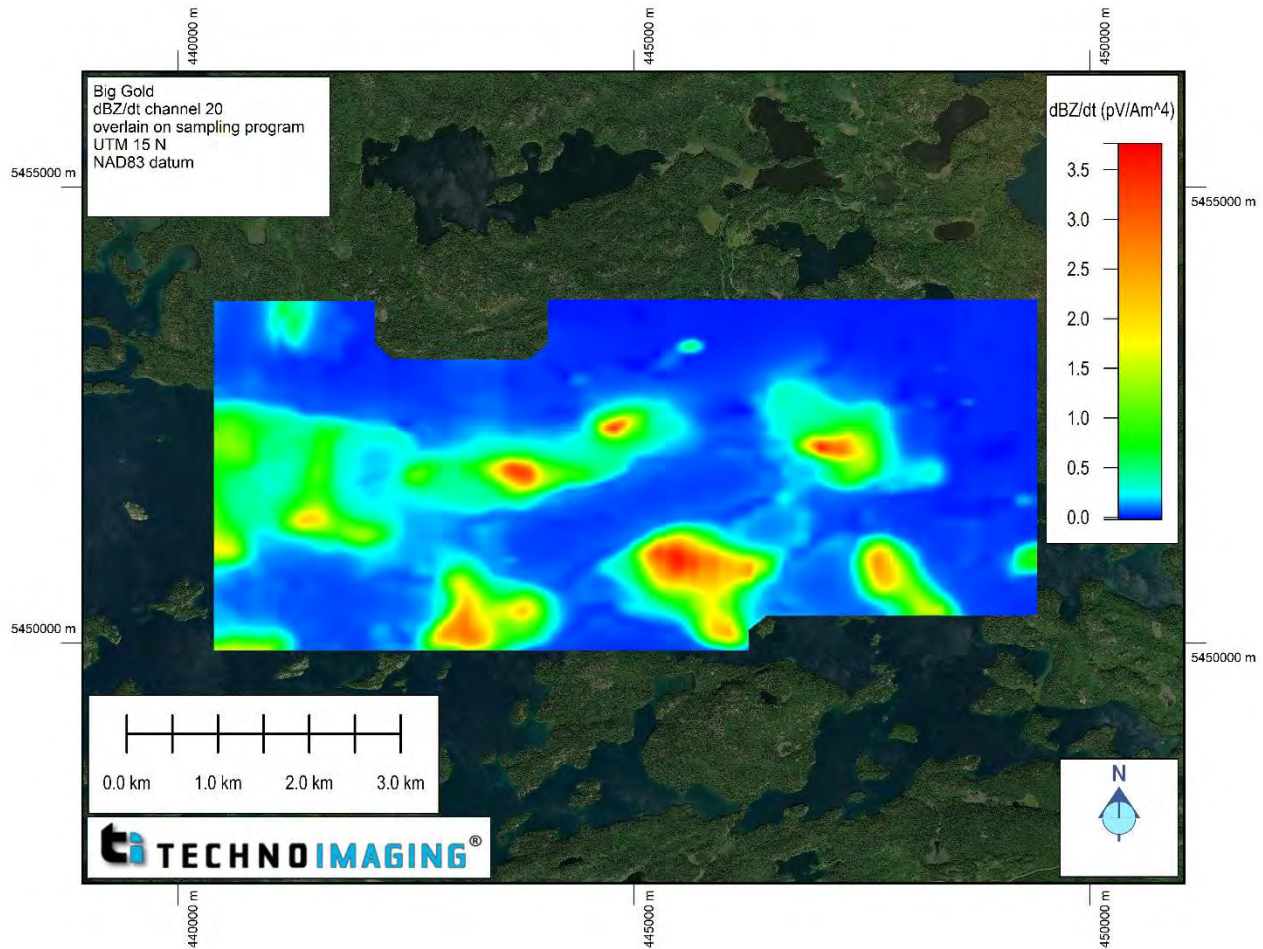
Figure 12. Martin Kenty VTEM dB/dt Z component field map Channel 20. The EM data primarily respond to lake bottom sediments. A few and quite weak anomalies are shown which are not imaged in the earlier time channel. These will be shown in more detail in the results.

4 Overview of the Modeling and Inversion Algorithms

4.1 Modeling of VTEM data

TechnoImaging uses both one-dimensional (1D) and three-dimensional (3D) inversions to process the data. In our standard workflow, 1D inversion is used to QC the data and create an approximate background model, while 3D inversion is used for final, higher accuracy inversion runs. One-dimensional inversion is typically faster than 3D inversion and can create accurate models in areas where the earth is laterally invariant. The 1D approximation is used to speed up calculations and makes the assumption that the earth is layered and these layers extend to infinity horizontally. Each transmitter-receiver position, or sounding location, has a 1D earth under it which is recovered during inversion. These are then gridded into a 3D model to create a more realistic earth picture, but in areas of strong lateral contrasts, especially such as strong vertical conductors and contacts, the modeling and physics are not accurate. In this area, the conductivity structure was conducive to pseudo-3D inversion, and this was used for the final results. In this case, full 3D stabilizers and

model discretization is used, while a 1D approximate is used for sensitivity calculations. TechnoImaging has multiple drivers for the EM inversions; please see Cox et al (2015) and Zhdanov (2015, 2018) for details.

4.1.1 Modeling Checks

TechnoImaging performs a variety of checks on the forward modeling response and approximations used in the inversion to determine the accuracy and increases modeling accuracy if needed when the assumptions do not hold.

4.2 VTEM™ plus Inversion

All inversions were carried out using TechnoImaging's proprietary Glass Earth® technology and EMVision® software package. The software uses a robust and stable method to solve for the 3D physical parameter distribution in the earth. Fast and accurate algorithms are used to model the physics, and flexibility in the software allows a wide selection of stabilizers, a priori models, and cooperative inversion techniques. The inversion method uses data weights to ensure fitting of the data to the appropriate noise level and model weights to normalize sensitivities of the data for increased depth resolution and stability.

The data weights for inversion are based on a two-part model: an absolute error plus a relative error. The absolute noise level considers the instrument noise floor and prevents small data values close to 0 from being overly important. The relative error level represents errors such as tilt and flight height errors. The estimate errors are listed for each survey individually. The inverse of these errors is used as data weights. Ideally, the inversion is run to a normalized χ^2 of 1, see equation (1) below:

$$\chi^2 = \frac{1}{N} \sum \left(\frac{d_i^p - d_i^o}{\varepsilon_i} \right)^2 \ (1)$$

where d^p is the predicated data, d^o is the observed data, and ε_i is the estimated error in the ith data point. The value of $\chi^2 = 1$ indicates an optimal data fit when the prediction errors are equal to the noise level in the observed data.

However, these errors should not be taken as exactly the error levels in the data, because these are also adjusted to change the fit and convergence of the inversion during the inversion parameter testing phase. The errors should be taken as an approximate (order of magnitude) estimate.

4.3 TMI Inversion

All inversions were carried out using TechnoImaging's proprietary Glass Earth® technology. A few technical highlights are detailed here.

4.3.1 Magnetization vector properties and susceptibility

In mineral exploration, magnetic data have traditionally been inverted to produce magnetic susceptibility models, which represent magnetization induced by the current magnetic field. This does not take into account the remanent magnetization of the rocks produced by the ancient magnetic field. More information about rock formations and geological processes can be obtained by inverting magnetic data for magnetization vector, as opposed to magnetic susceptibility only. This is demonstrated in Figure 13, which is an example taken from the Thunderbird V-Ti-Fe deposit in Ontario, Canada. All TechnoImaging's magnetic inversions include inversions for both these properties. For more technical details, please refer to Jorgensen and Zhdanov (2021).
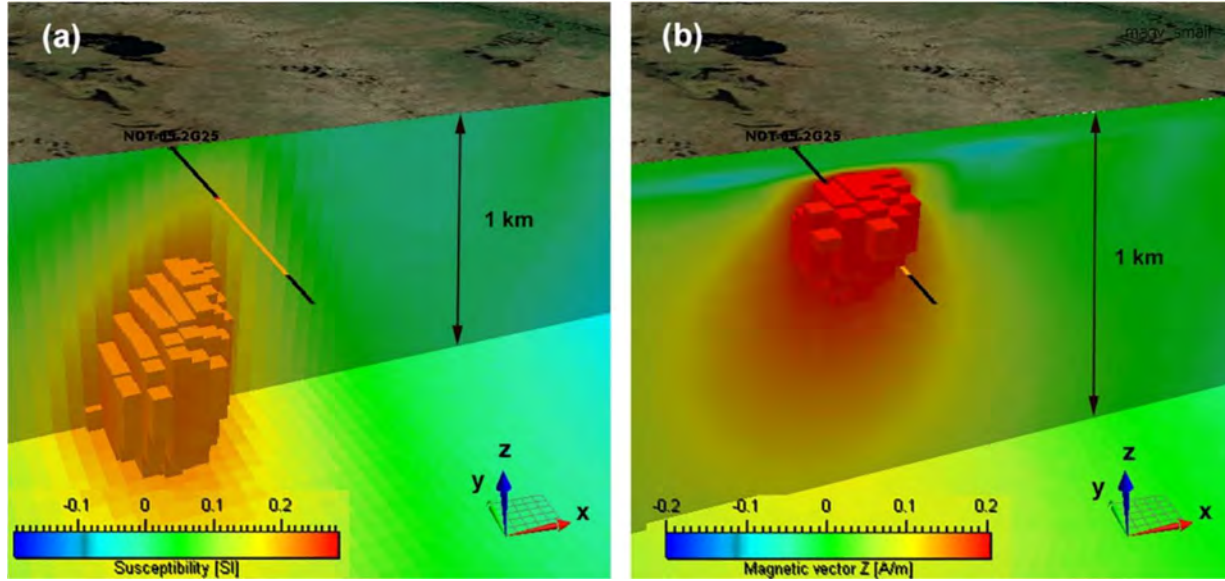
Figure 13. Comparison of 3D inverse models with drilling results. Left panel (a) shows the volume image of the inverse susceptibility model. Right panel (b) presents the volume image of the vertical component of the magnetization vector. The black–yellow–black solid line shows the location of the borehole drilled in the survey area. The yellow color indicates the mineralization zone confirmed by drilling. The recovered magnetization vector matches the drilling much better than the susceptibility only inversion..

4.3.2 Focusing regularization

Potential field data are finite and noisy. Their inversion is inherently non-unique, meaning that there is an infinite number of source distributions that can equally satisfy the observed data. In order to solve this inverse problem, regularization must be introduced. Regularization aims to recover the most geologically plausible solutions from the infinite number of mathematically equivalent solutions. As we generalized our inversion methodology for gravity data, we describe our model parameters by vector $\mathbf{m}$, of length N_m. Regardless of the iterative scheme used, most regularized inversions seek to minimize the Tikhonov parametric functional, $P^\alpha(\mathbf{m})$ shown in equation (2):

$$P^\alpha(\mathbf{m}) = \phi(\mathbf{m}) + \alpha s(\mathbf{m}) \rightarrow min, \quad (2)$$

where $\phi(\mathbf{m})$ is a misfit functional of the observed and predicted potential field data, $s(\mathbf{m})$ is a stabilizing functional, and α is the regularization parameter that balances the misfit and stabilizing functional (Zhdanov, 2002). Data and model weights can be introduced to equation (2) through data and model weighting matrices. We can also re-weight the inverse problem in logarithmic space in order to reduce the dynamic range of both the data and model parameters.

In our implementation, all weighting functions are selected based upon their integrated sensitivity (Zhdanov, 2002). Our weighting functions provide equal sensitivity of the observed data to cells located at different depths and at different horizontal positions. Thus, our weighting functions automatically introduce appropriate corrections for the vertical and horizontal distribution of the

density.

All geological constraints manifest themselves as regularization that can be quantified through a choice of data weights, model upper and lower bounds, model weights, an a priori model, and the type of stabilizing functional. The latter incorporates information about the class of models used in the inversion. The choice of stabilizing functional should be based on the user's geological knowledge and prejudice. In this section, we will briefly describe different smooth and focusing stabilizers.

A minimum norm (MN) stabilizer will seek to minimize the norm of the difference between the current model and an a priori model:

$$s(\mathbf{m}) = \iiint (\mathbf{m} - \mathbf{m}_{apr})^2 dv, (3)$$

and usually produces a relatively smooth model.

The Occam (OC) stabilizer implicitly introduces smoothness with the first derivatives of the model parameters:

$$s(\mathbf{m}) = \iiint (\nabla\mathbf{m} - \nabla\mathbf{m}_{apr})^2 dv, (4)$$

and can result in spurious oscillations and artifacts when the model parameters are discontinuous. A combination of stabilizers, (3) and (4), is often used (e.g., Li and Oldenburg, 1996, 1998).

Very little geology exhibits smooth density distributions. Usually, geology is characterized by sharp boundaries of contrasting density, for example, between an ore deposit and host rock, or across a discontinuity. As such, stabilizers (3) and (4) or their combinations produce results that bear no physical relevance to the actual geology. Portniaguine and Zhdanov (1999) introduced focusing stabilizers that make it possible to recover models with sharper boundaries and contrasts. We briefly describe these stabilizers here and refer the reader to Zhdanov (2002) for further details. First, we present the minimum support (MS) stabilizer:

$$s_{MS}(\mathbf{m}) = \iiint \frac{(\mathbf{m}-\mathbf{m}_{apr})^2}{(\mathbf{m}-\mathbf{m}_{apr})^2 + e^2} dv, (5)$$

where e is a focusing parameter introduced to avoid singularity when $\mathbf{m} = \mathbf{m}_{apr}$. The minimum support stabilizer minimizes the volume with non-zero departures from the a priori model, effectively recovering compact bodies. Thus, a smooth distribution of all model parameters with a small deviation from the a priori model is penalized. A focused distribution of the model parameters is penalized less. Similarly, we present the minimum gradient support (MGS) stabilizer:

$$s_{MGS}(\mathbf{m}) = \iiint \frac{\nabla(\mathbf{m}-\mathbf{m}_{apr}) \cdot \nabla(\mathbf{m}-\mathbf{m}_{apr})}{\nabla(\mathbf{m}-\mathbf{m}_{apr}) \cdot \nabla(\mathbf{m}-\mathbf{m}_{apr}) + e^2} dv. (6)$$

which minimizes the volume with non-zero gradients, i.e., sharp transitions in the model parameters are penalized less than smooth transitions.

While variations of equations (5) and (6) were derived in Zhdanov (2009), we base our solution on the re-weighted regularized conjugate gradient (RRCG) method (Zhdanov, 2002), which is easier to implement numerically. This method iteratively updates the vector of model parameters $\mathbf{m}$ so as to minimize the vector of residual errors, $\mathbf{r}$, akin to:

$$\mathbf{m}_{i+1} = \mathbf{m}_i + k \, \mathbf{A}^T \mathbf{r} \text{ subject to } \mathbf{r}_i \rightarrow min, (7)$$

where k_i is a step length and $\mathbf{A}^T$ is the conjugate transpose of the matrix of the gravity linear operator. The inversion proceeds to iterate in a manner similar to equation (7) until the residual error reaches a preset threshold, or a maximum number of iterations is reached. Upon completion, the quality of the inversion is appraised by the data misfit and visual inspection of the model.

4.3.3 The moving sensitivity domain approach

In principle, the regularized inversion outlined above can be applied to large-scale problems. Numerically, however, the computational complexity increases linearly with the size of the problem, meaning large-scale 3D inversion faces two major obstacles. First is the large amount of computer memory required for storing the kernels of the forward modeling operators, which double as sensitivities for linear problems. Even a small-sized 3D inversion of thousands of data to 3D earth models of hundreds of thousands of cells can exceed the memory available for desktop computers. The second obstacle is a large amount of CPU time required to apply the dense matrix of the forward modeling operators to data and model vectors. One may store the matrices outside RAM or generate them at the time of processing. An alternative approach has been to exploit the translational invariance of the kernels to reduce the matrices to Toeplitz block structure and use FFTs for matrix-vector multiplication (e.g., Pilkington, 1997; Zhdanov et al., 2004). Such strategies alleviate memory limitations and reduce the CPU time dramatically. However, these methods require the data to lie over a regular grid on a flat surface above the topography. Although applicable in some special cases, it cannot address the aforementioned difficulties for topography and variable altitude.

In potential fields, the sensitivity of the data to the density variations is expressed via the appropriate kernel functions of the forward modeling operators, i.e., via the corresponding Green's functions. It was demonstrated that at some limited distance, which we call the *sensitivity domain*, the receiver is no longer sensitive to the 3D earth model. Typically, the size of the sensitivity domain is less than the size of an airborne survey. The size of the sensitivity domain for gravity fields is proportional to $1/\mathbf{r}^2$; for gravity gradiometry fields, it is proportional to $1/\mathbf{r}^3$.

Cox and Zhdanov (2007) introduced the concept of the moving sensitivity domain for 3D inversion of airborne electromagnetic (AEM) data. They showed that there was no need to calculate the responses or sensitivities beyond the AEM's sensitivity domain for a single transmitter- receiver pair. The sensitivity matrix for the entire 3D earth model could be constructed as the superposition of the sensitivity domain from all transmitter-receiver pairs. Zhdanov et al. (2010) also introduced the sensitivity approach for the large-scale 3D inversion of the magnetotelluric (MT) data. The framework of this approach can be described as follows: for a given receiver, compute and store the Fréchet derivative for those inversion cells within a predetermined horizontal distance from this receiver, i.e., the sensitivity domain. The radius of the sensitivity domain is based on the rate of sensitivity attenuation.

5 Inversion of Martin Kenty Project Area

5.1 VTEM Inversion Specifications

5.1.1 Data processing

Powerlines and cultural features were not present in the area to an extent which required further processing or even rejecting data.

5.1.2 Components

The inversion used all Z channels, which extended from 21 µs to 8.8083 ms (channel centers).

5.1.3 Inversion parameters and workflow

The final workflow for the inversion was to run the 1D inversion using EMVision® on the Z component data. This initial inversion step uses 1D sensitivities, but full 3D stabilizers and runs on a voxel discretization of the model exactly as the 3D inversion. The model for the 1D inversion was discretized into 20 m x 50 m cells in the inline and cross-line directions horizontally, and vertically discretized into 16 cells from 4 m thick at the surface to 70 m thick at depth. The total thickness of the inversion domain was 650 m.

Conductivity, chargeability, and time constant were all inverted for using the generalized effective-medium model of induced polarization (GEMTIP model- Zhdanov, 2008, 2018). A simplified version of this model parameterizes the conductivity as a function of frequency to describe the observed induced polarization effect by the following equation (8):

$$\sigma(\omega) = \sigma_0 \left(1 + \eta \left[1 - \frac{1}{1 + (i \; \tau)^C} \right] \right) (8)$$

where σ_0 is the DC conductivity, η is the chargeability, τ is the time constant, and C is the relaxation coefficient. The relaxation coefficient was fixed at 0.9 for the entire inversion process.

The inversion used a minimum norm stabilizer combined with a 2nd derivative in the crossline and vertical directions. The stabilizer ensures the algorithm finds a geologically reasonable model which also satisfies the observed data. A 1e-4 S/m (10,000 Ohm-m) hard lower bound was used in the inversion. No upper bound was needed.

For data weighting, the percent and absolute errors are combined into a total error by the following equation (9):

$$e^t = |d_o| * \frac{e^p}{100} + e^a. (9)$$

The percent error was set to 6% and the absolute error was se to 0.001 pV/Am^4.

5.2 TMI Inversion

5.2.1 System parameters

The horizontal magnetic gradiometer consists of two Geometrics split-beam field magnetic sensors with a sampling interval of 0.1 seconds. These sensors are mounted 12.5 meters apart on a separate loop, 10 meters above the VTEM Transmitter-receiver loop. The average terrain clearance for the TMI survey was 50 m. A GPS and tilt help to determine the positions and tilt of the gradiometer. The data from the two magnetometers are corrected for position and orientation variations and for the diurnal variations using the base station data. Only one of the magnetometer data sets was used for the inversions.

5.2.2 Data processing

A first-degree polynomial was used to high pass filter the data and remove regional trends. No other processing was required. The data were microleveled by Geotech. Figure 14 shows the microleveled data as supplied from Geotech. Figure 15 shows the inversion-ready data after filtering.
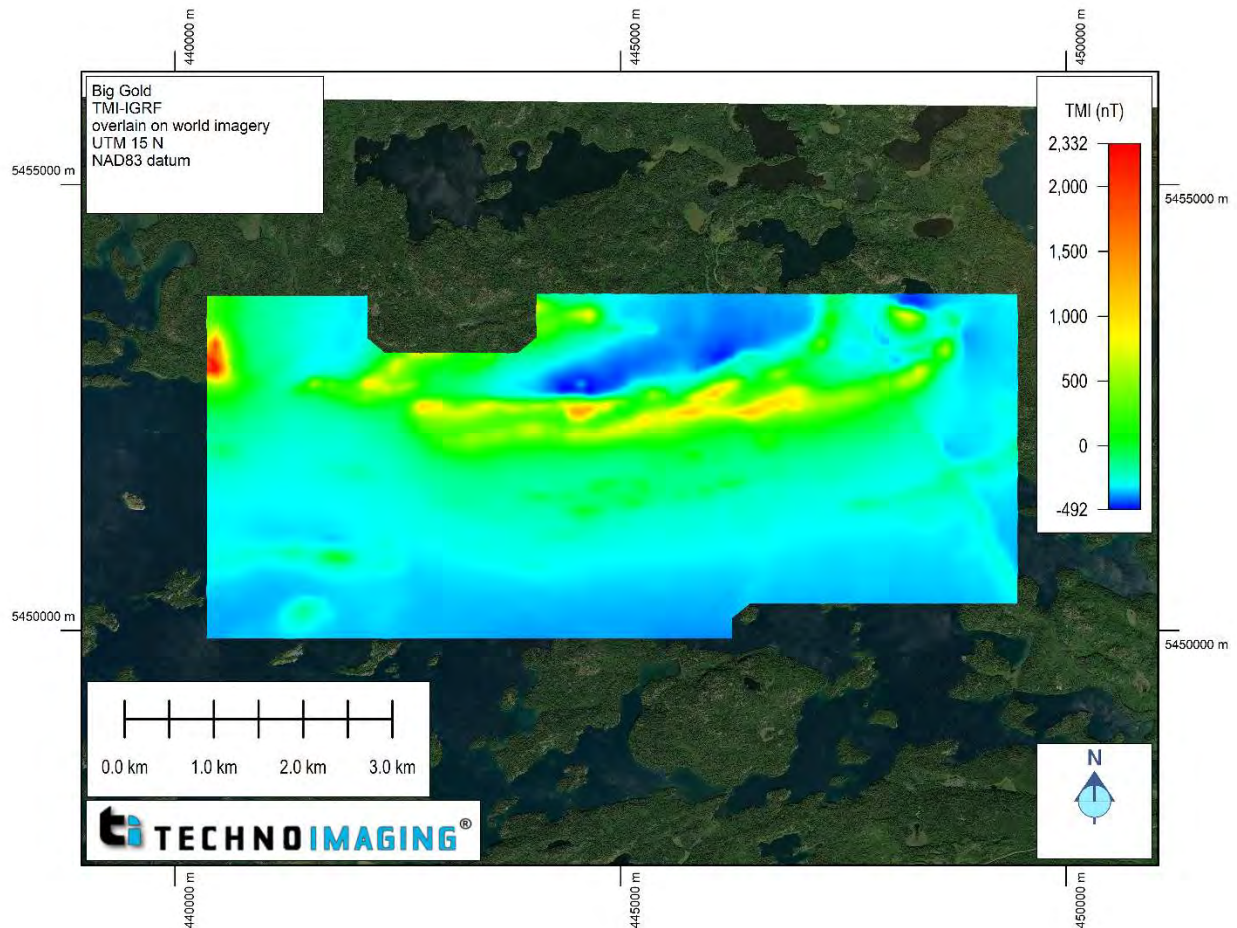

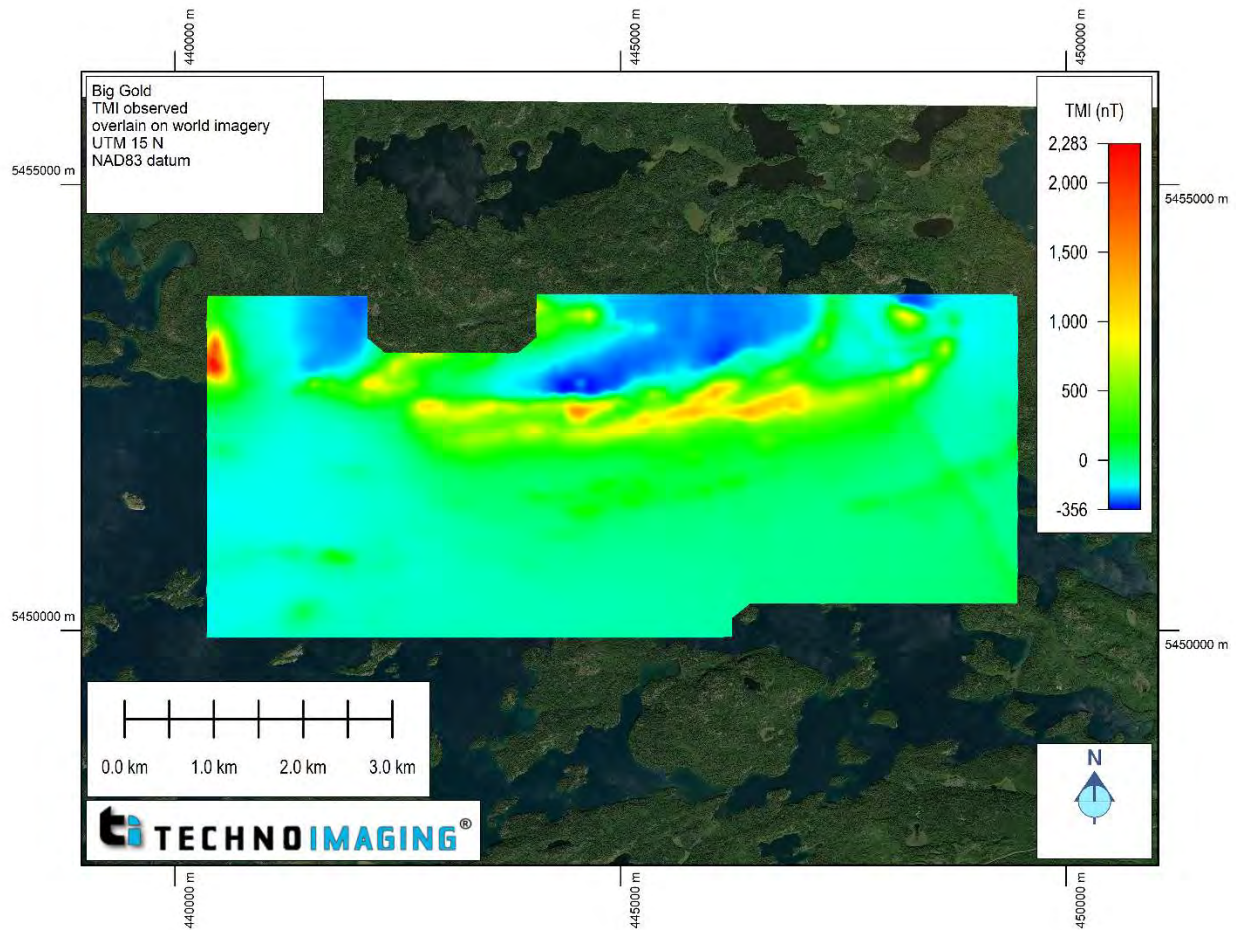*Figure 14. TMI data supplied by Geotech with the main field removed.*

Figure 15. Filtered TMI data used in the inversion.

5.2.3   Inversion parameters and workflow

The 3D inversion domain was discretized into 25 m x 50 m cells in the inline and crossline directions horizontally, and vertically discretized into 36 cells from 25 m thick at the surface to 300 m at depth. The total depth of the inversion domain was about 4000 m below the surface. The horizontal cell size of 50 m in the crossline direction is adequate due to the 100 m spaced flight lines. The errors used for the error model in the inversion are given in Table II. The final misfit converged to 5% globally and fit the data to the estimated error levels.

Table II. Estimated error levels in the Big Gold TMI survey used to compute the data weights.

Datum	Relative Error (%)	Absolute Error (nT)
Filtered TMI	5	0.02

The 3D inversion was run using a homogeneous half-space as the reference and initial model. The stabilizing constraint (stabilizer) used to ensure a robust inversion was the minimum norm of the departure of the model parameters from the reference model and the first derivative in the horizontal and vertical directions.

6   Discussion of the results

The 3D inversions results are presented here. This section presents our first observations, and we give examples of what can be done with this data set. The data set is very rich in information, and it should be approached as a model that will continue to be analyzed, when new geological and drill hole information becomes available. The 3D model files can be viewed in various ways, from map views, profile views, voxels, and isosurfaces. The interpretation needs to be done with a solid background understanding of the geology of the area and targets. TechnoImaging can aid with this interpretation and work with an area geologist or geophysicist to help get the process started.

6.1   VTEM Inversion Results

The VTEM data were inverted to a chargeability and conductivity model. Several methods were used to produce the best final models. Images of these results are shown in Figures 16 – 22.

Figures 16-19 show an overview of the recovered conductivity models at depths of 25, 125, 225, and 325 meters below the surface, respectively. The conductivity in the survey area varies from around 0.1 S/m (10 Ohm-m) to 2e-5 S/m (50,000 Ohm-m). Most of the variations are due to near-surface effects and are well correlated with sediments in lake area. The resolution below the conductive lakes is not as good as below islands because the conductive sediments mask the deeper material.

However, Figure 20 shows the recovered conductivity model at a depth of 425 meters below the surface. Two conductors of interest highlighted in this image, and other weaker bedrock conductors can also be seen in the image. These are small, single-line anomalies, but they are not noise or near-surface effects.
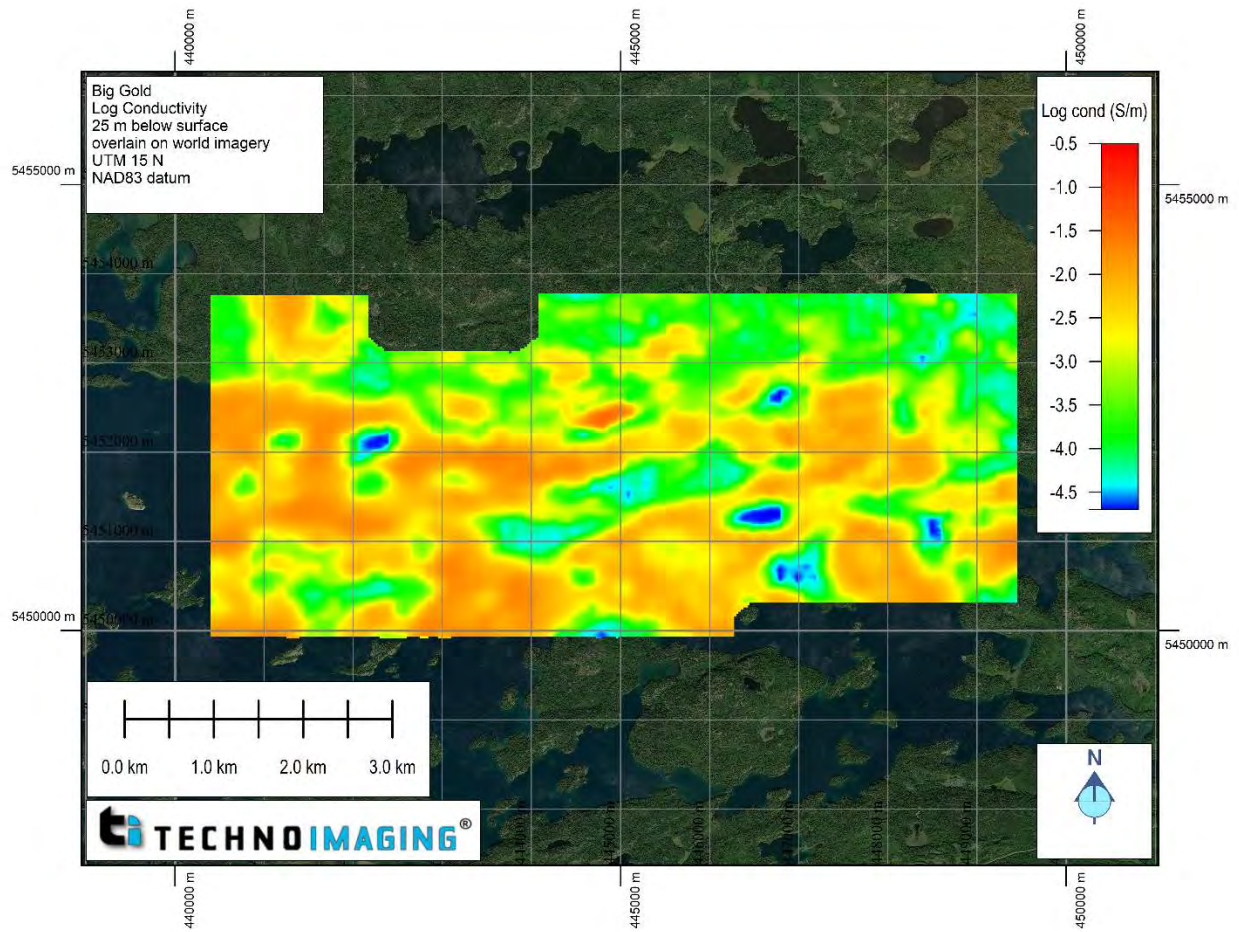
Figure 16. Conductivity inversion results at a depth of 25 m below the surface. The majority of the near-surface response is from lake sediments.
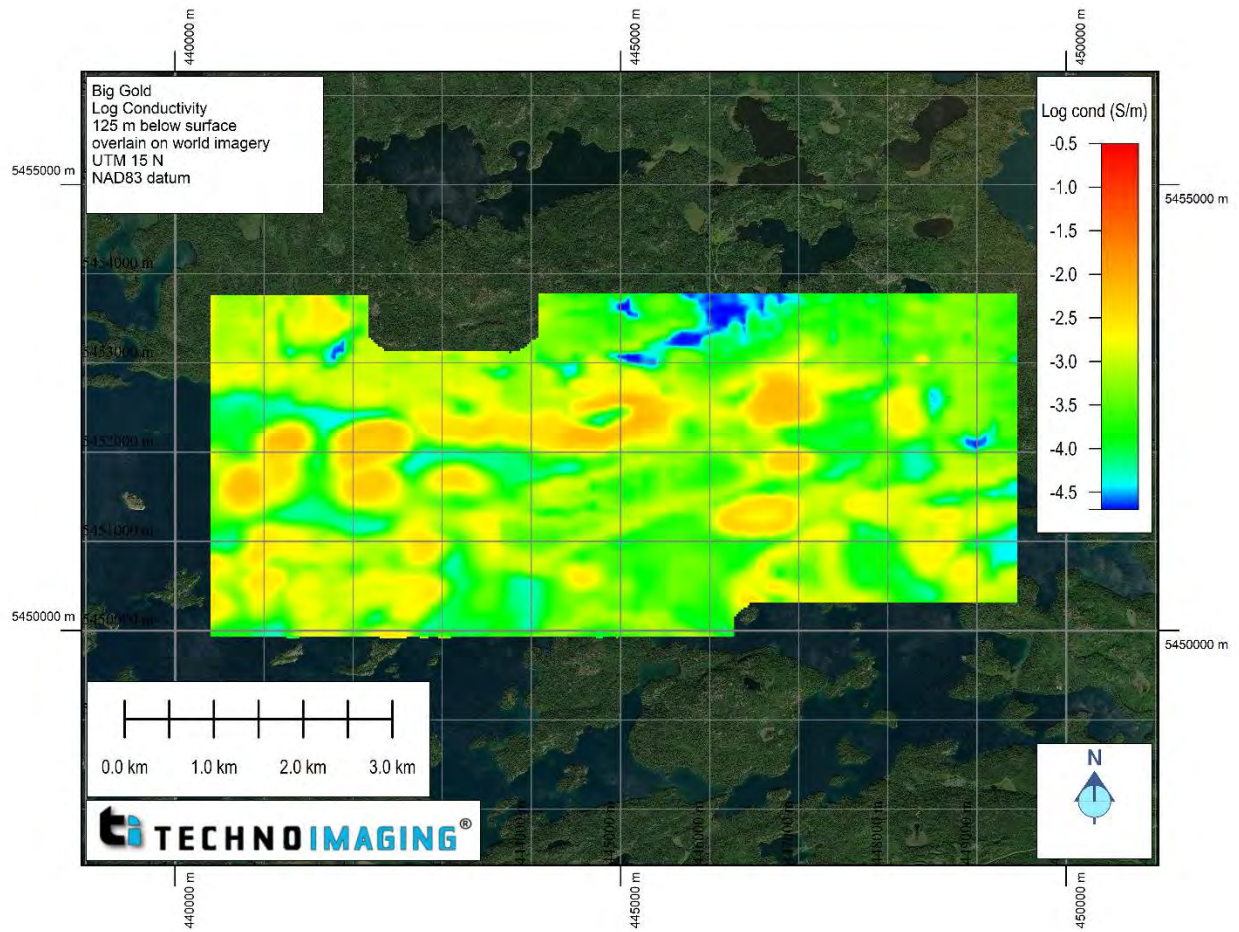
Figure 17. Conductivity inversion results at a depth of 125 m below the surface. The majority of the response is due to lakes.
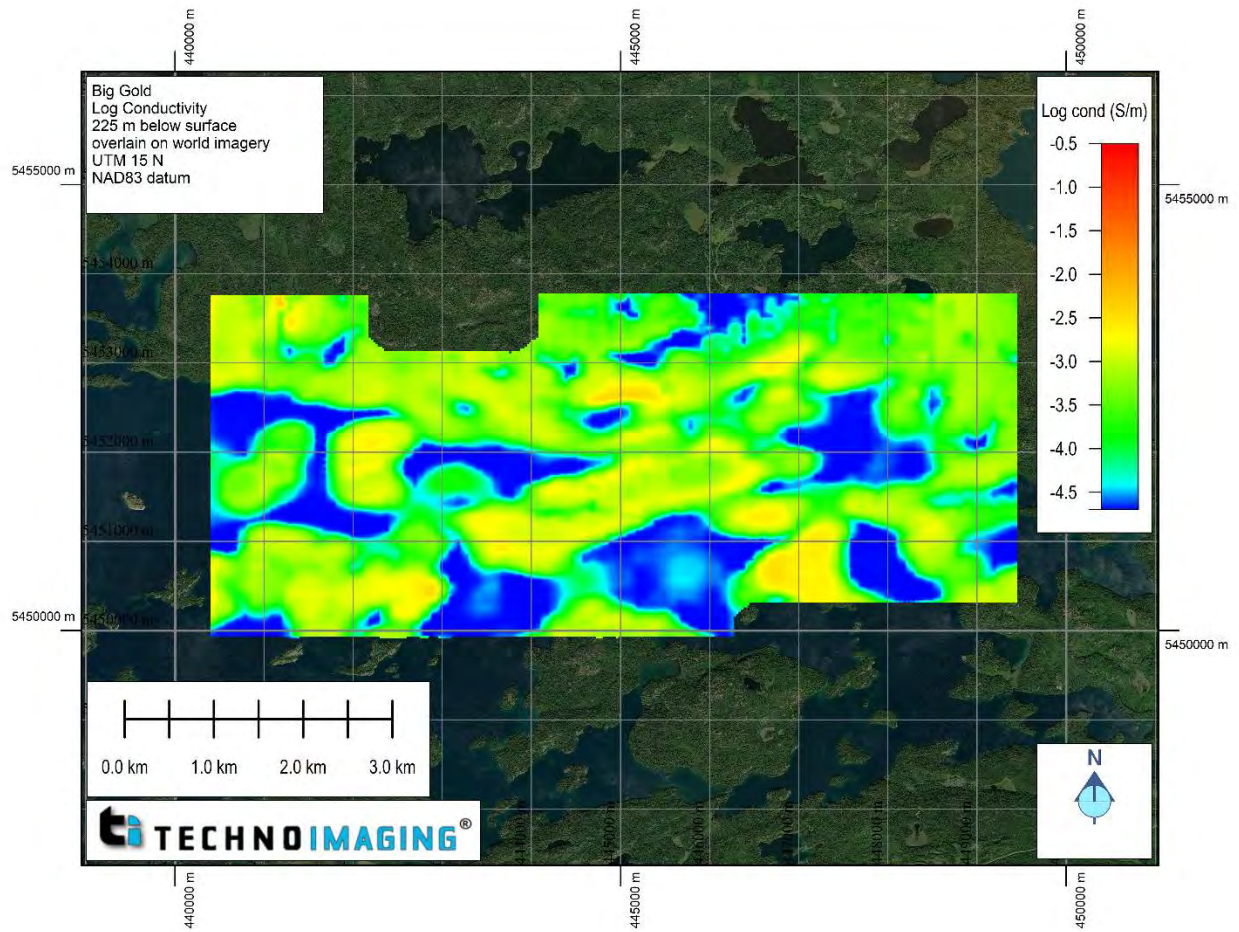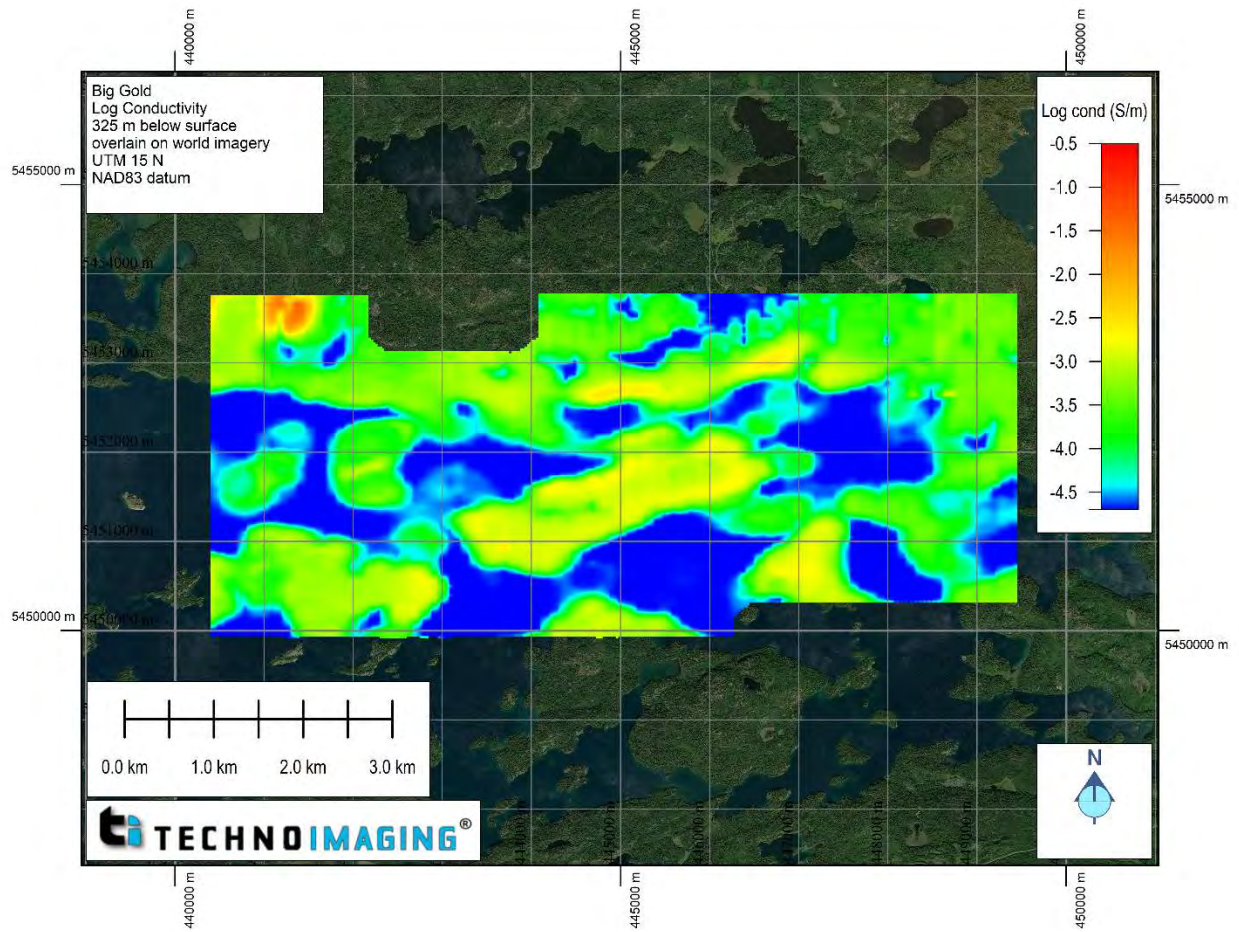
Figure 18. Conductivity inversion results at a depth of 225 m below the surface. The very resistive areas (cool colors) are likely not well imaged due to the conductive lake bottom sediments shielding deeper material.
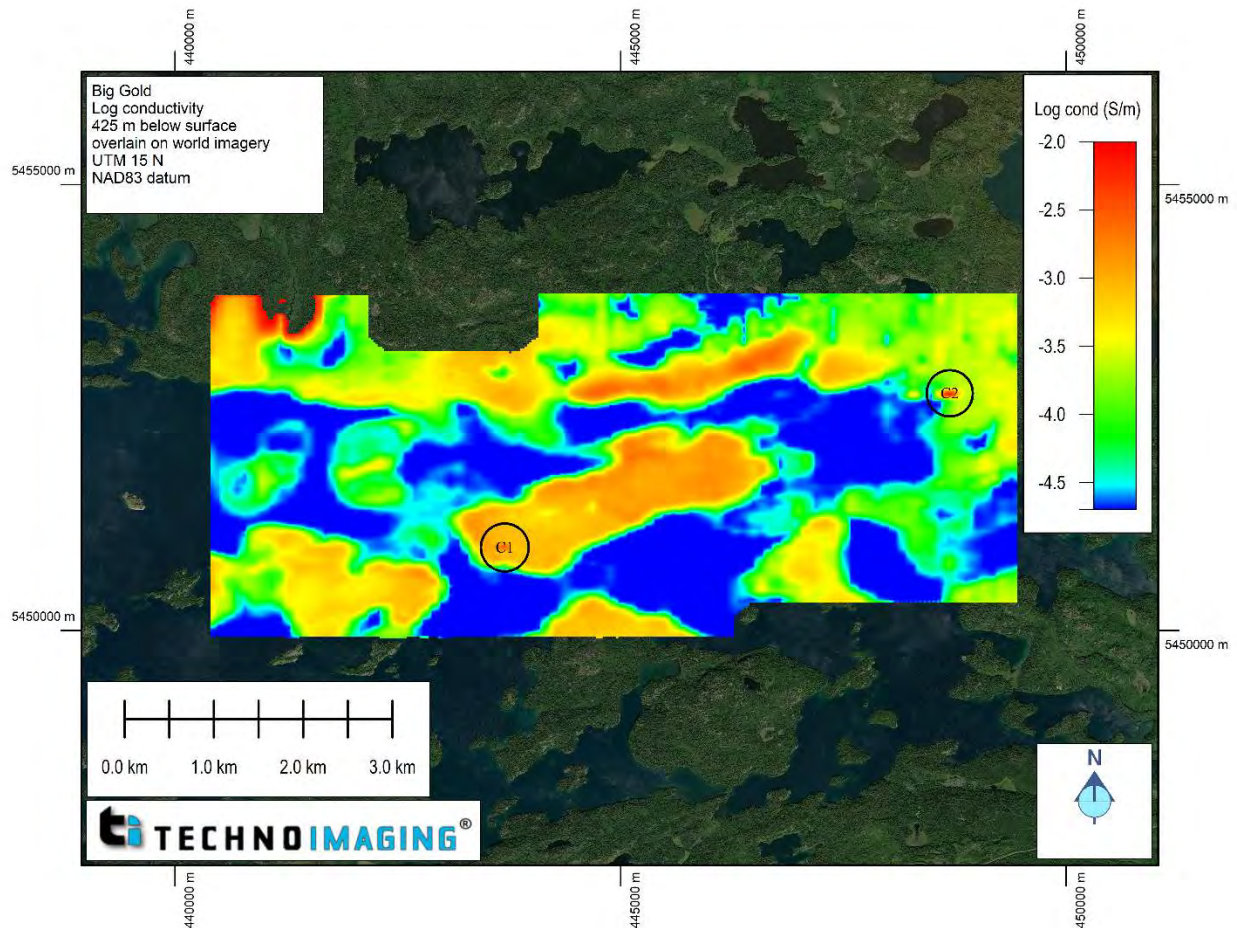
Figure 19. Conductivity inversion results at a depth of 325 m below the surface. The very resistive areas (cool colors) are likely not well imaged due to the conductive lake bottom sediments shielding deeper material.

Figure 20. Conductivity inversion results on a compressed color scale to bring out details at a depth of 425 m below the surface. Conductive targets C1 and C2 are shown by the black circles. These are well-confined conductors and could correspond to gold/silver or nickel deposits.

Figures 21 and 22 show the conductive anomalies C1 and C2 shown in detail, respectively. Both vertical planes of conductivity, plus isosurfaces at a constant conductivity are shown in the figures. Figure 21 shows the body C1 with an isosurface at 0.002 S/m, and Figure 22 shows the body C2 with a surface of 0.001 S/m. The geometry of the bodies can be clearly seen in these figures. However, these are single line anomalies, and extracting detailed geometries and conductivities cannot be done with a single flight line response. If these are of economic interest, tighter flight line spacing or ground follow-up would be needed to better describe these targets.
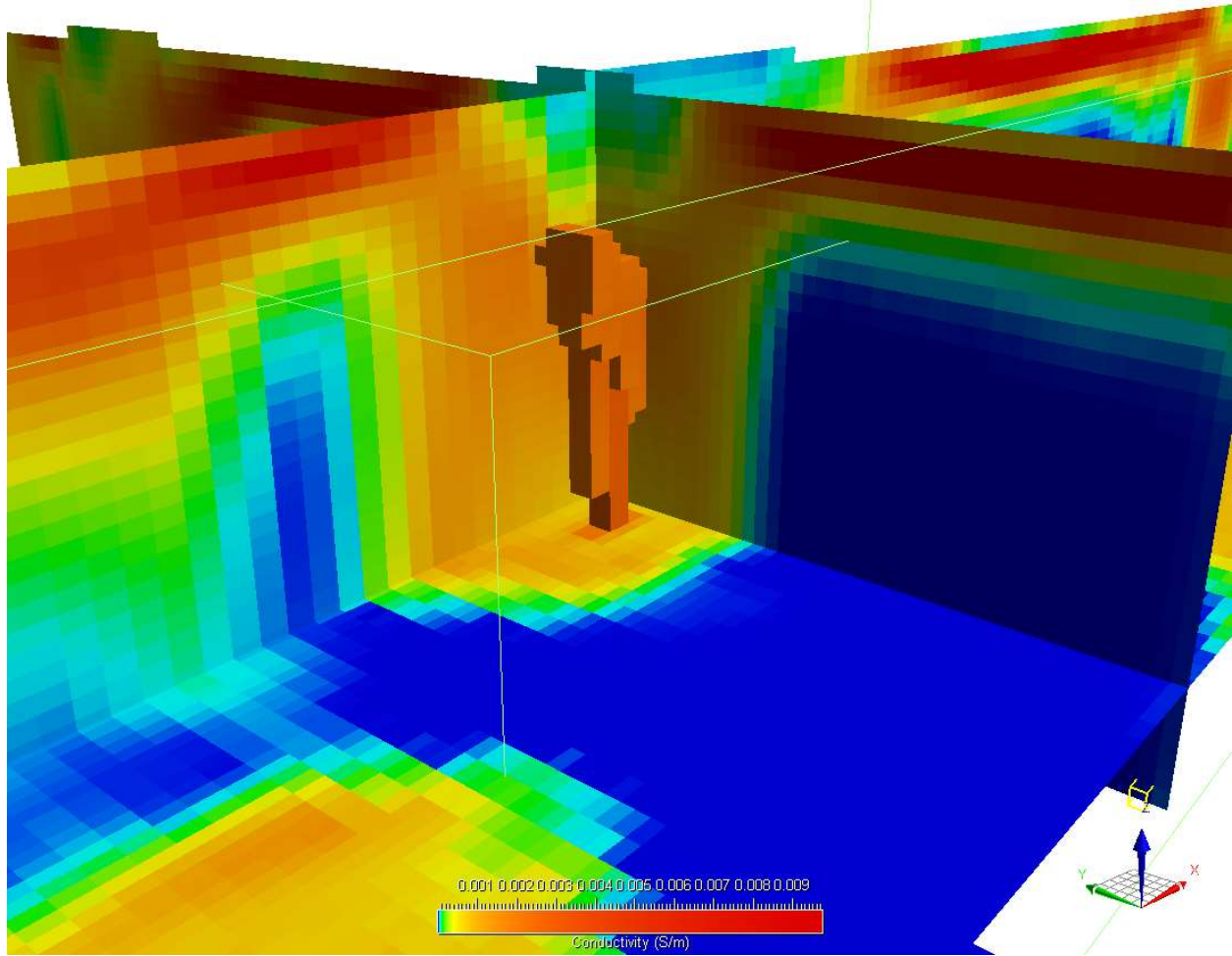
Figure 21. Detail of body C1 looking northeast. The isosurface is shown at 0.002 S/m. The body is about 400 m in depth extent and 200 m depth-to-top. The full section depth extent is about 600 m. The vertical exaggeration is 1.5.
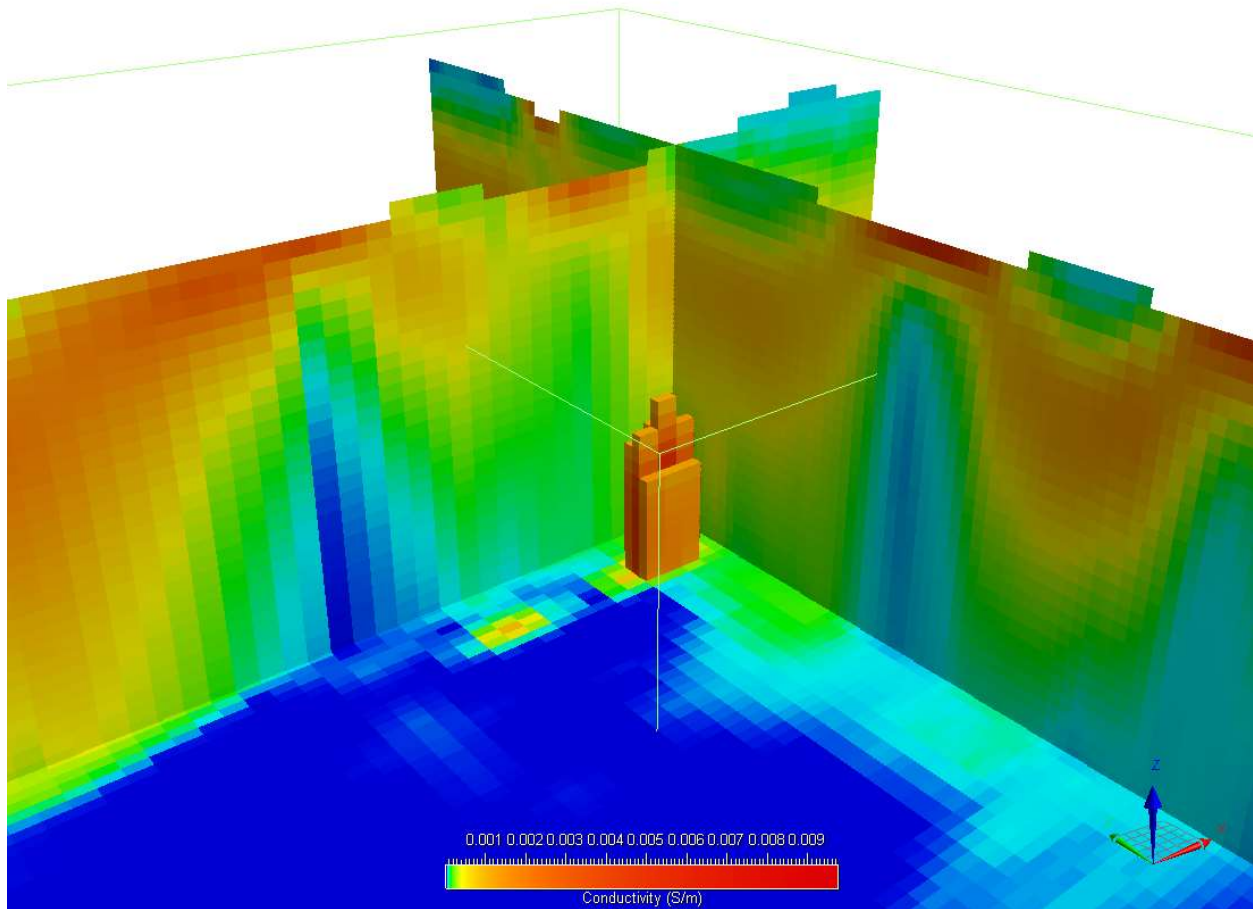
Figure 22. Detail of body C2 looking northeast. The isosurface is shown at 0.001 S/m. The body is about 300 m in depth extent and 300 m below depth-to-top. The full section depth extent is about 600 m. The vertical exaggeration is 1.5

6.1.1   Chargeability Inversion Results

The airborne derived chargeability results are illustrated here. The chargeability from the airborne inversion results typically do not and should not necessarily match with ground-based IP measurements. We believe this is primarily because of the greatly different bandwidth of ground-based systems (~1/4 Hz) and airborne systems (30 Hz). This gives two orders of magnitude difference in the time constants of media that they image. However the information presented in the two types of the surveys is complimentary, and the AEM systems provide useful chargeability measurements.

Images of the 3D chargeability distribution are shown in Figures 23-27. In the survey area, most of the chargeability anomalies align with lakes.
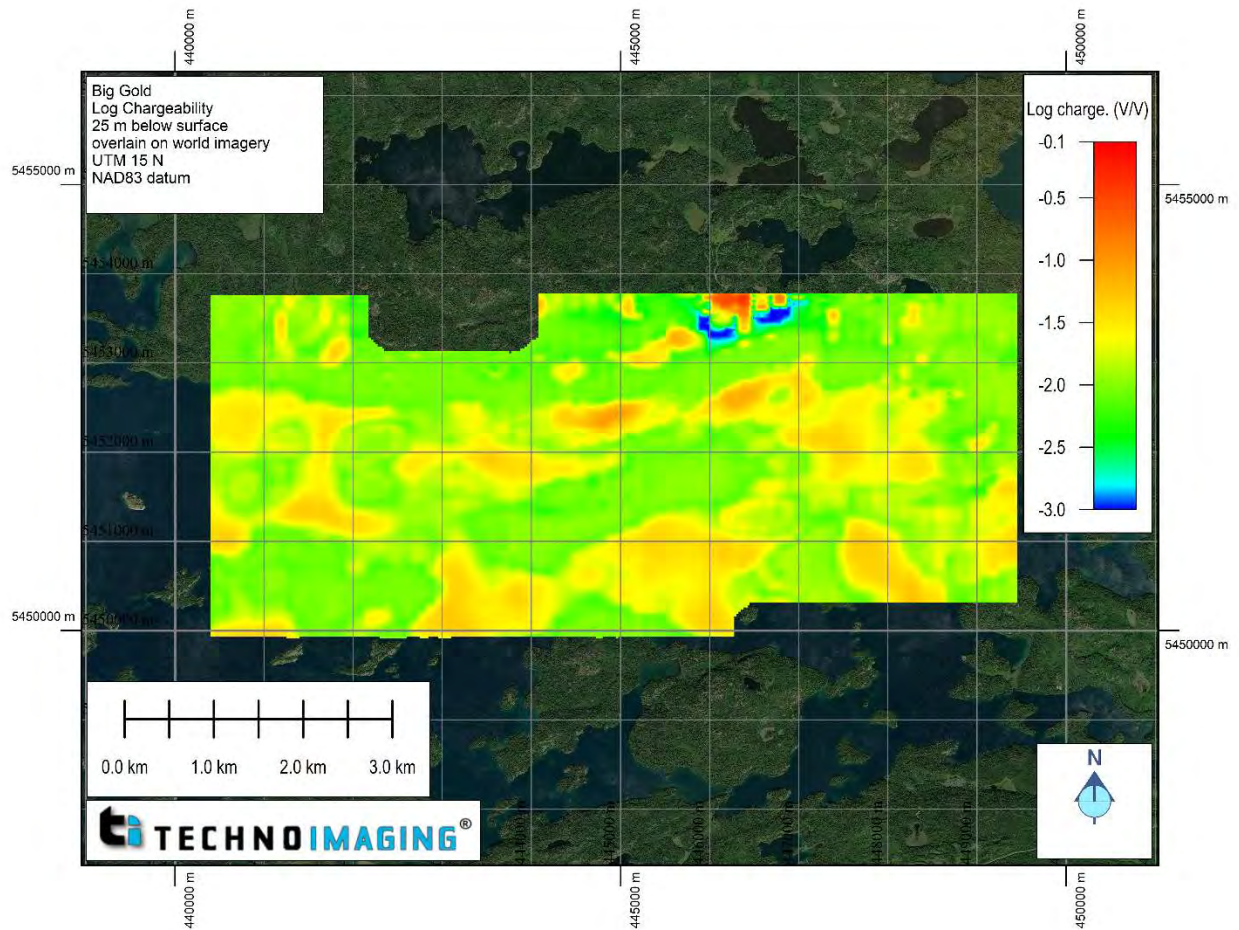
Figure 23. Chargeability inversion results at a depth of 25 m below the surface. Most of the chargeability anomalies are due to lake bottom sediments. However, anomalies not associated with lakes are of interest.
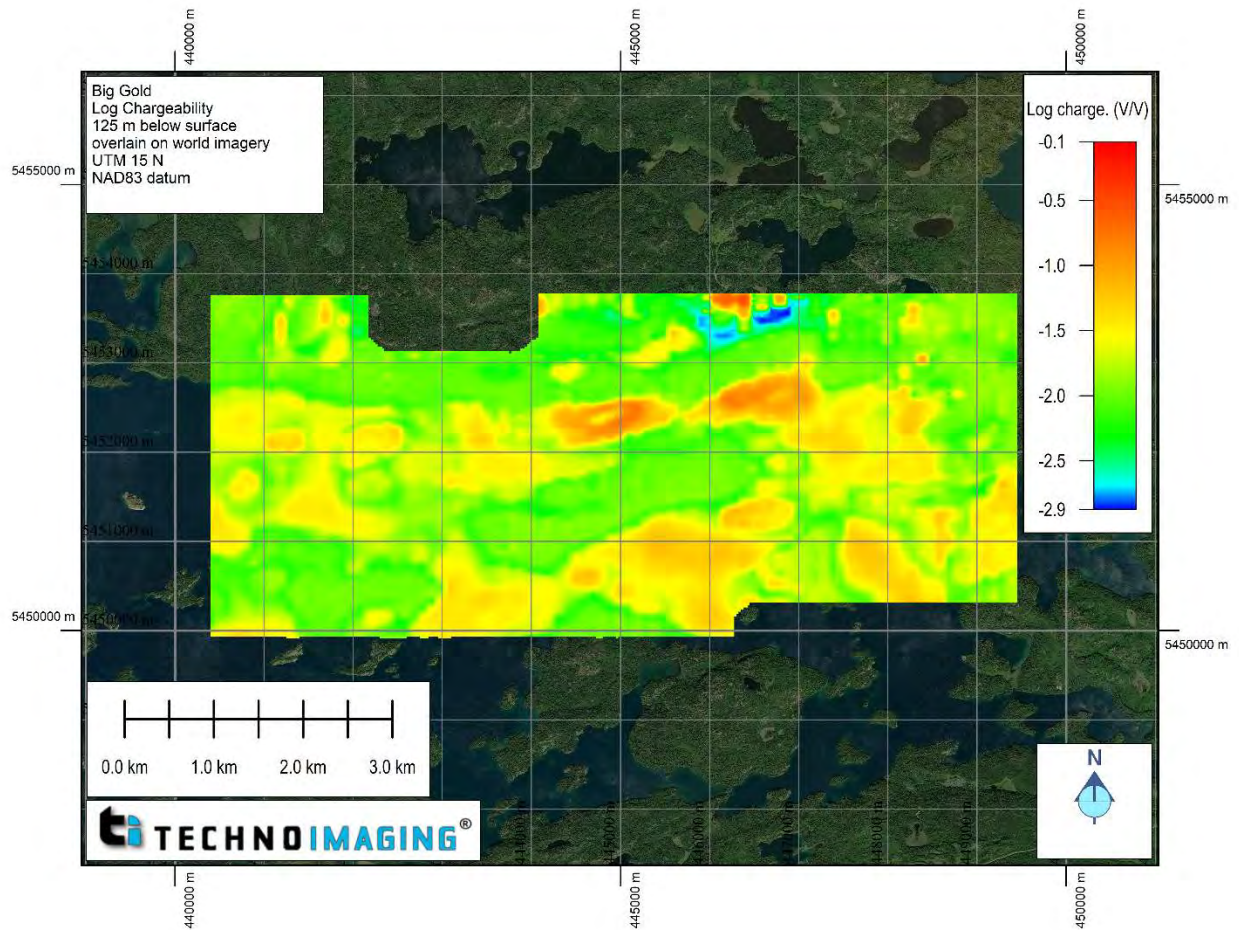
Figure 24. Chargeability inversion results at a depth of 125 m below the surface. We see an excellent correlation of the airborne chargeability with lakes, as the sediment bottoms are likely filled with clay and respond well to the time constants that fall within the airborne bandwidth.
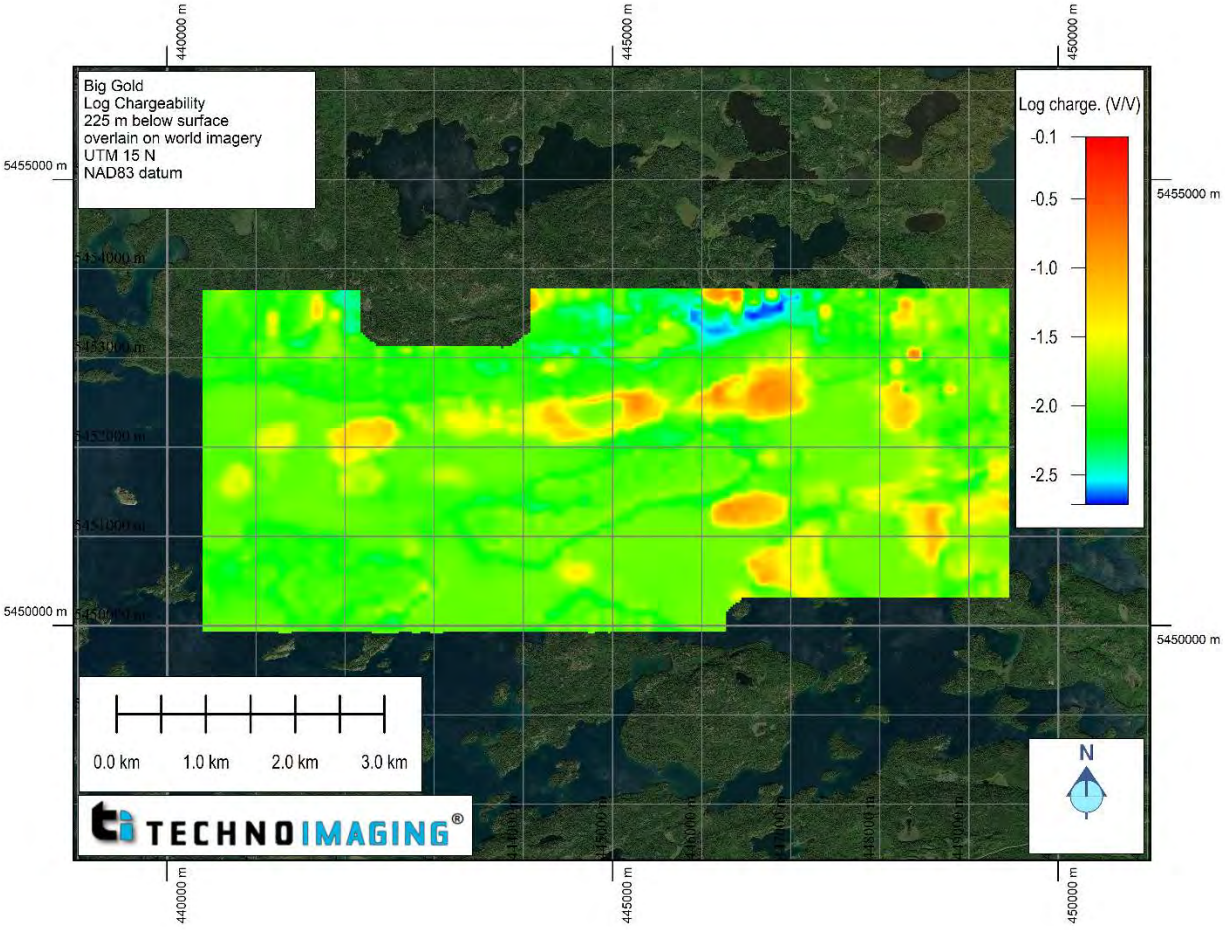
Figure 25. Chargeability inversion results at a depth of 225 m below the surface.
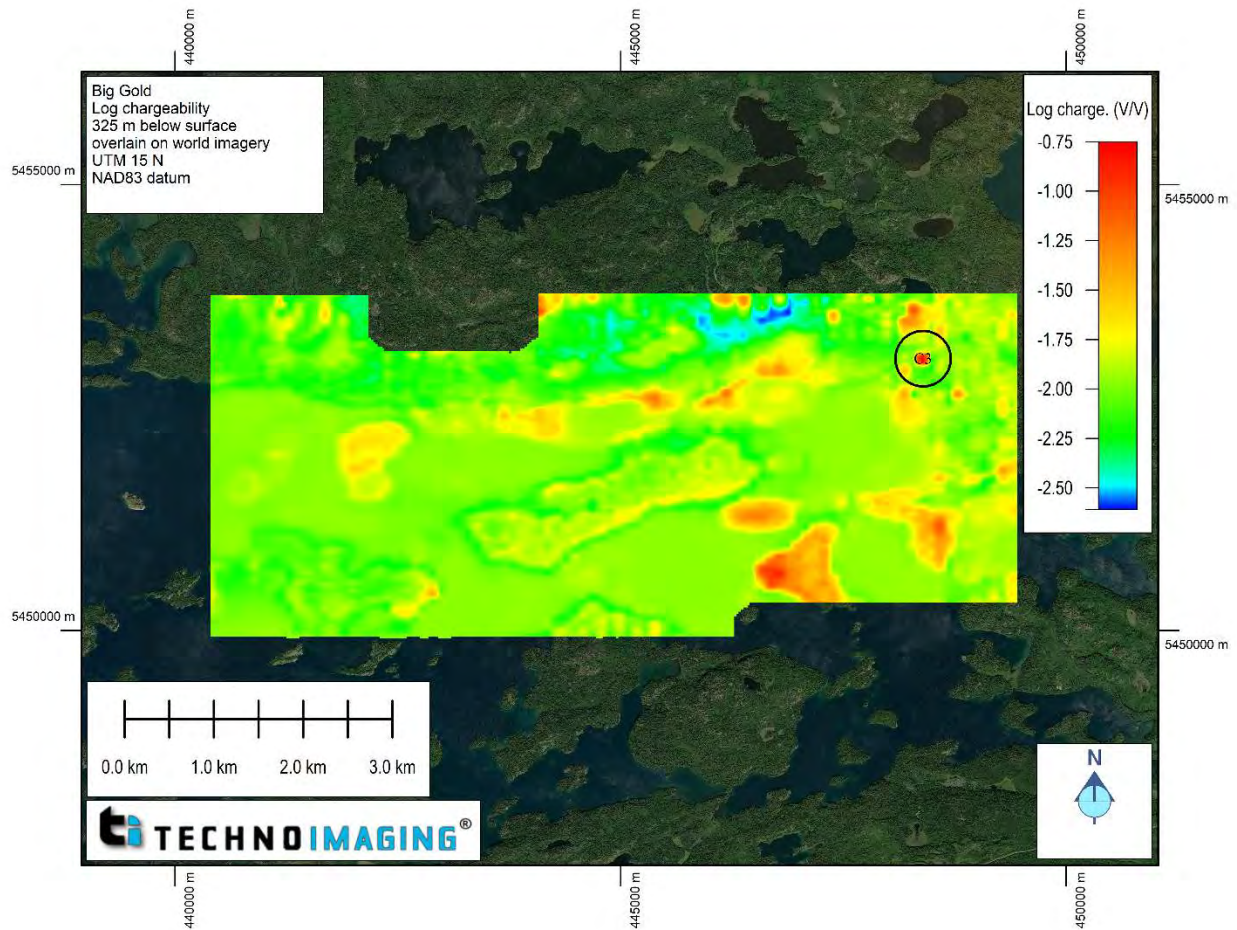
Figure 26. Chargeability at a depth of 325 m overlain on satellite imagery. The correlation between the lakes and the chargeability anomalies is apparent. However, anomaly C3 at 448400 mE and 5453050 mN show chargeability that is not associated with a lake. This anomaly is indicated by the black circle.

Figure 27 shows a three-dimensional detail of the chargeability anomaly C3. This is an interesting chargeable feature that does not have a strong conductivity associated with it. This could indicate sulphide mineralization. Several other similar but weaker anomalies are also shown.

37
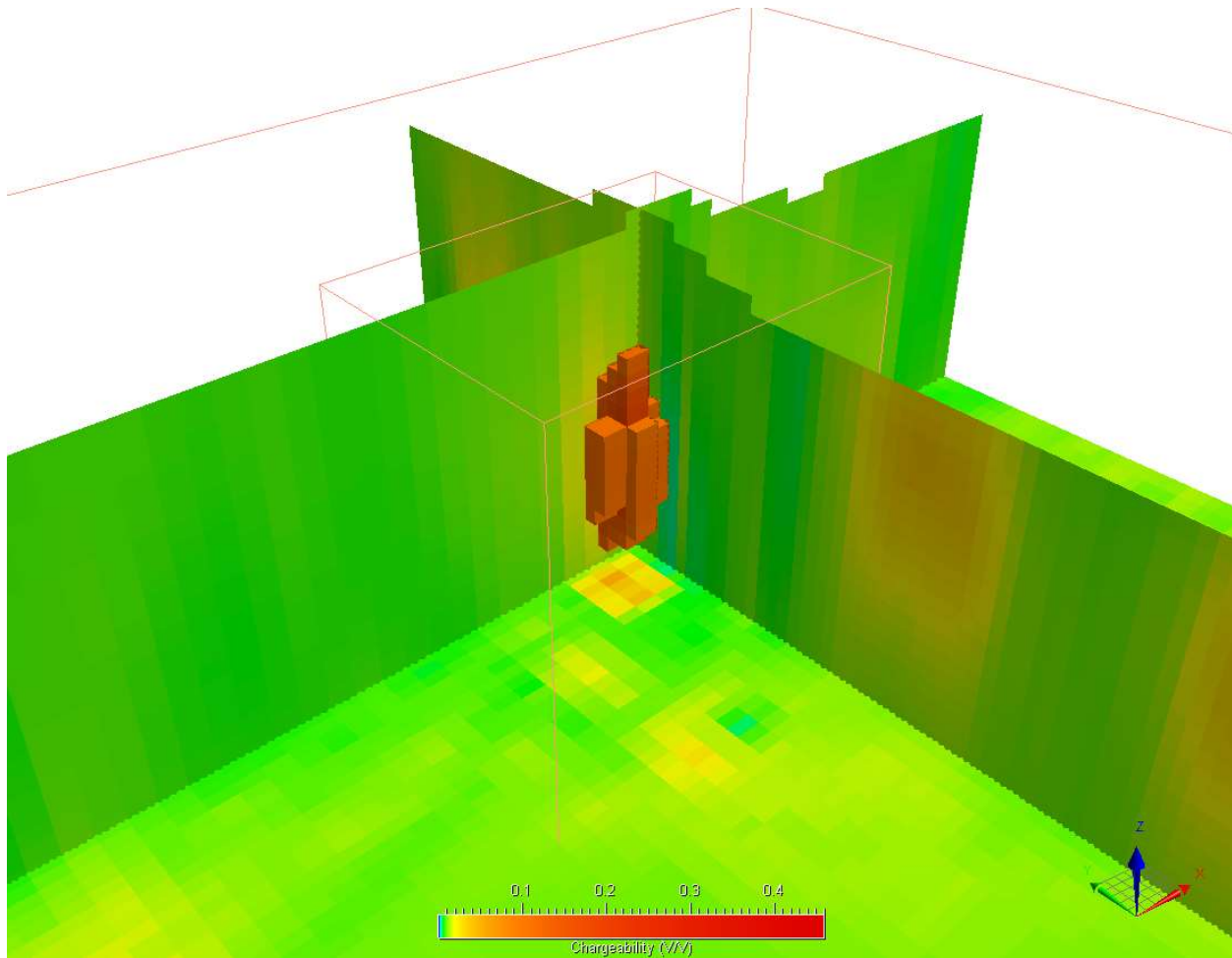
Figure 27. Chargeability anomaly C3 isosurface shown at a cutoff of 0.1 V/V. The anomaly is roughly 300 meters in depth extent and 200 meters depth-to-top. Vertical exaggeration is 1.5.

6.2   TMI Inversion Results

The TMI data were inverted to both susceptibility and magnetization vector models.   The susceptibility model is a standard product but cannot take into account remanent magnetization. The magnetization vector model considers both susceptibility and remanent magnetization and is the preferred product to study.   However, the three vector components are more challenging to visualize than one scalar value.   To overcome this difficulty, we present images of the scalar susceptibility and the amplitude of remanent magnetization. Figures 28 to 34 give overviews of the recovered magnetic models at depths of 25 m (near-surface lithologies), 125 m, and 525 m (deep-seated structures).   Shear lineaments, faults, dikes, and other areas of interest are shown in these images.

Figure 32 shows the amplitude of remanent magnetization with interpreted shear lineaments which are not as evident in the magnetic susceptibility model.   Similar responses are shown nearby, which could be worth follow-up work given a favorable geological setting.
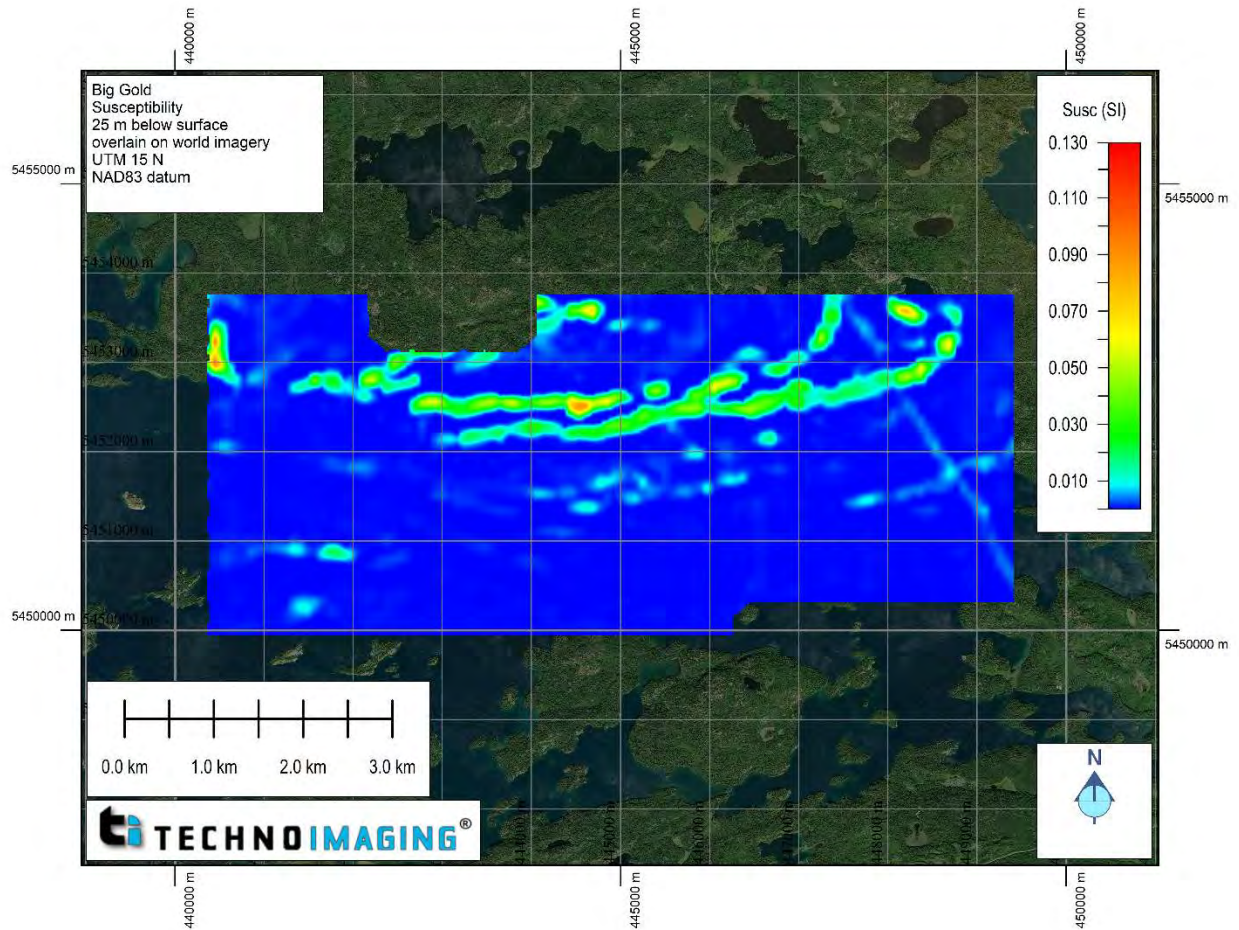
Figure 28. Horizontal section of magnetic susceptibility 25 m below the surface.
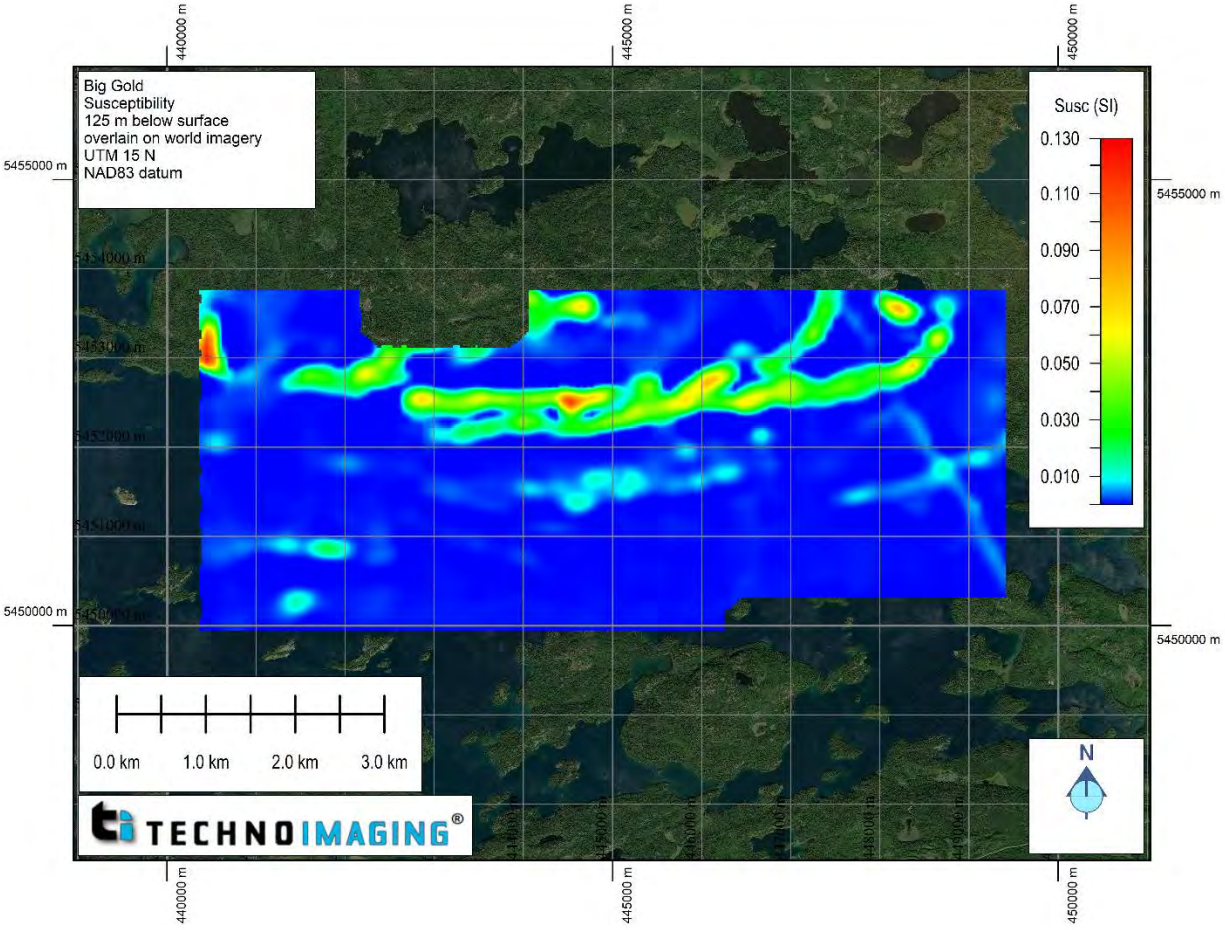
Figure 29. Horizontal section of magnetic susceptibility 125 m below the surface.
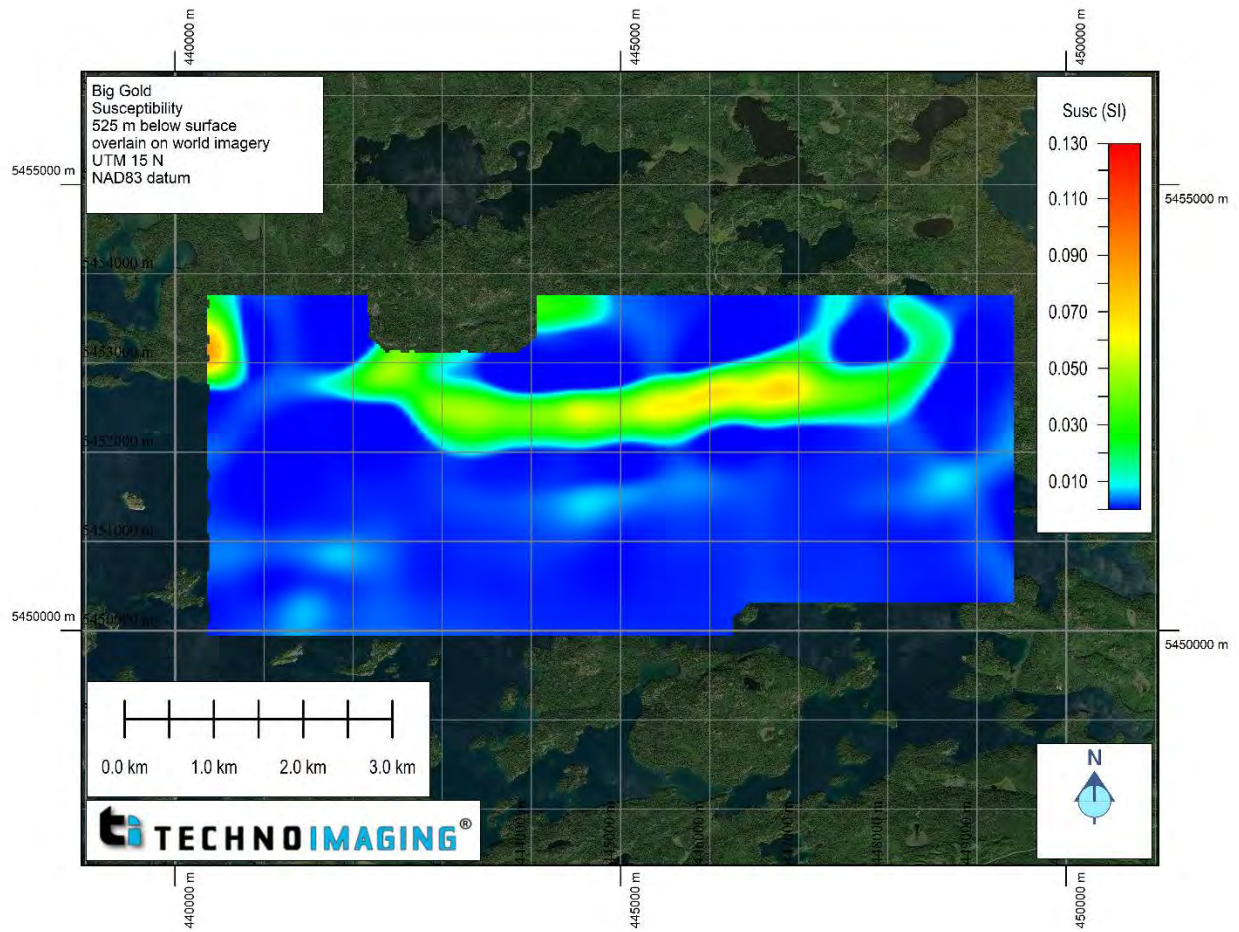
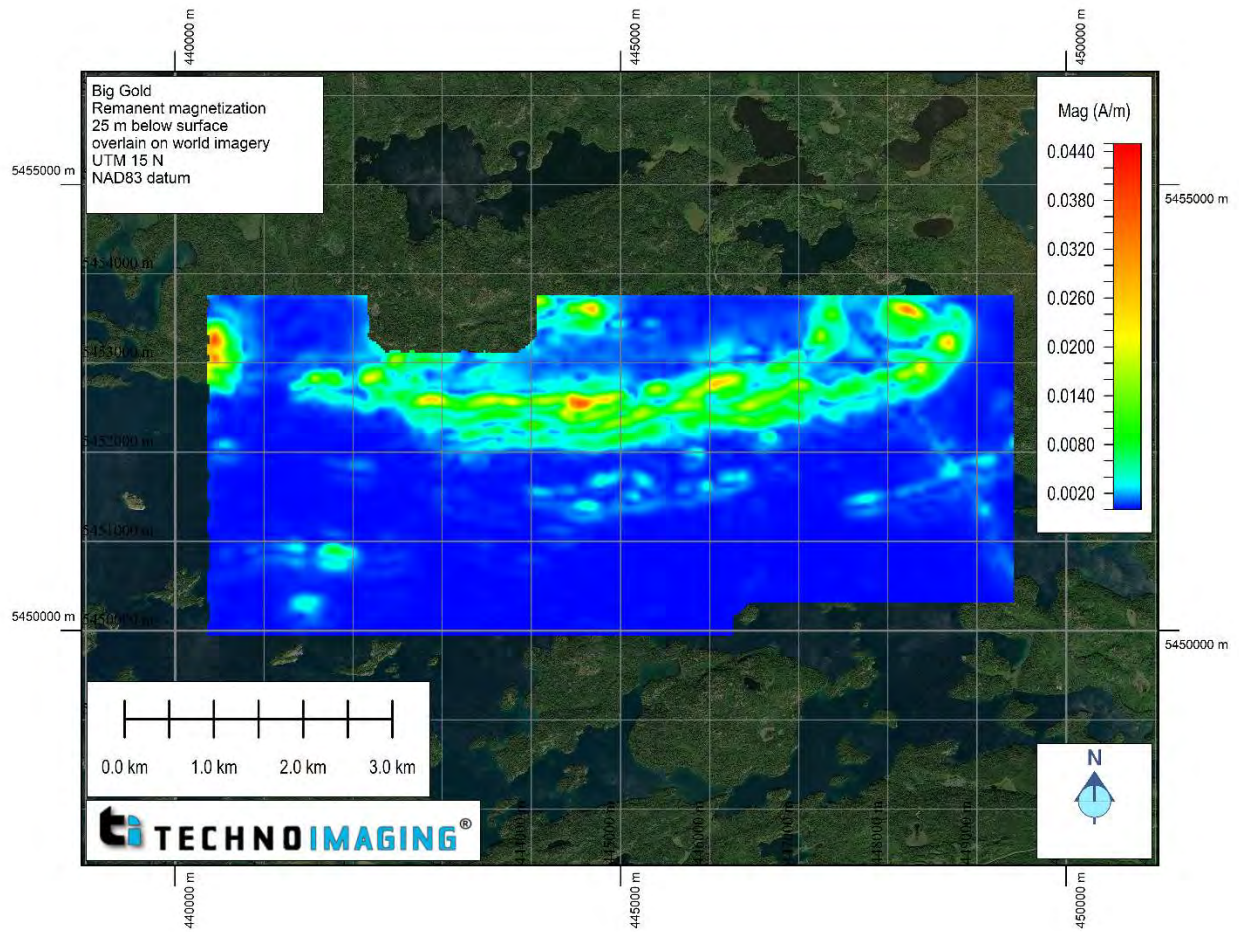*Figure 30. Horizontal section of magnetic susceptibility 525 m below the surface.*

Figure 31. Horizontal section of the amplitude of the remanent component of the magnetization vector at 25 m below the surface.
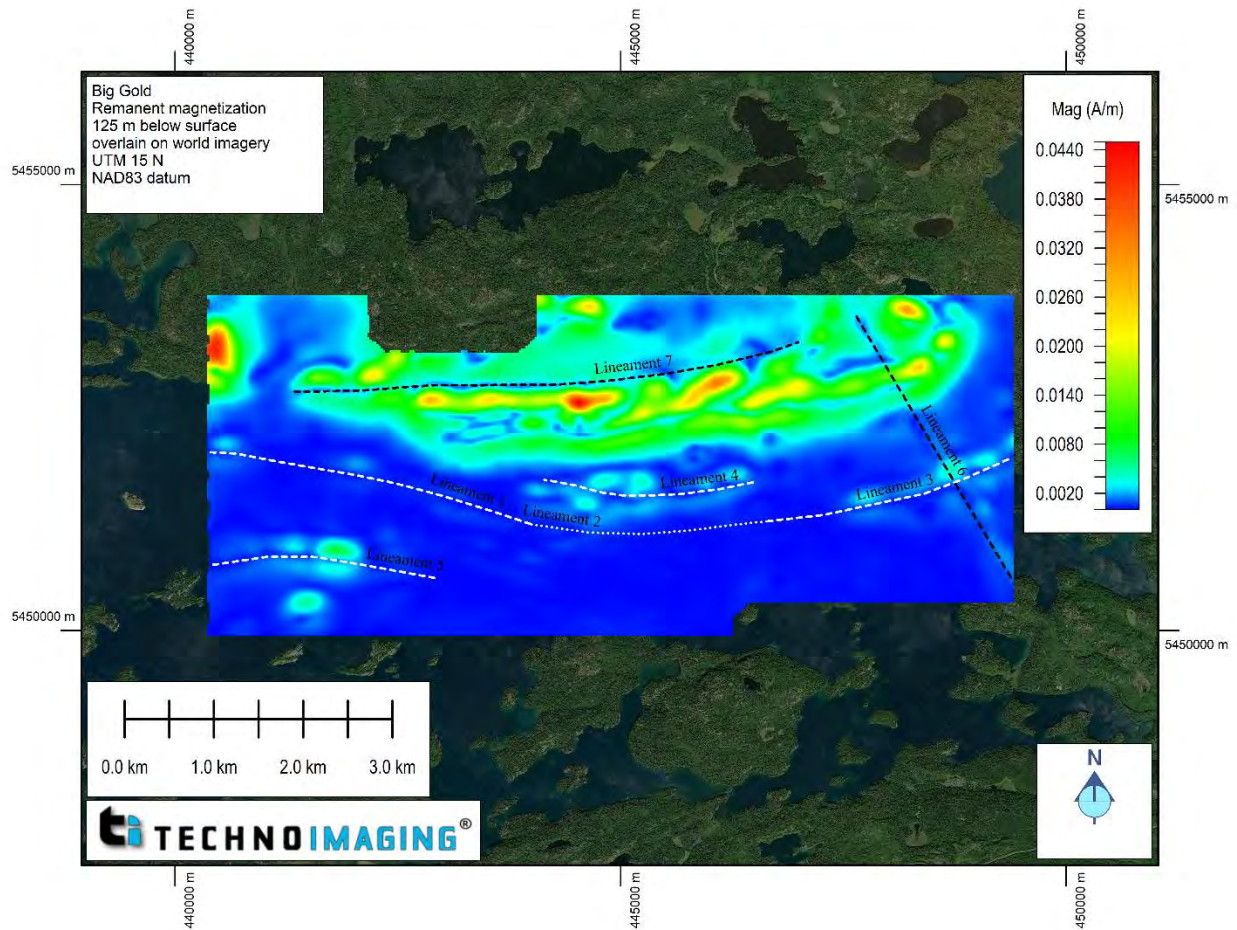
Figure 32. Horizontal section of the amplitude of the remanent component of the magnetization vector at 125 m below the surface. Interpreted lineaments of interest are shown. Lineaments 1,3,4,5 (white dashed lines) are on-trend or parallel to high gold intercepts from drillholes shown by lineament 2 (white dotted line). These lineaments are all of interest. N-S trending lineament 6 is a diabase dike. E-W trending lineament 7 (black dashed line) is an ultramafic/intermediate-felsic contact. The ultramafics are characterized by a high magnetic response and a prominent fold in evident in the north.
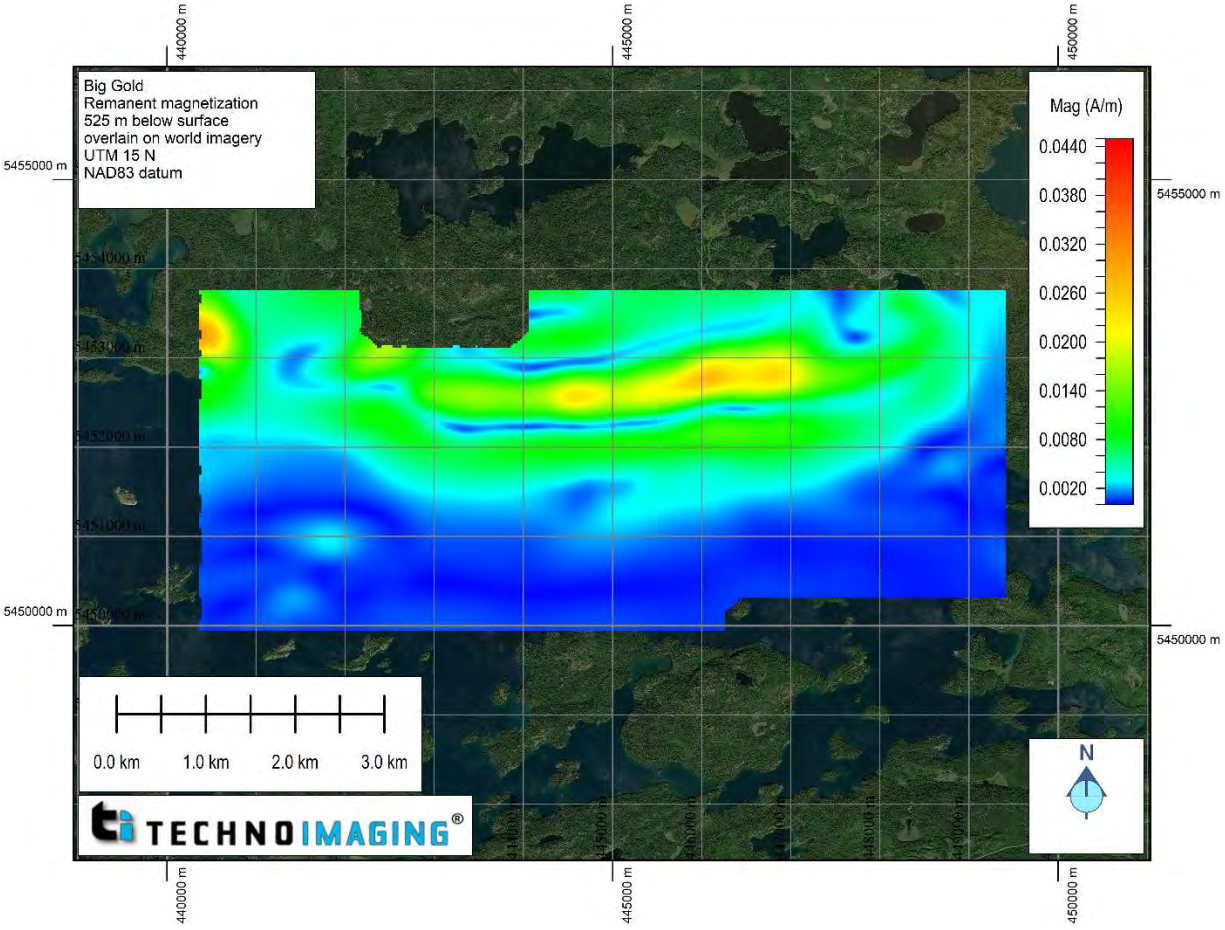
Figure 33. Horizontal section of the amplitude of the remanent component of the magnetization vector at 525 m below the surface.
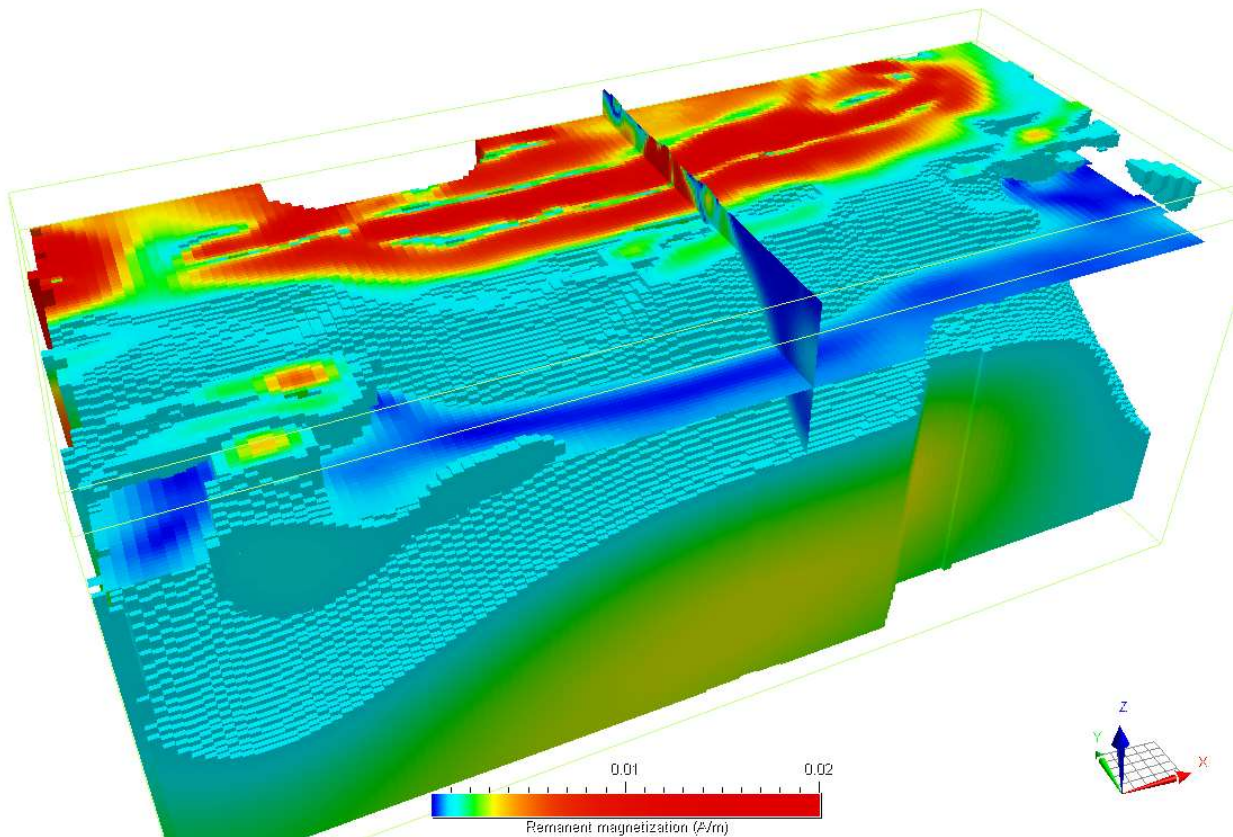
Figure 34.   An isosurface view of the the amplitude of the remanent component of the magnetization vector looking northeast. The lineaments 1,2,3 align with the dipping lithology shown in cyan, which is an isosurface with cutoff of 0.001 A/m. The full 4 km inversion domain is shown with no vertical exaggeration.

7   Digital Deliverables

All models are delivered in msh/model format:
- 3D volume of resistivity derived from AEM data,
- 3D volume of chargeability derived from AEM data,
- 3D volume of magnetic susceptibility derived from TMI data,
- 3D volume of inline component of magnetization vector derived from TMI data,
- 3D volume of remanent component of magnetization vector derived from TMI data,
- 3D volume of X component of magnetization vector derived from TMI data,
- 3D volume of Y component of magnetization vector derived from TMI data,
- 3D volume of Z component of magnetization vector derived from TMI data,
- Final report in PDF format.

The coordinate system for all deliverables is UTM Zone 15 N with a NAD 83 datum. The units are meters for depth, elevation, and horizontal distance. The UBC msh/model file parameters and null values are specified in the readme file provided with the deliverables.

8   Recommendations for a Follow-up Study

TechnoImaging recommends the following additional work to assist Big Gold with their mineral exploration projects over the Martin Kenty Property.

1) Target generation based on follow-up data interpretation and inversion results includes an enhanced study of prospective targets using constrained inversion over specific areas.
2) If small conductors are of interest, such as the examples shown as C1 and C2, an infill survey at 50 m line spacing allows a better definition of these targets and the possibility of detecting more targets that may have been missed at the 100 m flight line spacing.

9   Conclusions

This report provides a brief geological and geophysical setting for the Martin Kenty Project Area work by TechnoImaging. In addition, it documents the data collection methods and gives an overview of the theoretical processing applied to the data to generate 3D models.

The field data collection was of high quality, and three-dimensional conductivity, chargeability, susceptibility, and magnetic vector property models have been produced from the provided field data. The results correlate well with the known geology in the area. Several examples of potential targets have been suggested based on our understanding of the area, and an abbreviated summary is listed below:

- Lineaments 1,3,4,5 in the 3D remanent component of the magnetization vector are of interest. They are parallel to or adjoining the shear zone with high gold intercepts from drilling.

- Although the airborne-based chargeability highlights lake bottom sediments in the project area, there are other chargeability anomalies, i.e., chargeability anomaly C3, in other areas that warrant further investigation for gold and disseminated sulphide mineralization.

- Conductive anomalies C1 and C2, as well as chargeability anomaly C3, warrant follow-up. The geometries of these suggest nickel deposits, Barnes and Mungall (2018).

The inclusion of remanence in the TMI data interpretation and chargeability in the AEM data were instrumental in developing the above targets. These state-of-the-art techniques are standard in TechnoImaging's algorithms and interpretations.

This report provides a high-level overview of what we see in the results, and it gives ideas on how to view and integrate the 3D models and suggestions on how to perform the interpretation of the data. These models are rich with information, but a full interpretation of the geophysics requires a detailed geological understanding of the area and knowledge to build and test geological models. TechnoImaging would be pleased to help direct these initial efforts in collaboration with staff geologists and geophysicists.

10 References

Alfouzan, F., Alotaibi, A., Cox, L., and Zhdanov, M. S., 2020, Spectral Induced Polarization Survey with Distributed Array System for Mineral Exploration: Case Study in Saudi Arabia: Minerals, 10, 769.

Barnes, S. J. and Mungall, J. E. (2018), Blade-shaped dikes and nickel sulfide deposits: A model for the emplacement of ore-bearing small intrusions: Economic Geology, v. 113, no. 3, pp. 789–798.

Combrinck, M., Cox, L.H., Wilson, G.A., Zhdanov M. S., 2012, 3D VTEM inversion for delineating sub-vertical shear zones in the West African gold belt, ASEG Extended Abstracts, 2012:1, 1-4.

Cox, L., Endo, M., & Zhdanov, M. (2015, June). 3D Inversion of AEM Data Based on a Hybrid IE-FE Method and the Moving Sensitivity Domain Approach with a Direct Solver. In 77th EAGE Conference and Exhibition 2015 (Vol. 2015, No. 1, pp. 1-5). European Association of Geoscientists & Engineers.

Cox, L. H., and Zhdanov, M. S., 2008, Advanced computational methods of rapid and rigorous 3-D inversion of airborne electromagnetic data: Communications in Computational Physics, **3** (1), 160-179.

Cox, L. H., Wilson, G. A., & Zhdanov, M. S. (2012), 3D inversion of airborne electromagnetic data. *Geophysics*, *77*(4), WB59-WB69.

Čuma, M., and Zhdanov, M. S., 2014, Massively parallel regularized 3D inversion of potential fields on CPUs and GPUs: Computers & Geosciences, **62**, 80-87.

Jorgensen, M., and Zhdanov, M. S., 2021, Recovering magnetization of rock formations by jointly inverting airborne gravity gradiometry and total magnetic intensity data: Minerals, **11** (4), 366.

Zhdanov, M.S., Cox, L., and Rudd, J., 2013, Paradigm change in 3D inversion of airborne EM surveys: case study for oil sands exploration near Fort McMurray, Alberta: First Break, 31 (4), 45-49.

Zhdanov, M. S., 2008, Generalized effective-medium theory of induced polarization: Geophysics **73**, F197-F211

Zhdanov, M. S., 2015, Inverse theory and applications in geophysics. Elsevier.

Zhdanov, M.S., Zhu, Y., Endo, M., and Kinakin, Y., 2016, Novel approach to joint 3D inversion of EM and potential field data using Gramian constraints: First Break, **34**, 59-64.

Zhdanov, M. S., 2018, Foundations of geophysical electromagnetic theory and methods. Elsevier.

Zhdanov M. S., F. A. Alfouzan, L. Cox, A. Alotaibi, M. Alyousif, D. Sunwall, and M. Endo, 2018, Large-Scale 3D Modeling and Inversion of Multiphysics Airborne Geophysical Data: A Case Study from the Arabian Shield, Saudi Arabia: Minerals, **8**, 271.

Zhdanov M.S., Ellis R., and Mukherjee S., 2004, Three-dimensional regularized focusing inversion of gravity gradient tensor component data: Geophysics, **69** (4), 925-937

Zhu, Y., M.S. Zhdanov, and Čuma, M., 2015, Inversion of TMI data for the magnetization vector using Gramian constraints: 85th Annual International Meeting, SEG, Expanded Abstracts, 1602-1606.